Thu. Jun 3, 2021

[J] Poster | P (Space and Planetary Sciences)：P-CG Complex & General

5:15 PM - 6:30 PM JST | 8:15 AM - 9:30 AM UTC | Ch.01_2

[P-CG18] Planetary Magnetosphere, Ionosphere, and Atmosphere

convener:Kanako Seki(Graduate School of Science, University of Tokyo), Hiroyuki Maezawa(Department of Physical Science Osaka Prefecture University), Takeshi Imamura(Graduate School of Frontier Sciences, The University of Tokyo), Naoki Terada(Graduate School of Science, Tohoku University)

[PCG18-P01] Hybrid particle simulation on Mercury's dayside magnetopause

*Hideyuki Usui[1], Yohei Miyake[2], Naoshi Motoda[1], Masaharu Matsumoto[3] (1.Graduate school of system informatics Kobe University, 2.Education Center for Computational and Engineering Science, 3.Graduate school of information science and technology, The University of Tokyo)

[PCG18-P02] Numerical calculation of moist convection in Jupiter's atmosphere - A case study with an average cooling vertical profile based on a radiative transfer calculation -

Taro Sekiguchi[1], *Ko-ichiro SUGIYAMA[2], Masaki Ishiwatari[1], Kensuke Nakajima[3], Kiyoshi Kuramoto[1], Yoshi-Yuki Hayashi[4] (1.Department of Cosmoscience, Graduate School of Science, Hokkaido University, 2.National Institute of Technology, Matsue College, 3.Department of Earth and Planetary Sciences,Flculty of Sciences,Kyushu University, 4.Department of Planetology, Graduate School of Science, Kobe University / Center for Planetary Science (CPS))

[PCG18-P03] High dynamic range observation using a 1.8-m off-axis telescope PLANETS: feasibility study and telescope assembly

*Masato Kagitani[1], Takeshi Sakanoi[1], Kazuya Nagta[1], Yasumasa Kasaba[1], Yasuhiro Hirahara[2], Mikio Kurita[3], Jeffry Kuhn[4], Svetlana Berdyugina[5], Emilio Marcelo[6] (1.Planetary Plasma and Atmospheric Research Center, Graduate School of Science, Tohoku University, 2.Graduate School of Environmental Studies, Nagoya University, 3.Graduate School of Science, Kyoto University, 4.Institute for Astronomy, Univesity of Hawaii, USA, 5.Kiepenheuer Institute for Solar Physics, Germany, 6.Universidade Estadual de Ponta Grossa, Brazil)

[PCG18-P04] A search for atomic sodium and calcium in the atmosphere of the icy Galilean moons of Jupiter with ground-based telescope

*Seiko Takagi[1], Taro Matsuo[2], Jun Kimura[3], Kazuo Yoshioka[4] (1.Hokkaido University, Graduate School of Science, 2.Nagoya University, 3.Osaka University, 4.The University of Tokyo)

[PCG18-P05] Development of PLANETS telescope: An attempt to reduce polishing volume in final polishing process by using an active mirror support

*Kazuya Nagata[1], Masato Kagitani[1], Yasumasa Kasaba[1], Takeshi Sakanoi[1], Yasuhiro Hirahara[2], Mikio Kurita[3] (1.Graduate School of Science, Tohoku University, 2.Graduate School of Environmental Studies, Nagoya University, 3.Graduate School of Science, Kyoto University)

[PCG18-P06] Numerical simulations of 500eV-50keV electron elastic collisions with neutral H_2O around Enceladus ~estimation of electron loss rate and auroral brightness~

*Hiroyasu Tadokoro[1], Yuto Katoh[2] (1.Surugadai University, 2.Tohoku University)

[PCG18-P07] Development of the near-infrared camera TOPICS and the Echelle spectrograph ESPRIT for planetary observations

Ayumu Kambara[1], *Takeshi Sakanoi[1], Yasuhiro Hirahara[2], Takashi Ichikawa[3], Masato Kagitani[1], Yasumasa Kasaba[1], Aya Otomo[1], Kazuya Nagata[1] (1.Planetary Plasma and Atmospheric Research Center, Graduate School of Science, Tohoku University, 2.Graduate School of Environmental Studies, Nagoya University, 3.Astronomical Institute, Graduate School of Science, Tohoku University)

[PCG18-P08] Effects of the magnetic field configuration in the ionosphere on solar energetic electron precipitation into the Martian upper atmosphere observed by MAVEN

*Kanako Seki[1], Takuya Hara[2], Dave A Brain[3], Robert J Lillis[2], Darvin E Larson[2], Dave L Mitchell[2], Gina A Dibraccio[4], Janet G Luhmann[2], Bruce M Jakosky[3] (1.Graduate School of Science, University of Tokyo, 2.Space Sciences Laboratory, University of California, Berkeley, 3.Laboratory for Atmospheric and Space Physics, University of Colorado, Boulder., 4.Goddard Space Flight Center, NASA)

[PCG18-P09] Observations of minor constituents in the Venusian atmosphere, CO and SOx using the millimeter/submillimeter-wave band radio telescopes, SPART/ALMA

Ayaka Tomihara[1], Teppei Yonetsu[1], Yuki Hamaguchi[1], Hideo Sagawa[2], *Hiroyuki Maezawa[1] (1.Department of Physical Science Osaka Prefecture University, 2.Kyoto Sangyo University)

[PCG18-P10] Influences of solar energetic particles on the Martian ozone layer

*Sayano Hiruba[1], Yuki Nakamura[1], Hiromu Nakagawa[1], Naoki Terada[1], Shotaro Sakai[1], Isao Murata[1], Yoshifumi Futaana[2] (1.Dept. of Geophysics, Graduate school of science, Tohoku University, 2.Swedish Institute of Space Physics)

[PCG18-P11] Simultaneous remote and in-situ observations of ionospheric irregularities at Mars

*Hina Bando[1], Yuki Harada[1], Naoki Terada[2], Hiromu Nakagawa[2] (1.Kyoto University, 2.Tohoku University)

[PCG18-P12] Annual variability in the thermospheric wave perturbations at Mars

*Hiromu Nakagawa[1], Nao Yoshida[1], Kaori Terada[1], Naoki Terada[1], Yuki Harada[2], Shotaro Sakai[1], Takeshi Imamura[3], Hitoshi Fujiwara[4], Kanako Seki[5] (1.Planetary Atmosphere Physics Laboratory, Department of Geophysics, Graduate School of Science, Tohoku University, 2.Kyoto University, 3.Graduate School of Frontier Scienfes, The University of Tokyo, 4.Faculty of Science and Technology, Seikei University, 5.Graduate School of Science, University of Tokyo)

[PCG18-P13] **Study of atmospheric ion escape from exoplanet TOI-700 d**

*Tomoaki Nishioka[1], Kanako Seki[1], Ryoya Sakata[1], Kazuhiro Yamamoto[1], Naoki Terada[2], Hiroyuki Shinagawa[3] (1.Graduate School of Science, University of Tokyo , 2.Graduate School of Science, Tohoku University , 3.NICT)

[PCG18-P14] DSMC simulations of slow hydrodynamic escape from Earth-like and Mars-like planets

*Naoki Terada[1], Kaori Terada[1], Hitoshi Fujiwara[2], Masahiro Ikoma[3] (1.Graduate School of Science, Tohoku University, 2.Faculty of Science and Technology, Seikei University, 3.Graduate School of Science, The University of Tokyo)

[J] Poster | A (Atmospheric and Hydrospheric Sciences)：A-AS Atmospheric Sciences, Meteorology & Atmospheric Environment

5:15 PM - 6:30 PM JST | 8:15 AM - 9:30 AM UTC | Ch.02_2

[A-AS06] Stratosphere-troposphere Processes And their Role in Climate

convener:Takenari Kinoshita(Japan Agency for Marine-Earth Science and Technology), Takatoshi Sakazaki(Graduate School of Science, Kyoto University), Masashi Kohma(Department of Earth and Planet Science, Graduate School of Science, The University of Tokyo), Nawo Eguchi(Kyushu University)

[AAS06-P01] Radiosonde Observations in the 30-40 km Altitude Range Using 3000 g Balloons

*Takenari Kinoshita[1], Shin-Ya Ogino[1], Junko Suzuki[1], Ryuichi Shirooka[1], Takuji Sugidachi[2], Kensaku Shimizu[2], Matthew H Hitchman[3] (1.Japan Agency for Marine-Earth Science and Technology, 2.Meisei Electric Co. Ltd., 3.University of Wisconsin-Madison)

[AAS06-P02] Influence of a SH SSW in September 2019 on tropical tropospheric circulation and deep convective activity

*Kunihiko Kodera[1], Shunnsuke Noguchi[2], Nawo Eguchi[3], Tomoe Nasuno[2] (1.Meteorological Research Institute, 2.JAMSTEC, 3.Kyushu University)

[AAS06-P03] Dynamical analysis of extreme tropopause folding events in the coastal region of Antarctica

Masatoshi Mizukoshi[1], *Masashi Kohma[1], Kaoru Sato[1] (1.Department of Earth and Planet Science, Graduate School of Science, The University of Tokyo)

[AAS06-P04] Response of the Brewer-Dobson circulation to the major volcanic eruptions in reanalysis datasets

*Masatomo Fujiwara[1], Marta Abalos[2], Patrick Martineau[3], Jonathon Wright[4] (1.Faculty of Environmental Earth Science, Hokkaido University, 2.Universidad Complutense de Madrid, 3.JAMSTEC, 4.Tsinghua University)

[AAS06-P05] **Impact of the upper troposphere and stratosphere on the climate change around Japan**

*Yoshio Kawatani[1], Takeshi Horinouchi[2], Naoki Sato[3] (1.Japan Agency for Marine-Earth Science and Technology, 2.Faculty of Environmental Earth Science, Hokkaido University, 3.Tokyo Gakugei University)

[AAS06-P06] Analysis of Arctic spring ozone anomaly in the phases of QBO and 11-year solar cycle for 1979–2011

Yousuke Yamashita[1,2], *Hideharu Akiyoshi[1], Masaaki Takahashi[1,3] (1.National Institute for Environmental Studies, 2.Japan Agency for Marine-Earth Science and Technology, 3.Atmosphere and Ocean Research Institute, The University of Tokyo)

[AAS06-P07] Morphology of zonal asymmetry of QBO zonal wind

*Takatoshi Sakazaki[1], Kevin Hamilton[2], Yoshio Kawatani[3] (1.Graduate School of Science, Kyoto University, 2.International Pacific Research Center, University of Hawai'i, 3.Japan Agency for Marine-Earth Science and Technology)

[AAS06-P08] Relationships between Unusual Antarctic Ozone Hole in 2019 and Dynamical Fields

*Guangyu Liu[1], Toshihiko Hirooka[2], Nawo Eguchi[3] (1.Department of Earth and Planetary Sciences, Graduate School of Science, Kyushu University, 2.Department of Earth and Planetary Sciences, Faculty of Science, Kyushu University, 3.Research Institute for Applied Mechanics, Kyushu University)

[J] Poster | A (Atmospheric and Hydrospheric Sciences)：A-OS Ocean Sciences & Ocean Environment

5:15 PM - 6:30 PM JST | 8:15 AM - 9:30 AM UTC | Ch.03_3

[A-OS18] Kuroshio Large Meander

convener:Toru Miyama(Japan Agency for Marine-Earth Science and Technology, Application Laboratory), Norihisa Usui(Meteorological Research Institute), Hidetaka Hirata(Rissho University), Takashi SETOU(Japan Fisheries Research and Education Agency)

[AOS18-P01] Characteristics and evolution of the cyclonic eddy in the Kuroshio coastal area in association with the Kuroshio large meander

★Invited Papers

*Daiki Ito[1], Takashi Setou[1], Daisuke Ambe[1], Yugo Shimizu[1,2] (1.Fisheries Resources Institute, Japan Fisheries Research and Education Agency, 2.(Present affiliation) Fisheries Agency)

[AOS18-P02] The relationship between Kuroshio meander and observed tidal-regime shift along southern coast of Japan

*Takumi Kamura[1], Hiromi Matsuura[1], Katsuto Uehara[2] (1.Interdisciplinary Graduate School of Engineering Sciences, Kyushu University, 2.Research Institute for Applied Mechanics, Kyushu University)

[AOS18-P03] Eddy separation from the Kuroshio Large Meander in 2020

*Toru Miyama[1], Yasumasa Miyazawa[1], Sergey M Varlamov[1], Zhang Ruochao[1] (1.Japan Agency for Marine-Earth Science and Technology, Application Laboratory)

[AOS18-P04] Study on the temporal and spatial variation of the Kuroshio Current path

*Yuya Hirano[1], Kazuyuki Uehara[1] (1.Graduate School of Earth Environmental Science, Tokai University)

[AOS18-P05] Impact of a Marine Heatwave Attributable to a Kuroshio Large Meander on Extreme Heavy Rainfall Caused by an Extratropical Cyclone

*Eigo Tochimoto[1], Satoshi Iizuka[1] (1.National Research Institute for Earth Science and Disaster Resilience)

[AOS18-P06] **The Kuroshio volume transport in near future estimated by Reduced Gravity model**

*Takashi SETOU[1], Akira KUSAKA, Daisuke Ambe, Daiki Ito[1], Takashiko Kameda (1.Japan Fisheries Research and Education Agency)

[J] Poster | A (Atmospheric and Hydrospheric Sciences)：A-CC Cryospheric Sciences & Cold District Environment

5:15 PM - 6:30 PM JST | 8:15 AM - 9:30 AM UTC | Ch.04_1

[A-CC25] Glaciology in the new normal

convener:Hiroto Nagai(Waseda Univ., School of Education), Kzutaka Tateyama(National University Corporation Kitami Institute of Technology), Ishikawa Mamoru(Hokkaido University), Keiko Konya(Japan Agency for Marine-Earth Science and Technology)

[ACC25-P01] Evidence for long-range transport of atmospheric microplastic

*Osamu Nagafuchi[1], Koyomi Nakazawa[1] (1.Fukuoka Institute of Techology)

[ACC25-P02] **A discussion of the circumstances and causes of the massive avalanche that occurred at Mt. Kiso Ontake on May 21st 2019**

*Hideo Suzuki[1], Takeshi Saito[2], Kuniaki Makino[2] (1.Institute of Science, Academic Assembly School of Science and Technology, Shinshu University, 2.Department of Geology, Faculty of Science, Shinshu University)

[ACC25-P03] Preliminary observation report of snow-buried corner reflectors for SAR-based snow-depth monitoring in Nagaoka, Niigata (2020/2021)

*Hiroto Nagai[1,2], Sojiro Sunako[2], Katsuya Yamashita[2], Satoru Yamaguchi[2] (1.Waseda Univ., School of Education, 2.National Research Institute for Earth Science and Disaster Resilience)

[ACC25-P04] Radiation characteristics of thin sea ice in the ice tank experiment using multifrequency passive microwave radiometers

*Kzutaka Tateyama[1], Hiroyuki Enomoto[2], Masashige Nakayama[3], Naoto Shoji[1], Yurika Watanabe[1], Sae Ohira[1], Kohei Sato[1] (1.National University Corporation Kitami Institute of Technology, 2.Arctic Environment Research Center, National Institute of Polar Research, 3.National University Corporation Hokkaido University of Education, Kushiro campus)

[ACC25-P05] Polar snow monitoring by satellite microwave radiometer

*Nuerasimuguli Alimasi[1], Hiroyuki Enomoto[1] (1.National Institute of Polar Research)

[ACC25-P06] The observation plan of glacier research and its modification due to covid-19

*Keiko Konya[1] (1.Japan Agency for Marine-Earth Science and Technology)

[ACC25-P07] **Relationship between Haliaeetus pelagicus flights route over the Russian Far East and surface atmospheric conditions**

*Kazutoshi Sato[1], Kzutaka Tateyama[1], Saiko Shiraki[2], Yusuke Murata[1] (1.Kitami Institute of Technology, 2.Tokyo University of Agriculture)

[J] Poster | A (Atmospheric and Hydrospheric Sciences)：A-CC Cryospheric Sciences & Cold District Environment

5:15 PM - 6:30 PM JST | 8:15 AM - 9:30 AM UTC | Ch.04_2

[A-CC26] Ice cores and paleoenvironmental modeling

convener:Nozomu Takeuchi(Chiba University), Ayako Abe-Ouchi(Atmosphere and Ocean Research Institute, The University of Tokyo), Ryu Uemura(Nagoya University), Kenji Kawamura(National Institute of Polar Research, Research Organization of Information and Systems)

[ACC26-P01] **A biomass burning record over the past 350 years in an ice core from Northwest Greenland**

*Kumiko Goto-Azuma[1,2], Yoshimi Ogawa-Tsukagawa[1], Yutaka Kondo[1], Remi Dallmayr[9], Jun ogata[1], Nobuhiro Moteki[3], Sho Ohata[4], Tatsuhiro Mori[5], Makoto Koike[3], Kaori Fukuda[1], Motohiro Hirabayashi[1], Sumito Matoba[6], Yuki Komuro[1], Akane Tsushima[7], Naoko Nagatsuka[1], Koji Fujita[4], Naga Oshima[8], Kyotaro Kitamura[1], Kenji Kawamura[1,2], Wataru Shigeyama[1,2], Hideaki Motoyama[1,2], Teruo Aoki[1,2] (1.National Institute of Polar Research, 2.SOKENDAI, 3.University of Tokyo, 4.Nagoya Univeristy, 5.Tokyo University of Science, 6.Hokkaido University, 7.Chiba University, 8.Meteorological Research Institute, 9.Alfred Wegner Institute for Polar and Marine Research)

[ACC26-P02] Seasonal changes in concentration, metal composition and size distribution of mineral particles in recent snow at EGRIP, Greenland

*Yuki Komuro[1], Fumio Nakazawa[1,2], Kumiko Goto-Azuma[1,2], Motohiro Hirabayashi[1], Wataru Shigeyama[1,2], Naoko Nagatsuka[1] (1.National Institute of Polar Research, 2.The Graduate University for Advanced Studies, SOKENDAI)

[ACC26-P03] Implementation of higher-order advection schemes in a numerical ice-sheet model for ice-core studies

*Fuyuki SAITO[1], Takashi Obase[2], Ayako Abe-Ouchi[2] (1.Japan Agency for Marine-Earth Science and Technology, 2.Atmosphere and Ocean Research Institute, The University of Tokyo)

[ACC26-P04] An ice-flow modeling study for evaluation of sites for an oldest ice core around Dome Fuji, Antarctica

*Takashi Obase[1], Ayako Abe-Ouchi[1,2], Fuyuki SAITO[3], Shun Tsutaki[2], Shuji Fujita[2,4], Kenji Kawamura[2,4] (1.Atmosphere and Ocean Research Institute, the University of Tokyo, 2.National Institute of Polar Research, Japan, 3.Japan Agency for Marine-Earth Science and Technology, 4.SOKENDAI, the Graduate University for Advanced Studies)

[ACC26-P05] The effect of ocean circulation on glacial-interglacial cycles

*Ryotaro Todoroki[1], Ayako Abe-Ouchi[1], Fuyuki SAITO[2], Takashi Obase[1], Wing-Le Chan[1], Sam Sherriff-Tadano[3], Yasuto Watanabe[4] (1.Atmosphere and Ocean Research Institute, The University of Tokyo, 2.Japan Agency for Marine-Earth Science and Technology (JAMSTEC), 3.The University of Leeds, 4.The University of Tokyo)

[ACC26-P06] **Transient simulations of the last deglaciation using MIROC AOGCM and time evolving ice-topography**

*Tristan Vadsaria[1], Takashi Obase[1], Ayako Abe-Ouchi[1], Sam Sherriff-Tadano [2,1], Wing-Le Chan[1] (1.Atmosphere and Ocean Research Institute, The University of Tokyo, Japan, 2.School of Earth and Environment, The University of Leeds, Leeds, UK)

[ACC26-P07] **Inactivating microorganisms in melted snow and ice samples using ultraviolet germicidal radiation**

*Fumio Nakazawa[1,2], Kumiko Goto-Azuma[1,2] (1.National Institute of Polar Research, 2.The Graduate University for Advanced Studies, SOKENDAI)

[ACC26-P08] The origin of moisture inferred from water stable-isotopes of an ice-core drilled in the Pamir-Alay Mountains in Central Asia

*Daiki Seto[1], Nozomu Takeuchi[1], Aizen Vladimir[2], Akane Tsushima[3], Kenji Kawamura[4], Koji Fujita[5] (1.CHIBA university, 2.University of Idaho, 3.Graduate School of science, Chiba university, 4.Graduate School of Environmental Studies, Nagoya University, 5.National Institute of Polar Research, Research Organization of Information and Systems)

[ACC26-P09] Analyses of pollen grains and insoluble particles in an ice core drilled in the Pamir-Arai Mountains in central Asia

*Nozomu Takeuchi[1], Haruka Ogaya[1], Koji Fujita[2], Kenji Kawamura[3], Akane Tsushima[1], Vladimir Aizen[4] (1.Chiba University, 2.Nagoya University, 3.National Institute of Polar Research, 4.University of Idaho)

[J] Poster | A (Atmospheric and Hydrospheric Sciences)：A-CG Complex & General

5:15 PM - 6:30 PM JST | 8:15 AM - 9:30 AM UTC | Ch.07_1

[A-CG40] Coastal Ecosystems - 1. Water Cycle and Land-Ocean Interactions

convener:Masahiko Fujii(Faculty of Environmental Earth Science), Ryo Sugimoto(Faculty of Marine Biosciences, Fukui Prefectural University), Makoto Yamada(Faculty of Economics, Ryukoku University)

[ACG40-P01] Spatial extent of groundwater-derived heat in coastal area of volcanic sandy beach

*Makoto Yamada[1], Ryo Sugimoto[2], Toshimi Nakajima[2] (1.Faculty of Economics, Ryukoku University, 2.Faculty of Marine Biosciences, Fukui Prefectural University)

[ACG40-P02] Effects of fresh groundwater springs on phytoplankton primary productivity in a volcanic sandy beach

Kana Harada[1], *Ryo Sugimoto[1], Toshimi Nakajima[1], Osamu Tominaga[1] (1.Faculty of Marine Biosciences, Fukui Prefectural University)

[ACG40-P03] Spatial variation of ^{222}Rn concentration in river water and groundwater in the coastal area of Tokyo Bay

*Hiroya Kondo[1], Yu Umezawa[1], Misaki Ikari[1], Yosuke ONO[1], Shigeyoshi Otosaka[2], Muneoki Yoh[1] (1.Tokyo University of Agriculture and Technology , 2.Tokyo University)

[J] Poster | A (Atmospheric and Hydrospheric Sciences)：A-CG Complex & General

5:15 PM - 6:30 PM JST | 8:15 AM - 9:30 AM UTC | Ch.07_2

[A-CG41] Coastal Ecosystems -2. Coral reefs, seagrass and macroalgal beds, and mangroves

convener:Yu Umezawa(Tokyo University of Agriculture and Technology), Toshihiro Miyajima(Marine Biogeochemistry Group, Division of Ocean-Earth System Science, Atmosphere and Ocean Research Institute, The University of Tokyo), Atsushi Watanabe(The ocean policy research institute, The Sasakawa peace foundation), Tomihiko Higuchi(Atmosphere and Ocean Research Institute, The University of Tokyo)

[ACG41-P01] **Skeleton microstructures and *in situ* colony morphometry analysis of the corals collected during Tara Pacific Expedition**

*Guinther Hiromu Mitushasi[1], Yuko Kitano[2], Emilie Boissin[3], Serge Planes[3], Denis Allemand[4], Tara Pacific Consortium[1], Sylvain Agostini[1] (1.Shimoda Marine Research Center, University of Tsukuba, 2. National Institute of Environmental Science, Japan (Tsukuba), 3. CRIOBE, Universite de Perpignan (Perpignan), 4. Monaco Scientific Center (Monaco))

[ACG41-P02] Diversity of coral distributions and the difference in Sakiyamawan-Amitoriwan nature conservation area, Iriomote Island, Japan

*Shinya Shimokawa[1], Tomokazu Murakami[1], Hiroyoshi Kohno[2], Akira Mizutani[2] (1.National Research Institute for Earth Science and Disaster Resilience, 2.Okinawa Reagional Research Center, Tokai University)

[ACG41-P03] Characteristics of water temperature changes and coral breaching in Amitori Bay, Iriomote Island, Japan

*Shinya Shimokawa[1], Tomokazu Murakami[1], Hiroyoshi Kohno[2], Akira Mizutai[2] (1.National Research Institute for Earth Science and Disaster Prevention, 2.Okinawa Reagional Research Center, Tokai University)

[ACG41-P04] Coral bleaching countermeasures by supplying metal-containing feed ~evaluation the effect at gene expression levels~

*Ikuko Yuyama[1], Naoko Yasuda[2], Sayaka Higa[2], Sung-Yin Yang[3], Sylvain Agostini [3], Tomihiko Higuchi[4], Toshihiro Miyajima[4], Takashi Nakamura[5], Hiroyuki Fujimura[2] (1.Yamaguchi University, 2.University of the Ryukyus, 3.University of Tsukuba, 4.The University of Tokyo , 5.Tokyo Institute of Technology)

[ACG41-P05] Linear and non-linear analysis for high temperature and acidification event in the Great Barrier Reef based on the observation in the Coral Sea

*Tatsuki Tokoro[1,2], Shin-ichiro Nakaoka[1], Shintaro Takao[1] (1.National Institute for Environmental Studies, 2.Port and Airport Research Institute)

[ACG41-P06] Stratigraphy of seagrass bed at Bise in Okinawa Island.

*Wataru Sano[1], Kazuhiko Fujita[2], Yoshikatsu Nakano[3], Shoko Hirabayashi[4], Yusuke Yokoyama[5], Yosuke Miyairi[5], Naoko Isomura[6], Hironobu Kan[1] (1.Kyushu Univ., 2.Univ. of the Ryukyus, 3.Okinawa Institute of Science and Technology Graduate University , 4.Rissho Univ., 5.Univ. of Tokyo, 6.National Institute of Technology, Okinawa College)

[ACG41-P07] **Applying DPSIR framework for blue carbon ecosystems assessment: The case of Busuanga Island, Palawan, Philippines**

*Jay Mar Dioquito Quevedo[1], Yuta Uchiyama[2], Ryo Kohsaka[2] (1.Tohoku University, 2.Nagoya University)

[ACG41-P08] Detecting mangrove- and seagrass-derived eDNA from deep-sea sediment around Yaeyama Islands: Implication for offshore blue carbon sequestration

*Toshihiro Miyajima[1], Masami Hamaguchi[2], Takashi Nakamura[3], Hajime Katayama[4], Masakazu Hori[5] (1.Marine Biogeochemistry Group, Division of Ocean-Earth System Science, Atmosphere and Ocean Research Institute, The University of Tokyo, 2.National Research Institute of Fisheries Technology, Japan Fisheries Research and Education Agency, 3.School of Environment and Society, Tokyo Institute of Technology, 4.Geological Survey of Japan, National Institute of Advanced Industrial Science and Technology, 5.National Research Institute of Fisheries Resources, Japan Fisheries Research and Education Agency)

[ACG41-P09] Evaluation of the effect of differences in nitrogen loading on the chemical composition and decomposition characteristics of eelgrass(*Zostera marina*).

*Toru Miyata[1], Yu Umezawa[1], Takunari Ida[1], Yoshiki Horikawa[1], Makoto Watanabe[1], Shigeki Wada[2], Masahiro Nakaoka[3], Tomohiro Kuwae[4] (1.Tokyo University of Agriculture and Technology, 2.University of Tsukuba, 3.Hokkaido University, 4.Port and Airport Research Institute)

[J] Poster | A (Atmospheric and Hydrospheric Sciences)：A-CG Complex & General

5:15 PM - 6:30 PM JST | 8:15 AM - 9:30 AM UTC | Ch.07_3

[A-CG42] Water and sediment dynamics from land to coastal zones

convener:Shinichiro Kida(Research Institute for Applied Mechanics, Kyushu University), Yuko Asano(The University of Tokyo), Keiko Udo(International Research Institute of Disaster Science, Tohoku University), Dai Yamazaki(Institute of Industrial Sciences, The University of Tokyo)

[ACG42-P01] Representing terrestrial water dynamics within Earth system modelling framework

*Dai Yamazaki[1] (1.Institute of Industrial Sciences, The University of Tokyo)

[ACG42-P02] Breaching flood impact analysis of landslide dams in the Yarlung Tsangpo River Basin

*Danyi Shen[1,2], Zhenming Shi[1,2], Ming Peng[1,2] (1.Key Laboratory of Geotechnical & Underground Engineering of Ministry of Education, Tongji University, Shanghai 200092, China, 2.Department of Geotechnical Engineering, Tongji University, Shanghai 200092, China)

[ACG42-P03] Sediment transport analysis from the Abukuma river to the sea by typhoon No.19 in 2019

Makoto Kobayashi[1], *Daisuke Nakahara[1], Keiko Udo[1], Hiroshi Takebayashi[2] (1.International Research Institute of Disaster Science, Tohoku University, 2.Disaster Prevention Research Institute, Kyoto University)

[ACG42-P04] Structural characteristics of airflow and blown sand flux over fine-grained gravel surfaces in wind tunnel

*Jiaqi Liu[1], Reiji Kimura[1], Jing Wu[1] (1.Arid Land Research Center, Tottori University)

[ACG42-P05] Predictive simulations of redeposition and seawater transportation after a tsunami in Osaka Bay where bottom sediments were disturbed by tsunami

*Mitsuru Hayashi[1,2], Satoshi Nakada[4], Soichi Hirokawa[2], Shuto Fujisawa[3] (1.Research Center for Inland Seas, Kobe University, 2.Graduate School of Maritime Sciences, 3.Faculty of Maritime Sciences, 4. National Institute for Environmental Studies)

[ACG42-P06] Application of an isopycnal-layered model to islands

*Hiroaki Sato[1], Yosuke Alexandre Yamashiki[2] (1.Kyoto University, 2.Graduate School of Advanced Integrated Studies in Human Survivability Kyoto University)

[J] Poster | A (Atmospheric and Hydrospheric Sciences)：A-CG Complex & General

5:15 PM - 6:30 PM JST | 8:15 AM - 9:30 AM UTC | Ch.03_4

[A-CG43] Earth & Environmental Sciences and Artificial Intelligence/Machine Learning

convener:Tomohiko Tomita(Faculty of Advanced Science and Technology, Kumamoto University), Shigeki Hosoda(Japan Marine-Earth Science and Technology), Ken-ichi Fukui(Osaka University), Satoshi Ono(Kagoshima Univeristy)

[ACG43-P01] **Machine learning for remote sounding of the ionosphere in Taiwan**

*ALEXEI DMITRIEV[1] (1.National Central University, Jungli City, Taiwan)

[ACG43-P02] Precipitation predictions using RNN and LSTM with simple time series observations and the comparison between them.

*He Zhang[1], Tomohiko Tomita[2], Ken-ichi Fukui[3], Satoshi Ono[4] (1.Kumamoto University, 2.Faculty of Advanced Science and Technology, 3.The Institute of Scientific and Industrial Research, Osaka University, 4.Faculty of Engineering, Kagoshima University)

[ACG43-P03] Hindcast of the July 2018 torrential rainfall event in Kagoshima City using LSTM

*Genki Shirasawa[1], Ryusei Hamasaki[1], Shinichiro Kako[2], Hirohiko Nakamura[3] (1.Kagoshima University, Faculty of Engineering, 2.Graduate School of Science and Engineering, Kagoshima University, 3.Kagoshima University, Faculty of Fisheries)

[ACG43-P04] Real-time Data Quality Control of Phased Array Weather Radar by using Semantic Segmentation

*Isoda Fusako[1], Shinsuke Satoh[1], Masashi Kimura[2], Takemasa Miyoshi[3] (1.National Institute of Information and Communications Technology, 2.Convergence Lab., 3.RIKEN)

[ACG43-P05] A Preliminary Study on Developing a Smartphone Application for Weather Classification Using AutoML

*Satoshi Ono[1], Kento Wakamatsu[1], Yusaku Hayashi[1], Tomohiko Tomita[2] (1.Kagoshima Univeristy, 2.Kumamoto University)

[ACG43-P06] Fundamental Study on Weather Judgement of Image Data using Machine Learning Classification

*Tomohiko Tomita[1], Kosuke Tanaka[2] (1.Faculty of Advanced Science and Technology, Kumamoto University, 2.Faculty of Science, Kumamoto University)

[J] Poster | A (Atmospheric and Hydrospheric Sciences)：A-CG Complex & General

5:15 PM - 6:30 PM JST | 8:15 AM - 9:30 AM UTC | Ch.07_4

[A-CG44] Biogeochemical linkages between the surface ocean and atmosphere

convener:Sohiko Kameyama(Hokkaido University), Yoko Iwamoto(Graduate School of Integrated Sciences for Life, Hiroshima University), Noguchi Maki Aita(Japan Agency for Marine-Earth Science and Technology), Daisuke Sasano(Japan Meteorological Agency)

[ACG44-P01] Relationship between the variability in dissolved inorganic carbon in surface seawater and the formation volume of subtropical mode water along the 137°E line

*Ono Hisashi[1], Masao Ishii[1], Yosuke Iida[2], Kazutaka Enyo[2], Daisuke Sasano[2] (1.Meteorological Research Institute, 2.Japan Meteorological Agency)

[ACG44-P02] Verification of the effect of aerosol deposition on surface chlorophyll in subtropical oligotrophic waters using JRAero reanalysis datasets

*Naohiro Kosugi[1], Taichu Y Tanaka[1] (1.Meteorological Research Institute)

[ACG44-P03] Seasonal Variation of Phosphate in Atmospheric Aerosols in Higashi-Hiroshima

*Yoko Iwamoto[1], Mako Hirota[2], Kazuhiko Takeda[1], Hiroshi Sakugawa[1] (1.Graduate School of Integrated Sciences for Life, Hiroshima University, 2.School of Integrated Arts and Sciences, Hiroshima University)

[ACG44-P04] Modelling regional and global scale impacts of atmospheric nitrogen inputs on marine biogeochemistry

*Maki Noguchi Aita[1], Fumikazu Taketani[1], Yoko Iwamoto[2], Tomohiro Hajima[3] (1.Earth Surface System Research Center, Japan Agency for Marine-Earth Science and Technology, 2.Hiroshima University, 3.Research Center for Environmental Modeling and Application, Japan Agency for Marine-Earth Science and Technology)

[ACG44-P05] Contribution of lightning-induced nitgen oxide to nitrogen cycle in air-sea boundary estimated by plasma discharge in laboratory

Ryo Hashimoto[1], *Sohiko Kameyama[1], Kohki Satoh[2], Hiroshi Ogawa[3] (1.Hokkaido University, 2.Muroran Institute of Technology, 3.The University of Tokyo)

[J] Poster | H (Human Geosciences)：H-RE Resource and Engineering Geology

5:15 PM - 6:30 PM JST | 8:15 AM - 9:30 AM UTC | Ch.08_1

[H-RE12] Resource Geology

convener:Tsubasa Otake(Division of Sustainable Resources Engineering, Faculty of Engineering, Hokkaido University), Kenzo Sanematsu(Mineral Resource Research Group, Institute for Geo-Resources and Environment, Geological Survey of Japan, National Institute of Advanced Industrial Science and Technology), Ryohei Takahashi(Graduate School of International Resource Sciences, Akita University), Tatsuo Nozaki(Submarine Resources Research Center, Research Institute for Marine Resources Utilization, Japan Agency for Marine-Earth Science and Technology)

[HRE12-P01] Exploration of multiple geothermal resources in southern Yuzawa area, Akita prefecture

*Hayata Sato[1], Keishi Nunohara[1], Ryoichi Yamada[1], Nobuo Hirano[1], Noriyoshi Tsuchiya[1] (1.tohoku university)

[HRE12-P02] The Gold and Silver mineralization of layered yellow ore in Furutobe mine.

*Teruhiro Suzuki[1], Yasushi Watanabe[1], Takuya Echigo[1] (1.Graduate School of International Resource Sciences, Akita University)

[HRE12-P03] The significance of geology and sulfur isotope compositions of sulfates and sulfides at the ca.3.4 Ga Big Stubby Kuroko deposit in Pilbara, Western Australia

*Tomoaki Koya[1], Akizumi Ishida[1], Takeshi Kakegawa[1] (1.Graduate school of science, Tohoku University)

[J] Poster | H (Human Geosciences)：H-TT Technology & Techniques

5:15 PM - 6:30 PM JST | 8:15 AM - 9:30 AM UTC | Ch.08_2

[H-TT16] Development and application of environmental traceability methods

convener:Ichiro Tayasu(Research Institute for Humanity and Nature), Ki-Cheol Shin(Research Institute for Humanity and Nature), Nozomu Takeuchi(Chiba University)

[HTT16-P01] Oxygen and hydrogen isotopic signatures of surface and groundwater during a dry season in the Tonle Sap Lake basin

*Yumi Yoshioka[1], Takao Masumoto[2], Kumiko Tsujimoto[3], Yuji Ito[4] (1.Shimane University, 2.Akita Prefectural University, 3.Okayama Univerisity, 4.Kagoshima University)

[HTT16-P02] Identification of regional characteristics of the basin using elemental components as tracers

*Yusuke Hataya[1], Shiho Yabusaki[2], Seiki Kawagoe[3] (1.Fukushima University Faculty of Symbiotic Systems Science, 2.Research Institute for Humanity and Nature, 3.Fukushima University Faculty of Symbiotic Systems Sciences)

[HTT16-P03] Seasonal variation of $\delta^{34}S$ and $\delta^{18}O$ in sulfate in rain water and aerosols on the outskirts of Gifu City

*Masako Kagawa[1], Nagayoshi Katsuta[1], Yusuke Hashimoto[1], Yuto Yamagishi[1], Ichiro Tayasu[2], Chikage Yoshimizu[2] (1.Gifu University, Faculty of Education, 2.Research Institute for Humanity and Nature)

[HTT16-P04] Seasonal variations and trends of dissolved elements in rainwater and stream water in forest catchment area of central Japan

*Masayuki Morohashi[1], Hiroki Yotsuyanagi[1], Masaaki Takahashi[2], Tatsuyoshi Saito[2], Yayoi Inomata[3], Ki-Cheol Shin[4], Ichiro Tayasu[4], Tsuyoshi Ohizumi[1], Hiroyuki Sase[1] (1.Asia Center for Air Pollution Research, 2.Niigata Prefecture, 3.Kanazawa Univercity, 4.Research Institute for Humanity and Nature)

[HTT16-P05] Geochemical and isotopic study of river water from the Okayama and Tottori Prefectures, Japan.

*Katsuyuki Yamashita[1], Takahiro Kamei[1], Keisuke Kishimoto[1], Masahiko Mori[1], Yuga Kishimoto[2], Aya Ooi[2], Ayaka Onishi[2], Yoko Kurihara[2], Miyake Ryota[2], Ryosuke Yamano[2], Hitoshi Chiba[1], Takanori Nakano[3], Ki-Cheol Shin[4] (1.Graduate School of Natural Science and Technology, Okayama University, 2.Department of Earth Sciences, Okayama University, 3.Ono City, 4.Research Institute for Humanity and Nature)

[HTT16-P06] Stable sulfur isotope variations in lacustrine sediments in Mongolia and its paleo-environmental implication

Miku Yoichi[1], *Nagayoshi Katsuta[1], Shinya Ochiai[2], Sayuri Naito[1], Masako Kagawa[1], Yuma Masuki[1], Ichiro Tayasu[3] (1.Faculty of Education, Gifu University, 2.Institute of Nature and Environmental Technology, Kanazawa University, 3. Research Institute for Humanity and Nature)

[HTT16-P07] Variations in sedimentation rates of Tsuya River in the western Nobi Plain, central Japan over the last decades

*Takashi Tashiro[1], Ichiro Tayasu[2] (1.Nagoya University, 2.Research Institute for Huminity and Nature)

[HTT16-P08] Neutralization using recycled waste materials for acid wastewater from the Kusatsu hot spring area in Japan

*Takeshi Saito[1], Naoki Watanabe[2] (1.Graduate School of Science and Engineering, Saitama University, 2.Research Institute for Natural Hazards and Disaster Recovery, Niigata University)

[HTT16-P09] Evaluating temperature dependence of arsenic and boron adsorption onto sediments

*Keigo Kurita[1], Takeshi Saito[2] (1.Department of Civil and Environmental Engineering, Faculty of Engineering, Saitama University, 2.Graduate School of Science and Engineering, Saitama University)

[HTT16-P10] Soil food webs after more than a year since litter-removal experiment: an evaluation based on carbon and nitrogen stable isotope ratios

*Takashi F Haraguchi[1], Soshi Yoshida[2], Syuhei Fujimoto[2], Keiichiro Sato[2], Motohiro Hasegawa[2] (1.Biodiversity Research Center, RIEAF, Osaka, 2.Doshisha University Faculty of Science and Engineering, Environmental Systems Science)

[HTT16-P11] Evaluation of air pollution stress in roadside trees using stable carbon isotope ratio

*Yuko T. Hanba[1], Mayu Matsumoto[1], Takashi Kiyomizu[1], Tomomitsu Kinoshita[1], Atsushi Kume[2] (1.Kyoto Institute of Technology, 2.Kyushu University)

[HTT16-P12] **Effects of Traffic Volume on Photosynthetic Function and Water Use Efficiency of Tall Street Trees in Kyoto City**

*Takumi Matsuura[1], Yuko T. Hanba[1] (1.Kyoto Institute of Technology)

[HTT16-P13] Effect of flooding stress on photosynthesis of aquatic plants

*Yutaro Yasui[1], Yuko T. Hanba[1] (1.Kyoto Institute of Technology)

[HTT16-P14] The incubation method using ^{18}O-water and phosphate oxygen isotope for quantitative evaluation of bioavailable phosphate in soil.

*Takuya Ishida[1] (1.Hiroshima University)

[HTT16-P15] Trace element quantification in organic materials by low temperature plasma ashing

Taisuke Hino[1], Yuriko Umeda[1], Hibiki Shishime[1], Akane Ito[1], *Masaharu Tanimizu[1] (1.Kwansei Gakuin University)

[HTT16-P16] Metal element isotope analysis for Environmental Reference Materials

*Ki-Cheol Shin[1] (1.Research Institute for Humanity and Nature)

[J] Poster | H (Human Geosciences)：H-TT Technology & Techniques

5:15 PM - 6:30 PM JST | 8:15 AM - 9:30 AM UTC | Ch.08_3

[H-TT17] New Developments in Shallow Geophysics

convener:Kyosuke Onishi(Public Works Research Institute), Kunio Aoike(Oyo corporation), Tishiyuki Yokota(National Institute of Advanced Industrial Science and Technology), Toru Takahashi(Fukada Geological Institute)

[HTT17-P01] **An Atempt to Estimate the Water Level Change of Non-confined Groundwater by Earthing Resistance (III) - Characteristics of the Anniversary Changes -**

*Kunihiro Ryoki[1] (1.Polytechnic University)

[HTT17-P02] Estimation of underground structure beneath the debris control dams constructed during the Edo era based on the microtremor measurements

*Atsushi Mukai[1] (1.Faculty of Urban Management, Fukuyama City University)

[HTT17-P03] Measuring the distribution of surface thickness of pavement using ground-penetrating radar

*Kyosuke Onishi[1], Kobayashi Takayuki[1] (1.Public Works Research Institute)

[J] Poster | H (Human Geosciences)：H-CG Complex & General

5:15 PM - 6:30 PM JST | 8:15 AM - 9:30 AM UTC | Ch.09_3

[H-CG28] Earth surface processes related to deposition, erosion and sediment transport

convener:Koji Seike(Geological Survey of Japan, AIST), Masayuki Ikeda(University of Tokyo), Hajime Naruse(Department of Geology and Mineralogy, Graduate School of Science, Kyoto University), Hideko Takayanagi(Institute of Geology and Paleontology, Graduate School of Science, Tohoku University)

[HCG28-P01] Preliminary study on the relationships between landform of coastal to alluvial plain and sediments supply from watershed

*Taku Komatsubara[1] (1.Institute of Geology and Geoinformation, Advanced Industrial Science and Technology)

[HCG28-P02] Relationship between magnetic anisotropy and hydraulic conditions in modern flood deposits

*Ryo Tateishi[1], Ichiro Kimura[1], Naoto Ishikawa[1] (1.University of Toyama)

[HCG28-P03] Flume experiment on crevasse-splay deposits formed by the 2019 flooding of the Chikuma River

*Taichi Kato[1], Masaki Yamada[1], Hajime Naruse[2], Sakai Yuichi[2] (1.Department of Geology, Faculty of Science, Shinshu University, 2.Graduate school of Science, Kyoto University)

[HCG28-P04] Sedimentary environments and fluctuations in lake levels as recorded in the latest Pleistocene and Holocene core from the Suwa Basin, central Japan

*Nozomi Hatano[1], Ritsuho Kawano[2], Kohki Yoshida[2] (1.Natural Environment Division, Nagano Environmental Conservation Research Institute, 2.Department of Geology, Faculty of Science, Shinshu University)

[HCG28-P05] Microcodization in a Kasimovian section of the Omi Limestone (Niigata Prefecture, central Japan), the Upper Carboniferous

*Yoshihiro Kakizaki[1], Yasuhiro Ota[2], Kenji Kashiwagi[3], Akihiro Kano[1] (1.Department of Earth and Planetary Science, Graduate School of Science, The University of Tokyo, 2.Kitakyushu Museum of Natural History & Human History, 3. Graduate School of Science and Engineering for Research, University of Toyama)

[HCG28-P06] Coastal transport process of pebble along the Seisho Coast, Kanagawa Prefecture, estimated from changes in lithological composition and form of pebble particles

*Masaaki Shirai[1], Tomomi Akiyama[1], Kiyokazu Kawajiri[2], Takako UTSUGAWA[3], Takayuki Takahashi[4] (1.Tokyo Metropolitan University, 2.Sagamihara Cuty Museum, 3.Rissho University, 4.Tohoku University)

[HCG28-P07] A consideration of the age of the higher terraces in the southeastern part of the Kashiwazaki plain, Niigata Prefecture, central Japan.

*Satoshi Kaneko[1], Toshimichi Kaneto[1], Akiko Miyawaki[2], Akira Fukuchi[2], Mitsugu Momose[2] (1.Tokyo Electric Power Company Holdings, Inc., 2.Hanshin Consultants Co., Ltd.)

[HCG28-P08] Linear stability analysis of plane beds with active suspended load

Koji Ohata[1], *Hajime Naruse[1], Norihiro Izumi[2] (1.Department of Geology and Mineralogy, Graduate School of Science, Kyoto University, 2.Graduate School of Engineering)

[J] Poster | S (Solid Earth Sciences)：S-SS Seismology

5:15 PM - 6:30 PM JST | 8:15 AM - 9:30 AM UTC | Ch.10_1

[S-SS05] Crustal Deformation

convener:Masayuki Kano(Graduate school of science, Tohoku University), Tadafumi Ochi(Institute of Earthquake and Volcano Geology, Geological Survey of Japan, The National Institute of Advanced Industrial Science and Technology), Fumiaki Tomita(Japan Agency for Marine-Earth Science and Technology)

[SSS05-P01] Estimation of Afterslip Distribution and Viscoelastic Deformation by MCMC Method

*Ryoji Kawabata[1], Hiroshi Munekane[1] (1.GSI of Japan)

[SSS05-P02] Application of a slow slip objective detection method to GNSS 6-hour coordinates

*Akio Kobayashi[1] (1.Meteorological Research Institute, Japan Meteorological Agency)

[SSS05-P03] Long-term SSE along the Nankai trough detected by Geonet

*Shinzaburo Ozawa[1], Ryoji Kawabata[1], Hiroshi Munekane[1] (1.Geographical Survey Institute of Japan)

[SSS05-P04] Estimation of strain-rate field in the Japanese Islands using optimized distance-decaying constants

*Issei Kosugi[1], Yuta Mitsui[2] (1.Graduate School Of Science and Technology, Shizuoka University , 2.Faculty of Science, Shizuoka University)

[SSS05-P05] **Evaluation of inland seismic potential in southwest Japan using GNSS data and seismic catalog**

*Hiroki Sato[1], Takeo Ito[1] (1.Graduate School of Environmental Studies, Nagoya University)

[SSS05-P06] Re-evaluation of earthquake swarm activity in the offshore region to the northeast of Izu Peninsula focusing on crustal deformation for several months (1990-2011)

Keisuke Takeshita[1], *Kazuhiro Kimura[1], Takeshi Kimura[2] (1.Meteorological College, 2.National Research Institute for Earth Science and Disaster Resilience)

[SSS05-P07] Evaluation earthquake potential using a kinematic block motion model in Indonesia based on GNSS Observation

*Rio Raharja[1], Takeo Ito[1], Hiroshi Kimura[1], Irwan Meilano[2] (1.Graduate School of Environmental Studies, Nagoya University, Japan, 2.Faculty of Earth Sciences and Technology, Bandung Institute of Technology, Indonesia)

[SSS05-P08] **A recent example of active intraplate deformation in the Central Anatolia: Obruk-Bor (Nigde) earthquakes, Turkey**

*Dogan Kalafat[1] (1.Bogazici University Kandilli Observatory and Earthquake Research Institute Cengelkoy, Istanbul Turkey)

[SSS05-P09] Modification of computer program GOTIC2 for calculation of the ocean tidal loading effect - Application of Green's function to calculate theoretical strain at depth of borehole observation near coasts -

Osamu Kamigaichi[1,2], *Norio Matsumoto[2], Fuyuki Hirose[3] (1.Japan Meteorological Business Support Center, 2.Geological Survey of Japan, National Institute of Advanced Industrial Science and Technology (AIST), 3.Seismology and Tsunami Research Department, Meteorological Research Institute)

[SSS05-P10] Crustal deformation observed with Tenryu-Funagira laser strainmeter

*Takahiro Tsuyuki[1] (1.Meteorological Research Institute)

[SSS05-P11] Crustal movements due to the seismic motions observed in Kobe

*Atsushi Mukai[1] (1.Faculty of Urban Management, Fukuyama City University)

[J] Poster | S (Solid Earth Sciences)：S-SS Seismology

5:15 PM - 6:30 PM JST | 8:15 AM - 9:30 AM UTC | Ch.10_2

[S-SS06] Statistical seismology and underlying physical processes

convener:Yasuhiro Yoshida(Meteorological Research Institute, Japan Meteorological Agency)

[SSS06-P01] Accuracy improvement of DONET seismometer orientations estimated from seismic waveforms

*Shuichiro Yada[1], Takehiro Nishiyama[1], Keisuke Ariyoshi[1], Yojiro Yamamoto[1], Masaru Nakano[1], Kentaro Sueki[1], Takane Hori[1], Narumi Takahashi[2,1] (1.Japan Agency for Marine-Earth Science and Technology, 2.National Research Institute for Earth Science and Disaster Resilience)

[SSS06-P02] A preliminary study on data quality characterization for the DONET seismic catalogue

*Kazuyoshi Nanjo[1,2,3], Keisuke Ariyoshi[4], Narumi Takahashi[4,5], Shuichiro Yada[4], Yojiro Yamamoto[4], Takane Hori[4] (1.University of Shizuoka, 2.Shizuoka University, 3.Institute of Statistical Mathematics, 4.Japan Agency for Marine-Earth Science and Technology, 5.National Research Institute for Earth Science and Disaster Resilience)

[SSS06-P03] Aftershock activity of the 2015 M7.1 earthquake and back-arc rifting in the northern Okinawa Trough

*Hirotsugu Yanagida[1], Yukihiro Nakatani[2], Hiroshi Yakiwara[2], Shuichiro Hirano[1], Reiji Kobayashi[1], Yusuke Yamashita[3], Takeshi Matsushima[4], Hiroshi Shimizu[4], Kodo Umakoshi[5], Masanao Shinohara[6] (1.Graduate School of Science and Engineering, Kagoshima University, 2.Nansei-Toko Observatory for Earthquakes and Volcanoes, Kagoshima University, 3.Disaster Prevention Research Institute, Kyoto University, 4.Institute of Seismology and Volcanology, Faculty of Science, Kyushu University, 5.Graduate School of Fisheries and Environmental Sciences, Nagasaki University, 6.Earthquake Research Institute, the University of Tokyo)

[SSS06-P04] Microseismic Monitoring and Stress Inversion: before the 2018 Mw 6.4 Hualien earthquake and 2019 M_L 6.0 Ilan earthquake

*Wei-Jhe Wu[1], Chein-Min Su[1], Strong Wen[1], Yi-Heng Li[2], Chun-Rong Chen[2], Chau-Huei Chen[1] (1.National Chung Cheng University, 2.Industrial Technology Research Institute)

[SSS06-P05] Aftershock activity and its duration following inland earthquakes in Japan

*Taichi Honda[1], Takuji Yamada[2] (1.Ibaraki University, 2.Faculty of Science, Graduate School of Science and Technology, Ibaraki University)

[SSS06-P06] Whether the change in shear strain energy causes change in *b* value? Case study for the 2016 Kumamoto Earthquakes and the interplate coupling along the Nankai Trough

*Kohei Nagata[1], Akemi Noda[1], Koji Tamaribuchi[1], Fuyuki Hirose[1] (1.Meteorological Research Institute)

[SSS06-P07] Inter-plate aseismic slip determined from teleseismic similar earthquakes recorded by the Japanese seismic network

*Toshihiro Igarashi[1], Aitaro Kato[1] (1.Earthquake Research Institute, University of Tokyo)

[SSS06-P08] Seasonal variations in crustal seismicity and surface load

*Taku Ueda[1], Aitaro Kato[1] (1.Earthquake Research Institute, the University of Tokyo)

[J] Poster | S (Solid Earth Sciences)：S-SS Seismology

5:15 PM - 6:30 PM JST | 8:15 AM - 9:30 AM UTC | Ch.11_1

[S-SS07] Crustal Structure

convener:Mikiya Yamashita(National Institute of Advanced Industrial Science and Technology)

[SSS07-P01] Local variations of seismic scattering-attenuation structure around the volcanic front in Hokkaido

*Kiyoshi Yomogida[1], Hidekatsu Masuda[2], Takahiro Shiina[3], Kei Katsumata[4] (1.Department of Earth and Planetary Dynamics, Graduate School of Science, Hokkaido University, 2.Earth and Planetary Dynamics, Faculty of Natural History Sciences, Graduate School of Science, Hokkaido University, 3.National Institute of Advanced Industrial Science and Technology, 4.Institute of Seismology and Volcanology, Hokkaido University)

[SSS07-P02] Study of the delamination structure at the southern end of the Hidaka collision zone- Examination using numerical calculation-

*Masahiro Shimazaki[1], Noriko Tsumura[2] (1.Graduate School of Science and Engineering, Chiba University, 2.Graduate School of Science, Chiba University)

[SSS07-P03] Three-dimensional resistivity modeling in the eastern Iburi district, Hokkaido

*Ryo Ito[1], Takeshi Hashimoto[1], Tomohiro Inoue[1], Makoto Uyeshima[2], Hiroshi Ichihara[3], Yusuke Yamaya[4] (1.Graduate School of Science, Hokkaido University, 2.Earthquake Research Institute, The University of Tokyo, 3.Graduate school of environmental studies, Nagoya University, 4.National Institute of Advanced Industrial Science and Technology)

[SSS07-P04] Measurement of seismic velocity anisotropy in the Tohoku region, NE Japan by shear wave splitting analysis (3)

*Tatsuya Mizuta[1], Tomomi Okada[1], Martha Savage[2], Ryota Takagi[1], Keisuke Yoshida[1], Shin'ichi Sakai[3], Mako Ohzono[3,9], Masahiro Kosuga[4], Yoshiko Yamanaka[5], Hiroshi Katao[6], Takeshi Matsushima[7], Hiroshi Yakiwara[8], Takashi NAKAYAMA[1], Satoshi Hirahara[1], Toshio Kono[1], Toru Matsuzawa[1], _ Group for the aftershock observations of the 2011 off the Pacific coast of Tohoku Earthquake (1.Tohoku Univ., 2.Victoria University of Wellington, 3.Tokyo Univ., 4.Hirosaki Univ., 5.Nagoya Univ., 6.kyoto univ., 7.kyushu Univ., 8.Kagoshima Univ., 9.Hokkaido Univ.)

[SSS07-P05] Velocity structure of the uppermost mantle beneath central Japan

*Akio Katsumata[1] (1.Faculty of Sustainable Design, University of Toyama)

[SSS07-P06] Seismological structure revealed by regional deep-event records beneath the Kii peninsula

*Yasunori Sawaki[1], Takuo Shibutani[2], Yihuan Ruan[1], Yoshihiro Ito[2] (1.Graduate School of Science, Kyoto University , 2.Disaster Prevention Research Institute, Kyoto University)

[SSS07-P07] Deep crustal seismicity in Hiroshima Prefecture

*Azusa Shito[1] (1.Okayama University of Science)

[SSS07-P08] Seismic imaging of the subducting Kyushu-Palau ridge in relation to the distribution of tectonic tremors

*Yanxue Ma[1], Kimihiro Mochizuki[1], Rie Nakata[1], Seiichi Miura[2], Yasuyuki Nakamura[2], Ryuta Arai[2], Gou Fujie[2], Yuka Kaiho[2], Shuichi Kodaira[2] (1.Earthquake Research Institute, University of Tokyo, 2.Japan Agency for Marine-Earth Science and Technology)

[SSS07-P09] Analysis of JAMSTEC Seismic Survey Database site

*Yuka Kaiho[1], Seiichi Miura[1], Ayako Nakanishi[1], Tetsuo No[1], Kaoru Takizawa[1], Yasuyuki Nakamura[1], Gou Fujie[1], Koichiro Obana[1], Shuichi Kodaira[1] (1.Japan Agency for Marine-Earth Science and Technology)

[J] Poster | S (Solid Earth Sciences)：S-EM Earth's Electromagnetism

5:15 PM - 6:30 PM JST | 8:15 AM - 9:30 AM UTC | Ch.11_3

[S-EM14] Electromagnetic Induction in the Earth and Planetary Interiors, and Tectono-Electromagnetism

convener:Maki Hata(Earthquake Research Institute, the University of Tokyo), Mitsuru Utsugi(Aso Volcanological Laboratory, Institute for Geothermal Sciences, Graduate School of Science, Kyoto University)

[SEM14-P01] A research report on the fundamental investigations of an electrical resistivity structure beneath Chugoku and Shikoku regions, southwestern Japan(2020)

*Ichiro Shiozaki[1], Tomofumi Uto[1], Makoto Uyeshima[2], Hideki Murakami[3], Naoto Oshiman[4], Yoshihisa Iio[4] (1.Graduate School of Engineering, Tottori University, 2.Earthquake Research Institute, The University of Tokyo, 3.Research and Education Faculty, Kochi University, 4.Disaster Prevention Research Institute, Kyoto University)

[SEM14-P02] 1-D forward calculation of tidally-induced magnetic variation in the Lau Basin: Comparison of calculation and seafloor magnetic data and sensitivity analysis

*Nakaya Tokuma[1], Takuto Minami[1], Nobukazu Seama[1] (1.Kobe University)

[SEM14-P03] Detection of magnetic field variation induced by tsunami

*Ai Kataoka[1], Ikuko Fujii[1] (1.Japan Meteorological Agency)

[SEM14-P04] Repeated aeromagnetic survey of Tarumae volcano using an unmanned autonomous helicopter

*Keiichi Shibuya[1], Takeshi Hashimoto[2], Tomoya Hayakawa[3], Keitaro Yoshikawa[4] (1.Graduate School of Science, Hokkaido University, 2.Faculty of Science, Hokkaido University, 3.Nippon Koei Co., Ltd., 4.Hokkaido Regional Development Bureau)

[SEM14-P05] A magnetic inversion method to recover the subsurface block structures based on L1-TV1 regularization

*Mitsuru Utsugi[1] (1.Aso Volcanological Laboratory, Institute for Geothermal Sciences, Graduate School of Science, Kyoto University)

[J] Poster | S (Solid Earth Sciences)：S-IT Science of the Earth's Interior & Techtonophysics

5:15 PM - 6:30 PM JST | 8:15 AM - 9:30 AM UTC | Ch.12_2

[S-IT21] Innovation through the Integration of Solid Earth Science and Materials Science

convener:Kenji Kawai(Department of Earth and Planetary Science, School of Science, University of Tokyo), Jun Tsuchiya(Geodynamics Research Center, Ehime University), Ryuichi Nomura(Kyoto University), Satoshi Ohmura(Hiroshima Institute of Technology)

[SIT21-P01] Theoretical approach to the pattern formation in spin systems via the time-dependent Ginzburg-Landau equation

*Ryoji Anzaki[1], Shin-ichi Ito[1,2], Hiromichi Nagao[1,2], Masaichiro Mizumaki[3], Masato Okada[4], Ichiro Akai[5] (1.ERI/UTokyo, 2.IST/UTokyo, 3.JASRI, 4.GSFS/UTokyo, 5.IINa, Kumamoto Univ.)

[SIT21-P02] Waveform inversion for localized 3-D transversely isotropic structure in the lowermost mantle beneath the western Pacific using Thai Seismic Array (TSAR) data

*Yuki Suzuki[1], Kenji Kawai[2], Robert J. Geller[2], Satoru Tanaka[3], Weerachai Siripunvaraporn[4], Songkhun Boonchaisuku[4], Noisagool Sutthipong[4], Yasushi Ishihara[3], Taweoon Kim[3] (1.Department of Earth and Planetary Science School of Science Tokyo Institute of Technology, 2.Department of Earth and Planetary Science School of Science University of Tokyo, 3.Japan Agency for Marine-Earth Science and Technology, 4.Faculty of Science, Mahidol University)

[SIT21-P03] Measurements of local stress using TEM in-situ obserbation

*Akira Miyake[1], Satoko Motai[1], Yohei Igami[1], Ryuichi Nomura[1] (1.Kyoto University)

[SIT21-P04] Measurements of local strain in minerals using electron nanoprobe

★Invited Papers

*Yohei Igami[1], Akira Miyake[1] (1.Kyoto University)

[SIT21-P05] Elastic properties of fine-grained polycrystalline clinopyroxene under high *P-T* conditions

*Yumiko Tsubokawa[1,2], Masahiro Ishikawa[2] (1.Kyushu University, 2.Yokohama National University)

[SIT21-P06] Effect of Al on stability and crystal strucutre of superhydrous phase B

*Sho Kakizawa[1,2], Toru Inoue[1,2], Hiroto Nakano[3], Minami Kuroda[4], Takahiro Kuribayashi[5], Naoya Sakamoto[6], Hisayoshi Yurimoto[7] (1.Graduate School of Advanced Science and Engineering, Hiroshima University, 2.Hiroshima Institute of Plate Convergence Region Research (HiPeR), 3.Geodynamics Research Center, Ehime University, 4.Graduate School of Sciences, Hokkaido University, 5.Department of Earth Science, Graduate School of Science, Tohoku University, 6.Creative Research Institution, Hokkaido University, 7.Department of Natural History Sciences, Hokkaido University)

[J] Poster | S (Solid Earth Sciences)：S-VC Volcanology

5:15 PM - 6:30 PM JST | 8:15 AM - 9:30 AM UTC | Ch.13_1

[S-VC30] Volcanic and igneous activities, and these long-term forecasting

convener:Takeshi Hasegawa(Department of Earth Sciences, College of Science, Ibaraki University), Teruki Oikawa(GSJ, National Institute of Advanced Industrial Science and Technology), Daisuke MIURA(Department of Physical Science, Graduate School of Science, Osaka Prefecture University), Nobuo Geshi(Geological Survey of Japan, The National Institute of Advanced Industrial Science and Technology)

[SVC30-P01] **Yield strength obtained from lava flow and lava tube cave of Undara volcano**

*Tsutomu Honda[1] (1.Vulcano-speleological Society)

[SVC30-P02] **Survey on Fissure Cave and Lava Tube Cave in Kansuyama Lava Flow of Mt.Fuji**

*Tsutomu Honda[1], Masaru Hatanaka[1], Takayoshi Katumata[1] (1.Vulcano-speleological Society)

[SVC30-P03] The origin of bimodal magmatism in the Okinawa Trough, Japan

*Arran Peter Murch[1], Kenichiro Tani[1], Takashi Sano[1], Shigekazu Yoneda[1] (1.National Museum of Nature and Science, Tsukuba, Ibaraki, Japan)

[SVC30-P04] Reinvestigation of Holocene eruption history of Nikko-Shirane Volcano, central Japan

*Yuki Kusano[1], Yoshihiro Ishizuka[1], Teruki Oikawa[1], Osamu Ishizuka[1] (1.Geological Survey of Japan, AIST)

[SVC30-P05] Construction of Geochemical database of Kikai Caldera magmas for understanding the magmatic evolution prior to caldera-forming eruptions

*Satoru Haraguchi[1,2], Kenta Ueki[2], Kenta Yoshida[2], Tatsu Kuwatani[2], Morihisa Hamada[2], Iona McIntosh[2], Takashi Miyazaki[2], Takeshi Hanyu[2] (1.Earthquake Research Institute, University of Tokyo, 2.JAMSTEC)

[SVC30-P06] Reconstruction of the volcanic history of Nakadake volcano in Kirishima volcano group, Kyushu, Japan (1)

*Yasuhisa Tajima[1], Atsushi Yasuda[2], Mitsuru Okuno[3] (1.Research & Development Center, Nippon Koei Co.,LTD., 2.Earthquake Research Institute, University of Tokyo, 3.Faculty of Science Department of Earth System Science, Fukuoka University)

[SVC30-P07] The effect of dissolved water induced by lithostatic pressure on lava migration

*Akio Goto[1] (1.Center for Northeast Asian Studies, Tohoku University)

[SVC30-P08] An attempt to detect volcanic materials of Ogasawara Ioto (Iwojima) Volcano from the core sample of the turbidite layers deposited in the Palace Bella Basin

*Masashi NAGAI[1], Takahiro Miwa[1] (1. Volcano Research Department, National Research Institute for Earth Science and Disaster Resilience)

[J] Poster | S (Solid Earth Sciences)：S-TT Technology & Techniques

5:15 PM - 6:30 PM JST | 8:15 AM - 9:30 AM UTC | Ch.14_1

[S-TT34] Airborne surveys and monitoring of the Earth

convener:Shigekazu Kusumoto(Institute for Geothermal Sciences, Graduate School of Science, Kyoto University), Shigeo Okuma(Geological Survey of Japan, AIST), Takao Koyama(Earthquake Research Institute, The University of Tokyo), Yuji Mitsuhata(AdvancedIndustrial Science and Technology)

[STT34-P01] Geological structure survey by drone airborne electromagnetic survey method

*Youichi Yuuki[1], Akira Shinsei[1], Zenshiro Saito[1], Satoshi Tomimori[1], Akiyo Yamaguti[1], Akira Jomori[2], Atsuyoshi Jomori[2], Tatsuya Toyama[2] (1.Oyo corporation, 2.Neo Science)

[STT34-P02] Development of a Portable Infrared Camera system for Measuring Volcanic Surface Phenomena

*Tetsuya Jitsufuchi[1] (1.National Research Institute for Earth Science and Disaster Resilience)

[J] Poster | S (Solid Earth Sciences)：S-TT Technology & Techniques

5:15 PM - 6:30 PM JST | 8:15 AM - 9:30 AM UTC | Ch.14_2

[S-TT37] Seismic Big Data Analysis Based on the State-of-the-Art of Bayesian Statistics

convener:Hiromichi Nagao(Earthquake Research Institute, The University of Tokyo), Aitaro Kato(Earthquake Research Institute, the University of Tokyo), Keisuke Yano(The Institute of Statistical Mathematics), Takahiro Shiina(National Institute of Advanced Industrial Science and Technology)

[STT37-P01] Clustering seismic noises using semi-supervised learning

*Kotaro Sato[1], Keisuke Yano[2], Komaki Fumiyasu[1] (1.The University of Tokyo, 2.The Institute of Statistical Mathematics)

[STT37-P02] Convolutional Neural Network to Detect Deep Low-Frequency Tremors from Seismic Waveform Images

*Ryosuke Kaneko[1,2], Hiromichi Nagao[2,1], Shin-ichi Ito[2,1], Kazushige Obara[2], Hiroshi Tsuruoka[2] (1.Graduate School of Information Science and Technology, The University of Tokyo, 2.Earthquake Research Institute, The University of Tokyo)

[STT37-P03] A Convolutional Neural Network based classification of local earthquakes and tectonic tremors in Sanriku-oki using a single station S-net data and its generalization ability

*Masayuki Kano[1], Hidenobu Takahashi[1], Kazuya Tateiwa[1], Keisuke Yano[2] (1.Graduate school of science, Tohoku University, 2.The Institute of Statistical Mathematics)

[STT37-P04] Forecasting temporal variation of aftershocks immediately after a main shock using Gaussian process regression

*Kosuke Morikawa[1], Hiromichi Nagao[2,3], Shin-ichi Ito[2,3], Yoshikazu Terada[1,4], Shin'ichi Sakai[2,5], Naoshi Hirata[2,6] (1.Osaka University, 2.Earthquake Research Institute, The University of Tokyo,, 3.Graduate School of Information Science and Technology, 4.Center for Advanced Intelligence Project, 5.Interfaculty Initiative in Information Studies, The University of Tokyo, 6.National Research Institute for Earth Science and Disaster Resilience)

[STT37-P05] **Detection of deep low-frequency earthquakes based on matched filter technique using mutual information**

*Ryo Kurihara[1], Aitaro Kato[1], Hiromichi Nagao[1,2], Sumito Kurata[2] (1.Earthquake Research Institute, The University of Tokyo, 2.Graduate School of Information Science and Technology, The University of Tokyo)

[STT37-P06] Adjoint-based uncertainty quantification of frictional inhomogeneity on slow-slipping fault

*Shin-ichi Ito[1], Masayuki Kano[2], Hiromichi Nagao[1] (1.The University of Tokyo, 2.Tohoku University)

[STT37-P07] Sensor selection for seismic wavefield reconstruction based on sparse observation (Part II: Preliminary study on method based on data-driven low-dimensional model)

*Takayuki Nagata[1], Kumi Nakai[1], Yuji Saito[1], Taku Nonomura[1], Masayuki Kano[1], Shin-ichi Ito[2], Hiromichi Nagao[2] (1.Tohoku University, 2.Earthquake Research Institute, The University of Tokyo)

[J] Poster | S (Solid Earth Sciences)：S-CG Complex & General

5:15 PM - 6:30 PM JST | 8:15 AM - 9:30 AM UTC | Ch.15_2

[S-CG50] Dynamics in mobile belts

convener:Yukitoshi Fukahata(Disaster Prevention Research Institute, Kyoto University), Hikaru Iwamori(Earthquake Research Institute, The University of Tokyo), Kiyokazu Oohashi(Graduate School of Sciences and Technology for Innovation, Yamaguchi University)

[SCG50-P01] Seismic anisotropy of the dipping Pacific slab and adjacent mantle

*Dapeng Zhao[1], Zewei Wang[1] (1.Department of Geophysics, Tohoku University)

[SCG50-P02] Magnitude of east-west contraction forces acting to Japanese Islands since 3Ma estimated from altitude changes

*Ryohei Sasajima[1], Yukitoshi Fukahata[1] (1.Research Center For Earthquake Prediction, Disaster Prevention Research Institute, Kyoto University)

[SCG50-P03] Earthquake simulation based on Coulomb stress change on inland faults during megathrust earthquake cycles in southwest Japan

*Tsukasa MITOGAWA[1], Takuya NISHIMURA[2] (1.Graduate School of Science, Kyoto University, 2.Disaster Prevention Research Institute, Kyoto University)

[SCG50-P04] GNSS observation around the shear zone in southern Kyushu, southwest Japan (5)

*Tsuyoshi Watanabe[1], Koichi Asamori[1], Akiomi Shimada[1], Atsushi Saiga[1], Hiroki Ogawa[1], Umeda Koji[2], Akira Goto[1], Koji Shimada[1], Tsuneari Ishimaru[1] (1.Japan Atomic Energy Agency, 2.Graduate School of Science and Technology, Hirosaki University)

[SCG50-P05] Classification of faults using vertical gravity gradient data by machine learning

*Yuya Honda[1], Kohei Hotta[1] (1.University of Toyama)

[SCG50-P06] Hierarchical clustering of reduced stress tensors based on angular stress distance

*Noriaki Abe[1], Katsushi Sato[1] (1.Kyoto University)

[SCG50-P07] Characteristic of fault geometry and the subducting plate boundary in the focal area of the 2016 Mw7.8 Kaikoura earthquake, New Zealand inferred from high precision aftershock distribution

*Yuta Kawamura[1], Satoshi Matsumoto[1], Tomomi Okada[2], Miu Matsuno[2], Yoshihisa Iio[3], Tadashi Sato[2], Stephen Bannister[4], John Ristau[4], Martha Savage[5], Richard Sibson[6] (1.Kyushu University, 2.Tohoku University, 3.Kyoto University, 4.GNS Science, 5.Victoria University of Wellington, 6.University of Otago)

[SCG50-P08] Analysis of fault kinematics and internal structure of fracture zone at ISTL

*HIBIKI CHIBA[1], Kenta Kobayashi[1], Keita Takahashi[1] (1.Gradate School of Science and Technology Niigata University)

[SCG50-P09] Non-double-couple earthquake in the focal area of the 2000 Western Tottori earthquake by “0.1 manten” hyperdense seismic observation

*Takumi Motokoshi[1], Satoshi Matsumoto[2], Yoshihisa Iio[3], Shin'ichi Sakai[4], Aitaro Kato[4] (1.Department of Earth and Planetary Sciences, Graduate School of Science, Kyushu University, 2.Institute of Seismology and Volcanology, Faculty of Science, Kyushu University, 3.Disaster Prevention Research Institute, Kyoto University, 4.Earthquake Research Institute , the University of Tokyo)

[SCG50-P10] Transition from radial to parallel dike swarm in Amakusa, Japan and their paleostress analyses

*Kentaro Ushimaru[1], Atsushi Yamaji[1] (1.Division of Earth and Planetary Sciences, Graduate School of Science, Kyoto University)

[SCG50-P11] **Electrical conductivity in a brine-saturated granite under uni-axial compression**

*Yui Aikawa[1], Tohru Watanabe[1] (1.University of Toyama)

[SCG50-P12] Lithologic and thermal controls of seismicity in the northwestern Kii Peninsula, southern Honshu, Japan

*Sumire Maeda[1], Shinji Toda[2], Toru Matsuzawa[3], Makoto Otsubo[4] (1.National Research Institute for Earth Science and Disaster Resilience, 2.International Research Institute of Disaster Science, Tohoku University, 3.Graduate School of Science, Tohoku University, 4.Geological Survey of Japan, National Institute of Advanced Industrial Science and Technology)

[SCG50-P13] On approximations of EASY%R_o model to estimate maximum experienced temperature from vitrinite reflectance in rocks

*Shunya Kaneki[1], Hiroyuki Noda[1] (1.Disaster Prevention Research Institute, Kyoto University)

[J] Poster | S (Solid Earth Sciences)：S-CG Complex & General

5:15 PM - 6:30 PM JST | 8:15 AM - 9:30 AM UTC | Ch.12_3

[S-CG51] New perspectives of subduction zone earthquake dynamics through experiments across-scales

convener:Masataka Kinoshita(Earthquake Research Institute, University of Tokyo)

[SCG51-P01] For examining steady-state solution for pore pressure distribution in a plate-subduction zone incorporating fluid release by chemical reaction

*Shunya Kaneki[1], Hiroyuki Noda[1] (1.Disaster Prevention Research Institute, Kyoto University)

[SCG51-P02] A new method for large number of core sample CT scanning and preliminary results of Nankai Trough DSDP and ODP core samples

*Satoshi Tonai[1], Yusuke Kubo[2], Masataka Kinoshita[3], Keishi Okazaki[2] (1.Faculty of Science and Technology, Kochi University, 2.Kochi Institute for Core Sample Research, JAMSTEC, 3.Earthquake Research Institute, University of Tokyo)

[J] Poster | S (Solid Earth Sciences)：S-CG Complex & General

5:15 PM - 6:30 PM JST | 8:15 AM - 9:30 AM UTC | Ch.14_3

[S-CG52] Driving Solid Earth Science through Machine Learning

convener:Hisahiko Kubo(National Research Institute for Earth Science and Disaster Resilience), Yuki Kodera(Meteorological Research Institute, Japan Meteorological Agency), Makoto Naoi(Kyoto University), Keisuke Yano(The Institute of Statistical Mathematics)

[SCG52-P01] Automatic hypocenter determination by deep learning for microseismic networks in geothermal areas

*Kyosuke Okamoto[1], Yusuke Mukuhira[2], Hiroshi Asanuma[1], Markus Häring[3] (1.National Institute of Advanced Industrial Science and Technology, 2.Tohoku University, 3.Häring GeoProject)

[SCG52-P02] Toward development of dense low cost citizen seismic network: Performance comparison of different types of neural network architectures

*Ahyi KIM[1], Hiroki Uematsu[1], Yuji Nakamura[1], Yuta Takahashi[1], Momoko Nakamura[1] (1.Yokohama City University)

[SCG52-P03] Unsupervised automatic classification of seismic records based on a hierarchical clustering

*Yuki Kodera[1], Shin'ichi Sakai[2] (1.Meteorological Research Institute, Japan Meteorological Agency, 2.Earthquake Research Institute, the University of Tokyo)

[SCG52-P04] Hierarchical cluster analysis of F-net moment-tensor-solution catalogue in Japan

*Hisahiko Kubo[1], Takeshi Kimura[1], Katsuhiko Shiomi[1] (1.National Research Institute for Earth Science and Disaster Resilience)

[J] Poster | M (Multidisciplinary and Interdisciplinary)：M-IS Intersection

5:15 PM - 6:30 PM JST | 8:15 AM - 9:30 AM UTC | Ch.17_2

[M-IS21] Chemosynthetic community and mud volcano: biology, geochemistry, and geophysics of fluid discharge

convener:Yusuke Miyajima(Geomicrobiology Research Group, Research Institute for Geo-Resources and Environment, Geological Survey of Japan, National Institute of Advanced Industrial Science and Technology), Kayama Hiromi WATANABE(Japan Agency for Marine-Earth Science and Technology), Akira Ijiri(Japan Agency for Marine-Earth Science and Technology), Tomohiro Toki(Faculty of Science, University of the Ryukyus)

[MIS21-P01] Origin of noble gases in surface sediments from submarine mud volcanoes off Tanegashima

*Yuki Mitsutome[1], Tomohiro Toki[2], Takanori Kagoshima[3], Naoto Takahata[4], Yuji Sano[5], Yama Tomonaga[6] (1.University of the Ryukyus Graduate School of Science and Engineering, 2.Faculty of Science, University of the Ryukyus, 3.University of Toyama, 4.Atmosphere and Ocean Research Institute, the University of Tokyo, 5.Division Ocean and Earth Systems, Atmosphere and Ocean Research Institute, the University of Tokyo, 6.Eawag, Swiss Federal Institute of Aquatic Science and Technology)

[MIS21-P02] Subsurface structures and fluid transportation visualization by acoustic mapping in a shallow methane hydrate area off Sakata, eastern margin of the Sea of Japan

*Miho Asada[1], Mikio Satoh[1], Toshiyuki Yokota[1], Shusaku Goto[1] (1.NATIONAL INSTITUTE OF ADVANCED INDUSTRIAL SCIENCE AND TECHNOLOGY (AIST))

[MIS21-P03] Chemosynthesis, surface ruptures and possible methane eruption on the Kuroshima Knoll: a review from previous studies

*Takeshi Matsumoto[1] (1.Faculty of Science, University of the Ryukyus)

[MIS21-P04] Community composition and connectivity of hot vent endemic animals on the Izu-Bonin-Mariana Arc

*Hiromi Kayama WATANABE[1], Chong Chen[1], Shigeaki Kojima[2], Hiroyuki Yamamoto[1] (1.Japan Agency for Marine-Earth Science and Technology, 2.Atmosphere and Ocean Research Institute, the University of Tokyo)

[MIS21-P05] Population Genetic Structure and Gene Expression Plasticity of the Deep-Sea Vent and Seep Squat Lobster *Shinkaia crosnieri*

*Yao Xiao[1] (1.Hong Kong University of Science and Technology)

[MIS21-P06] A Decade to Study Deep-Sea Science

*Hiromi Kayama WATANABE[1], Kerry Howell[2] (1.Japan Agency for Marine-Earth Science and Technology, 2.University of Plymouth)

[J] Poster | M (Multidisciplinary and Interdisciplinary)：M-GI General Geosciences, Information Geosciences & Simulations

5:15 PM - 6:30 PM JST | 8:15 AM - 9:30 AM UTC | Ch.20_2

[M-GI33] Data-driven geosciences

convener:Tatsu Kuwatani(Japan Agency for Marine-Earth Science and Technology), Hiromichi Nagao(Earthquake Research Institute, The University of Tokyo), Kenta Ueki(Japan Agency for Marine-Earth Science and Technology), Shin-ichi Ito(The University of Tokyo)

[MGI33-P01] Numerical modeling of mantle melting degree based on major element composition of melt

*Kenta Ueki[1], Satoru Haraguchi[2,1], Hikaru Iwamori[1] (1.Japan Agency for Marine-Earth Science and Technology, 2.Earthquake Research Institute, The University of Tokyo)

[MGI33-P02] Bayesian modeling of the equation-of-state by integration of various data sets for liquid iron in Earth's outer core

*Taroujirou Matumura[1], Yasuhiro Kuwayama[2], Kenta Ueki[3], Tatsu Kuwatani[3], Ando Yasunobu[1], Kenji Nagata[4], Shin-ichi Ito[5], Hiromichi Nagao[5] (1.Research center for computational design of advanced functional materials, AIST, 2.Department of Earth and Planetary Science, The University of Tokyo, 3.Research Institute for Marine Geodynamics, Japan Agency for Marine-Earth Science and Technology, 4.Research Center for Advanced Measurement and Characterization, National Institute for Materials Science (NIMS), 5.Earthquake Research Institute, The University of Tokyo)

[MGI33-P03] Superresolution of X-ray CT images of rock core samples and applications to serpentinite in the Oman ophiolite

*Shoui Suzuki[1], Atsushi Okamoto[2], Katsuyoshi Michibayashi[3], Toshiaki Omori[1] (1.Kobe University, 2.Tohoku University, 3.Nagoya University)

[J] Poster | M (Multidisciplinary and Interdisciplinary)：M-GI General Geosciences, Information Geosciences & Simulations

5:15 PM - 6:30 PM JST | 8:15 AM - 9:30 AM UTC | Ch.18_2

[M-GI34] Earth and planetary informatics with huge data management

convener:Ken T. Murata(National Institute of Information and Communications Technology), Susumu Nonogaki(Geological Survey of Japan, National Institute of Advanced Industrial Science and Technology), Rie Honda(Department of Science and Technology, System of Natual Science, Kochi University), Keiichiro Fukazawa(Academic Center for Computing and Media Studies, Kyoto University)

[MGI34-P01] An attempt of local government disaster prevention WebGIS

*Ken T. Murata[1], Asanobu Kitamoto[2], Tomohiro Kawanabe[3], Keiichiro Fukazawa[4], Kazuya Muranaga[1], Kazunori Yamamoto[1], Yuki MURAKAMI[1] (1.National Institute of Information and Communications Technology, 2.National Institute of Informatics, 3.Institute of Physical and Chemical Research, 4.Kyoto University)

[MGI34-P02] Development of interface for PTZ Camera to use image processing technique

*Yuki MURAKAMI[1], Ken T. Murata[1], Michiharu Niimi[2], Yoshihide Kagatani[3], Minehito Ageno[3], Kazunori Yamamoto[1], Tomohiro Kawanabe[4] (1.National Institute of Information and Communications Technology, 2.Kyushu Institute of Technology, 3.GEO Solutions Co.Ltd., 4.Institute of Physical and Chemical Research)

[MGI34-P03] Development of LPWA and visual IoT techniques (2)

Mehdad Shirazi[1], *Takamichi Mizuhara[1], Toshiki Aoki[1], Yuua Kagebayashi[1], Takeshi Murata[2], Kazunori Yamamoto[2], Kazuya Muranaga[3] (1.CLEALINK TECHNOLOGY CO., LTD., 2.National Institute of Information and Communications Technology, 3.Systems Engineering Consultants Co.,LTD.)

[MGI34-P04] HpFP: development of high-speed data transfer applications (2)

Yasunori Kakizawa[1], Ayahiro Takaki[1], *Takamichi Mizuhara[1], Kazuya Muranaga[3], Kazunori Yamamoto[2], Takeshi Murata[2] (1.CLEALINK TECHNOLOGY CO., LTD., 2.National Institute of Information and Communications Technology, 3.Systems Engineering Consultants Co.,LTD.)

[MGI34-P05] Programming Techniques for visual IoT on Raspberry Pi (4)

Toshiki Aoki[1], *Takamichi Mizuhara[1], Takeshi Murata[2], Kazunori Yamamoto[2], Kazuya Muranaga[3] (1.CLEALINK TECHNOLOGY CO., LTD., 2.National Institute of Information and Communications Technology, 3.Systems Engineering Consultants Co.,LTD.)

[MGI34-P06] A large-scale distributed cloud system for research works on Earth and Planetary sciences

Kazunori Yamamoto[1], Kazuya Muranaga[2], *Ken T. Murata[1], Keiichiro Fukazawa[3], Atsushi Higuchi[4], Takeshi Nanri[5], Tomohiro Kawanabe[6], Yoshitaka Ohyoshi[7] (1.National Institute of Information and Communications Technology, 2.SEC, 3.Kyoto University, 4.Chiba University, 5.Kyushu University, 6.Institute of Physical and Chemical Research, 7.Virtual)

[MGI34-P07] Activity of preparing training data for study of space plasma with collaboration of observation, MHD simulation and machine leaning

*Keiichiro Fukazawa[1], Tomoki Kimura[2], Terumasa Tokunaga[3], Shin ya Nakano[4] (1.Academic Center for Computing and Media Studies, Kyoto University, 2.Frontier Research Institute for Interdisciplinary Sciences, Tohoku University, 3.Department of Systems Design and Informatics, Faculty of Computer Science and Systems Engineering, Kyushu Institute of Technology, 4.Department of Statistical Modeling, Institute of Statistical Mathematics)

[MGI34-P08] Development of a multi-station airglow imaging system using commercial cameras

*Shin Suzuki[1] (1.Faculty of Regional Policy, Aichi University)

[MGI34-P09] Super-resolution and colorization of small body images by Generative Adversarial Network

Rintaro Kishi[1], Ren Hashimoto[1], *Rie Honda[1], Kimikazu Tanase[1], Yasuhiro Yokota[2], Seiji Sugita[3], Tomokatsu Morota[3], Shingo Kameda[4], Naoya Sakatani[4], Eri Tatsumi[5], Yuichiro Cho[3], Toru Kouyama[6], Manabu Yamada[7], Masahiko Hayakawa[2], Hidehiko Suzuki[8], Kazuo Yoshioka[3], Chikatoshi Honda[9], Kazunori Ogawa[2], Hirotaka Sawada[2] (1.Kochi University, 2.ISAS/JAXA, 3.Univ. of Tokyo, 4.Rikkyo Univ., 5.Instituto de Astrofisica de Canarias, Univ. of La Laguna, 6.AIST, 7.Chiba Inst. Tech, 8.Meiji Univ., 9.Univ. of Aizu)

[J] Poster | M (Multidisciplinary and Interdisciplinary)：M-TT Technology & Techniques

5:15 PM - 6:30 PM JST | 8:15 AM - 9:30 AM UTC | Ch.20_3

[M-TT42] Frontiers in Geochemistry

convener:Tsuyoshi Iizuka(University of Tokyo), Yoshio Takahashi(Department of Earth and Planetary Science, Graduate School of Science, The University of Tokyo), Urumu Tsunogai(Graduate School of Environmental Studies, Nagoya University)

[MTT42-P01] High-precision La isotope measurements to apply early Solar System chronology and nuclear cosmochronology

*Mitsuru Suzuki[1], Tsuyoshi Iizuka[1], Kota Yamamoto[1], Takafumi Hirata[1] (1.The University of Tokyo)

[MTT42-P02] **Factors limiting the accuracy and precision of peak positions and intensity ratios in Raman spectra: Optimisation of optics and measurement environment for carbon isotope ratio measurements of CO_2**

*Yuuki Hagiwara[1], Junji Yamamoto[1] (1.Hokkaido University)

[MTT42-P03] Development and evaluation of wet-flow type isotope analyses for fluid-inclusions in speleothems

*Ryu Uemura[1] (1.Nagoya University)

[MTT42-P04] Sub-microgram sulfur isotope analysis for the biological, geological, and extraterrestrial samples by sensitivity-improved EA/IRMS

*Nanako O. Ogawa[1], Toshihiro Yoshimura[1], Takeru Kochi[2,1], Junichiro Kuroda[2,1], Yoshinori Takano[1], Naohiko Ohkouchi[1] (1.JAMSTEC, 2.AORI, Univ. Tokyo)

[J] Poster | M (Multidisciplinary and Interdisciplinary)：M-ZZ Others

5:15 PM - 6:30 PM JST | 8:15 AM - 9:30 AM UTC | Ch.19_2

[M-ZZ46] Marine Manganese Deposits: Origin, Exploration, and Development

convener:Akira Usui(Marine Core Research Center, Kochi University), Katsuhiko Suzuki(Submarine Resources Research Center, Japan Agency for Marine-Earth Science and Technology), Yoshio Takahashi(Department of Earth and Planetary Science, Graduate School of Science, The University of Tokyo), Takashi Ito(Faculty of Education, Ibaraki University)

[MZZ46-P01] Detrital minerals in hydrogenetic ferromanganese crusts as an alternative tool for archiving marine geological environments

*Akira Usui[1], Takashi Ito[2], Hirokuni Oda[3], Hitoshi Hasegawa[4] (1.Marine Core Research Center, Kochi University, 2.Ibaraki University, 3.AIST, 4.Kochi University)

[MZZ46-P02] Fluxes of sinking particles in the exploration area for cobalt-rich ferromanganese crusts in the Northwest Pacific

*Kyoko Yamaoka[1], Atsushi Suzuki[1], Yuichiro Tanaka[1], Masahiro Suzumura[2], Ayumi Tsukasaki[2], Tatsuo Fukuhara[3], Takeshi Fujii[3], Junpei Minatoya[4], Nobuyuki Okamoto[4], Yoshiaki Igarashi[4] (1.Geological Survey of Japan, National Institute of Advanced Industrial Science and Technology, 2.Environmental Management Research Institute, National Institute of Advanced Industrial Science and Technology, 3.KANSO Co., Ltd., 4.Japan Oil, Gas and Metals National Corporation)

[MZZ46-P03] Submarine erosion of basement sedimentary rocks around ferro-manganese crust fields

*Takashi Ito[1], Masaki Saito[1], Eri Shimizu[2], Takashi Miyazaki[3], Bogdan S. Vaglarov[3], Katsuhiko Suzuki[3], Akira Usui[4] (1.Faculty of Education, Ibaraki University, 2.JOGMEC, 3.JAMSTEC, 4.Center for Advanced Marine Core Research, Kochi University)

[MZZ46-P04] Local structure of rare earth elements in marine ferromanganese oxides by extended X-ray absorption fine structure analysis

*Makoto Nagasawa[1], Yoshio Takahashi[1] (1.Department of Earth and Planetary Science, Graduate School of Science, The University of Tokyo)

[MZZ46-P05] Reconstruction of rotation by paleomagnetic analysis of manganese nodules collected in the South Pacific

*Wataru Katanoda[1,2], Hirokuni Oda[2], Masafumi MURAYAMA[3], Akira Usui[3] (1. Kochi university Graduate school of Integrated Arts and Science, 2.National Institute of Advanced Industrial Science and Technology, 3.Kochi university)

[MZZ46-P06] Lamina-scale analysis of chemical composition of the mid-Cretaceous northern Shimanto belt, Kochi, Japan: implications for formative processes of bedded ferromanganese deposits

*Go-Ichiro Uramoto[1], Takaumi Nagata[1], Yoshiro Nishio[1] (1.Kochi University)

[MZZ46-P07] Biodiversity and connectivity of deep-sea amphipods at seamounts with cobalt-rich ferromanganese crusts in the Northwest Pacific

*Akira Iguchi[1], Eri Ikeuchi[1], Hiroyuki Yokooka[2], Hideki Sugishima[2], Kazumasa Ikeda[3], Ryuichi Miwa[4], Miyuki Nishijima[1], Nozomu Iwasaki[5], Yuichiro Tanaka[1], Taiga Kunishima[6], Shogo Kato[7], Junpei Minatoya[7], Yoshiaki Igarashi[7], Nobuyuki Okamoto[7], Atsushi Suzuki[1] (1.National Institute of Advanced Industrial Science and Technology, 2.IDEA Consultants, Inc., 3.Okamoto Glass Co., Ltd., 4.Kaiyo Engineering Co., Ltd., 5.Faculty of Geo-Environmental Science, Rissho University, 6.Wakayama Prefectural Museum of Natural History, 7. Japan Oil, Gas and Metals National Corporation)

[J] Poster | P (Space and Planetary Sciences)：P-CG Complex & General

Thu. Jun 3, 2021 5:15 PM - 6:30 PM JST | Thu. Jun 3, 2021 8:15 AM - 9:30 AM UTC | Ch.01_2

[P-CG18] Planetary Magnetosphere, Ionosphere, and Atmosphere

convener:Kanako Seki(Graduate School of Science, University of Tokyo), Hiroyuki Maezawa(Department of Physical Science Osaka Prefecture University), Takeshi Imamura(Graduate School of Frontier Sciences, The University of Tokyo), Naoki Terada(Graduate School of Science, Tohoku University)

Exploration of Mercury, Venus, Moon, Mars, Jupiter, Saturn, and beyond together with rapid developments of numerical simulations provides us new view of planetary environment. This session collects general contributions of new findings about planetary magnetosphere, ionosphere, and atmosphere. New methodology and technology development studies for future explorations are also welcome. In order to put the common knowledge at different planets into perspective, this session aims to facilitate discussions on comparative planetary environments.

[PCG18-P01] Hybrid particle simulation on Mercury's dayside magnetopause

*Hideyuki Usui[1], Yohei Miyake[2], Naoshi Motoda[1], Masaharu Matsumoto[3] (1.Graduate school of system informatics Kobe University, 2.Education Center for Computational and Engineering Science, 3.Graduate school of information science and technology, The University of Tokyo)

[PCG18-P02] Numerical calculation of moist convection in Jupiter's atmosphere - A case study with an average cooling vertical profile based on a radiative transfer calculation -

Taro Sekiguchi[1], *Ko-ichiro SUGIYAMA[2], Masaki Ishiwatari[1], Kensuke Nakajima[3], Kiyoshi Kuramoto[1], Yoshi-Yuki Hayashi[4] (1.Department of Cosmoscience, Graduate School of Science, Hokkaido University, 2.National Institute of Technology, Matsue College, 3.Department of Earth and Planetary Sciences,Flculty of Sciences,Kyushu University, 4.Department of Planetology, Graduate School of Science, Kobe University / Center for Planetary Science (CPS))

[PCG18-P03] High dynamic range observation using a 1.8-m off-axis telescope PLANETS: feasibility study and telescope assembly

*Masato Kagitani[1], Takeshi Sakanoi[1], Kazuya Nagta[1], Yasumasa Kasaba[1], Yasuhiro Hirahara[2], Mikio Kurita[3], Jeffry Kuhn[4], Svetlana Berdyugina[5], Emilio Marcelo[6] (1.Planetary Plasma and Atmospheric Research Center, Graduate School of Science, Tohoku University, 2.Graduate School of Environmental Studies, Nagoya University, 3.Graduate School of Science, Kyoto University, 4.Institute for Astronomy, Univesity of Hawaii, USA, 5.Kiepenheuer Institute for Solar Physics, Germany, 6.Universidade Estadual de Ponta Grossa, Brazil)

[PCG18-P04] A search for atomic sodium and calcium in the atmosphere of the icy Galilean moons of Jupiter with ground-based telescope

*Seiko Takagi[1], Taro Matsuo[2], Jun Kimura[3], Kazuo Yoshioka[4] (1.Hokkaido University, Graduate School of Science, 2.Nagoya University, 3.Osaka University, 4.The University of Tokyo)

[PCG18-P05] Development of PLANETS telescope: An attempt to reduce polishing volume in final polishing process by using an active mirror support

*Kazuya Nagata[1], Masato Kagitani[1], Yasumasa Kasaba[1], Takeshi Sakanoi[1], Yasuhiro Hirahara[2], Mikio Kurita[3] (1.Graduate School of Science, Tohoku University, 2.Graduate School of Environmental Studies, Nagoya University, 3.Graduate School of Science, Kyoto University)

[PCG18-P06] Numerical simulations of 500eV-50keV electron elastic collisions with neutral H_2O around Enceladus ~estimation of electron loss rate and auroral brightness~

*Hiroyasu Tadokoro[1], Yuto Katoh[2] (1.Surugadai University, 2.Tohoku University)

[PCG18-P07] Development of the near-infrared camera TOPICS and the Echelle spectrograph ESPRIT for planetary observations

Ayumu Kambara[1], *Takeshi Sakanoi[1], Yasuhiro Hirahara[2], Takashi Ichikawa[3], Masato Kagitani[1], Yasumasa Kasaba[1], Aya Otomo[1], Kazuya Nagata[1] (1.Planetary Plasma and Atmospheric Research Center, Graduate School of Science, Tohoku University, 2.Graduate School of Environmental Studies, Nagoya University, 3.Astronomical Institute, Graduate School of Science, Tohoku University)

[PCG18-P08] Effects of the magnetic field configuration in the ionosphere on solar energetic electron precipitation into the Martian upper atmosphere observed by MAVEN

*Kanako Seki[1], Takuya Hara[2], Dave A Brain[3], Robert J Lillis[2], Darvin E Larson[2], Dave L Mitchell[2], Gina A Dibraccio[4], Janet G Luhmann[2], Bruce M Jakosky[3] (1.Graduate School of Science, University of Tokyo, 2.Space Sciences Laboratory, University of California, Berkeley, 3.Laboratory for Atmospheric and Space Physics, University of Colorado, Boulder., 4.Goddard Space Flight Center, NASA)

[PCG18-P09] Observations of minor constituents in the Venusian atmosphere, CO and SOx using the millimeter/submillimeter-wave band radio telescopes, SPART/ALMA

Ayaka Tomihara[1], Teppei Yonetsu[1], Yuki Hamaguchi[1], Hideo Sagawa[2], *Hiroyuki Maezawa[1] (1.Department of Physical Science Osaka Prefecture University, 2.Kyoto Sangyo University)

[PCG18-P10] Influences of solar energetic particles on the Martian ozone layer

*Sayano Hiruba[1], Yuki Nakamura[1], Hiromu Nakagawa[1], Naoki Terada[1], Shotaro Sakai[1], Isao Murata[1], Yoshifumi Futaana[2] (1.Dept. of Geophysics, Graduate school of science, Tohoku University, 2.Swedish Institute of Space Physics)

[PCG18-P11] Simultaneous remote and in-situ observations of ionospheric irregularities at Mars

*Hina Bando[1], Yuki Harada[1], Naoki Terada[2], Hiromu Nakagawa[2] (1.Kyoto University, 2.Tohoku University)

[PCG18-P12] Annual variability in the thermospheric wave perturbations at Mars

*Hiromu Nakagawa[1], Nao Yoshida[1], Kaori Terada[1], Naoki Terada[1], Yuki Harada[2], Shotaro Sakai[1], Takeshi Imamura[3], Hitoshi Fujiwara[4], Kanako Seki[5] (1.Planetary Atmosphere Physics Laboratory, Department of Geophysics, Graduate School of Science, Tohoku University, 2.Kyoto University, 3.Graduate School of Frontier Scienfes, The University of Tokyo, 4.Faculty of Science and Technology, Seikei University, 5.Graduate School of Science, University of Tokyo)

[PCG18-P13] **Study of atmospheric ion escape from exoplanet TOI-700 d**

*Tomoaki Nishioka[1], Kanako Seki[1], Ryoya Sakata[1], Kazuhiro Yamamoto[1], Naoki Terada[2], Hiroyuki Shinagawa[3] (1.Graduate School of Science, University of Tokyo , 2.Graduate School of Science, Tohoku University , 3.NICT)

[PCG18-P14] DSMC simulations of slow hydrodynamic escape from Earth-like and Mars-like planets

*Naoki Terada[1], Kaori Terada[1], Hitoshi Fujiwara[2], Masahiro Ikoma[3] (1.Graduate School of Science, Tohoku University, 2.Faculty of Science and Technology, Seikei University, 3.Graduate School of Science, The University of Tokyo)

Hybrid particle simulation on Mercury’s dayside magnetopause

*Hideyuki Usui[1], Yohei Miyake[2], Naoshi Motoda[1], Masaharu Matsumoto[3]

1. Graduate school of system informatics Kobe University, 2. Education Center for Computational and Engineering Science, 3. Graduate school of information science and technology, The University of Tokyo

The purpose of the present study is to investigate the ion dynamics at the dayside magnetopause of Mercury's magnetosphere and the magnetopause location's dependence on the solar wind dynamic pressure by performing hybrid particle simulations. In the simulation model, a small planetary body that has an intrinsic dipole magnetic field is placed at the center, and the solar wind with the Southward or Northward IMF is injected from the simulation boundary. A magnetosphere is created in the simulation due to the interaction between the solar wind and planetary magnetic dipole field. Bow shock, magnetosheath, magnetopause, and cusp are formed in the magnetosphere. In this study, we focus on the ions' trajectories at the dayside magnetopause in the Southward IMF case and analyze the meandering motion and ExB drift motion of the ions at the magnetopause. We also performed simulations to study the magnetopause location in the extreme case of the solar wind condition. When the solar wind dynamics pressure is very high, the previous observations suggest that the possibility that the dayside magnetopause disappears and the solar wind bombard directly to Mercury's surface, called Disappearing Dayside Magnetopause (DDM). We simulate DDM and investigate the structure of the magnetosphere in terms of density and current profiles and the solar wind flux to the surface.

Keywords: Mercury, magnetosphere, hybrid particle simulation

©2021. Japan Geoscience Union. All Right Reserved.

Numerical calculation of moist convection in Jupiter's atmosphere - A case study with an average cooling vertical profile based on a radiative transfer calculation -

Taro Sekiguchi[1], *Ko-ichiro SUGIYAMA[2], Masaki Ishiwatari[1], Kensuke Nakajima[3], Kiyoshi Kuramoto[1], Yoshi-Yuki Hayashi[4]

1. Department of Cosmoscience, Graduate School of Science, Hokkaido University, 2. National Institute of Technology, Matsue College, 3. Department of Earth and Planetary Sciences,Flculty of Sciences,Kyushu University, 4. Department of Planetology, Graduate School of Science, Kobe University / Center for Planetary Science (CPS)

Active moist convections associated with condensation of H_2O and NH_3 and chemical reaction of NH_4SH are considered to occur in Jupiter's atmosphere. Since it is difficult to observe Jupiter's atmosphere covered with thick clouds by remote sensing, the structure of moist convection remains unclear. We have developed a cloud resolving model that includes cloud microphysical processes of condensation and chemical reactions of multiple components, and have investigated the structure of moist convection realized under Jupiter's atmospheric conditions (Sugiyama et al., 2009, 2011, 2014). Our calculations showed that periods of intense convective activity (active periods) and periods of weak convective activity (quiet periods) appear quasi-periodically. However, the settings of our previous studies were highly idealized. The purpose of this study is to examine the structure of moist convection in Jupiter's atmosphere that are established through a large number of life cycles of convective cloud elements by using the temperature and thermal forcing profiles based on the result of a one-dimensional vertical radiative-convective equilibrium calculation (Takahashi, Hokkaido University Ph. D. thesis, 2018).

The cloud resolving model developed by Sugiyama et al. (2009) is used. The temperature and pressure conditions and the abundances of condensible gases used in our calculation are based on the one-dimensional vertical radiative-convective equilibrium calculation (Takahashi, Hokkaido University Ph. D. thesis, 2018). The computational domain is two-dimensional, 1024 km in the horizontal direction and 300 km in the vertical direction. The resolution is set to 2 km in both the horizontal and vertical directions. One of the major differences between the settings of our calculation and those of Sugiyama et al. (2014) is the temperature profile of the basic state. The temperature profile used in our calculation is stable between 0.4 bar level and the tropopause (0.1 bar level). Another difference is the pressure range in which the model atmosphere is subject to an externally given body cooling that is a substitute for radiative cooling. The body cooling is applied below 0.4 bar level.

In our poster, we will present the characteristics of the structure of moist convection that emerge under more realistic conditions that are based on the one-dimensional vertical radiative-convective equilibrium calculation.

Keywords: planetary atmosphere, moist convection, cloud resolution model

©2021. Japan Geoscience Union. All Right Reserved.

High dynamic range observation using a 1.8-m off-axis telescope PLANETS: feasibility study and telescope assembly

*Masato Kagitani[1], Takeshi Sakanoi[1], Kazuya Nagta[1], Yasumasa Kasaba[1], Yasuhiro Hirahara[2], Mikio Kurita[3], Jeffry Kuhn[4], Svetlana Berdyugina[5], Emilio Marcelo[6]

1. Planetary Plasma and Atmospheric Research Center, Graduate School of Science, Tohoku University, 2. Graduate School of Environmental Studies, Nagoya University, 3. Graduate School of Science, Kyoto University, 4. Institute for Astronomy, Univesity of Hawaii, USA, 5. Kiepenheuer Institute for Solar Physics, Germany, 6. Universidade Estadual de Ponta Grossa, Brazil

High dynamic-range observation is one of the key techniques to reveal composition, distribution and dynamics of plasma and neutrals in the vicinity of planets and their moons in our solar system, e.g. water plumes on Europa and Enceladus, volcanic plumes on Io, escaping plasma and neutrals from Venus and Mars, and so on. A low-scattered light telescope PLANETS (Polarized Light from Atmospheres of Nearby Extra-Terrestrial Systems) will be a 1.8-m off-axis telescope atop Haleakala observatory in Hawaii in collaboration with Japan, USA, Germany and Brazil. Combined with contrast enhancement techniques such as coronagraphy, adaptive optics and high-resolution spectroscopy, the off-axis optical system enables us to achieve high dynamic range measurements without diffraction by support structure of secondary mirror. We present feasibility study of monitoring water plumes on Europa, neutral torus close to Enceladus, and ionosphere on Mars using PLANETS telescope and latest telescope design and assembly in Japan.

This “high dynamic-range” capability is largely dependent upon precision of telescope optics as well as atmospheric distortion. To test feasibility of high dynamic-range observation under actual conditions of wavefront error, we modeled propagation of light though the system based on Fraunhofer calculation taking into account for wavefront error made by atmospheric distortion and by primary mirror figure error. Then point spread function is calculated for several cases of figure errors under use of adaptive optics. The modeling result predicts that using moderate or high-precision primary mirror M1, a contrast level < 10^{-4} at 5 λ /D would be accomplished. We also derived signal-to-noise ratio expected for three observing targets in the vicinity of Saturn, Mars and Europa. The moderate or high-precision M1 is mandatory to achieve the HDR observations with signal-to-noise ratio > 2 to 3.

We also present latest design of the telescope structure and M1 active support structure. The most part of the telescope structure is reuse of prototype of Kyoto 3.8-m telescope (*Kurita and Sato*, 2009) which employs commercial truss component for architecture. The structure is characterized by its light-weight (6.4 tons) and high-stiffness. The primary thin mirror (100 mm thick on edge) is supported by 36-point whiffletrees in axial and 24-point Schwesinger support in lateral direction. 33 warping harnesses equipped to the axial support whiffletrees enable to compensate low-frequency wavefront error of M1. The laboratory experiment using a third part of prototype whiffletrees shows supporting force RMS repeatability < 0.005 kgf, and drive hysteresis < 0.7% of load range, which are precise enough to control or to keep the M1 surface figure.

We aim to complete the final M1 polish and assembling the telescope structures in the year of 2021.

©2021. Japan Geoscience Union. All Right Reserved.

A search for atomic sodium and calcium in the atmosphere of the icy Galilean moons of Jupiter with ground-based telescope

*Seiko Takagi[1], Taro Matsuo[2], Jun Kimura[3], Kazuo Yoshioka[4]

1. Hokkaido University, Graduate School of Science, 2. Nagoya University, 3. Osaka University, 4. The University of Tokyo

Study of the Galilean moon atmospheres has been advanced by space missions of the last 25 years, e.g., Voyager, Hubble Space Telescope, and Galileo, and numerous ground-based observations. Thus we now know these moons have tenuous atmosphere with SO_2 for Io and oxygen for Europa as primary species. On the other hand, minor species in the atmosphere can aid in investigation of surface composition and transportation processes between moons. For Io and Europa, numerous sets of observations exist of atomic sodium and potassium [Brown and Chaffee, 1974; Trafton, 1975; Brown and Hill, 1996; Brown, 2001]. For Io, the sodium D_1 (5,895.92 Å) and D_2 (5,889.95 Å) emission lines brightness of the sodium nebula has a positive correlation with Io's volcanic activity [Mendillo et al., 2004; Yoneda et al., 2015], which strongly suggests that the sodium originates from the Io’s interior. For Europa, spectrographic evidence on the surface acquired from the Galileo spacecraft suggests that hydrated salt minerals, such as magnesium and sodium sulfates, sodium carbonate and their mixtures, are concentrated at the linear features and in the chaotic terrains [McCord et al., 1999]. Furthermore, recent visible spectroscopic observations by the Hubble Space Telescope suggests the presence of sodium chloride on Europa [Trumbo et al. 2019]. The value of [Na]/[K] for the Europa’s atmosphere, ~25+/-3 [Brown et al., 2001], is used to express that Europa’s atmospheric alkalis are endogenic because of the relatively close to the predicted value for the Europa’s ocean [Zolotov and Shock, 2001] than the meteoroid source value of ~13 [Carlson et al., 2009]. However, we have no definitive conclusions about the endogenic or exogenic origin of Europa’s alkalis at present, and the compositional relationship between the Europa’s ocean, the surface and the atmosphere is unknown. In addition, although an emission signal from magnesium atoms has been expected, no positive signal has been reported [Horst and Brown, 2013]. Further observations expect to bring better understandings for the source of these materials and interaction processes on and around Europa.

We search minor species, on the icy Galilean moons of Jupiter using the ground-based telescope of Hokkaido University (Pirka telescope, the primary mirror is 1.6 m in diameter). The Pirka telescope and its on-board observation device has started full-scale operation in 2011 with priority to observe planetary bodies in the Solar System. The multi spectral imaging device [Watanabe et al., 2012] has been installed at the Cassegrain focus of the telescope and it allow us to obtain surface spectral data with wavelength between 350 and 1050 nm. We observed the Galileo satellite in 2018-2020 and searched for sodium and calcium in the Io and Europa atmospheres. Here we will report the investigation.

Keywords: Galilean moon, atmosphere, ground-based observation

©2021. Japan Geoscience Union. All Right Reserved.

Development of PLANETS telescope: An attempt to reduce polishing volume in final polishing process by using an active mirror support

*Kazuya Nagata[1], Masato Kagitani[1], Yasumasa Kasaba[1], Takeshi Sakanoi[1], Yasuhiro Hirahara[2], Mikio Kurita[3]

1. Graduate School of Science, Tohoku University, 2. Graduate School of Environmental Studies, Nagoya University, 3. Graduate School of Science, Kyoto University

PLANETS (Polarized Light from Atmospheres of Nearby Extra-Terrestrial Systems) telescope is a 1.85 m off-axis telescope. It is developed with technical support from Nagoya University and Kyoto University, and in international collaboration between Tohoku University, Hawaii, Germany, and Brazil. It is going to be temporally installed in Japan late in 2021, and will be finally installed at the Haleakala observatory, one of the world’ s best astronomical observation sites. PLANETS telescope is the only medium aperture telescope in Japan located at Hawaii longitude, and can be a base for collaborative observations with small and medium aperture telescopes in Japan. The main targets of the PLANETS telescope are faint luminous phenomena around bright bodies, such as material eruptions from Io, Europa, Enceladus, and other solar system objects, and the rarefied atmospheres around Mars and Venus. To achieve these observations, it is necessary to suppress the diffraction and scattering of light from the bright bodies effectively and to increase the contrast with the faint emission spreading to the surroundings. PLANETS telescope is one of the biggest off-axis telescopes except for solar telescopes. It uses a Gregorian type with a concave elliptic secondary mirror, and there is no obstacle on the light path such as secondary mirror and its support structure, so there is no diffraction from them. Combining the off-axis design with a coronagraph and an adaptive optics enables high-contrast observations. In addition, long-term continuous observations are necessary to understand such atmospheric and plasma phenomena. PLANETS telescope can make a significant contribution to understand planetary atmospheric phenomena because it will be used for dedicated observation of own instrument and can provide a large amount of observation time. In this presentation, we report an attempt to reduce the polishing volume by using an active support mechanism in the final polishing of the primary mirror, which will start in May 2021, and the results of a test to verify the operation of the support mechanism.

The primary mirror is a Clearceram-Z HS with a diameter of 1.85 m and an edge thickness of 100 mm. As of February 2021, the primary mirror has been figured to surface error of 1.50 μm RMS, and the final polishing scheduled for May 2021 aims to achieve the surface error < 20 nm RMS for 30-cm spatial scale. Large volume of mirror material to be removed by polishing (polishing volume) leads to an increase in the time and cost required, so smaller polishing volume is desirable. We will reduce the polishing volume by using both of the following two methods. In the first method, a radius of curvature of the off-axis paraboloid, an off-axis distance, tip-tilt of the mirror surface and a rotation angle are adjusted so that the polishing volume is minimized for the mirror surface error. Changes of these parameters deform the surface figure linearly and independently when the parameter changes are small amounts. By tuning these parameters, the best-fit parameters are determined so that the polishing volume is minimized. This minimization basically reduces polishing volume by less than half for the surface figure error expressed up to the third order of Zernike polynomial with 2μm RMS amplitude. In the second method, the active support mechanism of the primary mirror is also applied to correct the surface figure error to reduce the polishing volume. PLANETS telescope uses a 36-point whiffletree for the axial support of the primary mirror. The whiffletree is combined with 33 warping harnesses consisting of leaf springs and linear motors to control the support force at each support point. This axial support is also used in the final polishing to

©2021. Japan Geoscience Union. All Right Reserved.

reduce the polishing volume by decreasing the surface figure error on large spatial scales. We used finite element analysis to validate the second method. Combination of these two methods successfully deforms the mirror surface in shapes expressed as Zernike polynomials up to the third order and less than about 20% error. We also simulated the minimization of the polishing volume for the current figure error of the primary mirror in advance of the final polishing. As a result, it was expected that the mirror surface error could be reduced from 1.5 μm RMS to 0.28 μm RMS, and the amount of polishing could be reduced by 80.5 %.

Prior to the final polishing, we are making tests to confirm the control repeatability and stability of the active support mechanism using the primary mirror and autocollimator. We will report the latest results in this presentation.

Keywords: Off-axis optical system, Planetary atmosphere and plasma, Mirror polishing

©2021. Japan Geoscience Union. All Right Reserved.

Numerical simulations of 500eV-50keV electron elastic collisions with neutral H_2O around Enceladus ~estimation of electron loss rate and auroral brightness~

*Hiroyasu Tadokoro[1], Yuto Katoh[2]

1. Surugadai University, 2. Tohoku University

Saturn's inner magnetosphere is dominated by water group neutrals (H_2O, OH, and O) originated from Enceladus. Previous studies suggested that the neutrals contribute to loss processes of plasma in the inner magnetosphere. However, little has been reported on a quantitative study of the electron loss process due to electron-neutral collisions. *Tadokoro and Katoh* [2014] focused on the loss process of 1 keV electron through the elastic collision with neutral H_2O. They examined the time variations of equatorial electron pitch angle distribution and electrons within loss cone through 1keV electron pitch angle scattering due to elastic collisions around Enceladus, conducting one dimensional test particle simulation. The result showed that the electrons of 11.4 % are lost in the time scale (~380 sec.) of the co-rotation of the flux tube passing through the region of the dense H_2O in the vicinity of Enceladus. The examination of elastic collisions with other electron energy is required to understand the electron loss process due to elastic collision.

We calculate the electron elastic collision in the energy range of 500 eV –50 keV. We show the electron loss rate into the atmosphere of Saturn and auroral brightness based on the loss rate.

Keywords: Saturn, Enceladus, test particle simulation, elastic collision, auroral brightness

©2021. Japan Geoscience Union. All Right Reserved.

Development of the near-infrared camera TOPICS and the Echelle spectrograph ESPRIT for planetary observations

Ayumu Kambara[1], *Takeshi Sakanoi[1], Yasuhiro Hirahara[2], Takashi Ichikawa[3], Masato Kagitani[1], Yasumasa Kasaba[1], Aya Otomo[1], Kazuya Nagata[1]

1. Planetary Plasma and Atmospheric Research Center, Graduate School of Science, Tohoku University, 2. Graduate School of Environmental Studies, Nagoya University, 3. Astronomical Institute, Graduate School of Science, Tohoku University

We are developing a near-infrared imager TOPICS (Tohoku Planetary near-Infrared Camera System) and echelle spectrograph ESPRIT (Echelle Spectrometer for Planetary Research In Tohoku University) to carry out long-term observations of variations in planetary and satellite atmospheres at Haleakala Observatory (3,055 m) in Hawaii. In this study, we improved the electronics of the InSb 256 x 256 array by developing a proper and safe driving system of TOPICS, and conducted the vacuum and cooling tests of ESPRIT.

We summarized the results of TOPICS as follows. (1) Development of the precise ammeter: We developed the precise ammeter circuits with two specifications in the range of ±500 μA with the resolution of ~0.0209 μA, and in the range of ±10 mA with the resolution of ~0.418 μA. These ammeters were combined with the driving and readout electronics. Measuring with the science grade detector (Raytheon, SCA#108), we obtained current values as estimated for the all lines. These values are used as references in the future safe operation. (2) Development of voltage input sequence control system. We developed the electronics that control the turn on and turn off sequence of voltages to the detector using logic device and analog switches. (3) Test with the engineer grade detector (Raytheon, SCA#060): We got similar images of a halogen lamp to that in the previous tests by using a bandpass filter (a center wavelength is 2.295 μm). Therefore, we verified proper work of the new electronics. (4) Test with science-grade detector: We got the images of halogen lamp successfully. However, dark current was high (2,230 e^-/s) and the read noise was also huge (1,730 e^-_{rms}). We require the dark current less than 40 e^-/s , and the read noise less than 60 e^-_{rms} to observe Jovian thermospheric ion wind velocity with an accuracy of ±0.5 km from Doppler shift of the emission line of the Jovian H_3^+ aurora. We found that the main noise source is the pre-amplifier, and will improve it soon. For the dark current, we found that the detector temperature was 47 K of which optimal temperature is 30-35K.

We summarized the updates of ESPRIT (wavelength range 1–4 μm, wavelength resolution 20,000) as follows. (5) Vacuum test: We carried out vacuum and leak tests of ESPRIT chamber with optical system. The vacuum level reached to be 2.47×10^{-7} Torr which is sufficient for this spectrograph. (6) Development of thermal path: Thermal paths between 1st and 2nd stages of He refrigerator, radiation shield, and cold plate on which the detector is mounted. The thermal paths are made of oxygen-free copper mesh (wire diameter: ϕ0.23 mm, density: 50 mesh/inch). We found that the temperature of radiation shield and internal optical system reached to be 96 K, and cold plate to be 14 K which satisfies temperature requirements.

We will reduce the dark and read noises of TOPICS soon, and plan to install it on the T60 telescope at Haleakala. The electronics of ESPRIT is similar to that of TOPICS, and we are ready to develop the electronics for ESPRIT.

©2021. Japan Geoscience Union. All Right Reserved.

Keywords: planetary atmosphere, spectroscopy, near infrared

©2021. Japan Geoscience Union. All Right Reserved.

Effects of the magnetic field configuration in the ionosphere on solar energetic electron precipitation into the Martian upper atmosphere observed by MAVEN

*Kanako Seki[1], Takuya Hara[2], Dave A Brain[3], Robert J Lillis[2], Darvin E Larson[2], Dave L Mitchell[2], Gina A Dibraccio[4], Janet G Luhmann[2], Bruce M Jakosky[3]

1. Graduate School of Science, University of Tokyo, 2. Space Sciences Laboratory, University of California, Berkeley, 3. Laboratory for Atmospheric and Space Physics, University of Colorado, Boulder., 4. Goddard Space Flight Center, NASA

Discovery of the diffuse aurora at Mars in the region where the crustal magnetic field is absent, indicates precipitation of the high-energy electrons of ~100 keV down to the altitudes around 70 km along the draped IMF around the planet [Schneider et al., Science, 2015; GRL, 2018]. However, how the draped magnetic field configuration around Mars controls the SEP (solar energetic particle) electron precipitation to the atmosphere is far from understood. Moreover, global simulations of the solar wind-Mars interaction have shown that the existence of the crustal magnetic fields primarily in the southern hemisphere results in the complexed magnetic structure around entire Mars [e.g., Luhmann et al., GRL, 2015].

We here investigated SEP events observed by MAVEN from December 2014 to October 2017 in order to investigate effects of the magnetic field structure in the ionosphere, including both the crustal magnetic fields and penetrating draped IMF, on SEP pitch angle distributions (PADs) and energy dependent loss into the atmosphere. The PADs of the high-energy (30-210 keV) electrons observed in the Martian ionosphere are analyzed in details. Using the elevation angle of the local magnetic field, we also sorted the data so as to investigate the SEP electron loss below the MAVEN periapsis (~150 km altitude). The obtained PA distributions in the ionosphere are compared with the distributions of the source electrons in the magnetosheath. For some of the strong SEP events, one-to-one correspondence of the SEP distributions to the strength and dip angle of the local magnetic field was investigated.

In most of SEP events, the field-aligned component is pronounced for the precipitating electrons before entering the collisional region of the atmosphere, even if the source SEP electrons have isotropic pitch angle distributions. The highest energy of the SEP electrons lost into the Martian atmosphere depends on the magnetic field configuration draped around the planet. The SEP electron precipitation depleted in the region of the strong crustal magnetic field. Its loss into the atmosphere tend to be pronounced in the nightside, suggesting the deeper penetration of draped magnetic fields in the nightside than dayside. We will also report on the energy dependent precipitation seen in some SEP events and discuss role of the magnetic field to determine the precipitation flux of SEP electrons into the Martian atmosphere.

Keywords: Mars, Solar Energetic Particle, aurora, Induced Magnetosphere

©2021. Japan Geoscience Union. All Right Reserved.

Observations of minor constituents in the Venusian atmosphere, CO and SOx using the millimeter/submillimeter-wave band radio telescopes, SPART/ALMA

Ayaka Tomihara[1], Teppei Yonetsu[1], Yuki Hamaguchi[1], Hideo Sagawa[2], *Hiroyuki Maezawa[1]

1. Department of Physical Science Osaka Prefecture University, 2. Kyoto Sangyo University

As exoplanets are being explored, there is an urgent theme to understand the atmospheric environment of habitable planets. In Venus, it is known that there is an unsolved absorption spectrum in the cloud region in the ultraviolet wavelength region. The temperature and pressure at this altitude are close to those at the troposphere of the Earth, and the spectrum is similar to that caused by bacteria, so that the possibility of absorption by organisms has been discussed. Atmospheric environment of the earth-type planet whose main component is CO_2 such as Venus and the past earth seems to be comparatively universal. Therefore, study how materials circulate via cloud heights in the Venusian atmosphere is also important in understanding how such circulations influence planetary habitability/organisms.

Against this background, we have observed the minor constituents of the Venusian atmosphere using the 10m single dish radio telescope, SPATR at the Nobeyama Radio Observatory of Japan, and ALMA interferometers. The millimeter/submillimeter-wave band high-resolution heterodyne spectroscopies allow us to address the molecular abundances at a higher altitude than the H2S4 clouds layer on both dayside and nightside of Venus. Since 2011, SPART has been monitoring the rotational spectral lines of carbon monoxide (CO) in the 100 and 200 GHz bands. The mixing ratio of CO at an altitude of about 80 km observed during the time appeared to be anti-correlated with the intensity of solar UV in the 11-year solar cycle. These trends were compared with the abundance of SO_2 observed by Venus Express (VEX) and the albedo observed by VEX/Akatsuki satellite. In addition, the preliminary results obtained with ALMA show the latitude/longitude and altitudinal distributions of SO and SO_2 are anti-correlated. In this conference, a brief picture of the material circulations in the Venus middle atmosphere inferred from these results will be also discussed.

Keywords: planetary atmosphere, Solar system, Venus, terrestrial planet, millimeter/submillimeter-wave band telescope, heterodyne spectroscopy

©2021. Japan Geoscience Union. All Right Reserved.

Influences of solar energetic particles on the Martian ozone layer

*Sayano Hiruba[1], Yuki Nakamura[1], Hiromu Nakagawa[1], Naoki Terada[1], Shotaro Sakai[1], Isao Murata[1], Yoshifumi Futaana[2]

1. Dept. of Geophysics, Graduate school of science, Tohoku University, 2. Swedish Institute of Space Physics

Solar energetic particles (SEPs) consist of protons, electrons and heavy ions in the energy range between a few tens of keV and GeV. SEPs are originated from solar flares, shock waves driven by coronal mass ejections.

SEPs penetrate the Earth’ s atmosphere down to tens of kilometers at high geomagnetic latitudes. The penetrating SEPs can change the composition in the middle atmosphere. During the large solar flare that occurred in October 2003, penetrating SEPs caused NO_2 enhancement by several hundred percent, accompanied by ozone depletion of tens of percent between 36 and 60 km altitudes (e.g., Seppälä et al., 2004; Rohen et al., 2005).

In the same event, Martian Radiation Environment Experiment (MARIE) onboard Mars Odyssey was disabled by SEPs (Zeitlin et al., 2010). In addition, SEPs emitted by a solar flare in September 2017 reached Mars, where global diffuse-aurora was reported on the entire Martian night side (Schneider et al., 2018). The SEP penetration imposes a critical influence on deep atmospheres and impacts on surfaces of various planets. Considering the increasing human activities in space, like planned national and international missions to the Moon and Mars, understanding the SEP behaviors in the planetary environment is critical to assess influences on the missions and human bodies. In addition, the ozone layer is vital for understanding how NOx increases in the Martian environment. The increase of NOx can have implications on the aspects of astrobiology and the past Martian greenhouse effect.

In this study, we aim to identify the response of the Martian ozone layer to SEP events. We use vertical profiles of ozone number densities observed by stellar occultation measurements by IUVS onboard MAVEN, and the energy fluxes of electrons and ions monitored by Solar Energetic Particle onboard MAVEN (MAVEN/SEP). MAVEN/IUVS has regularly conducted stellar occultation campaigns (1-2 days per campaign) once every ~2-3 months (Groller et al., 2018). MAVEN/SEP can detect electron's and ion's energy spectra from 20 keV to 1 MeV and from 20 keV to 6 MeV in the differential flux range of $3\text{-}3\times10^6$ eV/cm^2 s sr eV (Larson et al., 2015).

As the first step of this study, we focus on a SEP event at Mars measured on 3-4 November 2015. Comparing the data during this SEP event with those during another period when the quiet period of solar activity under similar seasonal and latitudinal conditions, we found no significant differences in the ozone profiles.

We then estimated the amount of ozone depletion by oxygen atoms induced by the SEP flux using a Monte-Carlo model. In this model, we assumed that SEP-induced oxygen atoms would instantaneously destroy ozone for simplicity. The model suggests only ~0.1% of depletion of ozone number density from the background for the event in 2015. The depletion is too low to be detected by IUVS. On the other hand, the model suggests that the depletion of ozone is at detectable levels (about 100 % of the background) during the large flux SEP event in the September 2017 event. Note that the used model is yet simple. For example, we have to consider the ozone depletion by the catalytic cycle of HOx. The cycle

©2021. Japan Geoscience Union. All Right Reserved.

plays an essential role on the Earth. We will further develop a further photochemical model to assess the effect of SEPs on the photochemistry of the Martian atmosphere.

Since the MAVEN data are only available after 2014, we are analyzing the data from Mars Express (MEX). The vertical profiles of ozone number densities can be obtained from the observation by stellar occultation of SPICAM and the SEP flux is from the background counts of energetic particles observed by the Analyzer of Space Plasma and Energetic Atoms (ASPERA-3). MEX/SPICAM stellar occultations are applied to retrieve the ozone profiles since 2004. MEX/ASPERA-3 can record the penetrating energetic particles through the instrument structure as background counts (Ramstad et al., 2018). In this presentation, we will use these data for further analysis to evaluate the effect of SEPs on atmospheric chemistry on Mars.

Keywords: Mars, Solar Energetic Particles, ozone

©2021. Japan Geoscience Union. All Right Reserved.

Simultaneous remote and in-situ observations of ionospheric irregularities at Mars

*Hina Bando[1], Yuki Harada[1], Naoki Terada[2], Hiromu Nakagawa[2]

1. Kyoto University, 2. Tohoku University

It is known that the ionosphere of Mars contains a variety of irregularities. Gurnett et al., [2008] reported that “diffuse echoes”, the traces of which appear unusually diffuse in an ionogram, are sometimes observed by topside ionospheric sounding of Mars Express. These echoes are proposed to be caused by irregularities in the Martian ionosphere. Also, in addition to vertical echoes reflected from the horizontally stratified ionosphere, “oblique echoes” sometimes appear as hyperbola-shaped traces in a radargram. These echoes are typically found in regions where the Martian crustal magnetic field is nearly vertical, and they are interpreted as echoes reflected obliquely from electron density structures deviated from horizontally stratified ionosphere. However, the spatial scale lengths and generation mechanisms of ionospheric irregularities that cause diffuse and oblique echoes are still unknown, partly because comparative studies utilizing remote and in-situ measurements of ionospheric irregularities are yet to be conducted at Mars.

In this study, we surveyed conjunction events in which Mars Express and MAVEN observed the topside ionosphere of Mars at almost the same time and the same location, searching for cases with diffuse echoes or oblique echoes apparent in the Mars Express data. We then investigated variations of the electron, ion,and neutral densities, magnetic fields, and the presence or absence of the hot electron precipitation from MAVEN data. Based on the analysis, it is suggested that the spatial scale lengths of irregularities causing diffuse echo and oblique echoes range from tens to hundreds of kilometers. Additionally, we found an event that exhibits intense diffuse echoes in ionograms, and periodic variations of neutral and ion densities in in-situ data, implying ion-neutral coupling. These observations would provide an important clue as to the unidentified drivers of ionospheric irregularities causing diffuses echoes at Mars.

Keywords: Mars ionospheric irregularities

©2021. Japan Geoscience Union. All Right Reserved.

Annual variability in the thermospheric wave perturbations at Mars

*Hiromu Nakagawa[1], Nao Yoshida[1], Kaori Terada[1], Naoki Terada[1], Yuki Harada[2], Shotaro Sakai[1], Takeshi Imamura[3], Hitoshi Fujiwara[4], Kanako Seki[5]

1. Planetary Atmosphere Physics Laboratory, Department of Geophysics, Graduate School of Science, Tohoku University, 2. Kyoto University, 3. Graduate School of Frontier Scienfes, The University of Tokyo, 4. Faculty of Science and Technology, Seikei University, 5. Graduate School of Science, University of Tokyo

Although there have been very limited observations in the Martian thermosphere, especially on the night side, our understanding of the region has been rapidly enhanced in recent years by the MAVEN spacecraft (Bougher et al. (2015) ; Yigit et al. (2015) ; England et al; Siddle et al. (2019) ; Nakagawa et al. (2020) Recent observations have reported that wave-like perturbations are ubiquitously observed in the thermosphere, especially on the night side, with large amplitude density perturbations exceeding 50%. The anti-correlated amplitudes with the background temperature suggest the saturated atmospheric gravity wave (Terada et al., 2017). There are two possible excitation sources: (1) atmospheric gravity waves propagating upward from the lower atmosphere, and (2) energy injected from the upper atmosphere by external factors such as solar wind or energetic solar particles.

The widespread diffuse aurora on Mars (Schneider et al., 2015, 2020), recently discovered by the MAVEN spacecraft, is a luminous phenomenon that covers the entire Martian night side with the arrival of solar energetic particles (SEPs) and has an emission altitude of 60 km. This suggests that energetic particles can have a significant impact on the deep Martian atmosphere by globally injecting energy. In particular, ionization, dissociation, heating, and disturbance effects in the upper atmosphere can potentially have an impact on the escaping atmosphere, and are important for understanding the response of Mars, a non-magnetic planet, to space environment changes.

In this study, we use the MAVEN onboard mass spectrometer NGIMS to reveal the long-term interannual variation of density perturbation components in the Martian thermosphere. In particular, NGIMS has realized the multi-molecular observation since Viking, and here we focus on the difference in behavior between CO_2 and N_2 density perturbations in order to constrain the excitation source. In this study, we used the MAVEN/NGIMS data Level-2 and version-8 registered in NASA PDS.

In the evolution of the CO_2 density disturbance components over the five-year period from 2015 to 2020, we find that the amplitude of the density perturbations is significantly larger in the nighttime than in the daytime throughout the five-year period. This is consistent with the results of recent previous studies (Terada et al., 2017; Nakagawa et al., 2020). On the other hand, it should be noted that the amplitude of the density disturbance differs from year to year. In this paper, we will discuss in detail the relative importance of the lower and external factors on the interannual variation. Another important feature is the relationship between the perturbation amplitude components of CO_2 and N_2. The statistical results show that the two are basically well correlated, with CO_2 of a larger perturbation amplitude than N_2. This is consistent with the arguments of Cui et al. (2014) and England et al. (2016, 2017), because the disturbance amplitude normalized by the background density is anti-correlated to the scale height, and the amplitude ratio corresponds to the mass ratio of the molecular species. In fact, a scatter plot of the disturbance amplitudes of CO_2 and N_2 shows a distribution that follows with a mass ratio of 28/44 ~ 0.64, the mass ratio of CO_2 and N_2. Analysis of the perturbation components for each orbit shows that CO_2 and N_2 are well in phase with each other in many cases. On the other hand, we also find the N_2 perturbation

©2021. Japan Geoscience Union. All Right Reserved.

amplitude sometimes exceeds that of CO_2, meanwhile the perturbations seen in N_2 appear to be out of phase with those in CO_2. Interestingly, according to the predictions of the full-particle Direct Simulation Monte-Carlo (DSMC) modeling of the Martian upper atmosphere (Terada et al., 2016), the atmospheric waves excited at thermospheric altitudes during the injection of energetic particles from space have different wavelengths and amplitudes at each species. It is suggested that the amplitude of N_2 perturbations exceeds that of CO_2 at the distance from the source region (Terada et al., in prep.). In this paper, we compare and discuss the predictions with this numerical model and the implications of the observations.

Keywords: Mars, thermosphere, atmospheric wave

©2021. Japan Geoscience Union. All Right Reserved.

Study of atmospheric ion escape from exoplanet TOI-700 d

*Tomoaki Nishioka[1], Kanako Seki[1], Ryoya Sakata[1], Kazuhiro Yamamoto[1], Naoki Terada[2], Hiroyuki Shinagawa[3]

1. Graduate School of Science, University of Tokyo , 2. Graduate School of Science, Tohoku University , 3. NICT

An important purpose of detecting and characterizing exoplanets is to find habitable planets like Earth. Liquid water is essential for planetary habitability, and it is necessary to retain the atmosphere in strong stellar wind to maintain liquid water. By the Transiting Exoplanet Survey Satellite (TESS), exoplanet TOI-700 d was discovered in January 2020 (Gilbert et al., AJ, 2020; Rodriguez et al., AJ, 2020). This is the first Earth-sized planet in the habitable zone (HZ) discovered by TESS. The host star is a M dwarf star, which has lower surface temperature, thus closer HZ to the host star, and stronger X-ray and EUV (XUV) radiation in HZ than the solar system around a G-type star. Another important difference is that direction of the interplanetary magnetic field (IMF) around the planet may be dominated by the radial component because of the proximity to the host star and planet. The IMF orientation can change the atmospheric escape rate from the exoplanet. In this study, we investigated effects of the XUV radiation and IMF orientation on the atmospheric ion escape.

In order to simulate the atmospheric ion escape from TOI-700 d, we used multi-species MHD simulations (e.g., Terada et al., JGR, 2009; Sakata et al., JGR, 2020). Our model solved three-dimensional multispecies MHD equations including continuity equations for 10 ion species (O^+, O_2^+, CO_2^+, NO^+, CO^+, N_2^+, N^+, C^+, He^+, H^+) the bottom of the ionosphere to the inter-planetary space where a constant stellar wind is assumed. The model includes photoionization, electron impact ionization, charge exchange, ion-neutral reactions, dissociative recombination, collisions (ion-electron, ion-neutral, electron-neutral). As stellar wind conditions, number density, velocity, and temperature were set to 450 cm^{-3}, 470 km s^{-1}, and 1.3×10^6 K, respectively, by referring to previous studies (Cohen et al., ApJ, 2020; Dong et al., ApJL, 2020). IMF was assumed to be a Parker spiral with an angle of 4˚ or 45˚ degrees and a magnitude of 12 nT. Also, the stellar XUV flux was set either as 30 or 50 times larger than the current value of the Earth (referred as XUV30 and XUV50 hereafter). We assumed a Venus-like atmospheric composition that depends on the stellar XUV flux as the input neutral atmosphere based on Kulikov et al. (Space Sci. Rev., 2007).

The results show that the IMF Parker spiral angle affects the structure of the induced magnetosphere. Therefore, the path of atmospheric ion escape differs greatly depending on whether IMF Parker spiral angle is 4˚ or 45˚. In the case of 45˚, the escape flux is confined to the current sheet similar to Mars and Venus in the solar system. This is because a typical induced magnetosphere is formed and the magnetic tension force of the drape magnetic field in the polar region accelerates the local ionospheric plasma. In the case of 4˚, the escape from around SZA = 65˚ in the ionosphere becomes a ring-shaped escape flux in the induced magnetotail. The stellar XUV flux has a stronger effect on the escape rate of atmospheric ions than the IMF orientation. The larger the stellar XUV flux, the more atmospheric ions escape. This is because the scale height of atmospheric ions increases due to the increase in the stellar XUV flux. In the case of XUV50 and IMF angle 45˚, the atmospheric ion escape rate obtained in this study is ~2.3×10^{27} s^{-1}, which is about an order of magnitude larger than the value to be able to retain the 1-atm CO_2 atmosphere for about 10 billion years (Dong et al., ApJL, 2020). This result suggests that even if the atmosphere of TOI-700 d is Venus-like, it will be difficult to maintain it for a long time under strong XUV condition. This study also reveals that the escape rate of atmospheric ions, especially molecular ions, can be suppressed by small IMF Parker spiral angle which can become typical as the planet and the host star

©2021. Japan Geoscience Union. All Right Reserved.

get closer.

Keywords: exoplanet, atmospheric escape, MHD Simulation

©2021. Japan Geoscience Union. All Right Reserved.

DSMC simulations of slow hydrodynamic escape from Earth-like and Mars-like planets

*Naoki Terada[1], Kaori Terada[1], Hitoshi Fujiwara[2], Masahiro Ikoma[3]

1. Graduate School of Science, Tohoku University, 2. Faculty of Science and Technology, Seikei University, 3. Graduate School of Science, The University of Tokyo

We have developed full-particle simulation models that solve the slow hydrodynamic escape from Earth-like and Mars-like planets based on the Direct Simulation Monte Carlo (DSMC) method to understand the long-term evolution of the atmospheres of these planets. While hydrodynamic and Jeans escape processes are relatively well understood, the transition between the two, i.e., slow hydrodynamic escape process, has been less thoroughly investigated due to difficulties in its theoretical and numerical treatment. The slow hydrodynamic escape is one of the candidate processes that would have caused the drastic climate change on early Mars and have significantly changed the amount and composition of the atmosphere. The DSMC method is able to self-consistently solve the slow hydrodynamic escape without imposing a priori assumptions on the boundary condition and molecular diffusion. We first developed a full-particle DSMC model of the upper atmosphere of an Earth-like planet and then implemented photochemistry related to atomic carbon for a Mars-like planet. Our simulation results showed that the adiabatic cooling associated with the slow hydrodynamic expansion was weakened due to infrequent intermolecular collisions around the exobase, hence higher exobase temperature and escape rates were obtained than previous fluid models. In this presentation, we will show simulation results of Earth-like and Mars-like atmospheres subject to intense EUV radiation and compare them with fluid models.

Keywords: Atmospheric escape, DSMC simulation

©2021. Japan Geoscience Union. All Right Reserved.

[J] Poster | A (Atmospheric and Hydrospheric Sciences)：A-AS Atmospheric Sciences, Meteorology & Atmospheric Environment

Thu. Jun 3, 2021 5:15 PM - 6:30 PM JST | Thu. Jun 3, 2021 8:15 AM - 9:30 AM UTC | Ch.02_2

[A-AS06] Stratosphere-troposphere Processes And their Role in Climate

convener:Takenari Kinoshita(Japan Agency for Marine-Earth Science and Technology), Takatoshi Sakazaki(Graduate School of Science, Kyoto University), Masashi Kohma(Department of Earth and Planet Science, Graduate School of Science, The University of Tokyo), Nawo Eguchi(Kyushu University)



The dynamical, radiative, and chemical processes involved in the interactions between the stratosphere and troposphere are essential for understanding the present and future climate. Both observed data and high-resolution models have now clearly demonstrated that stratospheric processes can affect various tropospheric phenomena. On the other hand, it has been confirmed that the stratospheric processes are changing significantly with climate change. For example, the polar vortex was exceptionally strong, cold, and persistent in the Northern Hemisphere winter stratosphere in 2019-2020, resulting in record ozone depletion and contributing to unusually warm temperatures in mid-latitudes.
In this session, we will focus on stratospheric phenomena and invite presentations on the latest findings (case studies, long-term variations, predictability, etc.). We welcome studies on the effects of these phenomena on the troposphere and mesosphere. Inheriting the significance of the Stratosphere-troposphere Processes And their Role in Climate (SPARC) sessions held at JpGU, this division aims to enhance the development of this field in close cooperation with the atmospheric chemistry sessions.

[AAS06-P01] Radiosonde Observations in the 30-40 km Altitude Range Using 3000 g Balloons

*Takenari Kinoshita[1], Shin-Ya Ogino[1], Junko Suzuki[1], Ryuichi Shirooka[1], Takuji Sugidachi[2], Kensaku Shimizu[2], Matthew H Hitchman[3] (1.Japan Agency for Marine-Earth Science and Technology, 2.Meisei Electric Co. Ltd., 3.University of Wisconsin-Madison)

[AAS06-P02] Influence of a SH SSW in September 2019 on tropical tropospheric circulation and deep convective activity

*Kunihiko Kodera[1], Shunnsuke Noguchi[2], Nawo Eguchi[3], Tomoe Nasuno[2] (1.Meteorological Research Institute, 2.JAMSTEC, 3.Kyushu University)

[AAS06-P03] Dynamical analysis of extreme tropopause folding events in the coastal region of Antarctica

Masatoshi Mizukoshi[1], *Masashi Kohma[1], Kaoru Sato[1] (1.Department of Earth and Planet Science, Graduate School of Science, The University of Tokyo)

[AAS06-P04] Response of the Brewer-Dobson circulation to the major volcanic eruptions in reanalysis datasets

*Masatomo Fujiwara[1], Marta Abalos[2], Patrick Martineau[3], Jonathon Wright[4] (1.Faculty of Environmental Earth Science, Hokkaido University, 2.Universidad Complutense de Madrid, 3.JAMSTEC, 4.Tsinghua University)

[AAS06-P05] Impact of the upper troposphere and stratosphere on the climate change around Japan

*Yoshio Kawatani[1], Takeshi Horinouchi[2], Naoki Sato[3] (1.Japan Agency for Marine-Earth Science and Technology, 2.Faculty of Environmental Earth Science, Hokkaido University, 3.Tokyo Gakugei University)

[AAS06-P06] Analysis of Arctic spring ozone anomaly in the phases of QBO and 11-year solar cycle for 1979–2011

Yousuke Yamashita[1,2], *Hideharu Akiyoshi[1], Masaaki Takahashi[1,3] (1.National Institute for Environmental Studies, 2.Japan Agency for Marine-Earth Science and Technology, 3.Atmosphere and Ocean Research Institute, The University of Tokyo)

[AAS06-P07] Morphology of zonal asymmetry of QBO zonal wind

*Takatoshi Sakazaki[1], Kevin Hamilton[2], Yoshio Kawatani[3] (1.Graduate School of Science, Kyoto University, 2.International Pacific Research Center, University of Hawai'i, 3.Japan Agency for Marine-Earth Science and Technology)

[AAS06-P08] Relationships between Unusual Antarctic Ozone Hole in 2019 and Dynamical Fields

*Guangyu Liu[1], Toshihiko Hirooka[2], Nawo Eguchi[3] (1.Department of Earth and Planetary Sciences, Graduate School of Science, Kyushu University, 2.Department of Earth and Planetary Sciences, Faculty of Science, Kyushu University, 3.Research Institute for Applied Mechanics, Kyushu University)

Radiosonde Observations in the 30-40 km Altitude Range Using 3000 g Balloons

*Takenari Kinoshita[1], Shin-Ya Ogino[1], Junko Suzuki[1], Ryuichi Shirooka[1], Takuji Sugidachi[2], Kensaku Shimizu[2], Matthew H Hitchman[3]

1. Japan Agency for Marine-Earth Science and Technology, 2. Meisei Electric Co. Ltd., 3. University of Wisconsin-Madison

Observation of temperature and wind velocity in the 30–40 km altitude layer have been sparse since the elimination of the standard rocketsonde sounding network in 1990s. In an effort to the vertical range of radiosonde observations into the upper stratosphere, experiments were conducted with a 3000 g balloon at Tsukuba, Japan on November 5, 2019. Four radiosondes were launched, with two reaching above 40 km altitude. To confirm the accuracy of the obtained data, especially the temperature data, these profiles were compared with satellite and reanalysis data in the 30–40 km layer. The ability to quantify gravity wave parameters from the obtained data is described, with application to wave events detected near 38–40 km. This system extends the ability to provide information regarding gravity wave and planetary wave activity upward to ~40 km. Finally, we will introduce an enhanced observation campaign using this system.

Keywords: radiosonde, atmospheric waves

©2021. Japan Geoscience Union. All Right Reserved.

Influence of a SH SSW in September 2019 on tropical tropospheric circulation and deep convective activity

*Kunihiko Kodera[1], Shunnsuke Noguchi[2], Nawo Eguchi[3], Tomoe Nasuno[2]

1. Meteorological Research Institute, 2. JAMSTEC, 3. Kyushu University

A large stratospheric sudden warming (SSW) occurred in early September 2019 in the southern hemisphere (SH). Although stratospheric polar vortex was not broken up as the SSW in September 2002, changes associated with the Brewer-Dobson circulation were large and the tropical lower stratospheric temperature was largely decreased. A possible impact of the 2019 SH SSW on development of the tropical convection along the ascending branch of the Hadley circulation was demonstrated by Noguchi et al. (2020) by means of ensemble mean forecast experiment.

In the present study, we show that enhanced tropical convective activity induced by the SSW lead global development of tropical storms and cyclones in the Eastern and Western Pacific as well as the Atlantic sectors. Changes in the tropical convection also modified a distribution of subtropical high and subtropical jet. Accordingly, trajectory of the cyclone was influenced through change in environmental wind field. For instance, tropical cyclone Lingling, formed on 31 August over Philippine Sea, which has been forecasted to hit southwest of the Korean peninsula around 7 September, finally went slightly westward and landed on North Korea due to development of Bonin subtropical high. This development of Bonin high also produced a very high temperature over Japan in early September 2019, could also be related to an effect of this SH SSW on tropical convection.

Keywords: SSW, Tropical circulation, Convection

©2021. Japan Geoscience Union. All Right Reserved.

Dynamical analysis of extreme tropopause folding events in the coastal region of Antarctica

Masatoshi Mizukoshi[1], *Masashi Kohma[1], Kaoru Sato[1]

1. Department of Earth and Planet Science, Graduate School of Science, The University of Tokyo

Rapid and deep descent in the tropopause (the so-called tropopause folding; TF) is often observed in the extratropics. Previous studies examined the global distribution of frequency of TF events using reanalysis data [e.g., Škerlak et al., 2015]. They showed that the frequency of deep TF is maximized along the coast of Antarctica. However, the dynamics of TF in the Antarctic region have not yet been studied adequately. In the present study, the extreme TF in the Antarctic are examined using state-of-art reanalysis data to clarify the uniqueness of TF in the Antarctic.

Extreme TF events were defined as time periods during which the deviation of the dynamical tropopause height from 30 days running mean is negatively large. Fluctuations associated with the synoptic-scale eddies are extracted with a high-pass filter with a cut-off period of 10 days. Composite analyses of the extreme TF events at Syowa Station are performed.

When the negative anomaly of tropopause height is maximized, the significant downwelling is observed at the location of the extreme TF. From the analyses using Q-vector in the quasi-geostrophic equation, it is found that the divergence of the Q-vector is observed to the north of Syowa Station. The distribution of Q-vector is explained by the local westerly jet and strengthening of the frontal structure associated with a synoptic low-pressure system extending west-east centered at 70˚S over Antarctica and a high-pressure system.

The synoptic low-pressure system extending east-west centered at 70˚S over Antarctica is discussed based on ray tracing theory under the WKB approximation. The low-pressure system extends northeast-southwest from 24 hours before the lowest tropopause is observed, which means that this system has a southward group velocity. From the ray tracing theory, the meridional wavenumber increases with southward propagation of the wave packet since a strong meridional PV gradient associated with radiative cooling along the coast of Antarctica. Then, the meridional scale of the system becomes small. As a result, the westerly jet and frontal structure are enhanced along the coast of Antarctica. Then, the strong downward flow is located to the south of the entrance of the westerly jet. And thus, it is considered that the frequent occurrence of extreme TF along the coast of Antarctica is mainly due to the enhanced downwelling associated with shrinkage of the synoptic low-pressure system in the meridional direction.

Keywords: Tropopause folding, Antarctic

©2021. Japan Geoscience Union. All Right Reserved.

Response of the Brewer-Dobson circulation to the major volcanic eruptions in reanalysis datasets

*Masatomo Fujiwara[1], Marta Abalos[2], Patrick Martineau[3], Jonathon Wright[4]

1. Faculty of Environmental Earth Science, Hokkaido University, 2. Universidad Complutense de Madrid, 3. JAMSTEC, 4. Tsinghua University

The responses of the Brewer-Dobson circulation (BDC, i.e., the residual mean circulation) to the eruptions of Mt. Agung in March 1963, El Chichón in April 1982, and Mt. Pinatubo in June 1991 are investigated using global atmospheric reanalysis datasets, JRA-55, MERRA-2, and ERA-Interim. Multiple linear regression is applied to the zonal and monthly mean time series of temperature, zonal wind, BDC stream function, Eiassen-Palm flux divergence, and other variables/terms for two periods, 1980–2010 (for the three datasets) and 1958–2001 (for JRA-55 only), by considering explanatory factors of seasonal harmonics, linear trends, Quasi-Biennial Oscillation, solar cycle, and El Niño Southern Oscillation. The residuals are used to define the volcanic signals for the three eruptions separately.

Analysis using JRA-55 data showed the following: (1) in the first DJF season after each eruption, the Northern-Hemisphere BDC cell was weakened after Mt. Pinatubo and Mt. Agung eruptions, but was strengthened after El Chichón eruption; (2) in the second-year JJA, the Southern-Hemisphere BDC cell was weakened after El Chichón and Mt. Agung eruptions, but was strengthened after Mt. Pinatubo eruption. MERRA-2 and ERA-Interim showed qualitatively the same results for Mt. Pinatubo and El Chichó n eruptions as JRA-55. Thus, the BDC response was different for different eruptions and for different seasons. The EPFD response (anomaly) was found to correspond to the BDC (v_bar_star) response (anomaly) for all the cases. Interpretation of these results will be discussed at the meeting.

Keywords: Brewer-Dobson circulation, volcanic eruption

©2021. Japan Geoscience Union. All Right Reserved.

Impact of the upper troposphere and stratosphere on the climate change around Japan

*Yoshio Kawatani[1], Takeshi Horinouchi[2], Naoki Sato[3]

1. Japan Agency for Marine-Earth Science and Technology, 2. Faculty of Environmental Earth Science, Hokkaido University, 3. Tokyo Gakugei University

Impact of the upper troposphere and stratosphere on the climate change around Japan was investigated by analyzing CMIP5 model datasets for historical and rcp8.5 scenarios. Based on previous studies (Zappa and Shepherd 2017, Manzini et al. 2014), two remote drivers of climate were selected; tropical warming defined as temperature changes at 250 hPa in 30˚S-30˚N and stratospheric vortex strength defined as zonal mean zonal wind changes at 20 hPa in 70˚-80˚N. These indices were scaled by annual mean 2-m temperature changes associated with global warming. Here, climate response in cold season (November to April) was investigated by subtracting 1959-1990 from 2068-2099 mean data. Models with low tropical amplification and weak polar vortex projected southward shift of the subtropical jet over the east Asia. Higher SLP anomalies elongated from southeast Asia toward Japan, and negative precipitation anomalies extended from southwest to northeast. On the other hand, models with high tropical amplification and strong polar vortex projected northward shift of the subtropical jet. Higher SLP anomalies with an extreme value over the central Pacific were formed and their western parts covered most of Japan regions. Negative precipitation anomalies were seen in the southern part of Japan while positive anomalies were found in the northern part. These results demonstrate that different responses of global warming in the upper troposphere and lower stratosphere could affect climate changes around Japan.

Acknowledgement
This research was performed by the Environment Research and Technology Development Fund (JPMEERF20192004) of the Environmental Restoration and Conservation Agency of Japan.

Keywords: Troposphere-Stratosphere coupling

©2021. Japan Geoscience Union. All Right Reserved.

Analysis of Arctic spring ozone anomaly in the phases of QBO and 11-year solar cycle for 1979–2011

Yousuke Yamashita[1,2], *Hideharu Akiyoshi[1], Masaaki Takahashi[1,3]

1. National Institute for Environmental Studies, 2. Japan Agency for Marine-Earth Science and Technology, 3. Atmosphere and Ocean Research Institute, The University of Tokyo

This study investigates Arctic spring ozone in relation to the phase of quasi-biennial oscillation (QBO)/the 11-year solar cycle, using satellite observations, reanalysis data, and outputs of a chemistry climate model (CCM) during the period of 1979–2011. For this duration, we found that the composite mean of the Northern Hemisphere high-latitude total ozone in the QBO-westerly (QBO-W)/solar minimum (S_{min}) phase is slightly smaller than those averaged for the QBO-W/S_{max} and QBO-E/S_{max} years in March. An analysis of the passive ozone tracer defined at the pressure levels between 220 hPa and 12 hPa in the CCM simulation indicates that this negative anomaly is primarily caused by transport. The negative anomaly is consistent with a weakening of the residual mean downward motion in the polar lower stratosphere. The contribution of chemical processes estimated using the column amount difference between ozone and the passive ozone tracer is less than 6% of the total anomaly in February and between 10–20% in March. The lower ozone levels in the Arctic spring during the QBO-W/S_{min} years are associated with a stronger Arctic polar vortex from late winter to early spring, which is linked to the reduced occurrence of sudden stratospheric warming in the winter during the QBO-W/S_{min} years.

Keywords: Arctic, ozone, QBO, 11-year solar cycle, CCM, sudden stratospheric warming

©2021. Japan Geoscience Union. All Right Reserved.

Morphology of zonal asymmetry of QBO zonal wind

*Takatoshi Sakazaki[1], Kevin Hamilton[2], Yoshio Kawatani[3]

1. Graduate School of Science, Kyoto University, 2. International Pacific Research Center, University of Hawai'i, 3. Japan Agency for Marine-Earth Science and Technology

Although the QBO primarily shows a zonally symmetric nature, a smaller but significant eddy component is sometimes observed. This study demonstrates the basic morphology of zonal asymmetry in QBO zonal wind in the middle stratosphere based on the statistical analysis of the ERA5 dataset from 1958 to 2019. As pointed out by previous studies, the zonal eddy component is found to be statistically large in the westerly phase of QBO during boreal/austral winter seasons, since the tropical westerly allows a lateral, equatorward propagation of stationary planetary waves from the winter Hemisphere. Moreover, it is found that the QBO eddy component shows a strong inter-annual to decadal variability; the underlying processes (and possibly the uncertainty in QBO wind in reanalyses) will be discussed in the poster.

Keywords: Stratosphere, Quasi-biennial oscillation, Zonal asymmetry

©2021. Japan Geoscience Union. All Right Reserved.

Relationships between Unusual Antarctic Ozone Hole in 2019 and Dynamical Fields

*Guangyu Liu[1], Toshihiko Hirooka[2], Nawo Eguchi[3]

1. Department of Earth and Planetary Sciences, Graduate School of Science, Kyushu University, 2. Department of Earth and Planetary Sciences, Faculty of Science, Kyushu University, 3. Research Institute for Applied Mechanics, Kyushu University

Extreme ozone depletion occurs during early austral spring in the lower strarosphere over Antarctica, i.e., the Antarctic ozone hole, showing large interannual changes in its area as well as its ozone depletion amount. In 2019 a minor Antarctic sudden stratospheric warming (SSW) was observed in September and a smaller ozone hole was developed over Antarctica. Before this year, a small Antarctic ozone hole was also formed in 2017, even though there occurred no pronounced sudden stratospheric warmings. Hence, in this study, we use the Aura Microwave Limb Sounder (MLS) observations and the Japanese 55-year Reanalysis (JRA-55) data to try to find plausible mechanisms to bring about such small ozone holes in the two years. Resultantly, our ozone volume mixing ratio analyses show that positive volume mixing ratio anomalies from the climatological seasonal march appeared in the polar lower and middle stratosphere throughout the spring in both two years, which corresponds to the insufficient ozone hole development. We examined dynamical analyses based on Eliassen-Palm (E-P) flux and the residual mean meridional circulation and found that the wave activity of zonal wavenumber 1 was extremely strong in 2019 to cause the minor SSW while that of zonal wavenumbers 1 and 2 became strong intermittently in 2017; thus, the enhanced wave activity induced downward advection of ozone-rich air to bring about the small ozone holes.

Keywords: Antarctic Ozone Hole

©2021. Japan Geoscience Union. All Right Reserved.

[J] Poster | A (Atmospheric and Hydrospheric Sciences)：A-OS Ocean Sciences & Ocean Environment

Thu. Jun 3, 2021 5:15 PM - 6:30 PM JST | Thu. Jun 3, 2021 8:15 AM - 9:30 AM UTC | Ch.03_3

[A-OS18] Kuroshio Large Meander

convener:Toru Miyama(Japan Agency for Marine-Earth Science and Technology, Application Laboratory), Norihisa Usui(Meteorological Research Institute), Hidetaka Hirata(Rissho University), Takashi SETOU(Japan Fisheries Research and Education Agency)

The Kuroshio Large Meander that started in August 2017 is the second longest historic event in the observed record, next to the event in 1975-1980 (4 years and 8 months). In October 2020, a massive eddy separation occurred, and the Kuroshio path is beginning to take shape in a way that has not been seen before. There are strong public interests on the possible impacts of the Kuroshio Large Meander on fisheries and other phenomena along the coast. However, the actual impacts have not been well investigated. In addition, new findings such as the impacts of the Kuroshio Large Meander on weather are emerging. This session aims to shed light on this intriguing phenomenon by discussing its trends, dynamics, impacts, and comparison with past examples. Presentations from a variety of perspectives in the fields of ocean physics, biology, chemistry, and atmospheric effects will be welcomed.

[AOS18-P01] Characteristics and evolution of the cyclonic eddy in the Kuroshio coastal area in association with the Kuroshio large meander

★Invited Papers

*Daiki Ito[1], Takashi Setou[1], Daisuke Ambe[1], Yugo Shimizu[1,2] (1.Fisheries Resources Institute, Japan Fisheries Research and Education Agency, 2.(Present affiliation) Fisheries Agency)

[AOS18-P02] The relationship between Kuroshio meander and observed tidal-regime shift along southern coast of Japan

*Takumi Kamura[1], Hiromi Matsuura[1], Katsuto Uehara[2] (1.Interdisciplinary Graduate School of Engineering Sciences, Kyushu University, 2.Research Institute for Applied Mechanics, Kyushu University)

[AOS18-P03] Eddy separation from the Kuroshio Large Meander in 2020

*Toru Miyama[1], Yasumasa Miyazawa[1], Sergey M Varlamov[1], Zhang Ruochao[1] (1.Japan Agency for Marine-Earth Science and Technology, Application Laboratory)

[AOS18-P04] Study on the temporal and spatial variation of the Kuroshio Current path

*Yuya Hirano[1], Kazuyuki Uehara[1] (1.Graduate School of Earth Environmental Science, Tokai University)

[AOS18-P05] Impact of a Marine Heatwave Attributable to a Kuroshio Large Meander on Extreme Heavy Rainfall Caused by an Extratropical Cyclone

*Eigo Tochimoto[1], Satoshi Iizuka[1] (1.National Research Institute for Earth Science and Disaster Resilience)

[AOS18-P06] The Kuroshio volume transport in near future estimated by Reduced Gravity model

*Takashi SETOU[1], Akira KUSAKA, Daisuke Ambe, Daiki Ito[1], Takashiko Kameda (1.Japan Fisheries Research and Education Agency)

Characteristics and evolution of the cyclonic eddy in the Kuroshio coastal area in association with the Kuroshio large meander

*Daiki Ito[1], Takashi Setou[1], Daisuke Ambe[1], Yugo Shimizu[1,2]

1. Fisheries Resources Institute, Japan Fisheries Research and Education Agency, 2. (Present affiliation) Fisheries Agency

The Kuroshio coastal area, which is located between the south coast of Japanese islands and the Kuroshio, is nutrient-rich and becomes a major spawning grounds of various fishes. This area is occupied by the cyclonic eddy in association with the Kuroshio large meander. Therefore, during the Kuroshio large meander period, dynamical structures and evolutions of the cyclonic eddy greatly influence the marine resources and fisheries through the variation of the marine environment such as temperature, salinity (*S*) and dissolved materials. In addition, previous studies have demonstrated that the dynamical evolution of the cyclonic eddy is a key factor to predict the generation and decay of the Kuroshio large meander. While the monitoring and analysis of the cyclonic eddy are necessary in understanding of the dynamical processes and the variability of the marine resources, studies based on the observation are limited. To examine the characteristics and evolution of the cyclonic eddy in the Kuroshio coastal area in association with the Kuroshio large meander, we conducted hydrographic surveys in and around the cyclonic eddy and its upstream region in September 2020, along with analyzing fixed line observation data along 138˚E during the Kuroshio large meander period. The low-*S*and high-potential vorticity (*Q*) water in the surface layer was found in the Kuroshio coastal area from the small meander southeast of Kyushu to the cyclonic eddy. The high-*Q* water was in the similar density range, suggesting the supply of high-*Q* water into the cyclonic eddy from the upstream region. On the other hand, a cold eddy pinched off from the cyclonic eddy had a core of high-*Q* in the different density range from the cyclonic eddy. Eddy-eddy interaction associated with the Kuroshio large meander was discussed using the observation data, with particular attention to the magnitude of *Q*, the depth of cores, and the size of eddies. Moreover, the analysis of the fixed line observation data along 138˚E showed the temporal variation of *Q* in the cyclonic eddy from 2017 to 2021.

Keywords: Potential vorticity, Small meander, Eddy-eddy interaction

©2021. Japan Geoscience Union. All Right Reserved.

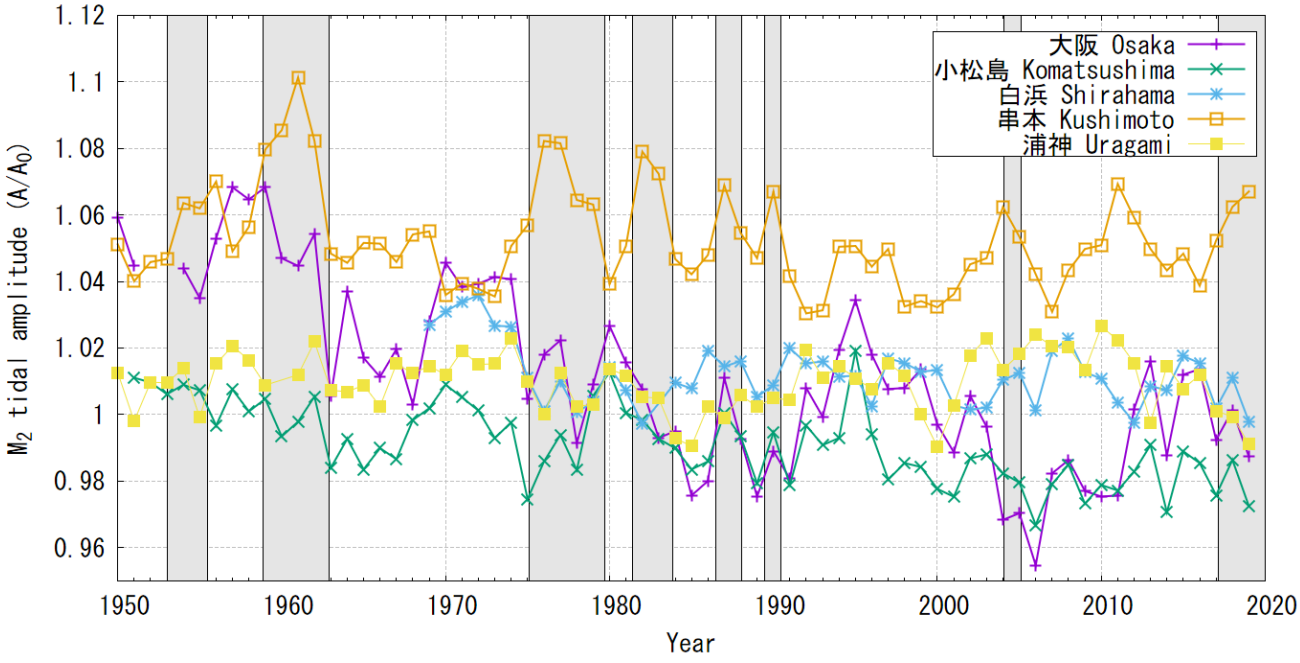
The relationship between Kuroshio meander and observed tidal-regime shift along southern coast of Japan

*Takumi Kamura[1], Hiromi Matsuura[1], Katsuto Uehara[2]

1. Interdisciplinary Graduate School of Engineering Sciences, Kyushu University, 2. Research Institute for Applied Mechanics, Kyushu University

Relationships between the Kuroshio meander and tidal changes over decadal time scales along Japanese coasts, which has not been well verified compared to the relationship between the meandering phase and the sea-level difference, were studied by conducting harmonic analyses of sea levels at five tide-gauge stations north of the major Kuroshio meandering region, Osaka, Komatsushima, Shirahama, Kushimoto, and Uragami, for duration from 1950 to 2019. It was found that at Kushimoto located on the western side of the southern end of the Kii Peninsula, M2 tidal amplitudes increased intermittently by about 4%, which have taken place at irregular intervals ranging from years to decades, and that the timing of such events coincided with the occurrence of the Kuroshio meander. This result indicates a relation between changes in coastal tides and the Kuroshio path.

Keywords: Kuroshio meandering, tides, sea level



©2021. Japan Geoscience Union. All Right Reserved.

Eddy separation from the Kuroshio Large Meander in 2020

*Toru Miyama[1], Yasumasa Miyazawa[1], Sergey M Varlamov[1], Zhang Ruochao[1]

1. Japan Agency for Marine-Earth Science and Technology, Application Laboratory

The Kuroshio Large Meander has been continuing since 2017. The large eddy was detached from the Meander in October 2020. The Large Meander temporarily ended. Correspondingly, Kushimoto-Urakami sea level difference, whose smallness is an indicator of the Large Meander, increased. Subsequently, the small meanders that existed east of Kyushu developed into the Large Meander by moving eastward and replacing the previous eddy, resulting in the continuation of the Large Meander. The Kushimoto-Urakami sea level difference decreased again. Alternatively, the eddy detached moved westward and formed a small meander by joining the Kuroshio southeast of Kyushu from the end of January to the beginning of February 2021. This behavior is different from the eddy HARUKAZE after the Harukaze Maru of the Kobe Marine Observatory, which was observed it in 1978 during the great Kuroshio Large Meander period of 1975–1980. In 2020, the Kuroshio Large Meandering Current was in a state of instability. Therefore, several small eddies shredded before the large eddy detachment described above. The instability was due to the small meander east of Kyushu and high sea level anomaly extended from the Kuroshio Extension. In this presentation, I will discuss the dynamics and predictability of the unstable Kuroshio Large Meander.

Keywords: kuroshio Large Meander, Eddy, ocean reanalysis, predictability

©2021. Japan Geoscience Union. All Right Reserved.

Study on the temporal and spatial variation of the Kuroshio Current path

*Yuya Hirano[1], Kazuyuki Uehara[1]

1. Graduate School of Earth Environmental Science, Tokai University

Kawabe (1995) classified the Kuroshio flowing along the southern coast of Honshu into three flow patterns: non-Large-Meander path (nearshore and offshore) and Large-Meander path. After this study, studies has been reported to show pattern of the Kuroshio Current paths, but the time-varying characteristics of the flow pattern have not been discussed. In this study, we therefore extracted the flow paths from the sea surface dynamic height data, then conducted time-frequency analysis for the Kuroshio detachment distance from the coast. In the result, we found the clear difference in periodicity from east to west, with the Kii Peninsula offshore as a border. West of the Kii Peninsula, the dominant peaks seen off southeast Kyushu at 30 days or less, 90-180 days, and 360 days gradually weakened while moved toward the Kii Peninsula. On the other hand, east of the Kii Peninsula, the stronger peaks with various periods were observed get closer to the Izu-Ogasawara Ridge.

Keywords: Kuroshio detachment distance, Wavelet analysis

©2021. Japan Geoscience Union. All Right Reserved.

Impact of a Marine Heatwave Attributable to a Kuroshio Large Meander on Extreme Heavy Rainfall Caused by an Extratropical Cyclone

*Eigo Tochimoto[1], Satoshi Iizuka[1]

1. National Research Institute for Earth Science and Disaster Resilience

Extratropical / Tropical cyclones often cause extreme rainfall events over eastern coastal region characterized by a western boundary current and an extended coastal mountain range. On 12–13 April, 2020, extreme heavy rainfall event was occurred over the east of the Kii Peninsula, Japan. Concurrently, the Kuroshio large-meander started from 2017 caused the notable positive sea surface temperature (SST) anomalies along the coast south of Japan. The present study examines the impact of the positive SST anomaly on the heavy rainfall event associated with an extratropical cyclone using numerical experiments. The control simulation (CNTL) showed that strong low-level easterly winds associated with a cold conveyor belt in the northeast of the cyclone brought humid airmass toward east of the Kii Peninsula, resulting in strong updraft and local intense precipitation. A sensitivity experiment in which the SST anomalies attributable to the LM was removed showed at least 25 % reduction of the maximum precipitation for 3 hours because of the smaller latent and sensible heat fluxes from the sea surface compared to those in CNTL. Thus, the SST anomalies attributable to the LM contributed to the heavy rainfall. Furthermore, additional numerical experiment without the evaporation of rainwater and ice pieces indicated that cold air temperature from the near surface to middle troposphere over land were maintained by the evaporation and contributed to the persistent of horizontal temperature gradient along the coastal region. Our results suggest that air-sea interaction on synoptic- and meso-scale can drive extreme precipitation. We have confirmed that there was another heavy rainfall event affected by warm SST anomalies attributable to the meander of the Kuroshio south of Japan on 2 May 2012. A sensitivity experiment in which SST values are replaced by those for climate values showed the reduction of total precipitation for CLM from CNTL.

Keywords: Kuroshio Large Meander, Extratropical Cyclone, Extreme rainfall

©2021. Japan Geoscience Union. All Right Reserved.

The Kuroshio volume transport in near future estimated by Reduced Gravity model

*Takashi SETOU[1], Akira KUSAKA, Daisuke Ambe, Daiki Ito[1], Takashiko Kameda

1. Japan Fisheries Research and Education Agency

In August 2017, for the first time in 12 years, the Kuroshio large meander event has occurred and is still continuing after three years and five months, making it the second-longest-lasting meander event in history among those that have occurred since 1970. Once the Kuroshio Meanders occur, the fishing environment in the surrounding seas will change and the fishing industry will be greatly affected. It is known that the duration of the Kuroshio large meander has an inverse linear relationship with the Kuroshio volumeflow transport, i.e., the lower the transport, the longer the duration (Usui et al. 2013). We has calculated the 137E eastward Kuroshio flow using a 1.5-layer Reduced Gravity model driven by wind stress, and then created a regression model to fit the 2017 Kuroshio Large Meander to the transport until 2020. As a result, it is estimated to continue for about 48 months, that is, until July 2021 (±7 months). However, as the transport will continue to be low in the future, there is a possibility that the large meander will become more prolonged.

Keywords: the Kuroshio large meander

©2021. Japan Geoscience Union. All Right Reserved.

[J] Poster | A (Atmospheric and Hydrospheric Sciences)：A-CC Cryospheric Sciences & Cold District Environment

Thu. Jun 3, 2021 5:15 PM - 6:30 PM JST | Thu. Jun 3, 2021 8:15 AM - 9:30 AM UTC | Ch.04_1

[A-CC25] Glaciology in the new normal

convener:Hiroto Nagai(Waseda Univ., School of Education), Kzutaka Tateyama(National University Corporation Kitami Institute of Technology), Ishikawa Mamoru(Hokkaido University), Keiko Konya(Japan Agency for Marine-Earth Science and Technology)

Glaciology conducts academic research on snow and ice using a wide variety of methods such as observation, sampling, laboratory experiments, and numerical calculations. Since 2020 Coronavirus disease (COVID-19) pandemic has had a critical impact on the global society, whereas it may derive "new-normal" regimes. Glaciological studies have also had some impacts, such as the cancellation of scheduled overseas surveys and user number restriction in laboratories, but their severity depends on their study methods.
How long period of data lacking is allowed on long-term continuous observations? Is there another alternative approach? Will information and communication technologies that are rapidly becoming widespread for web meeting and/or remote work contribute for glaciological studies?
In this session, regular reports of research results are welcomed. In addition, in this year, we will share various issues caused by the pandemic and their solutions. Discussing the new normal of the glaciology, furthermore, we aim to contribute for developing a more resilient and sustainable academic community of glaciology than before.

[ACC25-P01] Evidence for long-range transport of atmospheric microplastic

*Osamu Nagafuchi[1], Koyomi Nakazawa[1] (1.Fukuoka Institute of Techology)

[ACC25-P02] **A discussion of the circumstances and causes of the massive avalanche that occurred at Mt. Kiso Ontake on May 21st 2019**

*Hideo Suzuki[1], Takeshi Saito[2], Kuniaki Makino[2] (1.Institute of Science, Academic Assembly School of Science and Technology, Shinshu University, 2.Department of Geology, Faculty of Science, Shinshu University)

[ACC25-P03] Preliminary observation report of snow-buried corner reflectors for SAR-based snow-depth monitoring in Nagaoka, Niigata (2020/2021)

*Hiroto Nagai[1,2], Sojiro Sunako[2], Katsuya Yamashita[2], Satoru Yamaguchi[2] (1.Waseda Univ., School of Education, 2.National Research Institute for Earth Science and Disaster Resilience)

[ACC25-P04] Radiation characteristics of thin sea ice in the ice tank experiment using multifrequency passive microwave radiometers

*Kzutaka Tateyama[1], Hiroyuki Enomoto[2], Masashige Nakayama[3], Naoto Shoji[1], Yurika Watanabe[1], Sae Ohira[1], Kohei Sato[1] (1.National University Corporation Kitami Institute of Technology, 2.Arctic Environment Research Center, National Institute of Polar Research, 3.National University Corporation Hokkaido University of Education, Kushiro campus)

[ACC25-P05] Polar snow monitoring by satellite microwave radiometer

*Nuerasimuguli Alimasi[1], Hiroyuki Enomoto[1] (1.National Institute of Polar Research)

[ACC25-P06] The observation plan of glacier research and its modification due to covid-19

*Keiko Konya[1] (1.Japan Agency for Marine-Earth Science and Technology)

[ACC25-P07] **Relationship between Haliaeetus pelagicus flights route over the Russian Far East and surface atmospheric conditions**

*Kazutoshi Sato[1], Kzutaka Tateyama[1], Saiko Shiraki[2], Yusuke Murata[1] (1.Kitami Institute of Technology, 2.Tokyo University of Agriculture)

Evidence for long-range transport of atmospheric microplastic

*Osamu Nagafuchi[1], Koyomi Nakazawa[1]

1. Fukuoka Institute of Techology

In these days, marine, freshwater and terrestrial pollution with microplastics (MPs) has been discussed extensively, whereas there are few reports on long-range transport of atmospheric MPs. Here, we attempted to detect atmospheric MPs by focusing on rime-ice on mountain site located in the free troposphere. MPs were identified by Fourier transform infrared imaging in all samples. The MPs concentrations of rime-ice was significantly higher ($10^{\sim}20 \times 10^{-3}$ N liter^{-1}) than snow on same mountain (1×10^{-3} N liter^{-1}). The major polymer which detected was polyethylene. Most of particles were in the smaller size below 50mm. Furthermore, from the results of the back trajectory analysis, our data emphasize that atmospheric transport and deposition can be notable pathways for MPs.

Keywords: rime-ice, microplastic, long-range transport

©2021. Japan Geoscience Union. All Right Reserved.

A discussion of the circumstances and causes of the massive avalanche that occurred at Mt. Kiso Ontake on May 21st 2019

*Hideo Suzuki[1], Takeshi Saito[2], Kuniaki Makino[2]

1. Institute of Science, Academic Assembly School of Science and Technology, Shinshu University, 2. Department of Geology, Faculty of Science, Shinshu University

A large-scale snow avalanche that occurred on 21st May 2019 on the slope between Ichinoike and Ninoike craters at Mt. Kiso Ontake was unprecedented in terms of location and scale. This avalanche caused damage to the trail and Ninoike mountain lodge. On the same day, a collapse of the snow layer and mudflow occurred in the upper Yukawa River downstream from Ninoke crater. Similar collapse and mud flow were observed at Yukawa River in May 2011, suggesting that small collapse of snow layer and mud flow generation are common at Yukawa in snowmelt season. Ontake was erupted in September 2014, resulted in cohesive muddy volcanic ash deposits around the summit area. Not only appropriate weather and snow conditions but the presence of volcanic ash very likely promote sliding of the snow layer. In order to clarify the generation process of this avalanche, we carried out field observation. The sediments transported by the avalanches and water samples were analyzed. In addition, simple snow block sliding experiments were conducted in order to investigate snow conditions and the effect of volcanic ash.

As a result, several sharp-edged crown fractures were observed at the slope between Ichinoike and Ninoike craters. Snow slabs deposited at Ninoike maintains sedimentary structures formed before the avalanche generation, indicating the slabs simply slid the slope. Although Kunitomo et al. (2019) reported this avalanche was occurred as a slush avalanche, our results indicate the avalanche was generated as a surface-onset full-layer avalanche. At Yukawa River, the gully cracks were formed and slush was deposited on the levees, suggesting the avalanche was transformed to slush flows after entering Yukawa River.

Muddy volcanic ash derived from the 2014 eruption was deposited on the bed surface. The ash contains gypsum and the water sampled at Ichinoike and Ninoike craters showed high concentration of Ca and SO_4. These muddy gypsum bearing ash possibly promoted the avalanche generation. Simple snow block sliding experiments indicated that not only appropriate weather and snow conditions but the presence of volcanic ash promote sliding.
We concluded that the avalanche was possibly promoted by muddy water with volcanic ash in addition to appropriate weather and snow conditions (heavy rains and rapid temperature increasing around 0 degrees C).

Keywords: Avalanche, Slush, Clay volcanic ash, Mt. Kiso Ontake, Mudflow, Phreatic eruption

©2021. Japan Geoscience Union. All Right Reserved.



©2021. Japan Geoscience Union. All Right Reserved.

Preliminary observation report of snow-buried corner reflectors for SAR-based snow-depth monitoring in Nagaoka, Niigata (2020/2021)

*Hiroto Nagai[1,2], Sojiro Sunako[2], Katsuya Yamashita[2], Satoru Yamaguchi[2]

1. Waseda Univ., School of Education, 2. National Research Institute for Earth Science and Disaster Resilience

Understanding the distribution of snow depth over a wide area is basic information for disaster prevention. The number of ground-based observation points is limited especially in mountainous areas with heavy snowfall, therefore further development of observation systems is expected. Satellite-based synthetic aperture radars (SARs) are expected to observe a wide area and generate detailed information of snow depth distribution in such an area. SAR backscatter amplitude is decreased by snowpack, because reflection and scattering occur on the surface and inside of the snow cover. The backscatter amplitude is considered to depend on the depth and physical properties (water content) of the snow layer.
In this study, metal-made Corner Reflectors (CRs) for SAR are built and buried in actual snowpack. The signal on the CRs is significantly stronger than the surroundings. Using these, we aim to understand the microwave-propagation process in more detail and with lower noise than before.
The CRs are built with three 1-m squared panels. Steel-made CRs are made for extremely heavy snowpack (>3 m) in addition to stainless-made one. Totally four CRs are set in experimental fields operated by the National Research Institute for Earth Science and Disaster Resilience (NIED) in Nagaoka, Niigata Prefecture. CR installation was completed in November 2019. In addition, real-time camera monitoring system were installed and started on December 2020, which enables image transmission of snow-burring CRs in every 30-min. or 1-hours.
Significant heavy snowfall in a short time occurred on around December 14, 2021 around Niigata, Japan. This event caused social affects, for example, hundreds of cars getting stuck on the highway for a long time. The CR cameras captured the sudden increase of snow depth. Snow depth has not been lower than 50 cm in Nagaoka and not been lower than 1 m in Tochio-tashiro since this time. Regular automatic snow-depth measurement is operated at both points, but the snow depth is not completely uniform around the area. There is a slight spatial-heterogeneity caused by the shade, ground features, and wind direction. Especially in Nagaoka, the snow depth increases and decreases around 1 m, the CR’ s height. Because whether the CR is completely buried or partially exposed is important information in later analysis, the image from the camera shows the situation most reliably.
While recording the snow condition of CR, the Sentinel-1a/b satellites of the European Space Agency are conducting observations in multiple satellites/orbits, deriving three times observation opportunity in 12days for our study sites. In addition, Japanese SAR satellite "DAICHI-2" is scheduled to carry out observations twice in February in the high-resolution mode. In this presentation, we will analyze these satellite observation data and CR snow cover conditions, and give a preliminary report of the obtained results.

Keywords: SAR, Snow depth, Extreme weather, PALSAR-2

©2021. Japan Geoscience Union. All Right Reserved.

Radiation characteristics of thin sea ice in the ice tank experiment using multifrequency passive microwave radiometers

*Kzutaka Tateyama[1], Hiroyuki Enomoto[2], Masashige Nakayama[3], Naoto Shoji[1], Yurika Watanabe[1], Sae Ohira[1], Kohei Sato[1]

1. National University Corporation Kitami Institute of Technology, 2. Arctic Environment Research Center, National Institute of Polar Research, 3. National University Corporation Hokkaido University of Education, Kushiro campus

Microwave radiation characteristics of sea ice with a thickness ranged from 0 cm to around 30 cm was measured using the passive microwave radiometers having the observation frequencies of 6, 18, 36 GHz. Sea ice was grown in the ice tank which has a diameter of 2.6m and a depth of 0.9m and filled by 5 tons of saline water (32psu) transported from the Saroma-ko lagoon. The ice tank was set up outdoors next to the baseball ground in the campus of Kitami Institute of technology. In order to avoid the effects of melting by sunlight and disturbance by snow, a movable roof was installed and a refrigerator was installed inside the roof. Portable microwave radiometers MMRS2 were used and installed at same incident angle (55 degree) to GCOM-W/AMSR2.

The brightness temperature showed a rapid increasing from open water to newly formed sea ice. After maximum value appeared at a few centimeters thin ice, the brightness temperatures showed the tendency to decrease gradually with sea ice thickens.

Keywords: Sea ice, Remote sensing, Passive microwave radiometrer

©2021. Japan Geoscience Union. All Right Reserved.

Polar snow monitoring by satellite microwave radiometer

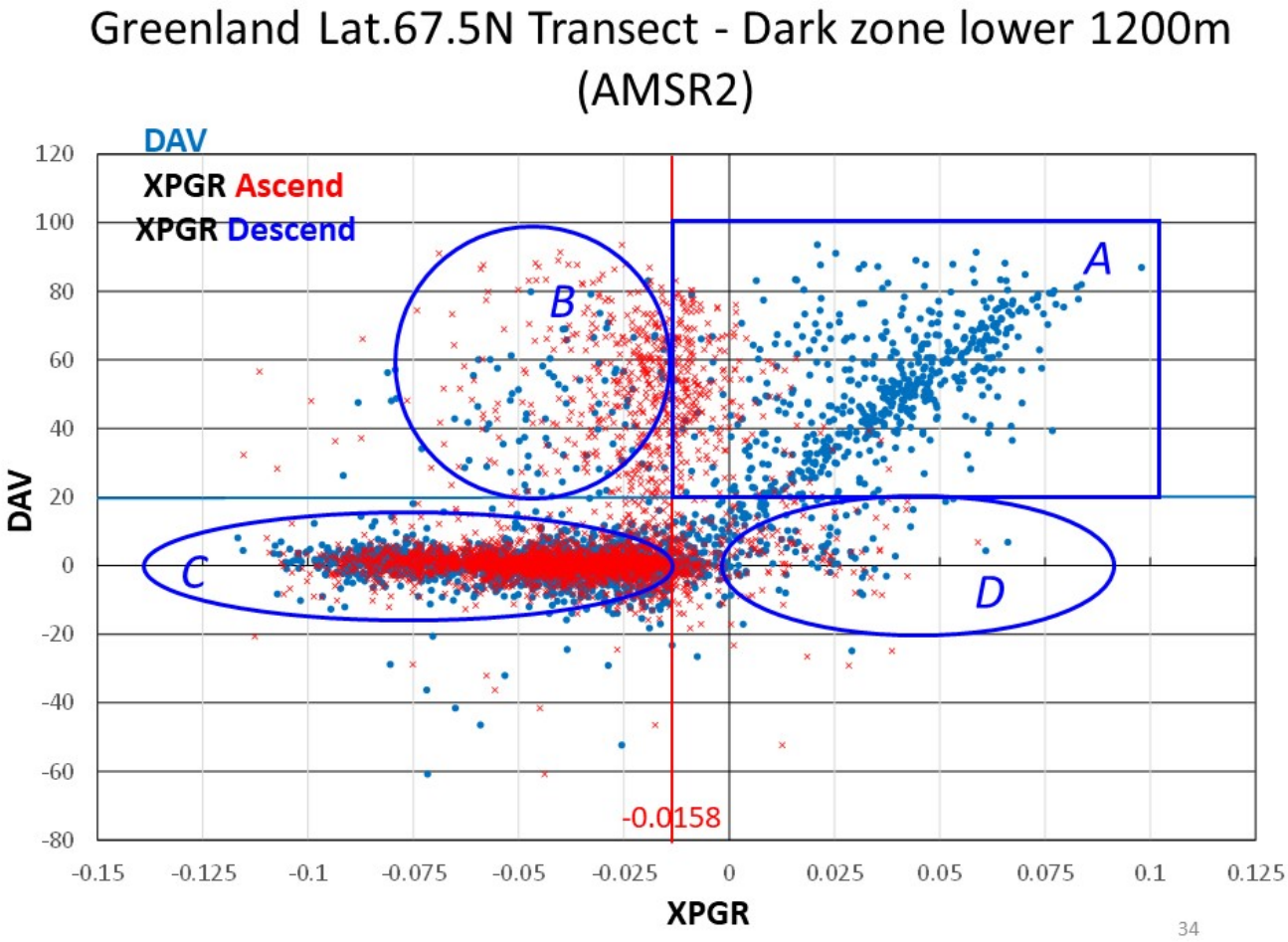
*Nuerasimuguli Alimasi[1], Hiroyuki Enomoto[1]

1. National Institute of Polar Research

The melting of snow covered areas, glacier and ice sheets is important information for the effects of climate change, the water cycle, and disaster prevention. Satellite observations are used to observe melting. There are methods such as investigating changes in the reflection characteristics of snow and ice with visible and near infrared observation, investigating that the temperature of snow and ice reaches the melting point by infrared observation, and detecting water contains by microwave radiation. Microwave observations, which allow observation of melting in all weather and at night, have been used since satellite microwave observations became possible in the 1980s. A method called XPGR (Cross-Polarization Gradient Ratio) has been used as the main observation algorithm since the latter half of the 1990s, and has been used for climate change research as an index of ice sheet melting. In addition, a method called the Diurnal Amplitude observation Variation (DAV) has been used to observe melting in snowy areas on land by observing daytime melting and nighttime freezing. The current study investigated the characteristics and precautions for use of XPGR and DAV.
In this study, we compared XPGR and DAV using ASMR_E and AMSR2 data. Although it is effective for DAV that the observation times are 13:30 (Ascending) and 01:30 (Descending). It turns out that XPGR should be careful when using Ascending data. XPGR was expected to overlook melting when it melted and the surface moisture increased.

Keywords: melt, DAV, glacier and ice sheets

©2021. Japan Geoscience Union. All Right Reserved.



©2021. Japan Geoscience Union. All Right Reserved.

The observation plan of glacier research and its modification due to covid-19

*Keiko Konya[1]

1. Japan Agency for Marine-Earth Science and Technology

As part of ArCSII project, observations of methane emitted from the Gulkana Glacier area in Alaska were planned for the summer of 2020. Methane is a greenhouse gas that has a large impact even in small amounts. In recent years, methane has been found to be emitted from the glacier area at the margin of the Greenland ice sheet and the Icelandic glacier area. While glacier areas are accounted for as new sources of methane, observation data are limited, and the mechanism of methane emission is unknown. Therefore, the authors have planned to conduct field measurements at the mountain glaciers area.
However, we found it impossible to carry out field observations due to covid-19. Since covid-19 was a global phenomenon, unlike SARS and MERS in the past, it was difficult to travel to countries where the number of infected people was higher than in Japan, or to areas where ethnic minorities lived in the Arctic region. In order to compensate for the missing data in 2020, we decided to construct a new method that is expected to get various data. As for 2021, the plan was divided into cases where observations could be conducted and cases where observations could not be conducted, and further changes were considered for the cases where observations could not be conducted.

Keywords: Glacier research, covid-19, the Arctic

©2021. Japan Geoscience Union. All Right Reserved.

Relationship between Haliaeetus pelagicus flights route over the Russian Far East and surface atmospheric conditions

*Kazutoshi Sato[1], Kzutaka Tateyama[1], Saiko Shiraki[2], Yusuke Murata[1]

1. Kitami Institute of Technology, 2. Tokyo University of Agriculture

The Haliaeetus pelagicus, which stays over the coastal region of Okhotsk sea of East Hokkaido during winter, is migratory bird. After breeding season over the coastal region of Okhotsk Sea in Russia during summer, they migrate southward in autumn and reach East Asia in early winter. However, no previous study has reported the influence of atmospheric conditions on migration route and timing of Haliaeetus pelagicus. Using reanalysis data and geolocation loggers data, we investigate the relationship between change in surface conditions (e.g. snow cover, sea ice cover, surface temperature) and migration factors (e.g. timing and route) of Haliaeetus pelagicus.
In autumn 2018, two birds stay over Khabarovsk area in Russia. Although departure and arrival areas of two birds are almost same, there are differences in departure date and route of migration of two birds. One bird starts migration toward south in middle of October 2018. After leaving Khabarovsk area, snow accumulation is seen over Khabarovsk area, meaning that this bird avoids snow. In contrast, another one stays over Khabarovsk area even high snow cover. However, this bird starts to migrate when temperature drops below -20 oC. In addition, Haliaeetus pelagicus selects high sea ice cover areas when they migrate northward after winter season. From these results, surface conditions would be an indicator of timing and route of Haliaeetus pelagicus.

Keywords: Haliaeetus pelagicus, Migratory bird, Sea of Okhotsk

©2021. Japan Geoscience Union. All Right Reserved.

[J] Poster | A (Atmospheric and Hydrospheric Sciences)：A-CC Cryospheric Sciences & Cold District Environment

Thu. Jun 3, 2021 5:15 PM - 6:30 PM JST | Thu. Jun 3, 2021 8:15 AM - 9:30 AM UTC | Ch.04_2

[A-CC26] Ice cores and paleoenvironmental modeling

convener:Nozomu Takeuchi(Chiba University), Ayako Abe-Ouchi(Atmosphere and Ocean Research Institute, The University of Tokyo), Ryu Uemura(Nagoya University), Kenji Kawamura(National Institute of Polar Research, Research Organization of Information and Systems)

Analyses of ice cores from polar and mountain regions have contributed to the reconstruction and understanding of the past environmental changes on timescales from years to several hundred thousand years. In this session, we welcome paleoenvironmental studies using ice cores and paleoclimatic modeling. Studies on reconstruction methods, recording processes and new paleoenvironmental proxies, technical aspects of paleo-modeling are also welcomed. Studies with marine sediment cores, terrestrial sediment cores and tree-rings on similar timescales are also important and welcomed, in order to discuss past environmental changes from multidisciplinary viewpoints.

[ACC26-P01] A biomass burning record over the past 350 years in an ice core from Northwest Greenland

*Kumiko Goto-Azuma[1,2], Yoshimi Ogawa-Tsukagawa[1], Yutaka Kondo[1], Remi Dallmayr[9], Jun ogata[1], Nobuhiro Moteki[3], Sho Ohata[4], Tatsuhiro Mori[5], Makoto Koike[3], Kaori Fukuda[1], Motohiro Hirabayashi[1], Sumito Matoba[6], Yuki Komuro[1], Akane Tsushima[7], Naoko Nagatsuka[1], Koji Fujita[4], Naga Oshima[8], Kyotaro Kitamura[1], Kenji Kawamura[1,2], Wataru Shigeyama[1,2], Hideaki Motoyama[1,2], Teruo Aoki[1,2] (1.National Institute of Polar Research, 2.SOKENDAI, 3.University of Tokyo, 4.Nagoya Univeristy, 5.Tokyo University of Science, 6.Hokkaido University, 7.Chiba University, 8.Meteorological Research Institute, 9.Alfred Wegner Institute for Polar and Marine Research)

[ACC26-P02] Seasonal changes in concentration, metal composition and size distribution of mineral particles in recent snow at EGRIP, Greenland

*Yuki Komuro[1], Fumio Nakazawa[1,2], Kumiko Goto-Azuma[1,2], Motohiro Hirabayashi[1], Wataru Shigeyama[1,2], Naoko Nagatsuka[1] (1.National Institute of Polar Research, 2.The Graduate University for Advanced Studies, SOKENDAI)

[ACC26-P03] Implementation of higher-order advection schemes in a numerical ice-sheet model for ice-core studies

*Fuyuki SAITO[1], Takashi Obase[2], Ayako Abe-Ouchi[2] (1.Japan Agency for Marine-Earth Science and Technology, 2.Atmosphere and Ocean Research Institute, The University of Tokyo)

[ACC26-P04] An ice-flow modeling study for evaluation of sites for an oldest ice core around Dome Fuji, Antarctica

*Takashi Obase[1], Ayako Abe-Ouchi[1,2], Fuyuki SAITO[3], Shun Tsutaki[2], Shuji Fujita[2,4], Kenji Kawamura[2,4] (1.Atmosphere and Ocean Research Institute, the University of Tokyo, 2.National Institute of Polar Research, Japan, 3.Japan Agency for Marine-Earth Science and Technology, 4.SOKENDAI, the Graduate University for Advanced Studies)

[ACC26-P05] The effect of ocean circulation on glacial-interglacial cycles

*Ryotaro Todoroki[1], Ayako Abe-Ouchi[1], Fuyuki SAITO[2], Takashi Obase[1], Wing-Le Chan[1], Sam Sherriff-Tadano[3], Yasuto Watanabe[4] (1.Atmosphere and Ocean Research Institute, The University of Tokyo, 2.Japan Agency for Marine-Earth Science and Technology (JAMSTEC), 3.The University of Leeds, 4.The University of Tokyo)

[ACC26-P06] Transient simulations of the last deglaciation using MIROC AOGCM and time evolving ice-topography

*Tristan Vadsaria[1], Takashi Obase[1], Ayako Abe-Ouchi[1], Sam Sherriff-Tadano [2,1], Wing-Le Chan[1] (1.Atmosphere and Ocean Research Institute, The University of Tokyo, Japan, 2.School of Earth and Environment, The University of Leeds, Leeds, UK)

[ACC26-P07] **Inactivating microorganisms in melted snow and ice samples using ultraviolet germicidal radiation**

*Fumio Nakazawa[1,2], Kumiko Goto-Azuma[1,2] (1.National Institute of Polar Research, 2.The Graduate University for Advanced Studies, SOKENDAI)

[ACC26-P08] The origin of moisture inferred from water stable-isotopes of an ice-core drilled in the Pamir-Alay Mountains in Central Asia

*Daiki Seto[1], Nozomu Takeuchi[1], Aizen Vladimir[2], Akane Tsushima[3], Kenji Kawamura[4], Koji Fujita[5] (1.CHIBA university, 2.University of Idaho, 3.Graduate School of science, Chiba university, 4.Graduate School of Environmental Studies, Nagoya University, 5.National Institute of Polar Research, Research Organization of Information and Systems)

[ACC26-P09] Analyses of pollen grains and insoluble particles in an ice core drilled in the Pamir-Arai Mountains in central Asia

*Nozomu Takeuchi[1], Haruka Ogaya[1], Koji Fujita[2], Kenji Kawamura[3], Akane Tsushima[1], Vladimir Aizen[4] (1.Chiba University, 2.Nagoya University, 3.National Institute of Polar Research, 4.University of Idaho)

A biomass burning record over the past 350 years in an ice core from Northwest Greenland

*Kumiko Goto-Azuma[1,2], Yoshimi Ogawa-Tsukagawa[1], Yutaka Kondo[1], Remi Dallmayr[9], Jun ogata[1], Nobuhiro Moteki[3], Sho Ohata[4], Tatsuhiro Mori[5], Makoto Koike[3], Kaori Fukuda[1], Motohiro Hirabayashi[1], Sumito Matoba[6], Yuki Komuro[1], Akane Tsushima[7], Naoko Nagatsuka[1], Koji Fujita[4], Naga Oshima[8], Kyotaro Kitamura[1], Kenji Kawamura[1,2], Wataru Shigeyama[1,2], Hideaki Motoyama[1,2], Teruo Aoki[1,2]

1. National Institute of Polar Research, 2. SOKENDAI, 3. University of Tokyo, 4. Nagoya Univeristy, 5. Tokyo University of Science, 6. Hokkaido University, 7. Chiba University, 8. Meteorological Research Institute, 9. Alfred Wegner Institute for Polar and Marine Research

Black carbon (BC) is one of the major light-absorbing aerosols, which can affect Earth’ s radiation budget. BC in the atmosphere absorbs sunlight and heats the atmosphere, whereas BC deposited on snow and/or ice reduces the surface albedo and enhances snowmelt. BC can also act as cloud condensation nuclei and ice nucleating particles, which play important roles in climate change. To understand the role of BC in climate change, we need to know concentrations, size distributions, and spatial and temporal variability in them. However, observations of BC in the atmosphere and snow have been started only recently. There have been no direct observations of BC in the preindustrial time, which was unaffected by anthropogenic input. Ice cores can provide proxy records of the past BC concentration and size distribution in the preindustrial period as well as the industrial period. The records from the preindustrial period are of special importance in understanding the role of BC in the pristine environment.

We analyzed an ice core drilled at SIGMA-D site, Northwest Greenland (Matoba et al., 2015), down to the depth of 113 m using a Continuous Flow Analysis (CFA) system developed at the National Institute of Polar Research. The CFA system enabled us to obtain high-resolution data of BC, stable isotopes of water, microparticles and six elements (Na, K, Mg, Ca, Fe, and Al). For BC analysis, we used a recently developed Wide-range (WR) SP2 (Single Particle Soot Photometer), which can detect BC particles in size range between 70 and 4000 nm (Mori et al., 2016). A combination of WR-SP2 and a high-efficiency nebulizer allowed us accurate measurements of BC concentrations and size distributions. We dated the core by annual layer counting using mainly Na and water stable isotopes. Our ice-core record covers the past 350 years. We divided each year into 12 months and calculated monthly averaged BC concentrations and size distributions.

Concentrations of BC started to increase in the 1870s, reached its maximum in the 1920s - 1930s, and decreased again since then. The increases are likely due to anthropogenic BC, which we as found to deposit mainly in fall and winter months. Before the increases started, the major source of BC was biomass burning, which showed summer peaks in BC concentrations. Based on the different seasonality of anthropogenic and biomass burning BC, we reconstructed temporal variability in biomass burning BC. Except for occasional large biomass burning events, we found relatively stable biomass burning BC concentrations over the past 350 years. We did not find particularly high summer BC concentrations in warm periods.

Keywords: Greenland, Black carbon, Biomass burning, Ice core

©2021. Japan Geoscience Union. All Right Reserved.

Seasonal changes in concentration, metal composition and size distribution of mineral particles in recent snow at EGRIP, Greenland

*Yuki Komuro[1], Fumio Nakazawa[1,2], Kumiko Goto-Azuma[1,2], Motohiro Hirabayashi[1], Wataru Shigeyama[1,2], Naoko Nagatsuka[1]

1. National Institute of Polar Research, 2. The Graduate University for Advanced Studies, SOKENDAI

Changes in meteorological and ground surface conditions can cause changes in mineral particle supply to the Greenland ice sheet and thus influence the particle concentration in snow. To reveal the factor causing the changes of the particle supply and concentration, an understanding of their source areas is required. Metal composition and size distribution of the particles should be able to estimate source areas of the particles. To clarify recent seasonal changes in the concentration of mineral particles in snow and their source area, we analyzed the total concentration of metals and particle distribution in snow pit samples obtained from EGRIP (East Greenland Ice Core Project).

In summer 2017, we dug a 2.01 m snow pit at EGRIP camp. Snow samples were collected at 0.03 m intervals. The snow samples were melted, then fractions of them were analyzed for the particle size distribution (0.52-12 μm) with a Coulter counter (Beckman Coulter: Multisizer 4). Other fractions of the samples were treated with a microwave acid digestion method to decompose particulates. Total concentrations of Al, Ca and Na in samples were measured by inductively coupled plasma mass spectrometry.

Concentrations of total Al (t-Al) and non-sea-salt Ca (nssCa) increased in winter to spring layers. This indicates that mineral particle concentration in the snow at EGRIP increased in the periods. In addition, volume fractions of fine particles (<4 μm) tended to be relatively high in the layers. This suggests that fine mineral particles from remote source areas were predominantly deposited on the snow at that time. Additionally, nssCa/t-Al ratios tended to be relatively high in those layers, having 2-3 times higher than the crustal average of Ca/Al ratio in some of the layers. Thus, it is suggested that mineral particles originated from remote desert areas were supplied to EGRIP in the periods. In contrast, in summer to autumn layers, the nssCa/t-Al ratios and volume fractions tended to be relatively low. This suggests the supplies from soil areas having Ca-poor compositions near Greenland in the periods.

Keywords: Greenland, snow, mineral dust

©2021. Japan Geoscience Union. All Right Reserved.

Implementation of higher-order advection schemes in a numerical ice-sheet model for ice-core studies

*Fuyuki SAITO[1], Takashi Obase[2], Ayako Abe-Ouchi[2]

1. Japan Agency for Marine-Earth Science and Technology, 2. Atmosphere and Ocean Research Institute, The University of Tokyo

Computation of temperature and age fields by numerical ice-sheet models is an important issue for ice-core related studies. Generally the evolution of temperature and/or age in an ice-sheet model is formulated using an advection equation. There are many variation of the formulation, which differ in numerical aspects such as stability, accuracy, numerical diffusivity, conservation and/or computational costs. Saito et al (2020, GMD) implement Rational Constrained Interpolation Profile (RCIP) scheme on vertical 1-d age computation of ice sheet, and demonstrate its efficiency, in particular, to preserve surface mass balance properties recorded at the deposit in terms of annual layer thickness. Successively, we have been extending the development using RCIP or similar higher-order advection schemes on 3-d age or temperature computation. In this study, we demonstrate 1-d temperature computation by various numerical schemes including classical upwind schemes and compare the accuracy of those schemes.

Keywords: ice-sheet model

©2021. Japan Geoscience Union. All Right Reserved.

An ice-flow modeling study for evaluation of sites for an oldest ice core around Dome Fuji, Antarctica

*Takashi Obase[1], Ayako Abe-Ouchi[1,2], Fuyuki SAITO[3], Shun Tsutaki[2], Shuji Fujita[2,4], Kenji Kawamura[2,4]

1. Atmosphere and Ocean Research Institute, the University of Tokyo, 2. National Institute of Polar Research, Japan, 3. Japan Agency for Marine-Earth Science and Technology, 4. SOKENDAI, the Graduate University for Advanced Studies

(notes: authors and texts will be edited by 2/18.)
The recovery of a new Antarctic ice core to cover one-million years before present will advance our understandings of the Quaternary climate. Previous ice flow modeling studies indicates that such old ice may exist in inland areas of the Antarctic continent, where the ice is thick enough, accumulation rate is low, basal temperature is well below the pressure melting point, and horizontal ice flow is slow. The 59th Japanese Antarctic Research Expedition (JARE59, 2017-2018 Antarctic summer) conducted glaciological field surveys for the selection of next deep drilling around Dome Fuji. In particular, a set of ground radar surveys were conducted around Dome Fuji for improved mapping of the bedrock topography as well as internal layers of the ice sheet.

In the present study, we use an one-dimensional ice flow model to investigate the influence of uncertain parameters, such as ice thickness, accumulation rate, geothermal heat flux, and thinning rate on the age estimation of ice especially in the lowest few hundred meters. The calculated age and temperature profiles are compared with previous depth-age models and borehole temperature at Dome Fuji for assessing the model performance for our purposes. The one-dimensional model is then applied to the vicinity of Dome Fuji along the transect of JARE 59 surveys, and simulated age profiles are compared with dated internal layers from the observation. We discuss the evaluation of potential site and the influences of uncertain parameters on the age of the deep ice core.

©2021. Japan Geoscience Union. All Right Reserved.

The effect of ocean circulation on glacial-interglacial cycles

*Ryotaro Todoroki[1], Ayako Abe-Ouchi[1], Fuyuki SAITO[2], Takashi Obase[1], Wing-Le Chan[1], Sam Sherriff-Tadano[3], Yasuto Watanabe[4]

1. Atmosphere and Ocean Research Institute, The University of Tokyo, 2. Japan Agency for Marine-Earth Science and Technology (JAMSTEC), 3. The University of Leeds, 4. The University of Tokyo

The climate of the Pleistocene is characterized by glacial cycles which are said to be driven by orbital forcing. On the other hand, the state of the ocean like the AMOC strength also has an important role in the earth system. For example, the AMOC is closely related to a bi-polar seesaw mechanism, not only during deglaciation, but it may also affect ice sheet extent throughout entire glacial cycle. Indeed, some recent studies showed the effect of millennial scale oscillations, namely Dansgaard-Oeschger events (DOE), on ice sheets using ice-sheet models. In this study, we use an ice-sheet model (IcIES; Abe-Ouchi et al., 2013) and introduce the effects of DOE by applying temperature anomalies from hosing experiments in GCM and NGRIP ice core $\delta^{18}O$ data, which can be seen as an indicator of the AMOC strength. Including the effects of a DOE-like ocean circulation in the ice-sheet model, the North American ice sheet retreats to the southern margins of the Hudson Bay and the total ice volume of the North American and Eurasian ice sheets decreases to 50m (SLE) in MIS3. As for the last deglaciation, during the Bølling-Allerød (B-A) interstadial, the Northern American and Eurasian ice sheets melt rapidly in accordance with AMOC recovery and both discharge meltwater. When applying the DOE effect, meltwater from the Eurasian ice sheet increases dramatically and the amount surpasses that from the North American ice sheet during peak melting, leading to a near-complete deglaciation of the Eurasian ice sheet during the B-A warming period.

Keywords: Glacial-Interglacial Cycles, Dansgaard-Oeschger Event

©2021. Japan Geoscience Union. All Right Reserved.

Transient simulations of the last deglaciation using MIROC AOGCM and time evolving ice-topography

*Tristan Vadsaria[1], Takashi Obase[1], Ayako Abe-Ouchi[1], Sam Sherriff-Tadano [2,1], Wing-Le Chan[1]

1. Atmosphere and Ocean Research Institute, The University of Tokyo, Japan, 2. School of Earth and Environment, The University of Leeds, Leeds, UK

The last deglaciation (from 21 to 9 ka BP, also called T1) is the transition from the last glacial maximum (LGM) to the present interglacial. From the LGM, the increase in global temperature rise was about +4˚C to +6˚C and the Atlantic Meridional Overturning Circulation was largely affected. Previous transient simulations were performed at the University of Tokyo, using transient greenhouse gases (GHC) and orbital parameters with LGM ice sheet topography and bathymetry throughout the simulation (Obase & Abe-Ouchi., 2019). The previous study shows that abrupt AMOC increase, associated with the Bolling-Allerod (BA, about 14.7 to 14.2 ka BP) event, can be caused by gradual warming induced by orbital and greenhouse gases forcing without meltwater addition, and, that different hosing transient experiments using meltwater reconstruction affect the BA event timing.

The aim of the current study is to realize similar transient experiment using time-evolving ice-sheet according to recent reconstruction (ICE-5G, Peltier et al., 2015). To date, several simulations using this protocol and the same model as Obase & Abe-Ouchi. (2019), have been performed with sensitivity to freshwater discharge after 16 ka BP (when northern ice-sheet retreat is accelerated) and ocean bathymetry.

To equivalent freshwater forcing –i.e., 0.04 Sv applied uniformly between 50 and 70˚N after 16 ka (“control” run in Obase & Abe-Ouchi., 2019) –the retreat of the northern ice sheet induces warming in the ice sheet margins especially over northern America Abrupt warming occurred simultaneously (about 15.5 ka) in hosing experiments (time-evolving ice-sheet vs fixed ice-sheet). This timing is delayed when greater meltwater is applied (0.05Sv) inducing a Greenland warming in good agreement with temperature proxies, in term of timing (14.5 ka) and amplitude (about +10˚C within 500 years).

Keywords: Last deglaciation, Transient experiments, Hosing experiments, PMIP protocol

©2021. Japan Geoscience Union. All Right Reserved.

Inactivating microorganisms in melted snow and ice samples using ultraviolet germicidal radiation

*Fumio Nakazawa[1,2], Kumiko Goto-Azuma[1,2]

1. National Institute of Polar Research, 2. The Graduate University for Advanced Studies, SOKENDAI

The storage of melted snow and/or ice samples from snow pits and ice cores in a refrigerator for long durations may be limited by an increase in particle concentration caused by microbial growth after approximately 1–2 weeks. In this study, we examined an ultraviolet (UV) disinfection method for the storage of melted snow and/or ice samples. Surface snow obtained from Glacier No. 31 in the Suntar-Khayata Range, eastern Siberia, Russia was divided into two portions for UV treatment and untreated controls. Particle concentrations in the samples were measured using a Coulter counter (Multisizer 4e; Beckman Coulter, USA). Whereas the particle concentration in untreated samples increased, no obvious increase was observed over 53 days in the samples subjected to UV treatment. In addition, the original particle concentrations were unaffected by UV treatment. These findings indicate that the antimicrobial effect of UV radiation is effective for long-term sample storage of melted water samples. A detailed analysis of the particle size distribution for untreated samples indicated that particles of 0.7–1.2 μm appeared within the first 7–14 days. Measurements using a viable particle counter (XL-10BT2 and XL-28A1; RION Co. Ltd., Japan) confirmed that these were biological particles, suggesting that microbial growth occurs during this period. Subsequently, the particles shifted to a smaller size and a higher concentration, suggesting that the decomposition of microorganisms occurred in the water samples. Therefore, the size distribution of particles in untreated samples reflected the growth and decomposition of microorganisms over time.

Keywords: biological particle, glacier, snow, sterilization, culture

©2021. Japan Geoscience Union. All Right Reserved.

The origin of moisture inferred from water stable-isotopes of an ice-core drilled in the Pamir-Alay Mountains in Central Asia

*Daiki Seto[1], Nozomu Takeuchi[1], Aizen Vladimir[2], Akane Tsushima[3], Kenji Kawamura[4], Koji Fujita[5]

1. CHIBA university, 2. University of Idaho, 3. Graduate School of science, Chiba university, 4. Graduate School of Environmental Studies, Nagoya University, 5. National Institute of Polar Research, Research Organization of Information and Systems

Central Asia is located in the central part of the Eurasia Continent and is characterized by arid climate. Precipitation occurs mostly in the alpine area and forms glaciers, which are important water resources in this region. To evaluate the mass balance of such alpine glaciers, understanding of the moisture sources of the central Asia is important. In this study, water stable isotopes of ice-core drilled in the Pamir-Alay Mountains in western Central Asia were analyzed to assess the origin and its variations of the moisture transported to this region.

An ice-core was drilled in August 2016, at the top of an ice cap in the Pamir-Alay Mountains at the elevation of 5300 m a.s.l. The mean of $\delta^{18}O$, δD, and d-excess of the ice core were -10.0‰, -58.0‰ and 22.3‰, respectively. The stratigraphy of the ice-core suggests that significant melting and refreezing occurred in the most of layers, and thus the stable isotope records of this ice-core appear to be disturbed. The mean stable isotope of the upper parts of the ice-core (above 15 m) was higher than those of the lower part (below 25 m), suggesting the recent warming trend. As the mean isotopes of ice-core was compared with those of river water and precipitation around the mountain range, the isotope of ice-core cannot be explained by elevation effect of river water and precipitation of the southern side of the mountains, while it is close to the isotope of river water and precipitation of the northern side of the mountains. The mean isotope of the ice-core was further compared with those of other ice cores obtained in Central Asia. The isotope of this ice-core is significantly higher than that of the ice-core from Pamir located in the southern side of the mountains, but is close to those of ice-cores from Tien Shan located in the northern side of the study site. Results suggest that the water vapor transported to the Pamir-Alay mountains is different from that of the southern side of Pamir-Alay mountains, which is originally from Indian Ocean, but is similar to that of the Tien Shan Mountains, which is transported from the Mediterranean.

Keywords: Central Asia, Pamir-Alay mountains, ice-core, stable isotope, moisture

©2021. Japan Geoscience Union. All Right Reserved.

Analyses of pollen grains and insoluble particles in an ice core drilled in the Pamir-Arai Mountains in central Asia

*Nozomu Takeuchi[1], Haruka Ogaya[1], Koji Fujita[2], Kenji Kawamura[3], Akane Tsushima[1], Vladimir Aizen[4]

1. Chiba University, 2. Nagoya University, 3. National Institute of Polar Research, 4. University of Idaho

We analyzed pollen grains and insoluble particles in an ice core drilled in the Pamir-Arai Mountains in central Asia. The ice core was drilled in August of 2016 on an ice cap of elevation 5300 m a.s.l. The length of the ice core was 36 m from the surface to the bedrock. Microscopy revealed that the ice core contained mainly three morphological types of pollen grains, which are likely to correspond the genus of Juniperus, Artemisia, and Ephedra. Using the variations in these pollen concentrations in the ice core, annual layers were determined from the surface to the depth of 15 m for 21 years. In the section between the depths of 15 m and 26 m, little pollen grains were found in the ice core. The lack of pollen grains in the section is probably due to refrozen ice originated from water filled in a crevasse. Below the depth of 26 m, the pollen grains appeared again down to the bottom of the ice core. We found the charcoal particles in several layers in the deeper part of the core, suggesting that forest fires occurred in the past in this region. We also found pure calcite particles in some layers, which appeared not to be derived from terrestrial surface, but from a geyser because silicate mineral particles were not contained in the layers. Although this ice core did not appear to preserve a continuous past climate information, particle analyses could reveal unique environment events in this region of central Asia.

Keywords: ice core, pollen, central asia

©2021. Japan Geoscience Union. All Right Reserved.

[J] Poster | A (Atmospheric and Hydrospheric Sciences)：A-CG Complex & General

Thu. Jun 3, 2021 5:15 PM - 6:30 PM JST | Thu. Jun 3, 2021 8:15 AM - 9:30 AM UTC | Ch.07_1

[A-CG40] Coastal Ecosystems - 1. Water Cycle and Land-Ocean Interactions

convener:Masahiko Fujii(Faculty of Environmental Earth Science), Ryo Sugimoto(Faculty of Marine Biosciences, Fukui Prefectural University), Makoto Yamada(Faculty of Economics, Ryukoku University)

Substances from land which are brought by river and/or submarine groundwater discharge are important for the process of biological production in coastal areas. This session focuses on land-ocean interactions through water cycle. The aim of this session is to create interdisciplinary discussions on the research of connectivity of ecosystems, water cycles in terrestrial and coastal areas, fishery resources and biodiversity. Comprehensive discussion on the mechanisms that promote productivity and biodiversity in coastal ecosystems will be made from the viewpoint of land-ocean interactions. Presentations on water-material cycle in terrestrial and coastal areas, fishery resources, biodiversity and connectivity of the ecosystems are encouraged.
A companion session proposed as "Coastal Ecosystems - 2. Coral reefs, seagrass meadows, and mangroves" focuses on benthic communities in shallow-water ecosystems such as coral reefs, seagrass meadows and mangroves and is dedicated to promote researches on comprehensive assessment and monitoring of ecosystem functions and development of effective means for conservation and restoration. Main focuses of these two sessions are different. However, there are much of information that covers both sessions. Scientists who work on the related field will be able to obtain information and share them with other scientists if they attend to both of these sessions.

[ACG40-P01] Spatial extent of groundwater-derived heat in coastal area of volcanic sandy beach

*Makoto Yamada[1], Ryo Sugimoto[2], Toshimi Nakajima[2] (1.Faculty of Economics, Ryukoku University, 2.Faculty of Marine Biosciences, Fukui Prefectural University)

[ACG40-P02] Effects of fresh groundwater springs on phytoplankton primary productivity in a volcanic sandy beach

Kana Harada[1], *Ryo Sugimoto[1], Toshimi Nakajima[1], Osamu Tominaga[1] (1.Faculty of Marine Biosciences, Fukui Prefectural University)

[ACG40-P03] Spatial variation of ^{222}Rn concentration in river water and groundwater in the coastal area of Tokyo Bay

*Hiroya Kondo[1], Yu Umezawa[1], Misaki Ikari[1], Yosuke ONO[1], Shigeyoshi Otosaka[2], Muneoki Yoh[1] (1.Tokyo University of Agriculture and Technology , 2.Tokyo University)

Spatial extent of groundwater-derived heat in coastal area of volcanic sandy beach

*Makoto Yamada[1], Ryo Sugimoto[2], Toshimi Nakajima[2]

1. Faculty of Economics, Ryukoku University, 2. Faculty of Marine Biosciences, Fukui Prefectural University

Fresh groundwater from coastal areas provides nutrients to the sea and influences coastal ecosystems, but such fresh groundwater also provides thermal energy as well as chemical components. In contrast to seawater, groundwater has thermal characteristics that do not change significantly throughout the year. In other words, compared to seawater, cold water flows in during the summer and warm water flows in during the winter. However, the actual situation of the heat supplied by such groundwater is incompletely understood. In this study, we measured the surface temperature distribution of the sandy beach area and the sea area by a drone equipped with a thermal camera at the beach along the coast of Chokai Volcano in August 2020, and verified the spatial extent of groundwater-derived heat. In addition, the amount of heat flowing into the coastal zone was estimated from the freshwater inflow and temperature. Groundwater discharge in the sandy beach area was mainly observed on land, and no discharge from the seabed was observed. Groundwater from the land area flowed a few meters on the surface and then flowed into the sea. The groundwater temperature immediately after the discharge was about 9 deg. C, but it became about 12 deg. C while flowing on the surface and flowed into the sea. In the sea area, the sea water temperature range from 20 to 25 deg. C was extended to about 50 m off the shoreline. Since the actual seawater temperature measured offshore was about 28 deg. C, it is thought that a seawater temperature area of 20 to 25 deg. C was formed due to the low temperature water flowing in from the land. The area of the sea affected by groundwater-derived heat was about 13,000 m^2 (about 300 m north-south and 50 m east-west).The amount of heat flowing from the groundwater into the sea was estimated to be about -16 GJ/day. These results indicate that groundwater discharged at the sandy beach plays a role in lowering the seawater temperature in a certain range of coastal areas during the summer.

Keywords: Groundwater, Coastal Area, Heat Influx, Thermal Image, Drone

©2021. Japan Geoscience Union. All Right Reserved.

Effects of fresh groundwater springs on phytoplankton primary productivity in a volcanic sandy beach

Kana Harada[1], *Ryo Sugimoto[1], Toshimi Nakajima[1], Osamu Tominaga[1]

1. Faculty of Marine Biosciences, Fukui Prefectural University

Research on how SGD nutrients impact marine biota has increased in recent years. The documented response of marine organisms to SGD is quite variable and site-specific, and can be positive or negative from a population or community perspective. Additionally, the response to SGD is sometimes unclear and could change depending on the specific location or time of the year. The most documented response to SGD-derived nitrogen and phosphorus loading is related to increasing the primary productivity of phytoplankton or microphytobenthos. However, in some cases, no response was found near sites receiving fresh groundwater springs, indicating SGD loading does not always induce an increase in primary productivity. Here, we present the phytoplankton primary productivity around fresh groundwater springs in the Chokai volcano coast assessed by the field experiments. Although fresh groundwater springs were significant nutrient sources, the primary productivity of phytoplankton decreased with increasing groundwater impact, possibly due to physical and physiological disturbances such as low salinity and temperature.

Keywords: Submarine groundwater discharge, 13C isotope tracer, Field experiment

©2021. Japan Geoscience Union. All Right Reserved.

Spatial variation of ^{222}Rn concentration in river water and groundwater in the coastal area of Tokyo Bay

*Hiroya Kondo[1], Yu Umezawa[1], Misaki Ikari[1], Yosuke ONO[1], Shigeyoshi Otosaka[2], Muneoki Yoh[1]

1. Tokyo University of Agriculture and Technology , 2. Tokyo University

It is important to correctly assess the source and amount of freshwater-derived nitrogen and phosphorus that enter from the land to shallow coastal areas. However, it is not possible to distinguish the contributions of groundwater and river water based only on salinity changes, and the impact of groundwater inflow on shallow coastal ecosystems has not been evaluated in the Tokyo Bay. Therefore, we aimed to (1) investigate the spatial distribution of ^{222}Rn in groundwater and river water in the coastal area of Tokyo Bay, and to explore the factors causing its variation and (2) confirm the significant difference in ^{222}Rn concentration between river water and groundwater in the coastal area, and to show the effectiveness of ^{222}Rn as an indicator of groundwater discharge to Tokyo Bay. Groundwater, spring water, and river water were collected from September 2020 to January 2021 in the coastal area of Tokyo Bay from Miura Peninsula to Boso Peninsula. ^{222}Rn concentrations were analyzed using an radon detector based on electrostatic collection of alpha-emitters (RAD7), and general water quality was analyzed using ion chromatography. ^{222}Rn concentration in groundwater (dpm/L) was 43-477 in the innermost part of the bay, 9-1480 in the western part of the bay, and 134-386 in the eastern part of the bay. The concentrations of ^{222}Rn in river water (dpm/L) were 24-30 in the innermost part of the bay, 10-62 in the western part of the bay, and 21-50 in the eastern part of the bay. In all areas, the difference in ^{222}Rn concentrations between groundwater and river water was about one to two orders. The factor causing the difference in ^{222}Rn concentration in each location will be discussed in the viewpoint of geology, topography, groundwater residence time, soil porosity/crack, and underground redox state.

Keywords: ^{222}Rn, groundwater, coastal area

©2021. Japan Geoscience Union. All Right Reserved.

[J] Poster | A (Atmospheric and Hydrospheric Sciences)：A-CG Complex & General

Thu. Jun 3, 2021 5:15 PM - 6:30 PM JST | Thu. Jun 3, 2021 8:15 AM - 9:30 AM UTC | Ch.07_2

[A-CG41] Coastal Ecosystems -2. Coral reefs, seagrass and macroalgal beds, and mangroves

convener:Yu Umezawa(Tokyo University of Agriculture and Technology), Toshihiro Miyajima(Marine Biogeochemistry Group, Division of Ocean-Earth System Science, Atmosphere and Ocean Research Institute, The University of Tokyo), Atsushi Watanabe(The ocean policy research institute, The Sasakawa peace foundation), Tomihiko Higuchi(Atmosphere and Ocean Research Institute, The University of Tokyo)

Coastal marine ecosystems are complex open system interacting with surrounding watersheds, outer ocean, and the atmosphere, providing a wealth of various ecosystem services to human life. Simultaneously, they are also influenced strongly and often negatively by human activities. This session, together with a companion session dedicated for the water cycle and land-ocean interactions, aims to provide a platform for interdisciplinary discussion covering various aspects of frontiers in coastal ecosystem sciences. This session particularly focuses shallow-water benthic communities ranging from temperate to tropical regions, such as coral reefs, seagrass and macroalgal beds, mangroves, intertidal flats, and saltmarshes. All these communities are characterized by intrinsically high primary production, active material cycling, and biodiversity hot spots. However, increasing human demand for coastal marine resources and industrial development concentrating on coastal regions incur the risk of rapid degradation and diminishment. Comprehensive assessment and monitoring of ecosystem functions and development of effective means for conservation and restoration are urgently needed for such communities. This session is dedicated to organizing and promoting such research and management activities by sharing state-of-the-art science and technology among ecologists, geologists, geochemists, biogeographers, etc. Field-based and modeling studies concerning the following topics are especially welcome: material cycling and ecosystem functions; community connectivity; environmental changes such as global warming, ocean acidification, and sea-level rise; ecosystem services such as carbon sequestration, nutrient regulation, and fisheries production; broad-scale comparison; long-term ecological researches.

[ACG41-P01] Skeleton microstructures and *in situ* colony morphometry analysis of the corals collected during Tara Pacific Expedition

*Guinther Hiromu Mitushasi[1], Yuko Kitano[2], Emilie Boissin[3], Serge Planes[3], Denis Allemand[4], Tara Pacific Consortium[1], Sylvain Agostini[1] (1.Shimoda Marine Research Center, University of Tsukuba, 2. National Institute of Environmental Science, Japan (Tsukuba), 3. CRIOBE, Universite de Perpignan (Perpignan), 4. Monaco Scientific Center (Monaco))

[ACG41-P02] Diversity of coral distributions and the difference in Sakiyamawan-Amitoriwan nature conservation area, Iriomote Island, Japan

*Shinya Shimokawa[1], Tomokazu Murakami[1], Hiroyoshi Kohno[2], Akira Mizutani[2] (1.National Research Institute for Earth Science and Disaster Resilience, 2.Okinawa Reagional Research Center, Tokai University)

[ACG41-P03] Characteristics of water temperature changes and coral breaching in Amitori Bay, Iriomote Island, Japan

*Shinya Shimokawa[1], Tomokazu Murakami[1], Hiroyoshi Kohno[2], Akira Mizutai[2] (1.National Research Institute for Earth Science and Disaster Prevention, 2.Okinawa Reagional Research Center, Tokai University)

[ACG41-P04] Coral bleaching countermeasures by supplying metal-containing feed ~evaluation the effect at gene expression levels~

*Ikuko Yuyama[1], Naoko Yasuda[2], Sayaka Higa[2], Sung-Yin Yang[3], Sylvain Agostini [3], Tomihiko Higuchi[4], Toshihiro Miyajima[4], Takashi Nakamura[5], Hiroyuki Fujimura[2] (1.Yamaguchi University, 2.University of the Ryukyus, 3.University of Tsukuba, 4.The University of Tokyo , 5.Tokyo Institute of Technology)

[ACG41-P05] Linear and non-linear analysis for high temperature and acidification event in the Great Barrier Reef based on the observation in the Coral Sea

*Tatsuki Tokoro[1,2], Shin-ichiro Nakaoka[1], Shintaro Takao[1] (1.National Institute for Environmental Studies, 2.Port and Airport Research Institute)

[ACG41-P06] Stratigraphy of seagrass bed at Bise in Okinawa Island.

*Wataru Sano[1], Kazuhiko Fujita[2], Yoshikatsu Nakano[3], Shoko Hirabayashi[4], Yusuke Yokoyama[5], Yosuke Miyairi[5], Naoko Isomura[6], Hironobu Kan[1] (1.Kyushu Univ., 2.Univ. of the Ryukyus, 3.Okinawa Institute of Science and Technology Graduate University , 4.Rissho Univ., 5.Univ. of Tokyo, 6.National Institute of Technology, Okinawa College)

[ACG41-P07] **Applying DPSIR framework for blue carbon ecosystems assessment: The case of Busuanga Island, Palawan, Philippines**

*Jay Mar Dioquito Quevedo[1], Yuta Uchiyama[2], Ryo Kohsaka[2] (1.Tohoku University, 2.Nagoya University)

[ACG41-P08] Detecting mangrove- and seagrass-derived eDNA from deep-sea sediment around Yaeyama Islands: Implication for offshore blue carbon sequestration

*Toshihiro Miyajima[1], Masami Hamaguchi[2], Takashi Nakamura[3], Hajime Katayama[4], Masakazu Hori[5] (1.Marine Biogeochemistry Group, Division of Ocean-Earth System Science, Atmosphere and Ocean Research Institute, The University of Tokyo, 2.National Research Institute of Fisheries Technology, Japan Fisheries Research and Education Agency, 3.School of Environment and Society, Tokyo Institute of Technology, 4.Geological Survey of Japan, National Institute of Advanced Industrial Science and Technology, 5.National Research Institute of Fisheries Resources, Japan Fisheries Research and Education Agency)

[ACG41-P09] Evaluation of the effect of differences in nitrogen loading on the chemical composition and decomposition characteristics of eelgrass(*Zostera marina*).

*Toru Miyata[1], Yu Umezawa[1], Takunari Ida[1], Yoshiki Horikawa[1], Makoto Watanabe[1], Shigeki Wada[2], Masahiro Nakaoka[3], Tomohiro Kuwae[4] (1.Tokyo University of Agriculture and Technology, 2.University of Tsukuba, 3.Hokkaido University, 4.Port and Airport Research Institute)

Skeleton microstructures and *in situ* colony morphometry analysis of the corals collected during Tara Pacific Expedition

*Guinther Hiromu Mitushasi[1], Yuko Kitano[2], Emilie Boissin[3], Serge Planes[3], Denis Allemand[4], Tara Pacific Consortium[1], Sylvain Agostini[1]

1. Shimoda Marine Research Center, University of Tsukuba, 2. National Institute of Environmental Science, Japan (Tsukuba), 3. CRIOBE, Universite de Perpignan (Perpignan), 4. Monaco Scientific Center (Monaco)

The taxonomy of scleractinian corals is still open to extensive debate due the high morphological variability among and within the numerous species. This variability can be associated with species plasticity and hybridization, phenotypic polymorphism, geographic variation and diverse environmental factors. Accurate and reproducible methods of taxonomic analysis are required for a better understanding of the distribution of coral communities and their response to climate change and anthropogenic stressors. Recent studies combining skeleton morphometry with genetic analysis have shown the relevance of landmark based skeleton morphometric analysis to identify coral species and the populations within. The Tara Pacific expedition collected more than 3000 samples from 30 different islands across two transects crossing the Pacific Ocean East-West and South-North. Three species, *Porites lobata*, *Pocillopora meandrina* and *Millepora platyphylla* were chosen for their relevance in the reef ecosystem and their presence across the whole Pacific. However, these species present great variations in their morphologies at both the colony and the skeleton levels making sampling and post-identification challenging. Here, we present the taxonomic identification of the corals collected during the Tara Pacific Expedition using morphometry landmark analysis of the coral colonies and their skeleton microstructures. The results will be further matched with the SNIPs based genotypes and linked with environmental and -omics data collected for the specimens.

Keywords: Tara Pacific, P. lobata, P. meandrina, skeleton morphometry, landmark analysis

©2021. Japan Geoscience Union. All Right Reserved.

Diversity of coral distributions and the difference in Sakiyamawan-Amitoriwan nature conservation area, Iriomote Island, Japan

*Shinya Shimokawa[1], Tomokazu Murakami[1], Hiroyoshi Kohno[2], Akira Mizutani[2]

1. National Research Institute for Earth Science and Disaster Resilience, 2. Okinawa Reagional Research Center, Tokai University

The Sakiyamawan-Amitoriwan nature conservation area, Iriomote Island, is the only oceanic nature conservation area in Japan. The area has no access roads; therefore, it conserves a natural environment with very little human impact and various coastal marine ecosystems such as those containing reef-building corals and *Enhalus acoroides* (a kind of seagrass; its northern distribution limit is the ocean area surrounding the Yaeyama Islands, Japan). Sakiyama and Amitori bays are adjacent, but the coral distributions in both bays are largely different because of the difference of the geographical environmental gradients such as water depth, bay length and bay shape.
In this study, the difference of coral distributions between both bays are investigated from a view of diversity index (MacArthur and MacArthur, 1961, Clark & Warwick, 2001, McCune and Grace, 2002) and intermediate disturbance hypothesis (Connell, 1978) based on the results of coral distribution field survey, physical environmental observation such as wave height and soil particle number, and numerical simulations using the observation data that we have conducted since 2011 (e.g., Shimokawa et al., 2014, 2015, 2016, 2020).
In Amitori Bay, the diversity index (here, based on colony shapes) was at the maximum in the middle part of the bay, and intermediate disturbance hypothesis was realized by considering wave height and soil particle as external disturbance. Also, *Enhalus acoroides* is scarce and there is no large community. On the other hands, in Sakiyama Bay, the diversity index was at the maximum in the edge of coral reef and intermediate disturbance hypothesis was not realized. Also, *Enhalus acoroides* is distributed broadly from the inner part of the bay to the middle part of the bay. In the presentation, the reason of the difference between both bays is also stated from a view of the difference of the effect of soil particle inflow due to geographical environmental gradients between both bays.

References:

Clarke, K. R. and R. M. Warwick (2001), Changes in marine communities: an approach to statistical analysis and interpretation, 2nd ed., PRIMER-E, Plymouth, pp. 176.
Connell, J. H. (1978), Diversity in Tropical Rain Forests and Coral Reefs, Science, 199, 1302-1310.
MacArthur, R. H. and J. W. MacArthur (1961), On bird species diversity, Ecology, 42, 594-598.
McCune, B. and J. B. Grace. (2002), Analysis of Ecological Communities, MjM Software Design, Oregon, pp.300.
Shimokawa, S., T. Murakami, A. Ukai, H. Kohno, A. Mizutani and K. Nakase (2014): Relationship between coral distributions and physical variables in Amitori Bay, Iriomote Island, Japan, J. Geophys. Res.: Oceans, 119, 8336-8356 (doi: 10.1002/2014JC010307).
Shimokawa, S., H. Kohno, T. Murakami, A. Mizutani, T. Shibayama, Y. Yamamoto, A. Ukai and K. Nakase (2015): Relationship between massive coral distribution and physical variables in Amitori Bay, Iriomote Island, Japan. Ann. J. Civil Eng. Ocean B3, 71, 969-974 (in Japanese with English abstract).
Shimokawa, S., H. Kohno, T. Murakami, S. Miyauchi, M. Suzuki and A. Mizutani (2016): Relation between coral distributions and Physical variables in Sakiyama Bay, Iriomote Island, Japan. Ann. J. Civil Eng. Ocean

©2021. Japan Geoscience Union. All Right Reserved.

B2, 72, 1435-1440 (in Japanese with English abstract).
Shimokawa, S., T. Murakami and H. Kohno eds. (2020), Geophysical Approach to Marine Coastal Ecology -The Case of Iriomote Island, Japan, Springer, 273 pp.

Keywords: Reef building coral, Diversity index, Intermediate disturbance hypothesis

©2021. Japan Geoscience Union. All Right Reserved.

Characteristics of water temperature changes and coral breaching in Amitori Bay, Iriomote Island, Japan

*Shinya Shimokawa[1], Tomokazu Murakami[1], Hiroyoshi Kohno[2], Akira Mizutai[2]

1. National Research Institute for Earth Science and Disaster Prevention, 2. Okinawa Reagional Research Center, Tokai University

Amitori Bay is located in the northeast region of Iriomote Island, Japan, and is a small bay but has a wide variety of environments with little human impacts and coastal ocean ecosystem such as reef building corals and mangrove forests. We have investigated the relationship between coral distributions and physical variables since 2011. In summer of 2016, a wide area breaching of the corals was caused also in the bay. The changes of water temperature in the bay are considered to have a large effect on the breaching.
In this study, the changes of water temperature in Amitori Bay are investigated from the observational data during 2014-2017. The results showed that no typhoon approached in this area in summer of 2016 caused high water temperature for a long term compared to the other years, and resulting the breaching of the corals. In the presentation, characteristics of seasonal changes of water temperature in Amitori Bay are also stated from the results of data analysis and numerical simulations.

Reference:

Shimokawa, S., T. Murakami and H. Kohno eds. (2020), Geophysical Approach to Marine Coastal Ecology -The Case of Iriomote Island, Japan, Springer, 273 pp.

Keywords: Reef building coral, Water temperature, Typhoon

©2021. Japan Geoscience Union. All Right Reserved.

Coral bleaching countermeasures by supplying metal-containing feed ~evaluation the effect at gene expression levels~

*Ikuko Yuyama[1], Naoko Yasuda[2], Sayaka Higa[2], Sung-Yin Yang[3], Sylvain Agostini [3], Tomihiko Higuchi[4], Toshihiro Miyajima[4], Takashi Nakamura[5], Hiroyuki Fujimura[2]

1. Yamaguchi University, 2. University of the Ryukyus, 3. University of Tsukuba, 4. The University of Tokyo , 5. Tokyo Institute of Technology

Under high temperature stress, the reactive oxygen species (ROS) generated from symbiotic algae triggers the coral bleaching response. There is a possibility that the antioxidant enzymes containing metal ions such as Fe, Mn, and Zn, have an effect on the mitigation of ROS stress. Therefore, we hypothesized that the supply of metal ions promotes antioxidant activity and mitigates the bleaching response. In this study, the corals were fed with a metal-containing diet, and investigated the effect on the bleaching response at gene expression level.

We used *Acropora hyacinthus* collected around Sesoko Island, and they were fed with Artemia and metal-fortified yeast. Furthermore, the coral was incubated at an increasing temperature, and physiological responses and gene expression change of coral and their symbiotic algae were investigated. Coral was fixed at the time point when the bleaching response was observed, and large-scale gene expression analysis by Next Generation Sequencing was performed. We identified 25,069 contigs derived from *Acropora hyacinthus* by de novo assembled of the short reads. Then, expression levels of each contigs were estimated, and the gene expression related to the physiological response of corals was investigated. Results showed that the expression level of genes related to proto-oncogene and CuZnSOD of corals was increased by temperature stress. [H1] These gene expression changes tended to be mitigated by feeding with artemia or yeast. Furthermore, a result of canonical correlation analysis (CCA) using the physiological data and the gene expression data showed that genes related to mucin metabolism and vitamin B12 were associated with the changes in symbiont density. Based on these gene expression levels, we discussed the effects of metal-containing diet on mitigating coral bleaching reactions.

Keywords: coral bleaching, feeding effect, RNA-seq

©2021. Japan Geoscience Union. All Right Reserved.

Linear and non-linear analysis for high temperature and acidification event in the Great Barrier Reef based on the observation in the Coral Sea

*Tatsuki Tokoro[1,2], Shin-ichiro Nakaoka[1], Shintaro Takao[1]

1. National Institute for Environmental Studies, 2. Port and Airport Research Institute

For predicting the health of coral reefs in the future, it is important to evaluate the impact of global fluctuations caused by the open ocean as well as the effect from the land area. For example, the widespread bleaching of the Great Barrier Reef (GBR) in 2016-2017 was attributed to the high temperature of seawater associated with El Nino event, but past El Nino events and GBR bleaching had not been necessarily linked. Therefore, the detailed analysis is required for future prediction of global fluctuation effects on coral reefs. In addition, the decrease in aragonite saturation state (Ω) due to the ocean acidification will lead to the inhibition of coral growth, but the study about the quantitative evaluation of Ωin coral reefs and the combined process with the high temperature event have not been enough at present.

In this study, we used the data in the Coral Sea, which corresponds to the oceanic endmember of GBR, from 2006 to 2018 observed by the National Institute for Environmental Studies (NIES) as the Volunteer Observation Ship program to identify the high temperature event and the Ωfluctuations in the GBR. In the analysis, the nonlinear analysis by machine learning (Random Forest and Gaussian Process) was applied to construct a regression model of the objective variables and extract the important explanatory variables. We used the Degree Heating Week (DHW; obtained from NOAA Coral Reef Watch), which is a high correlation index with the coral bleaching, and the Dissolved Inorganic Carbon concentration normalized to salinity of 35 (nDIC; calculated from the observation data of NIES), which is the main caution of the fluctuation of Ωas the objective variable of the high temperature event and the acidification, respectively.

The results of the regression model by Random Forest analysis are shown in Fig. 1. For the high temperature event, the atmospheric pressure on the Coral Sea was extracted as an important parameter in addition to the Southern Oscillation Index (SOI). This indicates that there are several meteorological patterns in the GBR during El Nino event, and that certain patterns, such as the increase in the amount of solar radiation, might cause the high temperature event in the GBR. It was also clarified that the fluctuation of Ωwas strongly influenced by the sea surface temperature and the concentration of atmospheric CO_2. However, the correlation with the former parameter is considered to be apparently significant because both the sea surface temperature and nDIC in the Coral Sea have increased by the recent global warming and acidification. No significant correlation was confirmed between the objective variables DHW and nDIC. This suggests that the high temperature and acidification in the GBR are independent phenomena each other. In the presentation, we will show the results of the linear regression analysis and will show more detailed analysis using the improved regression models.

Keywords: Great Barrier Reef, high temperature process, Acidification

©2021. Japan Geoscience Union. All Right Reserved.

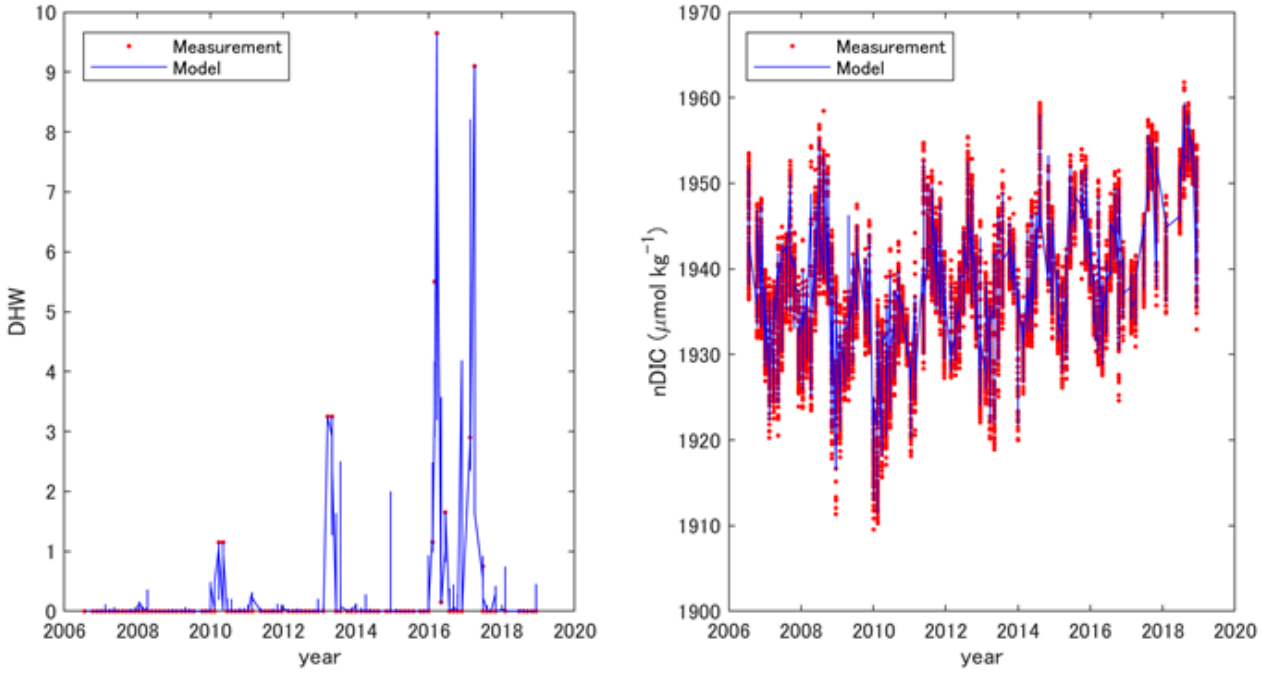


Figure 1
Results of regression model (blue) and the measurements (red);
DHW in GBR (left: r^2=0.98), nDIC in the Coral Sea (right: r^2=0.95).

©2021. Japan Geoscience Union. All Right Reserved.

Stratigraphy of seagrass bed at Bise in Okinawa Island.

*Wataru Sano[1], Kazuhiko Fujita[2], Yoshikatsu Nakano[3], Shoko Hirabayashi[4], Yusuke Yokoyama[5], Yosuke Miyairi[5], Naoko Isomura[6], Hironobu Kan[1]

1. Kyushu Univ., 2. Univ. of the Ryukyus, 3. Okinawa Institute of Science and Technology Graduate University , 4. Rissho Univ., 5. Univ. of Tokyo, 6. National Institute of Technology, Okinawa College

Coral reef seagrass bed is a community of seagrass formed in the lagoon off the beach, where fish and benthic organisms live and spawn, and play a role in the carbon cycle in shallow coastal area (Nellemann et al., 2009; Unsworth et al., 2018).
The surface substrate of the seagrass beds in Bise, Okinawa Island, was muddy sand sediments and a living branch coral (*Montipora digitata*). It has been proposed that seagrass and coral are in a symbiotic relationship by the rhizome of *Thalasia hemprichii* is entwined with the underground part of Montipora digitata in this area (Ninomiya et al., 2016). In addition, past aerial photographs show that the almost seagrass beds in Bise was disappeared in the 1960s, but recovered rapidly after 1980s.
It is necessary to clarify how the seagrass beds, which is an ecologically highly unique place and is thought to be sensitive to environmental changes in the coral reef lagoon, has accumulated during the process of coral reef development in the Holocene. It is very important to conserve the seagrass beds and consider the factors that form the zonal trend of coral reefs including the seagrass beds.
In this study, we used the five sediment cores (maximum penetration depth 253 cm) collected from the seagrass beds in Bise by hand boring. We focused on coral fossils and large benthic foraminifera contained in the core sediments to clarify the sedimentary structure of the seagrass beds.
The top part of the core sediment (0-40 cm; 157 cm below MSL) was muddy sand sediments indicating seagrass bed. The bottom part below 86 cm was a coarse-graine sediment including many fossil corals (*Acropora* sp.), and 40-86 cm was a transition facies in which muddy sand including fossil *Acropora* fragments.
As a result, it was clarified that the habitat of branch coral (*Acropora* sp.) was buried by muddy sand sediments and gradually formed a modern seagrass beds.

Keywords: Seagrass beds, Coral reefs, Foraminifera, Intertidal flats, Ryukyus

©2021. Japan Geoscience Union. All Right Reserved.

Applying DPSIR framework for blue carbon ecosystems assessment: The case of Busuanga Island, Palawan, Philippines

*Jay Mar Dioquito Quevedo[1], Yuta Uchiyama[2], Ryo Kohsaka[2]

1. Tohoku University, 2. Nagoya University

Mangrove forests, seagrass meadows, and tidal marshes or collectively known as blue carbon ecosystems (BCEs) play important roles in reducing the risks and impacts of climate change through carbon sequestration and other essential ecosystem services. Despite this, records show that they are declining at various scales due to their vulnerability to natural and anthropogenic disturbances. Similar trends are observed at a local scale, particularly in the case of Busuanga Island, Palawan province in the Philippines, where BCEs along with other marine and coastal ecosystems are perceived to be threatened by a number of factors. To better understand and capture the state changes of coastal ecosystems with emphasis on BCEs, this study collected the drivers and pressures and their impacts on the coastal environments as well as existing management responses by interviewing 17 stakeholders representing community organizations, non-government organizations, and municipal level government units from the municipality of Busuanga. The interview results were analyzed by applying the Drivers-Pressures-State-Impact-Response (DPSIR) framework. The results of this study show that lack of institutional capacities (indirect driver) is the leading factor that hinders the progress or efficacy of coastal management. Most pronounced pressures caused by direct drivers to BCEs include overexploitation and coastal developments. The responses collected in the interviews can be grouped into ecosystems management, capacity building development, policies and implementation, and welfare and livelihood development. These results can be used to enhance or update existing management responses into more precise and contextualized measures in addressing specific impacts observed in the local areas.

Keywords: blue carbon ecosystems, DPSIR framework, stakeholders, Philippines

©2021. Japan Geoscience Union. All Right Reserved.

Detecting mangrove- and seagrass-derived eDNA from deep-sea sediment around Yaeyama Islands: Implication for offshore blue carbon sequestration

*Toshihiro Miyajima[1], Masami Hamaguchi[2], Takashi Nakamura[3], Hajime Katayama[4], Masakazu Hori[5]

1. Marine Biogeochemistry Group, Division of Ocean-Earth System Science, Atmosphere and Ocean Research Institute, The University of Tokyo, 2. National Research Institute of Fisheries Technology, Japan Fisheries Research and Education Agency, 3. School of Environment and Society, Tokyo Institute of Technology, 4. Geological Survey of Japan, National Institute of Advanced Industrial Science and Technology, 5. National Research Institute of Fisheries Resources, Japan Fisheries Research and Education Agency

Coastal vegetated ecosystems (mangroves, salt marshes, seagrass beds) have been recognized as potential carbon dioxide (CO_2) sink due to their capacity to capture CO_2 and store organic carbon (OC) in anoxic sediment inside them. At the same time, these ecosystems are exporting OC (a.k.a. blue carbon) to outer ocean through tidal action, and the magnitude of OC export is believed to be as large as or even greater than that of OC burial within the ecosystems. Although the fate of exported OC has not been assessed due to technical difficulty, a part of exported OC may be transported across the pycnocline to deep ocean and isolated from the atmosphere for long term. For comprehensive evaluation of carbon sequestration capacity of coastal ecosystems, we need to clarify the fate of OC exported from these ecosystems, focusing on whether and to what extent OC may be sequestered in deep ocean.

In this study, we tested applicability of environmental DNA (eDNA) for detecting and estimating mangrove- and seagrass-derived OC in offshore sediments including those from the bathypelagic zone (>1000 m). As a case study, we focused OC export from mangroves and subtropical seagrass beds around Sekisei Lagoon, Okinawa, Japan, to the Lagoon and further to offshore area off Yaeyama Islands. Surface sediment samples were collected and analyzed for eDNA concentration by quantitative PCR, as well as OC, $\delta^{13}C_{OC}$, and specific surface area. Target species of the eDNA analysis include dominant plant species in this region, i.e., *Rhizophora stylosa*, *Bruguiera gymnorhiza*, and *Sonneratia alba* for mangroves, and *Thalassia hemprichii*, *Cymodocea rotundata*, and *Enhalus acoroides* for seagrasses.

Due to relatively high-energy conditions, shallow sediments of Sekisei Lagoon were mostly composed of coarse carbonate sand and often lacked any traces of mangrove and seagrass eDNA. However, significant concentrations of both mangrove and seagrass DNA fragments were detected from sediments of narrow nearshore area of Nagura Bay, where silty sediment supplied by the Nagura River prevailed. Offshore sediments commonly contained OC with the bulk $\delta^{13}C$ of -23‰ to -19‰, indicating that pelagic primary producers are the predominant source for OC stored in pelagic sediments. Nevertheless, DNA fragments of mangroves, but not seagrasses, could be detected in offshore sediments outside the Lagoon. Mangrove-derived eDNA was often detected significantly in bathypelagic sediments collected from northern area of Yaeyama Island. The concentration of bulk OC was also relatively high (>500 μmol C g^{-1}) in these sediments.

These observations suggest that: (i) organic detritus produced in coastal habitats such as mangroves and seagrass beds is exported by tidal action; (ii) exported OC is not accumulated significantly in shallow lagoon outside the habitats due to high-energy physical environment, but (iii) flushed away further to offshore water by tidal residual current, which usually flows from south to north across the lagoon; (iv) a

©2021. Japan Geoscience Union. All Right Reserved.

part of OC then sinks down to bathypelagic zone and stored in deep-sea sediment. Thus, deep-sea sediment located downstream of major coastal vegetated habitats can serve as potentially important blue carbon sink.

Keywords: Coastal vegetated ecosystems, Organic carbon export, Carbon sequestration, Deep-sea sediment, Environmental DNA

©2021. Japan Geoscience Union. All Right Reserved.

Evaluation of the effect of differences in nitrogen loading on the chemical composition and decomposition characteristics of eelgrass(*Zostera marina*).

*Toru Miyata[1], Yu Umezawa[1], Takunari Ida[1], Yoshiki Horikawa[1], Makoto Watanabe[1], Shigeki Wada[2], Masahiro Nakaoka[3], Tomohiro Kuwae[4]

1. Tokyo University of Agriculture and Technology, 2. University of Tsukuba, 3. Hokkaido University, 4. Port and Airport Research Institute

Nitrogen is one of the elements that can limit the primary production of plants, therefore nitrogen supply potentially affects coastal primary production. On the other hand, it is known that some secondary metabolites such as phenolic compounds that are not directly involved in growth and catabolism such as photosynthesis, respiration, and assimilation act as protective compounds against predators and pathogens. Some report that the abundance of these substances varies with the supply of nitrogen. Thus, differences in nitrogen supply may contribute not only to the growth of these plants, but also to the biodegradation properties of the plant.

In this study, we focused on the eelgrass (*Zostera marina*) widely distributed in the coastal area of Japan, and examined the followings, potential effects of the nitrogen supply in the coastal area on the function as “blue carbon”.

1) Possibility of measuring nitrogen content in eelgrass leaf using portable nitrogen meter

The measured values of multiple portable nitrogen meters for land herbs were compared with the chlorophyll content and actual nitrogen content of the eelgrass Z. marina. Conditions that enable us to effectively estimate the nitrogen content of eelgrass are discussed.

2) Relationship between nitrogen content and the amount of structural and repellent substances in the eelgrass leaves

The amount of structural substances and repellent substances of eelgrass plants were evaluated using chemical (KOH, $NaClO_2$, and NaOH) treatments and Folin-ciocalteu method, respectively, and compared with the nitrogen content.

3)Evaluation of the decomposition characteristics of eelgrass in the different environmental conditions

Effects of nitrogen load on the decomposition characteristics of eelgrass were evaluated by monitoring in the different environmental conditions.

Keywords: Blue carbon, Nitrogen load, Refractory organic carbon, Eelgrass(Zostera marina)

©2021. Japan Geoscience Union. All Right Reserved.

[J] Poster | A (Atmospheric and Hydrospheric Sciences)：A-CG Complex & General

Thu. Jun 3, 2021 5:15 PM - 6:30 PM JST | Thu. Jun 3, 2021 8:15 AM - 9:30 AM UTC | Ch.07_3

[A-CG42] Water and sediment dynamics from land to coastal zones

convener:Shinichiro Kida(Research Institute for Applied Mechanics, Kyushu University), Yuko Asano(The University of Tokyo), Keiko Udo(International Research Institute of Disaster Science, Tohoku University), Dai Yamazaki(Institute of Industrial Sciences, The University of Tokyo)

The dynamics of water and sediments from land to the ocean, such as hillslope runoff generation, river flow and flooding, sediment transport and geomorphology, and coastal river plumes, are inter-connected through processes with various spatial- and temporal-scales. As compound disasters and environmental changes often involve these processes occurring simultaneously at multiple scales, integrated understanding of the dynamics of water and sediments across hillslope, floodplain, river mouth, and coastal-zone are required. We welcome wide-range studies related to the dynamics of water and sediments from land to the ocean with theoretical, observational, and simulation-based approaches such as basic process understanding, in-situ and remote-sensing observations, big-data analysis and supercomputing.

[ACG42-P01] Representing terrestrial water dynamics within Earth system modelling framework

*Dai Yamazaki[1] (1.Institute of Industrial Sciences, The University of Tokyo)

[ACG42-P02] Breaching flood impact analysis of landslide dams in the Yarlung Tsangpo River Basin

*Danyi Shen[1,2], Zhenming Shi[1,2], Ming Peng[1,2] (1.Key Laboratory of Geotechnical & Underground Engineering of Ministry of Education, Tongji University, Shanghai 200092, China, 2.Department of Geotechnical Engineering, Tongji University, Shanghai 200092, China)

[ACG42-P03] Sediment transport analysis from the Abukuma river to the sea by typhoon No.19 in 2019

Makoto Kobayashi[1], *Daisuke Nakahara[1], Keiko Udo[1], Hiroshi Takebayashi[2] (1.International Research Institute of Disaster Science, Tohoku University, 2.Disaster Prevention Research Institute, Kyoto University)

[ACG42-P04] Structural characteristics of airflow and blown sand flux over fine-grained gravel surfaces in wind tunnel

*Jiaqi Liu[1], Reiji Kimura[1], Jing Wu[1] (1.Arid Land Research Center, Tottori University)

[ACG42-P05] Predictive simulations of redeposition and seawater transportation after a tsunami in Osaka Bay where bottom sediments were disturbed by tsunami

*Mitsuru Hayashi[1,2], Satoshi Nakada[4], Soichi Hirokawa[2], Shuto Fujisawa[3] (1.Research Center for Inland Seas, Kobe University, 2.Graduate School of Maritime Sciences, 3.Faculty of Maritime Sciences, 4. National Institute for Environmental Studies)

[ACG42-P06] Application of an isopycnal-layered model to islands

*Hiroaki Sato[1], Yosuke Alexandre Yamashiki[2] (1.Kyoto University, 2.Graduate School of Advanced Integrated Studies in Human Survivability Kyoto University)

Representing terrestrial water dynamics within Earth system modelling framework

*Dai Yamazaki[1]

1. Institute of Industrial Sciences, The University of Tokyo

Within the framework of Earth System modelling, land sub-models usually represent water dynamics as vertical 1-dimentional processes to provide lower boundary conditions for the atmospheric model. In addition, river sub-models represent water transport along the river network to represent global hydrological cycle across atmosphere, land and oceans. Thus, terrestrial water dynamics has been represented as simplified “1D:vertical + 1D:along river” processes. While the actual terrestrial water dynamics is more complex, including horizontal dynamics such as flooding, surface flow, and sub-surface flow. They affect land-atmosphere interactions and global material cycles by changing surface water extent, moisture redistribution and vegetation type distribution, thus should be better represented in climate modelling. However, representing these detailed terrestrial water dynamics within Earth system model had been difficult because of the discrepancy of spatial scales. In very recent years, there are significant advancements in representing detailed terrestrial water dynamic such as flooding and hillslope moisture redistribution by utilizing sub-grid scale physics approaches, and also due to the development of high precision global topography datasets. Here, we review recent advances in global-scale terrestrial water dynamics modelling and discuss the potential applications in Earth system modelling.

Keywords: Earth System Modelling, Terrestrial Water Dynamics

©2021. Japan Geoscience Union. All Right Reserved.

Breaching flood impact analysis of landslide dams in the Yarlung Tsangpo River Basin

*Danyi Shen[1,2], Zhenming Shi[1,2], Ming Peng[1,2]

1. Key Laboratory of Geotechnical & Underground Engineering of Ministry of Education, Tongji University, Shanghai 200092, China, 2. Department of Geotechnical Engineering, Tongji University, Shanghai 200092, China

Breaching floods of landslide dams occur frequently in mountainous area, and pose great threats to people and infrastructures downstream. Evidences show dam-break floods resulted in extremely catastrophic in the Yarlung Tsangpo River due to its high relief, narrow river gorges and numerous tributaries. On 9 April 2000, a large landslide occurred at the Zhamu Creek and blocked the Yigong Tsangpo River (a tributary of the Yarlung Tsangpo River). On 17 October 2018, another large landslide blocked the main course of the Yarlung Tsangpo River near Gyalha. The breaching of the Yigong and Gyalha landslide dams caused mega floods with peak discharge of 124,000 m^3/s and 32,000 m^3/s, respectively. Previous researches mainly focused on breaching floods of a single dam or cascade dams in the same river. However, the impact of breaching floods caused by simultaneous dam-break of mainstream and its tributaries on downstream are significantly different from that of a single dam-break flood.

This study presents works on flood routing caused by failures of the Yigong and Gyalha landslide dams in the Yarlung Tsangpo River and its tributaries, amplified floods by considering overlapping effects on the basis of these two landslide dams, and possible measures taken to mitigate breaching floods downstream. The erosion-based physical model is applied to predict flood hydrographs at dam site, and the one-dimensional hydrodynamic model is used to simulate the flood routing along the river and its tributaries.

Based on results of simulation, the peak discharge at dam sites and corresponding outflow rate along rivers agree well with field observations. The attenuation of peak outflow rate and flood propagation time along the river is decreased with the increase of peak discharge at dam site. The peak outflow rate is amplified when breaching floods of the mainstream and its tributaries are overlapping. Both flood peaks and inundated area downstream can be reduced by changing discharge magnitude and desynchronizing peak flow in different rivers. The work can serve as basis to predict overlapping floods of landslide dams and manage flood risks in the Yarlung Tsangpo River and its tributaries.

Keywords: Landslide dam, breaching flood, peak discharge, overlapping effects, flood attenuation

©2021. Japan Geoscience Union. All Right Reserved.

Sediment transport analysis from the Abukuma river to the sea by typhoon No.19 in 2019

Makoto Kobayashi[1], *Daisuke Nakahara[1], Keiko Udo[1], Hiroshi Takebayashi[2]

1. International Research Institute of Disaster Science, Tohoku University, 2. Disaster Prevention Research Institute, Kyoto University

A large amount of sediment was run off in the Abukuma river because of the record-breaking heavy rainfall of Typhoon No.19 in October 2019. This kind of heavy flood occurs in the Abukuma river once every few years, and it is important from the viewpoints of the river and coastal management to clarify the influence of sediment transport on the shape of the riverbed and the amount of sediment in the downstream area. To clarify the long-term sediment transport characteristics in the Abukuma river, the purposes of this study are to calculate the long-term sediment dynamics in the lower reaches of the Abukuma river and to estimate the sediment supply to the coast for each particle size with a one-dimensional mixed-grain riverbed fluctuation analysis model.

The Abukuma River, which is the subject of this study, is a first-class river with a drainage area of 5390 km² and a trunk river channel length of 239 km. The source of the water originates in Asahidake, Fukushima Prefecture, it flows into the Kakuda Basin through alternating plains and narrow areas and joins the Shiraishi River, the largest tributary, to flow into the Pacific Ocean. The calculated section is 36.4 km from Marumori to Arahama in the lower reaches of the Abukuma Valley, and the riverbed slope of the calculated section is about 1/3700 to 1/2000. The target runoffs are 47 runoffs with flow rates exceeding 1000 m³/s, when sediment transport generally starts, from 2000 to 2019 when water level and flow data are available. The initial riverbed level was obtained from the measured riverbed level in 1999, The initial riverbed level was obtained from the measured riverbed level in 1999 provided by the Tohoku Regional Development Bureau of the Ministry of Land, Infrastructure, Transport and Tourism, and 101 riverbed levels were given for each transect of 0.2 km in the longitudinal direction. The data from the Marumori Water Level Station was used for the upstream flow rate, and the data from the Arahama Water Level Station was used for the downstream water level. The flow rate of the Shiraishi River was measured using data from the Funaoka Bridge water level station located approximately 6 km upstream from the confluence. The particle size distribution of the riverbed material is based on the measured data of 2002 provided by the Tohoku Regional Development Bureau of the Ministry of Land, Infrastructure, and Transport. The calculation results were validated using the estimated sediment discharge associated with the seven runoff events that recorded 3000 m³/s at the Iwanuma water level observation station from 1999 to 2007.

To validate the one-dimensional riverbed fluctuation model, we compared the results of the analysis and the estimated values of the sediment discharge associated with the seven runoffs from 1999 to 2007. Although there is a tendency to overestimate the amount of fine sand (0.075-0.25mm) discharge when the discharge scale is large, the analysis results for other particle sizes are generally good, and it is judged that this model can be used to study sediment discharge in the Abukuma River. The annual average sediment discharge is about 140,000 m³ of fine sand, about 30,000 m³ of medium sand (0.25-0.85 mm), and about 0.3 m³ of coarse sand (0.85-2 mm), for a total of about 180,000 m³/year. In Typhoon No. 19 in 2019, it was estimated that about 400,000 m³ of sediment was supplied to the coast from rivers, including about 240,000 m³ of fine sand, 140,000 m³ of medium sand, and 20,000 m³ of coarse sand.

©2021. Japan Geoscience Union. All Right Reserved.

Keywords: Long-term sediment dynamics, Sediment supply, One-dimensional mixed-grain riverbed fluctuation analysis model, The Abukuma river

©2021. Japan Geoscience Union. All Right Reserved.

Structural characteristics of airflow and blown sand flux over fine-grained gravel surfaces in wind tunnel

*Jiaqi Liu[1], Reiji Kimura[1], Jing Wu[1]

1. Arid Land Research Center, Tottori University

To reduce damage caused by wind-blown sand, it is necessary to clarify the mechanism of soil erosion under various surface conditions. In the present study, we investigated the influence of gravel coverage on aerodynamic characteristics of airflow and blown sand flux in a compact wind tunnel developing boundary layer equipped with a turbulence generator and a piezoelectric blown sand meter.

The vertical profile of wind-blown sand over a flat sand surface showed an exponential distribution at all wind speeds, whereas the profile over fine-grained gravel surfaces of 20% or greater coverage showed a non-monotonic vertical distribution. At 20% to 30% gravel coverages, a peak of wind-blown sand flux developed between 6 and 10 cm above the ground at all wind speeds because of less energy loss due to grain-bed collisions at that level. We found that the wind-blown sand flux at 4 cm height accounted for about 20% of the total flux regardless of wind speed and gravel coverage. This finding can simplify future estimations of total near-surface wind-blown sand flux based on field observations because such measurements can be taken at just one height.

The effect of fine-grained gravel coverage on drag coefficient, wind-speed gradient, and turbulent transfer coefficient was investigated to understand the structure characteristic of blown sand flux. The drag coefficient of the gravel surface reached the maximum value at 15% coverage and then tended to stabilize at gravel coverage 20% and greater. At a height of 4 cm, near-surface airflow on gravel surfaces can be divided clearly into upper and lower sublayers, defined as the inertial and roughness sublayers, respectively. The coefficient of variation of wind speed over gravel surfaces in the roughness sublayer was 8.6 times as much as that in the inertial sublayer, indicating a greater effect of gravel coverage on wind-speed fluctuations in the lower layer. At the height of 4 cm, changes in gravel coverage had the same degree of effect on wind-speed fluctuations under the observed wind speeds. In addition, an energy-exchange region, where sand particles can absorb more energy from the surrounding airflow, was found between the roughness and inertial sublayers (6-10 cm), enhancing the erosional state of wind-blown sand. This finding can be applied to evaluate the aerodynamic stability of the gravel surface and provide a theoretical basis for elucidation of the vertical distributions of wind-blown sand flux.

Keywords: wind erosion, vertical profiles, blown sand flux, piezoelectric blown sand meter, wind tunnel developing boundary layer

©2021. Japan Geoscience Union. All Right Reserved.

Predictive simulations of redeposition and seawater transportation after a tsunami in Osaka Bay where bottom sediments were disturbed by tsunami

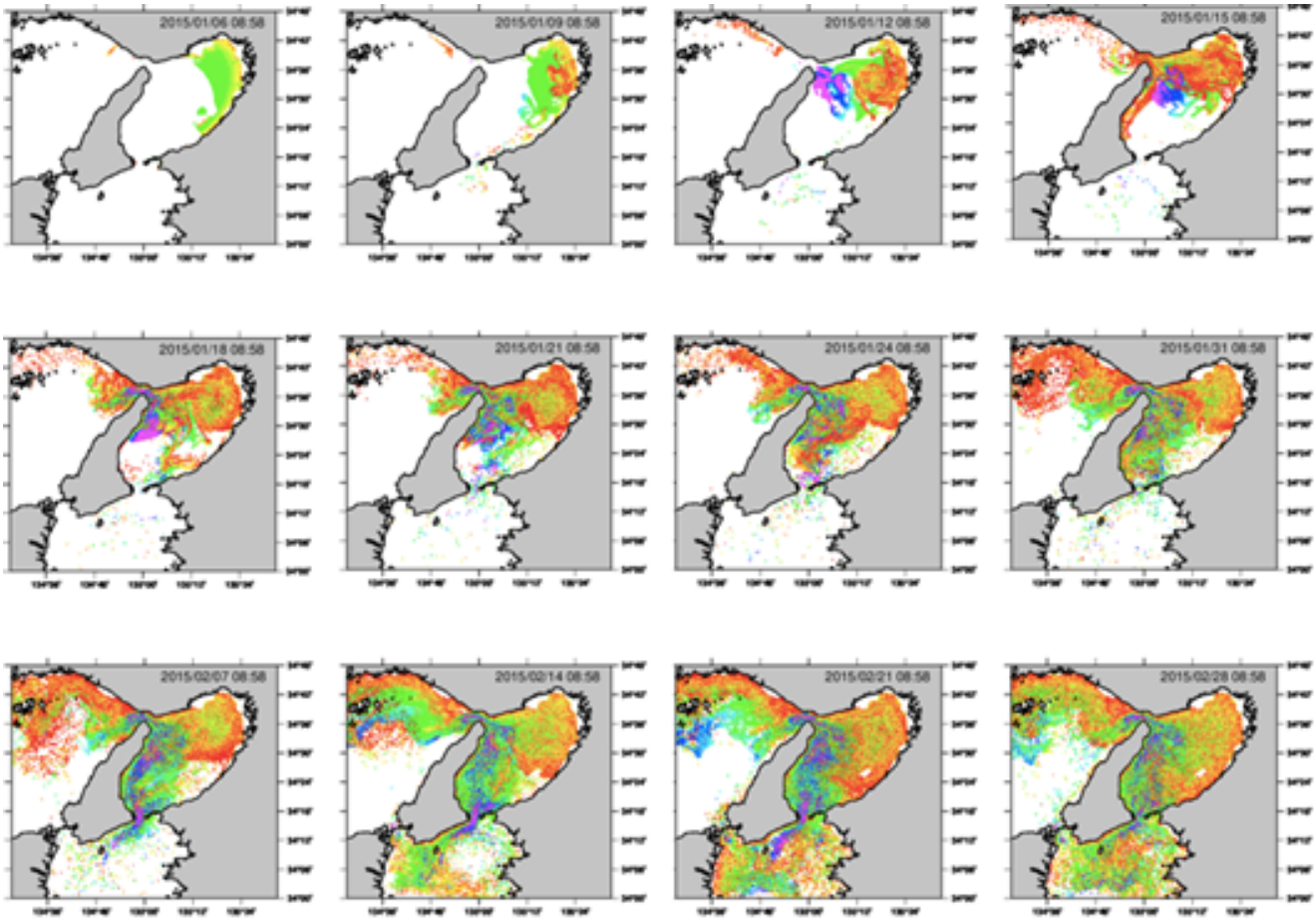
*Mitsuru Hayashi[1,2], Satoshi Nakada[4], Soichi Hirokawa[2], Shuto Fujisawa[3]

1. Research Center for Inland Seas, Kobe University, 2. Graduate School of Maritime Sciences, 3. Faculty of Maritime Sciences, 4. National Institute for Environmental Studies

Tsunami caused by Nankai Trough Earthquake will disturb marine bottom sediments in Osaka Bay. This disturbance is the first large-scale disturbance for Osaka Bay after the rapid economic growth. The sediments contain several materials such as nutrients, cysts of harmful algae, bacteria and heavy metals. It is necessary to predict the changes in the marine environment and ecosystems caused by tsunamis for the ocean SDGs. Nakada *et al.* (2018) predicted by the tsunami simulation that the sediments would be disturbed at the inner part (the eastern half) of Osaka Bay. The sediments were disturbed particularly at the mouth of the harbor and estuary, and the total flux for 10 hours after the earthquake is more than 10 kg/m^2. Transportation and redeposition of the sediments and transportation of seawater with dissolved materials in Osaka Bay after the tsunami were simulated in this study by ocean models. The transport and redeposition of the sediments were calculated by a tidal simulation. The deposition rate was given by the Stokes' low. The sediments were redeposited along the shore line and Okinose where the water depth was shallow and along the oceanic fronts by the tidal residual current as the results of the calculation for one month after the earthquake. Seawater transportations were simulated by the three-dimensional ocean model, FVCOM. Calculations were carried out for six cases for two months with different timing of earthquake occurrence every two month. The path and speed of seawater transportation inside Osaka Bay, and the timing and speed of outflow from the bay were different for each case.

Keywords: Tsunami, Osaka Bay, Marine Bottom Sediment, Simulation, Redeposition, Seawater transportation

©2021. Japan Geoscience Union. All Right Reserved.



©2021. Japan Geoscience Union. All Right Reserved.

Application of an isopycnal-layered model to islands

*Hiroaki Sato[1], Yosuke Alexandre Yamashiki[2]

1. Kyoto University, 2. Graduate School of Advanced Integrated Studies in Human Survivability Kyoto University

An isopycnal-layered model can effectively solve the dynamics of surface runoff, river flow, and oceanic flow seamlessly without determining specific arrangements for each component. Therefore, we presume that it is an adequate model for solving the entire island's hydrological processes using a single model. We applied an isopycnal-layered model into three islands, Yakushima, Iriomoteshima, and Ishigakishima, located southwest of Japan's main islands. To verify the simulation, we used in situ measured vertical profile of temperature and salinity. We aim to use satellite remote-sensing data to confirm the simulation in the next step.

Keywords: entire island's hydrological processes

©2021. Japan Geoscience Union. All Right Reserved.

[J] Poster | A (Atmospheric and Hydrospheric Sciences)：A-CG Complex & General

Thu. Jun 3, 2021 5:15 PM - 6:30 PM JST | Thu. Jun 3, 2021 8:15 AM - 9:30 AM UTC | Ch.03_4

[A-CG43] Earth & Environmental Sciences and Artificial Intelligence/Machine Learning

convener:Tomohiko Tomita(Faculty of Advanced Science and Technology, Kumamoto University), Shigeki Hosoda(Japan Marine-Earth Science and Technology), Ken-ichi Fukui(Osaka University), Satoshi Ono(Kagoshima Univeristy)

In recent years, we have been required to explore various gigantic data leading earth and environmental sciences such as modern meteorology, oceanography, hydrology and so on to accomplish Society 5.0 and Sustainable Development Goals (SDGs). To examine such gigantic environmental data faithfully, it may be required to use the techniques of artificial intelligence/machine learning (AI/ML) including spatiotemporal data modeling of AI, prediction and detection by ML, techniques of automated data mining, and so forth. At the present, AI/ML is also expected to lead the data-driven science as a bridge connecting science and big data. This session calls for various studies applying the techniques of AI/ML to scientific/environmental issues and will discuss them in both natural and information sciences.

[ACG43-P01] Machine learning for remote sounding of the ionosphere in Taiwan

*ALEXEI DMITRIEV[1] (1.National Central University, Jungli City, Taiwan)

[ACG43-P02] Precipitation predictions using RNN and LSTM with simple time series observations and the comparison between them.

*He Zhang[1], Tomohiko Tomita[2], Ken-ichi Fukui[3], Satoshi Ono[4] (1.Kumamoto University, 2.Faculty of Advanced Science and Technology, 3.The Institute of Scientific and Industrial Research, Osaka University, 4.Faculty of Engineering, Kagoshima University)

[ACG43-P03] Hindcast of the July 2018 torrential rainfall event in Kagoshima City using LSTM

*Genki Shirasawa[1], Ryusei Hamasaki[1], Shinichiro Kako[2], Hirohiko Nakamura[3] (1.Kagoshima University, Faculty of Engineering, 2.Graduate School of Science and Engineering, Kagoshima University, 3.Kagoshima University, Faculty of Fisheries)

[ACG43-P04] Real-time Data Quality Control of Phased Array Weather Radar by using Semantic Segmentation

*Isoda Fusako[1], Shinsuke Satoh[1], Masashi Kimura[2], Takemasa Miyoshi[3] (1.National Institute of Information and Communications Technology, 2.Convergence Lab., 3.RIKEN)

[ACG43-P05] A Preliminary Study on Developing a Smartphone Application for Weather Classification Using AutoML

*Satoshi Ono[1], Kento Wakamatsu[1], Yusaku Hayashi[1], Tomohiko Tomita[2] (1.Kagoshima Univeristy, 2.Kumamoto University)

[ACG43-P06] Fundamental Study on Weather Judgement of Image Data using Machine Learning Classification

*Tomohiko Tomita[1], Kosuke Tanaka[2] (1.Faculty of Advanced Science and Technology, Kumamoto University, 2.Faculty of Science, Kumamoto University)

Machine learning for remote sounding of the ionosphere in Taiwan

*ALEXEI DMITRIEV[1]

1. National Central University, Jungli City, Taiwan

A. V. Dmitriev and NCU AI group

Global Navigation Satellite System (GNSS) plays crucial role for positioning and navigation. The GNSS accuracy is directly controlled by the conditions in the ionosphere. Routing monitoring of the ionospheric conditions is conducted by ground-based ionosondes, which provide experimental information about radio-echoes from ionospheric layers, so-called ionograms. The ionograms contain a lot of noise from numerous artificial transmitters such that the recovery of ionospheric signals becomes a very difficult problem. We present application of various machine learning (ML) techniques for determination of the signals from ionospheric E and F layers in very noisy environment of Taiwan, where the noise is comparable with the signal (SNR ~ 1). It is shown that deep ML techniques allow increasing of the determination accuracy up to 80% even for extremely nosy conditions.

NCU AI group: Chang Y.-C., Dmitriev A., Hsieh M.-C., Hsu H.-W., Huang G.-H., Li Y.-H., Lin C.-H., Lin Y.-C., Mendoza M., Tsai L.-C., Tsogtbaatar E.

Keywords: ionospheric sounding, machine learning

©2021. Japan Geoscience Union. All Right Reserved.

Precipitation predictions using RNN and LSTM with simple time series observations and the comparison between them.

*He Zhang[1], Tomohiko Tomita[2], Ken-ichi Fukui[3], Satoshi Ono[4]

1. Kumamoto University, 2. Faculty of Advanced Science and Technology, 3. The Institute of Scientific and Industrial Research, Osaka University, 4. Faculty of Engineering, Kagoshima University

Precipitation prediction is one of most difficult predictions in weather and climate but strongly required for society. It is well known that there are three problems when artificial neural network (ANN) is employed to predict precipitation. The first is that the predicted local maximum in precipitation is not large enough; the second is that the time of occurrence of the maximum is lagged one interval time; the third is that the state of zero precipitation cannot be accurately represented. In this study, RNN and LSTM were employed to replace the multi-layer Perception (MLP) of ANN for the precipitation prediction, and the outputs were compared so as to explore the degree to which the above three problems could be improved.

Using simple time series observations, three different ANN models, that is, MLP, RNN, LSTM, were tested, two experiments were carried out for these three models. The data sets used in this study are observational time series data compiled by the Japan Meteorological Agency. The stations are five, i.e., Kumamoto, Kikuchi, Mashiki, Nagasaki, and Yatsushiro located in Kyushu of Japan. The used variables are six, that is, hourly precipitation, temperature, pressure, vapor pressure, wind speed, and wind direction. The evaluation functions are SS and RMSE, where SS is the ratio of observed values to predicted values larger than 10 mm/h, which varies between 0 and 1, and the large value means the better prediction performance.

When MLP was used for prediction, the predicted local maximum was less than one third of the observed value, and the occurrence of the maximum was delayed one hour. When RNN was used for prediction, this problem was obviously improved. The predicted maximum can reach about 90% of the observed one, but the maximum's occurrence was still delayed one hour. Finally, when we employed LSTM, the maximum's occurrence time was adjusted with large predicted maximum, which means the time-lag problem was certainly improved. When the ANN model is transformed from RNN to LSTM, the structure of LSTM seemed to improve the short-term dependency bottleneck of RNN, which means that the time series data can be better processed. Some unnecessary data can be forgotten and discarded, and the key data can be retained, which greatly improve the accuracy of the prediction.

When only data of Kumamoto was used for prediction, the best result of MLP was SS=0.45, RMSE=1.36, and for using 5 sites' data, it came to SS=0.54, RMSE=1.04. By adjusting the number of nodes in the two hidden layers, the results were further improved to SS=0.45, RMSE=1.04 for one site's experiment and SS=0.60, RMSE=1.04 in 5 sites' experiment. The results of RNN came to SS=0.46, RMSE=0.96 in one site's experiment and SS=0.61, RMSE=0.96 in 5 sites’ experiment. Finally, when the LSTM model was employed, our prediction reached the best so far, which was SS=0.62, RMSE=1.01 in one site's experiment and SS=0.72, RMSE=0.88 in 5 sites' experiment.

Keywords: precipitation forecast, evalution functions, RNN

©2021. Japan Geoscience Union. All Right Reserved.

Hindcast of the July 2018 torrential rainfall event in Kagoshima City using LSTM

*Genki Shirasawa[1], Ryusei Hamasaki[1], Shinichiro Kako[2], Hirohiko Nakamura[3]

1. Kagoshima University, Faculty of Engineering, 2. Graduate School of Science and Engineering, Kagoshima University, 3. Kagoshima University, Faculty of Fisheries

In this study, we constructed a long short-term memory (LSTM) model to hindcast the torrential rainfall event that occurred in Kagoshima City in July 2018. In this model, automated meteorological data acquisition system (AMeDAS) and radar–AMeDAS rainfall data from Kyushu were used as training data. Our LSTM model could hindcast the time variation of the rainfall event; however, it tended to underestimate the rainfall event observed by AMeDAS, and in some cases the start times of the precipitation events were late. Underestimation and phase lags were probably because the LSTM model was optimized for light rainfall events that occur frequently. To further improve the prediction accuracy of our model, it was necessary to improve the reproducibility of the magnitude of the precipitation amplitude. Therefore, we selected further training data such as physical quantities over the East China Sea that contribute to the forecast/hindcast of torrential rainfall events. The use of radar–AMeDAS rainfall data as training data over the ocean in the southern part of Kagoshima significantly improved the accuracy of our LSTM model compared to that without this additional training data.

Keywords: LSTM, Torrential rain, Radar AMeDAS, AMeDAS, Hindcast/Forecast of rainfall event

©2021. Japan Geoscience Union. All Right Reserved.

Real-time Data Quality Control of Phased Array Weather Radar by using Semantic Segmentation

*Isoda Fusako[1], Shinsuke Satoh[1], Masashi Kimura[2], Takemasa Miyoshi[3]

1. National Institute of Information and Communications Technology, 2. Convergence Lab., 3. RIKEN

The observation data of Phased Array Weather Radar (PAWR) which performs volume scan every 30 seconds is used for real-time precipitation prediction such as 3D precipitation nowcast (Otsuka, et al., 2016. doi: 10.1175 / WAF-D-15-0063.1) and the smartphone application "3D Amagumo Weather". The data quality control (QC) of PAWR is necessary to make accurate predictions, and It is important to remove non-precipitation echoes (clutters derived from buildings on the ground and mountains, fake echoes appear before and after strong echoes which is called range side-lobe echoes). In the current real-time QC, clutter discrimination is performed using thresholds of the Doppler velocity and the texture information of the reflectivity. However, if the data QC is performed in various cases with a certain threshold value, erroneous judgment may occur. Therefore, to perform appropriate QC in various cases, we apply semantic segmentation, one of the deep learning applications that detects objects from images in pixel units.

We report the results using ESPNet (Mehta, et al., 2018.arXiv: 1803.06815v3), which has high inferences speed. The data was selected from 10 cases of convective rainfall observed by PAWR installed at the Osaka University from 2015 to 2017, and a total of 666 images with elevation angles 6 to 12 (corresponding to elevation angles 4.4 ˚to 9.4 ˚) were prepared. For stratiform rainfall, another 10 cases were selected, and 644 images were prepared. By using color images of reflectivity and annotation images (0 = no data, 1 = precipitation data, 2 = non-precipitation data) as training data, two models for convection and stratiform rainfall were created. For the annotations, the QC flag created by the conventional method was used, and the flag data that was considered to be false judgments by visual inspection was removed as much as possible.

Figure 1 shows the inference results of convective (left) and stratiform rainfall (right) with an elevation angle of 6.2 ˚converted to PPI in the Cartesian coordinates. They are examples of input data (reflectivity: upper row), inference results (middle row), and the QC flag (lower row: as ground truth). In the result of inferences and the QC flag, black part is judged to be a non-precipitation echo. In the inference of convective rainfall, the range side-lobe echoes are discriminated, and the judgment is very similar to the QC flag. Looking at the inference results of stratiform rainfall, the non-precipitation echoes were hardly identified on this elevation angle, and the model inference was performed correctly.

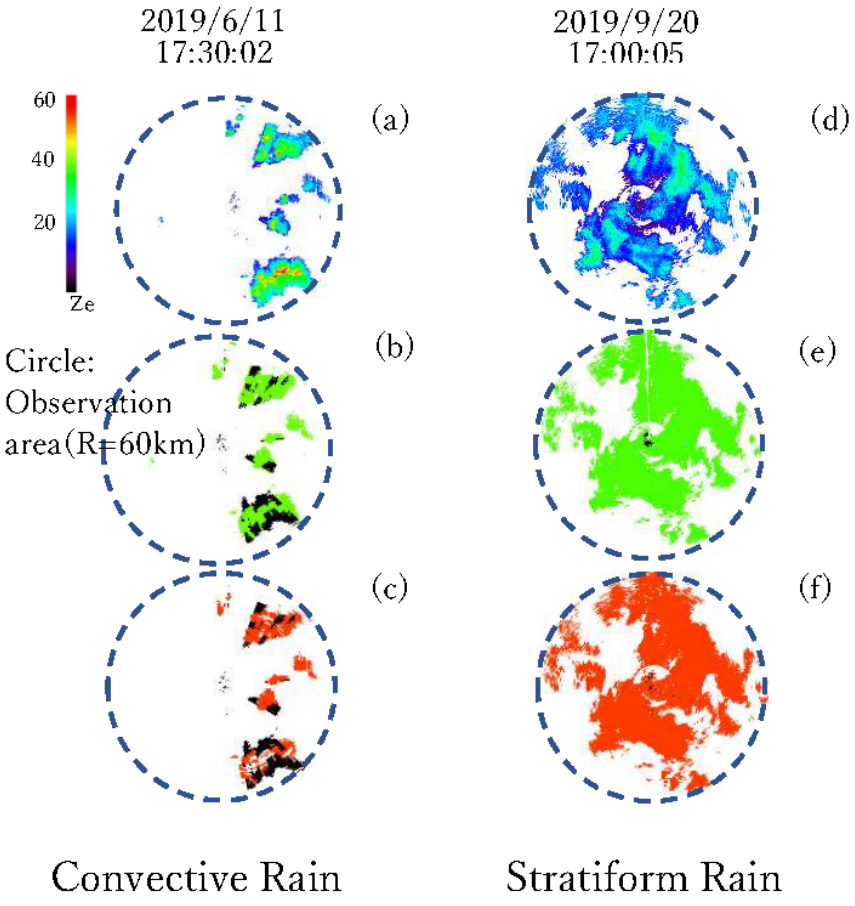
In this study, learning and inference were performed on a Linux server equipped with one GeForce RXT 2080 Ti. For convective rainfall, it took about 0.02 seconds to inference the data for one elevation angle, and for stratiform precipitation with a large precipitation area, it took about 0.04 seconds. The reading of observation data was accelerated by calling a C program using Cython (0.035 seconds / file, 1 file is about 40MB). Considering the data processing of 110 elevation angles obtained by the PAWR observation every 30 seconds, it was expected that QC processing would be performed in a few seconds.

As a future work, it is necessary to create other models for each elevation angles, because the types of non-precipitation echoes in the data near lower elevation and zenith angles are different from the above. In order to further improve the accuracy of inference, we think that it is necessary to tune the QC flag used as annotations for each case, create more correct ground truth, and increase the number of learning data. The goal is to complete a processing system that can process data reading, convection / stratiform judgment by CNN, segmentation of total elevation angles data, aggregation and output of inferences results within 10 seconds.

©2021. Japan Geoscience Union. All Right Reserved.

This work was supported by JST AIP Grant Number JPMJCR19U2, Japan.

Keywords: Phased Array Weather Radar, Semantic Segmentation, Quality Control



©2021. Japan Geoscience Union. All Right Reserved.

A Preliminary Study on Developing a Smartphone Application for Weather Classification Using AutoML

*Satoshi Ono[1], Kento Wakamatsu[1], Yusaku Hayashi[1], Tomohiko Tomita[2]

1. Kagoshima Univeristy, 2. Kumamoto University

In recent years, the need for local weather observation has increased for various applications. For instance, predicting local weather phenomena such as guerrilla rains and tornadoes requires detailed ground-based observation networks. In addition, recording weather conditions in an individual's environment can be used to treat physical illnesses caused by climate and weather changes, known as weather-related diseases. Therefore, this study develops a smartphone application that discriminates the weather as a tool to realize a local meteorological observation network or to record meteorological factors to patients. This study utilizes an automatic machine learning design technique (AutoML) that include neural architecture search and hyper-parameter optimization to design deep neural network architecture for weather classification and compresses the designed architecture to implement it on smartphones.

Keywords: machine learning, artificial intelligence, AutoML, neural architecture search, weather classification

©2021. Japan Geoscience Union. All Right Reserved.

Fundamental Study on Weather Judgement of Image Data using Machine Learning Classification

*Tomohiko Tomita[1], Kosuke Tanaka[2]

1. Faculty of Advanced Science and Technology, Kumamoto University, 2. Faculty of Science, Kumamoto University

The sky and ground conditions in many image data, i.e., pictures and video images, are valuable weather information. Using the multi-class classification technique of machine learning, this study investigated the potential how well the technique judged the weather condition involved in image data. For this purpose, about 30,000 pictures were taken with a 10-minute interval (144 pictures per day) by a field monitoring camera fixed in the Kumamoto University. Corresponding weather condition was then assigned from the published data of Kumamoto weather station. At this timing, the weather conditions were summarized into three categories, i.e., sunny, cloudy, and rainy conditions. The supervised training, validation, and test data were prepared from these pictures and weather condition data. This study employed simple multilayer perceptron with two hidden layers for building a classification model, and investigated the accuracy of the three-category classification of following four cases: (1) all pictures, (2) daytime, (3) nighttime pictures and (4) pictures around sunrise and sunset times. The results showed that the accuracy rates of four cases all reached about 85%. It is interesting that our classification model could judge weather conditions even using nighttime and around sunrise and sunset pictures. However, we confirmed that the significant difference appeared the time until when the accuracy rate reached 80% in the training process. That is, the training of the nighttime pictures needed longer time than the daytime ones. It was suggested that our model might have trained using relative brightness of pictures without convolution.

Keywords: machine learning multi-class classification, judgement of weather conditions in image data

©2021. Japan Geoscience Union. All Right Reserved.

[J] Poster | A (Atmospheric and Hydrospheric Sciences)：A-CG Complex & General

Thu. Jun 3, 2021 5:15 PM - 6:30 PM JST | Thu. Jun 3, 2021 8:15 AM - 9:30 AM UTC | Ch.07_4

[A-CG44] Biogeochemical linkages between the surface ocean and atmosphere

convener:Sohiko Kameyama(Hokkaido University), Yoko Iwamoto(Graduate School of Integrated Sciences for Life, Hiroshima University), Noguchi Maki Aita(Japan Agency for Marine-Earth Science and Technology), Daisuke Sasano(Japan Meteorological Agency)

Multi-scale vertical and horizontal ocean mixing processes can strongly influence the distribution of dissolved and suspended substances including macro- and micro-nutrients, and may impact on the global carbon cycles. The changes in nutrient dynamics generally affect the abundance, composition and metabolic activity of marine organisms such as phytoplankton and bacteria during the bloom. Marine phytoplankton can produce volatile organic compounds (VOCs) and marine atmospheric aerosols, which strongly influence on atmospheric chemistry. Primary and secondary organic and inorganic components produced via marine phytoplankton activity can contribute to the Earth's radiative forcing, and in turn marine ecosystems including biogeochemical processes directly or indirectly. Therefore, the biogeochemical cycles have a tight linkage between the ocean and the atmosphere. In order to understand physical, chemical and biological processes relevant to phytoplankton bloom formation in the ocean, dynamics of VOCs and marine aerosols in the atmosphere, and the biogeochemical linkage between the ocean and the atmosphere, we welcome new interdisciplinary presentations and active discussions on physical, chemical, and biological sciences both from ocean and atmospheric fields in this session. Studies linked to the Surface Ocean-Lower Atmosphere Study (SOLAS) project are good examples, but other related studies are also invited.

[ACG44-P01] Relationship between the variability in dissolved inorganic carbon in surface seawater and the formation volume of subtropical mode water along the 137°E line

*Ono Hisashi[1], Masao Ishii[1], Yosuke Iida[2], Kazutaka Enyo[2], Daisuke Sasano[2] (1.Meteorological Research Institute, 2.Japan Meteorological Agency)

[ACG44-P02] Verification of the effect of aerosol deposition on surface chlorophyll in subtropical oligotrophic waters using JRAero reanalysis datasets

*Naohiro Kosugi[1], Taichu Y Tanaka[1] (1.Meteorological Research Institute)

[ACG44-P03] Seasonal Variation of Phosphate in Atmospheric Aerosols in Higashi-Hiroshima

*Yoko Iwamoto[1], Mako Hirota[2], Kazuhiko Takeda[1], Hiroshi Sakugawa[1] (1.Graduate School of Integrated Sciences for Life, Hiroshima University, 2.School of Integrated Arts and Sciences, Hiroshima University)

[ACG44-P04] Modelling regional and global scale impacts of atmospheric nitrogen inputs on marine biogeochemistry

*Maki Noguchi Aita[1], Fumikazu Taketani[1], Yoko Iwamoto[2], Tomohiro Hajima[3] (1.Earth Surface System Research Center, Japan Agency for Marine-Earth Science and Technology, 2.Hiroshima University, 3.Research Center for Environmental Modeling and Application, Japan Agency for Marine-Earth Science and Technology)

[ACG44-P05] Contribution of lightning-induced nitgen oxide to nitrogen cycle in air-sea boundary estimated by plasma discharge in laboratory

Ryo Hashimoto[1], *Sohiko Kameyama[1], Kohki Satoh[2], Hiroshi Ogawa[3] (1.Hokkaido University, 2.Muroran Institute of Technology, 3.The University of Tokyo)

Relationship between the variability in dissolved inorganic carbon in surface seawater and the formation volume of subtropical mode water along the 137˚E line

*Ono Hisashi[1], Masao Ishii[1], Yosuke Iida[2], Kazutaka Enyo[2], Daisuke Sasano[2]

1. Meteorological Research Institute, 2. Japan Meteorological Agency

1. Introduction

Based on the data of partial pressure of CO2 in seawater (pCO_2^{sea}) along the 137˚E since the beginning of the 1980s, we previously reported the growth rates of dissolved inorganic carbon (DIC) in surface seawater from subtropic to tropic zone by means of a multiple regression analysis (Ono et al., 2019). In addition, we showed that the rates varied greatly on a decadal time scale in the Kuroshio recirculation. Besides, the paper by Kobashi et al. (2020) indicated the decadal scale variability of the North Pacific subtropical mode water (STMW) and its influence on the pycnocline along the 137˚E. In this study, we investigate the relationship between the variability in DIC in surface seawater, STMW thickness and the depth of isopycnal surface at 30˚N along the 137˚E line.

2. Data & Methods

We mainly used measurement data at 30˚N along the 137˚E line in each summer acquired by Japan Meteorological Agency (JMA). Based on the measurement data of DIC since 1994, the long-term trend of DIC in surface seawater was calculated by linear regression analysis. And the time-series of DIC was detrended. Using the data acquired by CTD system, we evaluated the temporal variability of the depth of isopycnal surface and STMW thickness which was defined as a layer of potential vorticity (PV) less than 2.0×10^{-10} $m^{-1}s^{-1}$. From these data, 3-year running means and correlations of each time-series were calculated.

3. Result & Discussion

Temporal variability of salinity-normalized DIC (nDIC) in surface seawater corresponded with those of STMW thickness and depth of isopycnal surface (Figure a-c). Significant correlations between them were seen and their coefficients were 0.69 ($p<0.01$) and -0.77 ($p<0.01$), respectively. These results indicate the thicker STMW and the shallower isopycnal surfaces are, the higher DIC is. Namely, higher values of nDIC around 2015 are considered to be caused by the heaving of isopycnal surfaces and the relatively larger supply of DIC from subsurface to surface by vertical mixing in winter.

It has been reported that the STMW thickness varies corresponding to the decadal variability of the Kuroshio Extension and which are fluctuated in association with the Pacific Decadal Oscillation (PDO) (e.g., Qiu and Chen, 2005). The time lag correlation analysis between nDIC in surface seawater and PDO index showed the maximum coefficient of -0.77 ($p<0.01$) with 4-year lag applied.

These results suggest that the temporal variability of nDIC in surface seawater in the Kuroshio recirculation along the 137˚E line is directly attributed to the fluctuation of STMW formation and isopycnal surface, and originally affected by PDO whose influence is transmitted in around 4 years.

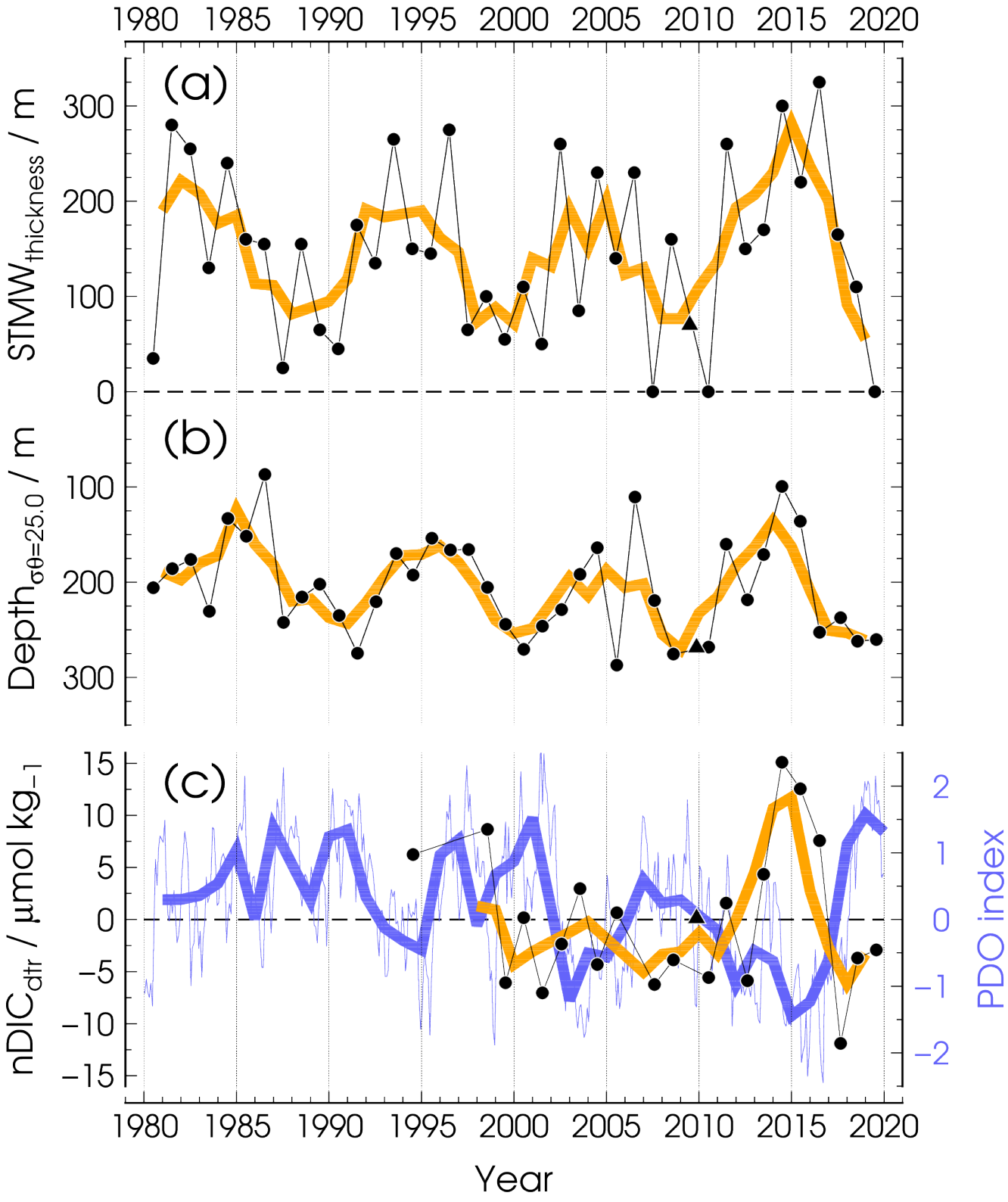
Figure caption

Time-series of (a) STMW thickness, (b) depth of isopycnal surface (σ_θ=25.0 kg/m^3), and (c) detrended nDIC in surface seawater in summer at 30˚N, 137˚E. The thick yellow lines in (a)-(c) represent 3-year running means. The thin and thick blue lines in (c) indicate monthly means and 3-year running means of

©2021. Japan Geoscience Union. All Right Reserved.

PDO index, respectively.

Keywords: 137°E section, Dissolved inorganic carbon, Subtropical mode water, Isopycnal surface, Decadal scale variability, PDO



©2021. Japan Geoscience Union. All Right Reserved.

Verification of the effect of aerosol deposition on surface chlorophyll in subtropical oligotrophic waters using JRAero reanalysis datasets

*Naohiro Kosugi[1], Taichu Y Tanaka[1]

1. Meteorological Research Institute

Introduction

Aerosols emitted from highly populated areas in East Asia contain inorganic nitrogen as a form of nitrate ion (NO_3^-) and ammonium ion (NH_4^+). Some of them deposit in the subtropical zone of the western North Pacific. This area is called “the desert of the ocean” due to its oligotrophy and low productivity. The aerosol deposition is supposed to be a valuable source of nutrients in this region. According to model calculations, significant increases in surface chlorophyll concentration and gross primary production are estimated in the western North Pacific due to the deposition [Taketani et al., 2018]. However, there are few examples of verifying the effect of the deposition on biochemical processes using observational data. In this study, the effects of the deposition on ocean biochemical parameters are examined by using the data obtained in research vessels and Japanese Reanalysis for Aerosol (JRAero) [Yumimoto et al., 2017].

Data

Hydrographic data obtained by research vessels “Ryofu-Maru” and “Keifu-Maru” which belong to Japan Meteorological Agency is used for our analysis. The study area and period are 20-30N, 130-165E, and winter (January, February, and March) from 2011 to 2017, respectively. Temperature, salinity, and chlorophyll data obtained from 10 m depth are used. Nitrate and ammonia are not recorded in JRAero although they supply inorganic nitrogen and stimulate biological activity in the ocean. Black carbon was used as a substitute index of nitrate and ammonia.

Results

The chlorophyll concentration in winter tended to be high as the temperature was low (see Figure). This is thought to be due to the vertical mixing and the entrainment of nitrates was promoted in cold water. On the other hand, the chlorophyll concentration was variable even at the same water temperature. This means chlorophyll concentration depended on factors other than the water temperature. In an incubation experiment onboard, chlorophyll concentration increases within 24-48 hours after the deposition [Zhang et al., 2019]. Therefore 24-hours accumulated amount of black carbon deposition was calculated. As a result, when the water temperature was about the same, the chlorophyll concentration tended to be

©2021. Japan Geoscience Union. All Right Reserved.

higher when the amount of black carbon deposition was large.

In our study, the possibility that atmospheric deposition stimulates biological activity in the subtropical oligotrophic region is shown by actual observations. However, quantitative evaluation is difficult as the number of data is too small spatially and temporally. For more accurate verification, more detailed observations of both the atmosphere and the ocean are essential.

References

Taketani et al., Scientific Report, 2018.

Yumimoto et al., Geosci. Model Dev., 2017.

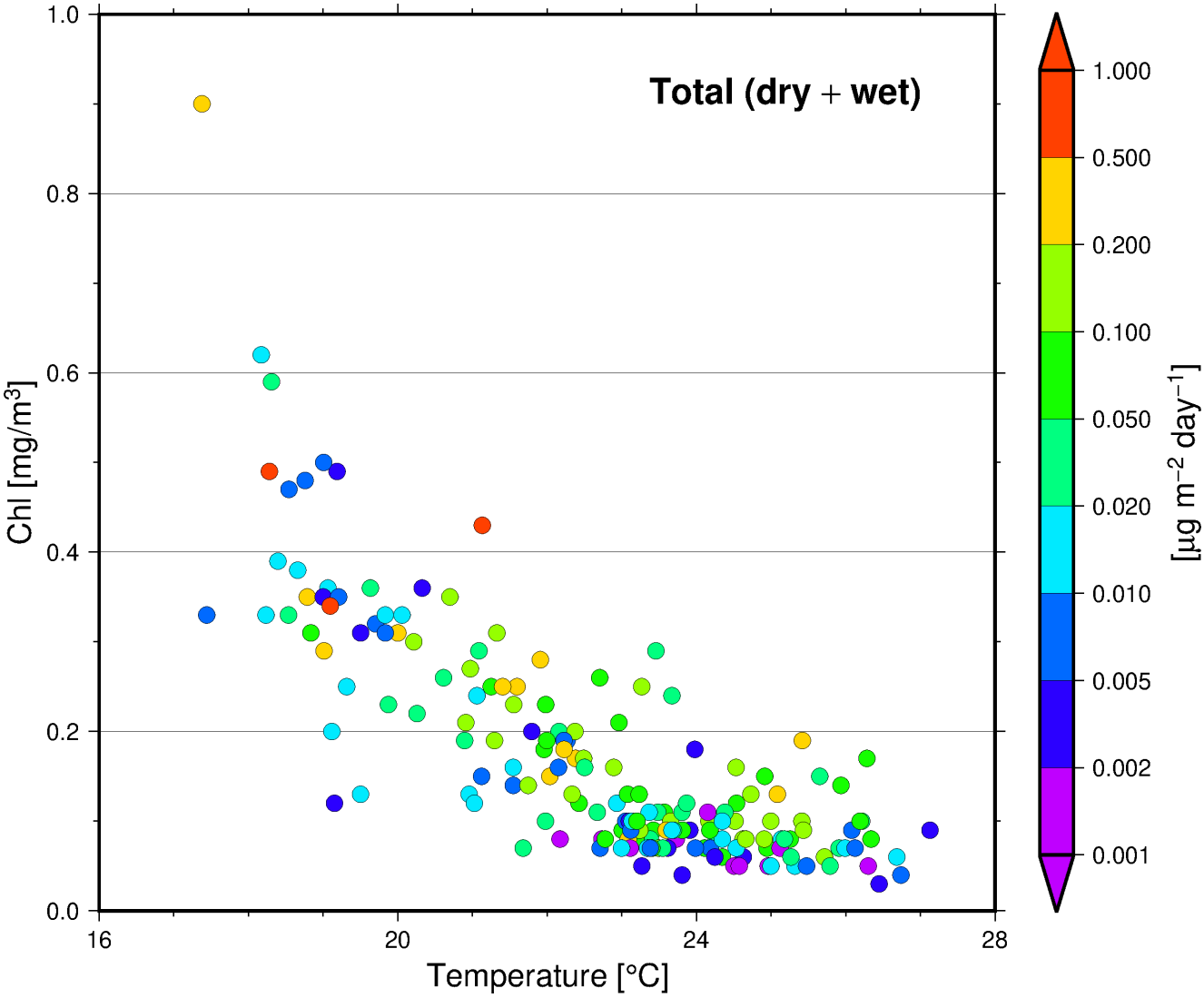
Zhang et al., Global Biogeochemical Cycles, 2019

Figure caption

Relationship between the water temperature and chlorophyll concentration at a depth of 10 m. The color shows the amount of black carbon deposition (dry + wet) in 24 hours before observation at the grid point of JRAERO closest to the observation point.

Keywords: depotision, aerosol

©2021. Japan Geoscience Union. All Right Reserved.



©2021. Japan Geoscience Union. All Right Reserved.

Seasonal Variation of Phosphate in Atmospheric Aerosols in Higashi-Hiroshima

*Yoko Iwamoto[1], Mako Hirota[2], Kazuhiko Takeda[1], Hiroshi Sakugawa[1]

1. Graduate School of Integrated Sciences for Life, Hiroshima University, 2. School of Integrated Arts and Sciences, Hiroshima University

Phosphorus is an essential element for the life support of all living organisms, but it can be depleted in the surface layer of the ocean and may control the primary productivity. The supply of phosphorus into the oceans is primarily from rivers, with atmospheric deposition accounting for about 5% of the supply. Atmospheric deposition can be an important source of phosphorus in the Seto Inland Sea, where the amount of phosphorus flowing into rivers has decreased in recent years and the primary productivity has decreased. However, reports on the source and behavior of phosphorus in the atmosphere are limited. In this study, we focused on phosphate (PO_4^{3-}), which is most easily utilized by organisms, and investigated the concentration range, seasonal variation, and source of phosphate in atmospheric aerosols in Higashi-Hiroshima, Japan.

Atmospheric aerosol samples were collected on cellulose fiber filters using a high-volume air sampler from December 2017 to June 2020 at the campus of Hiroshima University in Higashi-Hiroshima, Japan. The molybdenum blue method was used to determine the concentration of phosphate in the samples. Water-soluble inorganic ions were also measured by ion chromatography. In order to estimate the source of phosphate, backward trajectory analysis, comparison with meteorological data, and principal component analysis were conducted.

Concentrations of phosphate in atmospheric aerosols during the observation period ranged from 1.7 to 49.0 ng m^{-3} and tended to be high in spring and low in winter. Principal component analysis showed that phosphate had the same factor as non seasalt- (nss-) Ca^{2+} and K^+. Because the concentration of phosphate is high in spring and mineral dust is a source of phosphorus in the atmosphere, the peaks of phosphate in spring was considered to originate from Kosa. However, the peak of nss-Ca^{2+}, which is an indicator of mineral dust, coincided with the Kosa periods, but slightly deviated from the peaks of phosphate. Furthermore, backward trajectory analysis showed that the air mass during the period of phosphate peaks did not pass through the arid regions of the Asian continent. On the other hand, the variation of phosphate concentration was similar to that of nss-K^+, an indicator of plant origin, suggesting that the source of phosphate is plant in addition to mineral particles. Specifically, the high concentration of phosphate in spring, a positive correlation with solar radiation, and the presence of phosphorus as a major component of pollen suggested that pollen contributed to the origin of phosphate. Although the calculated dry deposition flux of phosphate was as small as 0.21 to 0.54 mg m^{-2} $month^{-1}$, phosphate from the atmosphere is suggested to be used for phytoplankton production in the Seto Inland Sea, where phosphorus is depleted particularly in spring.

Keywords: Atmospheric aerosol, Phosphorus, Pollen, Dry deposition flux

©2021. Japan Geoscience Union. All Right Reserved.

Modelling regional and global scale impacts of atmospheric nitrogen inputs on marine biogeochemistry

*Maki Noguchi Aita[1], Fumikazu Taketani[1], Yoko Iwamoto[2], Tomohiro Hajima[3]

1. Earth Surface System Research Center, Japan Agency for Marine-Earth Science and Technology, 2. Hiroshima University, 3. Research Center for Environmental Modeling and Application, Japan Agency for Marine-Earth Science and Technology

The spatio-temporal distribution and seasonality of oceanic primary producers may be altered by various external factors, including atmospheric deposition of anthropogenic aerosols, rising water temperature, increasing frequency of typhoons, and changing ocean mixing due to global warming (*e.g.*, IPCC AR5). Primary producers in the surface ocean are sustained by nitrogenous nutrients supplied via five main processes: nitrification, vertical mixing, nitrogen fixation, atmospheric aerosol deposition (including rainfall), and inflows from rivers. Over the last several decades, atmospheric aerosol emissions from East Asia have increased rapidly. However, the effects of "atmospheric aerosols" on primary producers have not yet been well quantified (*e.g.*, Steffen *et al.*, 2015). To investigate the impact of atmospheric nitrogen deposition on primary producers, we conducted simulations using a marine ecosystem model combined with an atmospheric chemistry transport model. Our results showed that aerosol deposition enhanced primary production in the surface ocean by a factor 1.7 in the subtropical North western Pacific (Taketani *et al.*, 2018). This is because aerosol deposition has enhanced the supply of essential nutrients such as nitrogen, phosphorus and iron, which typically limit production under natural conditions near the ocean surface. Statistical analyses of observed sea surface nutrient concentrations in the North Pacific over the past 50 years have revealed decreasing trends for phosphate and silicate concentrations, whereas no significant trend was detected for nitrate concentration (Yasunaka *et al.*, 2016). The lack of a clear trend for nitrate may reflect the net effect of increased anthropogenic nitrogen sources combined with reduced supply of nitrogen from deep waters as mixed layer depths have decreased due to global warming. We will review previous studies using marine ecosystem models and Earth System Models, focusing on the effects of atmospheric nitrogen inputs on marine biogeochemistry during short- and long-term climate change and global warming.

Keywords: atmospheric aerosol, nitrogen deposition, ocean biogeochemical cycle, primary production, marine ecosystem model

©2021. Japan Geoscience Union. All Right Reserved.

Contribution of lightning-induced nitgen oxide to nitrogen cycle in air-sea boundary estimated by plasma discharge in laboratory

Ryo Hashimoto[1], *Sohiko Kameyama[1], Kohki Satoh[2], Hiroshi Ogawa[3]

1. Hokkaido University, 2. Muroran Institute of Technology, 3. The University of Tokyo

Lightning discharge is one of the important phenomena in atmospheric chemistry because it promotes oxidation of nitrogen in the atmosphere and is a major factor in production of nitrogen oxides derived from nature. It is known the lightning discharge occurs frequently not only in land areas but also in sea areas. In addition, tropical and subtropical sea areas, which are known as oligotrophic sea areas, are areas where the lightning discharge is particularly frequent. Recent studies have predicted an increase in the lightning discharge due to global warming and increasing in particle emissions from ships, resulting in enhancement of oceanic primary production. Consequently, the amount of nitrogen oxides deposited to the sea, which is the main nutrient supporting oceanic productivity, may increase. Therefore, in this study, we simulated the lightning discharge near sea surface by artificial plasma discharge with various environmental factors in laboratory and evaluated the generation/consumption of nitrogen oxides. As a result of laboratory experiments, we confirmed that nitrogen oxides are produced by the plasma discharge significantly. In addition, based on the results, we estimated effects of the lightning discharge in a wide area of oligotrophic waters and we suggested the lightning discharge may locally activate biological production.

Keywords: lightning discharge, nitrogen fixation, oligotrophic oceanic region

©2021. Japan Geoscience Union. All Right Reserved.

[J] Poster | H (Human Geosciences)：H-RE Resource and Engineering Geology

Thu. Jun 3, 2021 5:15 PM - 6:30 PM JST | Thu. Jun 3, 2021 8:15 AM - 9:30 AM UTC | Ch.08_1

[H-RE12] Resource Geology

convener:Tsubasa Otake(Division of Sustainable Resources Engineering, Faculty of Engineering, Hokkaido University), Kenzo Sanematsu(Mineral Resource Research Group, Institute for Geo-Resources and Environment, Geological Survey of Japan, National Institute of Advanced Industrial Science and Technology), Ryohei Takahashi(Graduate School of International Resource Sciences, Akita University), Tatsuo Nozaki(Submarine Resources Research Center, Research Institute for Marine Resources Utilization, Japan Agency for Marine-Earth Science and Technology)

Ore deposits containing valuable elements and minerals at high concentrations in supracrustal rocks are formed by the Earth's dynamics including magmatism, hydrothermal activity, metamorphism, and weathering. The formation of ore deposits is also closely associated with global environmental changes and biological evolution in the Earth's history. Involvement of difference academic fields in earth sciences including geology, petrology, geochemistry, mineralogy, and microbiology is required to understand the genesis of ore deposits. The field of resource geology is essential not only for efficient exploration and development of ore deposits but also for better understanding and assessment of hazardous elements that may be caused by the resource development. This session widely covers various topics of field investigation and observation, laboratory experiments, theoretical calculation, development of analytical methods and others related to the supracrustal migration and concentration of elements.

[HRE12-P01] Exploration of multiple geothermal resources in southern Yuzawa area, Akita prefecture

*Hayata Sato[1], Keishi Nunohara[1], Ryoichi Yamada[1], Nobuo Hirano[1], Noriyoshi Tsuchiya[1] (1.tohoku university)

[HRE12-P02] The Gold and Silver mineralization of layered yellow ore in Furutobe mine.

*Teruhiro Suzuki[1], Yasushi Watanabe[1], Takuya Echigo[1] (1.Graduate School of International Resource Sciences, Akita University)

[HRE12-P03] The significance of geology and sulfur isotope compositions of sulfates and sulfides at the ca.3.4 Ga Big Stubby Kuroko deposit in Pilbara, Western Australia

*Tomoaki Koya[1], Akizumi Ishida[1], Takeshi Kakegawa[1] (1.Graduate school of science, Tohoku University)

Exploration of multiple geothermal resources in southern Yuzawa area, Akita prefecture

*Hayata Sato[1], Keishi Nunohara[1], Ryoichi Yamada[1], Nobuo Hirano[1], Noriyoshi Tsuchiya[1]

1. tohoku university

Multiple geothermal resource exploration was conducted in the southern part of Yuzawa city, Akita prefecture.

The Sanzugawa caldera is distributed around this area, and in this caldera, there are basement rocks of pre-tertiary granitic and metamorphic rocks from the lower part, and the Doroyu and Torageyama formations are distributed in the upper part. In particular, the Torageyama formation is composed of partially fused tuff and is widely distributed in this area. The upper part of the Torageyama formation includes the Sanzugawa formation, the Kabutoyama formation, and the Takamatsudake volcanic rocks. In this study, we carried out Thermoluminescence measurements and identification of alteration minerals.

Thermoluminescence geothermal prospecting is a method of analyzing the luminescence produced by heating quartz particles in igneous rocks, and is used to evaluate the thermal effects of the rocks.

Alteration minerals can be broadly classified into acidic, neutral, and alkaline alteration minerals. The alkaline alteration zone was observed in Yunomatazawa in the western part of this area. Pyrophyllite was also found in the middle reaches of the Minasegawa, and it can be assumed that there was strong acidic alteration in this area. Furthermore, acidic and alkaline alteration minerals are distributed locally, while neutral alteration minerals are distributed over a wide area.

As a result of TL measurement, low TL values were detected near the lower reaches of the Minasegawa, and the surrounding streams were also found to have low TL values. Furthermore, the TL values decreased as the elevation decreased from Torageyama to Minasegawa. This indicates that there is a strong thermal influence from Torageyama to Minasegawa.

We developed a thermal structure model of the subsurface in this area by coupling the decay rate equation of TL with temperature and the unsteady heat conduction model to estimate the location of the heat source. The heat source was modeled as a heat source on a uniform flat plate, with a source temperature of 700℃ and initial surface and subsurface temperatures of 15℃. The TL values at the surface were best explained when the heat sources were located at a depth of 5000 m near Toragesawa and 4000 m downstream of the Minasegawa. In the middle reaches of the Toragesawa river, the TL values are consistent with the case where the heat source is located at 4500 m below the ground surface. From the above, it can be inferred that the subsurface thermal structure in the target area is not a uniform heat source, but a shallow heat source in parts.

Keywords: geothermal resources

©2021. Japan Geoscience Union. All Right Reserved.

The Gold and Silver mineralization of layered yellow ore in Furutobe mine.

*Teruhiro Suzuki[1], Yasushi Watanabe[1], Takuya Echigo[1]

1. Graduate School of International Resource Sciences, Akita University

An important ore was discovered in the Furutobe deposit to represent the gold and silver mineralization of the kuroko type deposit. In this study, we interpret the formation of this ore and the precipitation process of gold and silver. This ore has a layered structure, and characteristic mineral assemblages are identified in each layer. These layers are classified into five types of mineral assemblages A to E, identified by microscopic and macroscopic observation.

Bornite is the main component of A zone and chalcocite, silver-bearing tetrahedrite, stromeyerite, chalcopyrite, galena, sphalerite, and barite are accessory components. This zone includes barite lens. Pyrite and bornite are main components of B zone and chalcopyrite, galena, tetrahedrite are associated. This zone have lens-shaped chalcopyrite. Pyrite, bornite and barite are main components of C zone and accessory components are galena, sphalerite, tetrahedrite, and electrum. The amount of bornite decreases away from B zone in this zone. Pyrite, chalcopyrite and barite are main components of D zone and sphalerite, galena, and tetrahedrite are accessory components. Bornite is rare in this zone. Zone E consists of barite, pyrite and chalcopyrite.

Barite and pyrite increase from A zone to E zone. Bornite and Cu-S minerals are more abundant on the A band side, and chalcopyrite, galena and sphalerite are abundant on the E band side.

Mineral paragenesis in this ore are determined as that pyrite is the earliest, followed by copper minerals, sphalerite, and galena. Although chalcopyrite and bornite occur in different layers, their paranegentic stages are similar. Chalcopyrite and bornite either fill the pyrite grain boundaries or substitute pyrite and other minerals. Electrum in A zone occurs as small droplets in silver-bearing tetrahedrite and chalcocite. Electrum in C zone occurs along the grain boundaries and in voids of chalcopyrite and pyrite.

The occurrence of ore minerals indicates that this ore formation started by a large amount of pyrite precipitation. The reason why pyrite is small in amount on the A zone side is that it is substituted by bornite and chalcopyrite. Bornite and Cu-S minerals are abundant on A zone side, and chalcopyrite is more abundant on E zone side. This indicates that A zone side ore was formed at higher temperature and higher sulfur fugacity than that of E zonee. From the above, this ore was originally void-rich, mainly composed of pyrite, and the void-rich layers in the ore becames the hydrothermal flow path. In the center of the hydrothermal path (zone A and B), a solution of relatively high temperature and high sulfidation flowed and precipitated bornite, chalcocite, and stromeyerite. In outer C zone, seawater was mixed to create a medium-temperature, high-to-medium sulfidation solution, which precipitated bornite, chalcopyrite, and tetrahedrite. Finally, due to rapid cooling and decreaseed sulfur fugacity of the solution led the precipitation of electrum to fill the grain boundaries of the previously crystallized minerals. More involvement of sea water formed barite, sphalerite and galena at the latest in the ore.

Keywords: Kuroko, Gold and silver, Hydrothermal, Sea water

©2021. Japan Geoscience Union. All Right Reserved.

The significance of geology and sulfur isotope compositions of sulfates and sulfides at the ca.3.4 Ga Big Stubby Kuroko deposit in Pilbara, Western Australia

*Tomoaki Koya[1], Akizumi Ishida[1], Takeshi Kakegawa[1]

1. Graduate school of science, Tohoku University

The Big Stubby deposit is located at the Pilbara district in Western Australia. The age of this deposit is ca. 3.4 Ga and considered as the oldest Kuroko deposit. On the other hand, it has been unknown if Big Stubby and Miocene Kuroko deposits were formed by the same geological conditions (problem 1). The seawater sulfate had an important role for the formation of Miocene Kuroko deposits. On the other hand, the sulfate-poor ocean model is popular for the Archean age, and it is unknown if Big Stubby deposit could have formed under “sulfate-poor” conditions, differing from the Miocene Kuroko deposits (problem 2). In order to approach above problems, comparative studies between the Big Stubby and Miocene Kuroko deposits are performed in the present study.
Paleo-geological structures of the Big Stubby deposit was reconstructed in the present study combining pre-existing geological information and detailed examination of core samples. As a result, massive and Keiko (silicified) ores developed at the interface between rhyolite dome and tuff. Distal massive or disseminated sulfates overlain altered rhyolite dome. Those geological, mineralogical and geochemical information suggest that the Big Stubby deposit was formed by the similar mechanism as the Miocene Kuroko formed (answer to problem 1).
The $\delta^{34}S$ values for sulfate and sulfide minerals in the Big Stubby deposit range from +11 to+16‰ (V-CDT) and -1 to +1‰ (V-CDT), respectively. The isotope fractionation factor between sulfate and sulfides at the Big Stubby deposit are interestingly the identical to those at the Miocene Kuroko deposits. Such commonness suggests the circulation of sulfate-rich seawater in deep footwall rocks was responsible to generate ca. 3.4 Ga black smokers, accompanied with high temperature sulfate reduction in depth (answer to problem 2). The $\Delta^{33}S$ values indicate that the sulfate and sulfide minerals in the Big Stubby deposit are surprisingly following the MDF trend. This finding is different from the MIF signature found in other Archean sulfides and sulfates. This further rises possibility that MIF of sulfur was not global but local at the middle Archean age.

©2021. Japan Geoscience Union. All Right Reserved.

[J] Poster | H (Human Geosciences)：H-TT Technology & Techniques

Thu. Jun 3, 2021 5:15 PM - 6:30 PM JST | Thu. Jun 3, 2021 8:15 AM - 9:30 AM UTC | Ch.08_2

[H-TT16] Development and application of environmental traceability methods

convener:Ichiro Tayasu(Research Institute for Humanity and Nature), Ki-Cheol Shin(Research Institute for Humanity and Nature), Nozomu Takeuchi(Chiba University)

Modern society uses almost all the elements present in the natural world. Although there have long been calls for the sustainable use of the resources that provide these elements and the building of human societies that are in harmony with the environment, the survival of the human race is increasingly at risk as a result of qualitative changes to the environment as a whole. Implementation by the society of methodologies for diagnosing and tracking these various elements of the natural environment and their relationships with humans are now required.
Elements cycle within and among the Earth system spheres, human society, and the human body. Information on the concentrations and stable isotopes of elements is a powerful tool for tracing this cycling and has been applied in studies of atmosphere-hydrosphere circulation, ecological systems, and the life, health, and history of humans. We propose a session to discuss the development and applications of environmental traceability methods toward the goal of establishing traceability in natural and human systems.
We encourage the presentation of research integrating isotopic information in various disciplines, such as geochemistry, hydrology, ecology, geology, mineralogy, anthropology, food science, and forensics. We call the research Environmental Isotope Study.

[HTT16-P01] Oxygen and hydrogen isotopic signatures of surface and groundwater during a dry season in the Tonle Sap Lake basin

*Yumi Yoshioka[1], Takao Masumoto[2], Kumiko Tsujimoto[3], Yuji Ito[4] (1.Shimane University, 2.Akita Prefectural University, 3.Okayama Univerisity, 4.Kagoshima University)

[HTT16-P02] Identification of regional characteristics of the basin using elemental components as tracers

*Yusuke Hataya[1], Shiho Yabusaki[2], Seiki Kawagoe[3] (1.Fukushima University Faculty of Symbiotic Systems Science, 2.Research Institute for Humanity and Nature, 3.Fukushima University Faculty of Symbiotic Systems Sciences)

[HTT16-P03] Seasonal variation of $\delta^{34}S$ and $\delta^{18}O$ in sulfate in rain water and aerosols on the outskirts of Gifu City

*Masako Kagawa[1], Nagayoshi Katsuta[1], Yusuke Hashimoto[1], Yuto Yamagishi[1], Ichiro Tayasu[2], Chikage Yoshimizu[2] (1.Gifu University, Faculty of Education, 2.Research Institute for Humanity and Nature)

[HTT16-P04] Seasonal variations and trends of dissolved elements in rainwater and stream water in forest catchment area of central Japan

*Masayuki Morohashi[1], Hiroki Yotsuyanagi[1], Masaaki Takahashi[2], Tatsuyoshi Saito[2], Yayoi Inomata[3], Ki-Cheol Shin[4], Ichiro Tayasu[4], Tsuyoshi Ohizumi[1], Hiroyuki Sase[1] (1.Asia Center for Air Pollution Research, 2.Niigata Prefecture, 3.Kanazawa Univercity, 4.Research Institute for Humanity and Nature)

[HTT16-P05] Geochemical and isotopic study of river water from the Okayama and Tottori Prefectures, Japan.

*Katsuyuki Yamashita[1], Takahiro Kamei[1], Keisuke Kishimoto[1], Masahiko Mori[1], Yuga Kishimoto[2], Aya Ooi[2], Ayaka Onishi[2], Yoko Kurihara[2], Miyake Ryota[2], Ryosuke Yamano[2], Hitoshi Chiba[1], Takanori Nakano[3], Ki-Cheol Shin[4] (1.Graduate School of Natural Science and Technology, Okayama University, 2.Department of Earth Sciences, Okayama University, 3.Ono City, 4.Research Institute for Humanity and Nature)

[HTT16-P06] Stable sulfur isotope variations in lacustrine sediments in Mongolia and its paleo-environmental implication

Miku Yoichi[1], *Nagayoshi Katsuta[1], Shinya Ochiai[2], Sayuri Naito[1], Masako Kagawa[1], Yuma Masuki[1], Ichiro Tayasu[3] (1.Faculty of Education, Gifu University, 2.Institute of Nature and Environmental Technology, Kanazawa University, 3. Research Institute for Humanity and Nature)

[HTT16-P07] Variations in sedimentation rates of Tsuya River in the western Nobi Plain, central Japan over the last decades

*Takashi Tashiro[1], Ichiro Tayasu[2] (1.Nagoya University, 2.Research Institute for Huminity and Nature)

[HTT16-P08] Neutralization using recycled waste materials for acid wastewater from the Kusatsu hot spring area in Japan

*Takeshi Saito[1], Naoki Watanabe[2] (1.Graduate School of Science and Engineering, Saitama University, 2.Research Institute for Natural Hazards and Disaster Recovery, Niigata University)

[HTT16-P09] Evaluating temperature dependence of arsenic and boron adsorption onto sediments

*Keigo Kurita[1], Takeshi Saito[2] (1.Department of Civil and Environmental Engineering, Faculty of Engineering, Saitama University, 2.Graduate School of Science and Engineering, Saitama University)

[HTT16-P10] Soil food webs after more than a year since litter-removal experiment: an evaluation based on carbon and nitrogen stable isotope ratios

*Takashi F Haraguchi[1], Soshi Yoshida[2], Syuhei Fujimoto[2], Keiichiro Sato[2], Motohiro Hasegawa[2] (1.Biodiversity Research Center, RIEAF, Osaka, 2.Doshisha University Faculty of Science and Engineering, Environmental Systems Science)

[HTT16-P11] Evaluation of air pollution stress in roadside trees using stable carbon isotope ratio

*Yuko T. Hanba[1], Mayu Matsumoto[1], Takashi Kiyomizu[1], Tomomitsu Kinoshita[1], Atsushi Kume[2] (1.Kyoto Institute of Technology, 2.Kyushu University)

[HTT16-P12] **Effects of Traffic Volume on Photosynthetic Function and Water Use Efficiency of Tall Street Trees in Kyoto City**

*Takumi Matsuura[1], Yuko T. Hanba[1] (1.Kyoto Institute of Technology)

[HTT16-P13] Effect of flooding stress on photosynthesis of aquatic plants

*Yutaro Yasui[1], Yuko T. Hanba[1] (1.Kyoto Institute of Technology)

[HTT16-P14] The incubation method using ^{18}O-water and phosphate oxygen isotope for quantitative evaluation of bioavailable phosphate in soil.

*Takuya Ishida[1] (1.Hiroshima University)

[HTT16-P15] Trace element quantification in organic materials by low temperature plasma ashing

Taisuke Hino[1], Yuriko Umeda[1], Hibiki Shishime[1], Akane Ito[1], *Masaharu Tanimizu[1] (1.Kwansei Gakuin University)

[HTT16-P16] Metal element isotope analysis for Environmental Reference Materials

*Ki-Cheol Shin[1] (1.Research Institute for Humanity and Nature)

Oxygen and hydrogen isotopic signatures of surface and groundwater during a dry season in the Tonle Sap Lake basin

*Yumi Yoshioka[1], Takao Masumoto[2], Kumiko Tsujimoto[3], Yuji Ito[4]

1. Shimane University, 2. Akita Prefectural University, 3. Okayama Univerisity, 4. Kagoshima University

Tonle Sap Lake located in Cambodia is the largest lake in South Asia. This lake has several inflow rivers and one outflow river. It is connected to the Mekong River via the outflow river and the Mekong river water inflows to the lake during wet seasons. Thus, the lake is characterized by key fluctuations of water levels and surface area. There is a need for better understanding of water supply to the lake from surface or under surface water. The contribution of groundwater is still unknown. Stable isotopes in water are often used to identify lake water balances. We therefore conducted a sampling campaign in February 2020 of a dry season. We collected water samples for four lake waters, nine river waters including inflow rivers, outflow river, and subbranch of the Mekong River, eight groundwater, and eleven commercial bottled water made in Cambodia and Thailand. Major dissolved ions, dissolved silica (DSi), and stable isotope ratios of oxygen and hydrogen ($\delta^{18}O$ and $\delta^{2}H$) were analyzed. Isotopic composition of rain obtained in earlier studies were used for data analyses. The highest ratios were observed in the lake and were ranging from 0.0 to 2.2 ‰for $\delta^{18}O$ and -18 to -9 ‰for $\delta^{2}H$. The isotopic ratios became higher in the order of subbranch of the Mekong River, the inflow rivers, and the outflow river. The isotopic composition of the groundwater varied widely: from -7.3 to -2.3 ‰for $\delta^{18}O$ and -52 to -21 ‰for $\delta^{2}H$. Average isotopic composition of groundwater was consistent with the volume-weighted average isotopic compositions of rain. Isotope signatures of groundwater did not depend on the depths of the wells. The regression line was delineated on a dual-isotope plot by samples of the lake and outflow river, and it was defined as the local evaporated line (LEL). The slope of LEL was 5.0. In addition, the slopes of regression lines for inflow river and groundwater were 4.9 and 6.2, respectively. The flatter slopes than that of the LMWL indicated that surface and groundwater were more evaporative than the source water, and isotope compositions were enriched by the kinetic isotope effect during evaporation even in river water. Small isotopic differences (ratios and slopes) between groundwater and commercial bottled water were observed. The intersect of LEL and LMWL, which is the initial composition before isotopic enrichment process, was fall near samples of groundwater and the average isotopic compositions of rain. The DSi concentration is used as a residence time indicator in groundwater. The higher concentration in the lake (less than 20 mg/L) than in inflow rivers (less than 10 mg/L) was consistent with the contribution of groundwater to the lake. Water sampling survey with monthly interval has been implemented since May 2020. Further works are monitoring of isotopic fluctuation throughout dry and rainy seasons, and tracing water source of the lake.

Keywords: Stable isotope, Groundwater, Kinetic isotope effect , Lake water balance, Mekong River, Cambodia

©2021. Japan Geoscience Union. All Right Reserved.

Identification of regional characteristics of the basin using elemental components as tracers

*Yusuke Hataya[1], Shiho Yabusaki[2], Seiki Kawagoe[3]

1. Fukushima University Faculty of Symbiotic Systems Science, 2. Research Institute for Humanity and Nature, 3. Fukushima University Faculty of Symbiotic Systems Sciences

1.Introduction

1.1 background

Changes in the environmental dynamics of the basin are expected in response to "land use development due to human modification" and "extreme temperature rise and precipitation due to climate change", and research on the impact assessment of eutrophication is being developed especially in closed water areas. Has been done. Along with internal production, it is necessary to understand the inflow effect of external load on the drastic environmental changes. Predicting the future image of water quality can be evaluated more precisely based on detailed information on both internal production according to the shape scale of each basin and external load according to regional characteristics.

1.2 Research purpose

In this research, as part of the purpose of developing an external load database that can be used for land cover and current conditions, and for assessing the water environment impact of climate change, the Abukuma River basin, which is a first-class river in the Tohoku region, was set as the target area and numerical geography. Based on the information, we attempted to compare and examine the relationship between regional characteristics (vegetation, land cover, soil, geology) and sampled and analyzed chemical outflow components (chemical component content due to multiple elements) for each small basin. ,

In the basin condition analysis, the types of basin conditions of the basin were classified using cluster analysis. We decided to compare the characteristics of the global region with the values obtained from chemical analysis (content of elements).

2.Main subject

2.1. Results of multi-element analysis using ICP-MS

Inductively coupled plasma mass spectrometry (ICP-MS) was used for analysis to determine the amount of elements contained in the Abukuma River basin (Na, Mg, Al, Si, K, Ca, Mn, Fe, P).

The chemical composition (element content) of the Abukuma River main river increases from the upstream to the middle basin, with the confluence with the Ose River at its maximum and decreasing toward the downstream.

In addition, in the results of this analysis, the value of Arakawa was the largest among the main river and tributary points. Above all, the concentration of Mg was more than twice as high as that of other

©2021. Japan Geoscience Union. All Right Reserved.

tributaries.

At each concentration, Na and Ca varied at each point, so it is considered that there are some regional characteristics.

2.2 Results of Regional Characteristics Analysis

2.2.1 Classification results by cluster analysis

For the sake of convenience, the classification by cluster analysis was integrated, and the integration numbers were shown as equivalent values in the relative positional relationship, and a total of three groups were shown. Vegetation in the Abukuma River basin was divided into 5 groups, 5 categories for land cover, 4 categories for soil, and 5 categories for geology. The classification categories of "4334 (Fujita River, Sasahara River)", "5112 (Suwon River, Yashiro River)", and "2113 (Kitasu River, Yui River)" have overlapping basin characteristics. Depending on the conditions, there is a high possibility that similar chemical component outflow will occur.

2.2.2 Comparison with multi-element analysis results

As basin conditions that are considered to contribute to the outflow of chemical components, vegetation includes deciduous and evergreen broad-leaved forests in the Yabutsubaki class area, land cover includes basins that occupy a high proportion of urban areas, and soil includes Andosols. In terms of humus and geology, the basin has a high occupation ratio related to volcanic ejecta. From the transition of the material outflow component (element content) as the material circulation route in the Abukuma River basin, it became clear that it changes depending on the basin where the outflow is artificially high due to the urban area and the regional characteristics due to the contribution of forests and volcanoes. ..

3.Conclusion

From the chemical analysis (content of elements) and the comparative study of the basin conditions, the elements of deciduous / evergreen broadleaf forest zone, urban area, humus, and volcanic ejecta were shown as basin conditions that contribute to the formation of water quality in the Abukuma River basin.

Furthermore, it is shown that classification by natural factors and social factors is necessary as a pattern of load increase due to basin conditions.

This time, the analysis was performed without considering the item of estimated population as the basin condition, so we plan to add some conditions in the future and work on the elucidation of the chemical composition and its material cycle.

Keywords: Elemental component, Tracer, Regional characteristics, Land cover

©2021. Japan Geoscience Union. All Right Reserved.

Seasonal variation of $\delta^{34}S$ and $\delta^{18}O$ in sulfate in rain water and aerosols on the outskirts of Gifu City

*Masako Kagawa[1], Nagayoshi Katsuta[1], Yusuke Hashimoto[1], Yuto Yamagishi[1], Ichiro Tayasu[2], Chikage Yoshimizu[2]

1. Gifu University, Faculty of Education, 2. Research Institute for Humanity and Nature

1. Introduction

Reportedly, Lake Ijira, which is located on the outskirts of Gifu City, has the highest deposition of non-sea-salt sulfate ion (nss-SO_4^{2-}) and the hydrogen ion (H^+) in Japan (Ministry of the Environment, 2004). It has also been demonstrated that its outflow of SO_4^{2-} is about twice its inflow (Ministry of the Environment, 2004). Based on these results, we sampled atmospheric aerosols and rainwater before deposition from November 2018 until the present (2021) to measure the contained sulfate ion, its sulfur isotope ratio ($\delta^{34}S$) and oxygen isotope ratio ($\delta^{18}O$) for this study. Thereafter, we examined the source of sulfur derived from the atmosphere and accumulated on the soil surface around Lake Ijira.

2. Methods for Observations and Analyses

Rainwater was sampled using a simple rainwater collector: a PET bottle equipped with polypropylene funnel. For ion analyses, atmospheric aerosols were sampled onto a 0.2-μm PTFE filter at an 8–10 L/min flow rate with a vacuum pump. For isotope analyses, atmospheric aerosols were sampled onto a quartz filter (QR-100®; Advantec) at a suction flow rate of 1000 L/min once a week using a high-volume air sampler (HV-RW; Sibata Scientific Technology Ltd.).After the samples filtered through membrane filter, they were subjected to quantitative analysis for concentrations using ion chromatography (ICS-1100; Thermo Fisher Scientific Inc.) for anions and inductively coupled plasma atomic emission spectrometry (ICP-AES) (ULTIMA2; Horiba Ltd.) for cations.For the sulfur isotope ratio and the oxygen isotope ratio were precipitate SO_4^{2-} in the sample as $BaSO_4$. It was analyzed using S-IRMS (Flash EA 2000 + ConFlo IV + delta V plus; Thermo Fisher Scientific Inc.) and OH-IRMS (TC/EA+ConFlo III+Delta plus XP; Thermo Fisher Scientific Inc.) installed in the Research Institute for Humanity and Nature.

3. Results

3-1. Changes in SO_4^{2-} and NO_3^- concentrations during the lockdown period in China

In early 2020, China adopted a lockdown policy because of the outbreak of COVID-19. Itabashi *et al.* (2020) reported that the concentrations of PM2.5, SO_4^{2-}, and NO_3^- were measured for three years of 2018–2020 at four sites (Goto Islands, Oki Islands, Maki, and Nonodake), the mean concentrations of PM2.5, SO_4^{2-}, and NO_3^- during January–March were lower than the prior year at all observation sites in the lockdown period of China during January–March. For Lake Ijira, comparison of SO_4^{2-} and NO_3^- concentrations of January–March between 2019 and 2020 indicated a remarkable decrease, suggesting a decrease in concentrations of atmospheric aerosols because of decreased economic activities resulting from lockdowns.

3-2. $\delta^{34}S$

$\delta^{34}S$ in the sulfate ions in rainwater during December 2018 –December 2020 was 4–12‰ in winter and 2–4‰ in summer, exhibiting clear seasonal changes to decrease in winter and increase in summer. $\delta^{34}S$

©2021. Japan Geoscience Union. All Right Reserved.

in sulfate aerosols was 5–6‰ in winter and 2–6‰ in summer, reflecting seasonal changes, although there were variations.

3-3. Analysis by back-trajectory analysis
Back-trajectory analysis was applied using NOAA HYSPLIT data every day during the observation period, to be classified into eight categories (Figure 1). Figure 2 shows nss-SO_4^{2-} and NO_3^- concentrations and the $\delta^{34}S$ value of each category from December 2019 through December 2020. The most frequently classified category was CE (route that passes the eastern side of the Korean Peninsula) followed by the second-most frequent, CN (route that passes the western side of the Korean Peninsula). Air masses from the Eurasian continent accounted for 80% of air masses that arrived at the observation points. It is therefore considered that most of the atmosphere comes from the Eurasian continent.

Keywords: sulfate ion, sulfur isotope, atmospheric aerosol, rain water

©2021. Japan Geoscience Union. All Right Reserved.

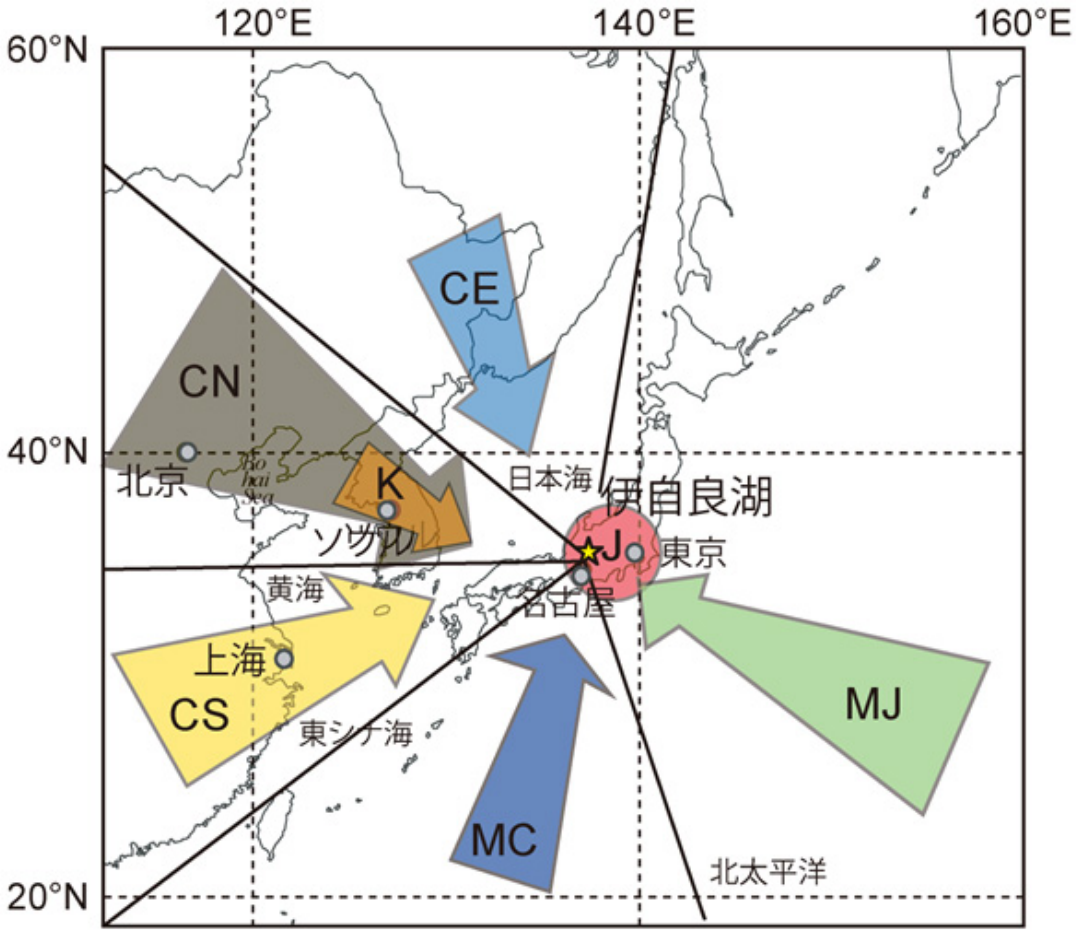


図 1. 気塊経路の後方流跡線による分類

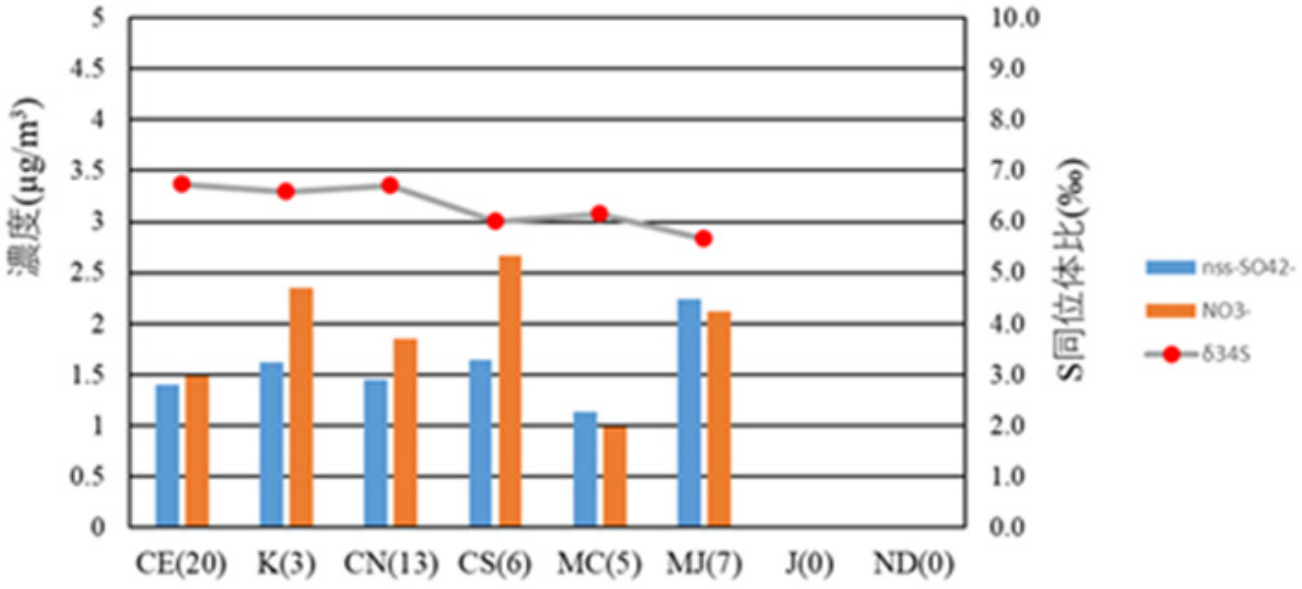


図 2. 気塊経路ごとの nss-SO_4^{2-}, NO_3^-濃度と $\delta^{34}S$ 値

©2021. Japan Geoscience Union. All Right Reserved.

Seasonal variations and trends of dissolved elements in rainwater and stream water in forest catchment area of central Japan

*Masayuki Morohashi[1], Hiroki Yotsuyanagi[1], Masaaki Takahashi[2], Tatsuyoshi Saito[2], Yayoi Inomata[3], Ki-Cheol Shin[4], Ichiro Tayasu[4], Tsuyoshi Ohizumi[1], Hiroyuki Sase[1]

1. Asia Center for Air Pollution Research, 2. Niigata Prefecture, 3. Kanazawa Univercity, 4. Research Institute for Humanity and Nature

Metal elements released into the atmosphere by human activities such as fossil fuel combustions flow into forest ecosystems by wet deposition (precipitation) and dry deposition (particulate matters), and some of them flow out of the system via mountainous stream water. Some elements are essential for lives, but excessive intake is harmful. It is important to grasp the concentration level of dissolved metal elements, because they are easily taken into the living organisms.

The Kajikawa catchment site in Niigata Prefecture, which is located on the continental side of central Japan, has been suffering to a large amount of acidic substances deposited due to its geographical conditions and meteorological seasonality, and is affected by transboundary air pollution originating from the Asian continent. In this study, concentrations of trace elements dissolved in rainfall (RF) and mountain stream water (SW) were clarified in order to evaluate the effects of transboundary air pollution in forest ecosystems more comprehensively. In addition, stable isotope ratio analysis was used to analyze the dynamic mechanism in more detail.

RF were collected by using bulk samplers at the end of each month, and SW were also collected on the same day during the period from 2014 to 2018. Trace element concentrations were quantified by ICP-MS and major inorganic ion concentrations by using ion chromatography. At the same time, pH, electrical conductivity, precipitation amount and flow rate were measured. In this study, we focus on Al, V, Cr, Zn, As, Sr, and Pb as trace elements. In addition, stable isotope ratios were measured for Sr and Pb.

Concentrations of trace elements and major inorganic ions in RF tended to be high in winter and low in summer. Fluxes of many trace elements also increased in winter, reflecting the high amount of precipitation in winter. The enrichment factors (EFs) calculated based on Al (as an index of earth crust) was high in winter and low in summer. The EFs for many elements were found to be above 10, suggesting that they are derived from anthropogenic sources, such as fossil fuel combustion. The EFs of many elements showed an upward trend, while that of Pb showed a downward trend.

The isotopic ratio of Sr increased over the years, especially in the spring, possibly due to the influence of the Asian dust (yellow sand). At the time of poster presentation, we will compare and discuss the change in the isotope ratio of Pb.
This work was supported by grants from the Japan Society for the Promotion of Science (JSPS) KAKENHI Grant Numbers JP19H00955 and JP18K11616.

Keywords: trace element, Forest catchment, Isotope ratio analysis

©2021. Japan Geoscience Union. All Right Reserved.

Geochemical and isotopic study of river water from the Okayama and Tottori Prefectures, Japan.

*Katsuyuki Yamashita[1], Takahiro Kamei[1], Keisuke Kishimoto[1], Masahiko Mori[1], Yuga Kishimoto[2], Aya Ooi[2], Ayaka Onishi[2], Yoko Kurihara[2], Miyake Ryota[2], Ryosuke Yamano[2], Hitoshi Chiba[1], Takanori Nakano[3], Ki-Cheol Shin[4]

1. Graduate School of Natural Science and Technology, Okayama University, 2. Department of Earth Sciences, Okayama University, 3. Ono City, 4. Research Institute for Humanity and Nature

Geochemical and isotopic properties of river water are influenced by various processes such as evaporation, interaction with rocks and soils, and input from human activities. In order to understand the cause of geochemical variation observed in river water from the Okayama and Tottori Prefectures, Japan, we have collected over 700 samples from 539 locations over the past ten years. All samples were filtered with 0.2 μm acetate cellulose disposable filter prior to the analyses for major dissolved components, trace element concentration, and O-H-S-Sr isotopes. The data from these analyses were used to construct high-resolution geochemical maps of the two Prefectures. Many elements, such as Ca, Rb, Cs, V and Si show geographic variations that are consistent with the geochemistry of the rocks exposed in the area. For example, high concentration of Ca is observed in the western Okayama Prefecture where limestones are widely exposed, and high concentrations Rb, Cs, V and Si are observed around Mt. Daisen of dacitic volcanic rocks. These regional variations exceed seasonal variation and thus we attribute this to the chemical weathering of watershed rocks.

Regional variation is also seen in various isotopic signatures. New Sr isotope data show that $^{87}Sr/^{86}Sr$ is low (<0.706) in the area near Mt. Daisen and Hiruzen, where Quaternary volcanic rocks are exposed. On the other hand, $^{87}Sr/^{86}Sr$ in excess of 0.709 is seen in areas where Paleozoic sedimentary rocks distribute. Such correlation between $^{87}Sr/^{86}Sr$ and the average age of rocks exposed in the area supports the idea that Sr (and perhaps Ca) in the river water is largely derived from rocks and soils in the vicinity of the river. The sulfur isotopic signature ($\delta^{34}S$), on the other hand, is high (>12‰) in the central to western Tottori Prefecture, and low in the Okayama Prefecture (<6‰). The high $\delta^{34}S$ seen in the river water from the Tottori Prefecture may be ascribed to sulfur originating from combusted Chinese coals and sea-salt during the winter with high rainfall. The $\delta^{34}S$ of the river water from the Okayama Prefecture tends to converge to ~0 ‰as the SO_4 concentration increases. This correlation may imply that Okayama river water with low $\delta^{34}S$ is enriched in artificial sulfur of domestic origin (e.g. sulfur released from breakdown of fertilizer), whose $\delta^{34}S$ is about 0 ‰.

Keywords: River water, Okayama Prefecture, Tottori Prefecture

©2021. Japan Geoscience Union. All Right Reserved.

Stable sulfur isotope variations in lacustrine sediments in Mongolia and its paleo-environmental implication

Miku Yoichi[1], *Nagayoshi Katsuta[1], Shinya Ochiai[2], Sayuri Naito[1], Masako Kagawa[1], Yuma Masuki[1], Ichiro Tayasu[3]

1. Faculty of Education, Gifu University, 2. Institute of Nature and Environmental Technology, Kanazawa University, 3. Research Institute for Humanity and Nature

In this study, we present the results of stable isotope variations since the last 300 years of lake sediment samples, southwest Mongolia, and discuss its environmental implication.

Keywords: lake sediment, stable sulfur isotope, permafrost zone

©2021. Japan Geoscience Union. All Right Reserved.

Variations in sedimentation rates of Tsuya River in the western Nobi Plain, central Japan over the last decades

*Takashi Tashiro[1], Ichiro Tayasu[2]

1. Nagoya University, 2. Research Institute for Huminity and Nature

The Nobi Plain has been formed with the fluvial processes of the Kiso Three Rivers (composed of the Kiso, Ibi and Nagara rivers), central Japan. Tsuya River, a branch of the Ibi River is flowing at the eastern foot of Yoro Mountains, Gifu prefecture, in the western margin of the plain with abundant groundwater. Because the current main channel of Tsuya River has the modern continuous levee only on its eastern side, it flows across ends of their alluvial fans with receiving a lot of spring water and sediment via its western side derived from the Yoro Mountains. This study is conduced to describe the environmental changes of Tsuya River from the viewpoints of sedimentation dynamics with natural and artificial impacts.
Sediment dynamics over the last decades in the Tsuya River are evaluated with the lead (Pb) -210 dating method. The sedimentation rates were determined by applying CIC (Constant Initial Concentration) and CRS (Constant Rate of Supply) models to the sediment cores in the pond linked to the right/western bank of main channel. The CRS model mostly agreed with the Cs-137 dating, which the CIC model was not applicable because of fluctuations in the lead 210 profiles. The average sediment rates of 0.24 - 0.44 g cm^{-2} yr^{-1} were obtained, which were larger than the reported values in most of the lakes in Japan. Furthermore, the higher sedimentation rates with the maximal values such as 0.59, 0.71 and 2.62 g cm^{-2} yr^{-1} were obtained from 1961 to 1984, which could respectively correspond to flood events and construction works in Tsuya River watershed during the same period by according to conventional literatures. Consequently, these results might clarify the river sediment dynamics also be explained with the classical lead-210 method (CRS model).

Keywords: sedimentation rate, flood history, Pb-210 dating, Tsuya River

©2021. Japan Geoscience Union. All Right Reserved.

Neutralization using recycled waste materials for acid wastewater from the Kusatsu hot spring area in Japan

*Takeshi Saito[1], Naoki Watanabe[2]

1. Graduate School of Science and Engineering, Saitama University, 2. Research Institute for Natural Hazards and Disaster Recovery, Niigata University

Acid river waters from active volcanos and mines influence seriously to ecosystems in the river basins. This study is paid attention to the Yukawa River that is characterized by markedly lower pH value (less than 2.0) and higher concentration of harmful elements such as arsenic (As) and lead (Pb) and that is the acid discharged water from the Kusatsu hot spring and closed sulfur mines located in the eastern foot of Kusatsu-Shirane Volcano in central Japan. The neutralization treatment of this river water using crushed limestone has been continuously carried out by the Ministry of Land, Infrastructure, Transport and Tourism (government of Japan) for more than 50 years. We have examined the applicability of recycled waste materials as alternative liming agents to the neutralization treatment using crushed limestone through batch neutralization experiments in laboratory. The neutralization experiments for the acid wastewater were performed the mixing of water from the Kusatsu hot spring with fly ash, clinker ash, steel slug, autoclaved lightweight aerated concrete, recycled concrete, wood ash, oyster shell, and calcium carbonate as a reference liming agent. The experimental conditions are as follows. Centrifuge tubes with 50 mL volume were filled with appropriate weight of each recycled waste material and 40 mL of the acid wastewater to have the solid-liquid ratio of 1:10 to 1:4000. Water samples are separated by centrifugation after shaking for 10 minutes. Subsequently we measured pH, electric conductivity (EC), and concentrations of harmful elements (As and Pb) immediately. As the results, neutralization performance of steel slug and recycled concrete was significantly higher than that of other recycled waste materials. For removal performance of both As and Pb, steel slug, recycled concrete, and wood ash revealed clearly higher comparing with calcium carbonate as a common liming agent. The above results suggest that steel slug and recycled concrete are promising alternative liming agents to calcium carbonate.

Keywords: Kusatsu hot spring area, Acid wastewater, Neutralization treatment, Recycled waste materials

©2021. Japan Geoscience Union. All Right Reserved.

Evaluating temperature dependence of arsenic and boron adsorption onto sediments

*Keigo Kurita[1], Takeshi Saito[2]

1. Department of Civil and Environmental Engineering, Faculty of Engineering, Saitama University, 2. Graduate School of Science and Engineering, Saitama University

Subsurface temperature increase likely due to global warming and urbanization has been observed all over the world. This phenomenon may cause changes in physical, chemical, and microbial processes in subsurface environment, resulting in groundwater quality changes. The effect of temperature increase on subsurface environment including groundwater system has not been sufficiently clarified. The objective of this study was therefore to clarify temperature dependence of arsenic and boron adsorption onto sediments based on batch adsorption experiments under 20°C and 40°C conditions. Completely different two samples of Holocene (non-marine sediment) and Miocene deposits (marine sediment) were used in this study. The adsorbed amount of arsenic at 40°C was significantly higher than that at 20°C, suggesting clear temperature dependence for arsenic. Oppositely, the adsorbed amount of boron was not clearly affected by temperature.

Keywords: Temperature dependence, Adsorption, Arsenic, Boron, Sediment

©2021. Japan Geoscience Union. All Right Reserved.

Soil food webs after more than a year since litter-removal experiment: an evaluation based on carbon and nitrogen stable isotope ratios

*Takashi F Haraguchi[1], Soshi Yoshida[2], Syuhei Fujimoto[2], Keiichiro Sato[2], Motohiro Hasegawa[2]

1. Biodiversity Research Center, RIEAF, Osaka, 2. Doshisha University Faculty of Science and Engineering, Environmental Systems Science

Organic layer on soil surface is vertically heterogeneous habitat and one of the important endmembers; i.e. their source of energy and nutrients, for soil fauna. The vertical heterogeneity of soil organic matter is primarily ascribed to decomposition process from plant litter to different matters so called fumus and humin. Many studies have shown that species composition of soil fauna is changed by perturbations of soil organic matter, mainly because the spatial heterogeneity is disrupted. On the other hand, effects of the disturbances to biological interactions between predator and prey; food web structures, are little described. In this study, we aimed to elucidate response of diets of soil microarthropods to ecological disturbances and compared carbon and nitrogen stable isotope ratios of them between those from litter removal plots and those from control plots.

Litter removal manipulation was conducted at a Japanese cypress forest (*Chamaecyparis obtusa*) in Kamigamo Experimental Station, Kyoto, Japan on July 12th, 2019. Litter manipulation plot was comprised of three 4 m x 4 m quadrates settled in one-line, and two 2 m x 4 m quadrates on both sides of the litter removal plot were defined as control plot. All quadrates were split into 2 m x 2 m subplots, and at least two soil cores were sampled from every subplot for the extraction of soil microarthropods by Tullgren apparatus. The extracted microarthropods in September 2019, were identified to order or suborder for the measurements of stable isotope ratios of carbon and nitrogen (δ^{13}C and δ^{15}N) for the following taxa; Oribatida (detritivore), Collembola (detritivore), Prostigmata (Predator or microbivore), and Gamasida (predator). Part of the soil cores were used for the δ^{13}C and δ^{15}N measurements of the following four collembola species; *Tetracanthella sylvatica*, *Tomocerus varius*, *Folsomia octoculata*, and *Isotoma carpenteli*. In 2020, only Gamasida and the four collembola species were chosen for measurements of the stable isotope ratios.

To test the effect of manipulation and sample type on the δ^{13}C or δ^{15}N values, ANOVA-like GLMM considering effect of plot as block factor, were conducted for each of soil organic layer, three Acari suborders with Collembola, and four Collembola species. Goodness of fit was evaluated by AIC, and in case singular fit was returned, block random factor was removed and GLM was re-selected. Post-hoc test was also conducted by model selection of GLMM for every sample type.
Based on the models, effect of litter removal was selected for δ^{13}C, δ^{15}N of Collembola species and δ^{15}N of Acari suborders and Collembola. δ^{15}N of organic layers were slightly different between manipulated plots and control plots, although the effects were not consistent between the sample types: δ^{15}N of litter layer was increased, while δ^{15}N of humus was decreased by litter removal. Collembola species living in the deeper organic layer showed in higher δ^{13}C and δ^{15}N than surface-living species, as shown in previous studies. Gamasida in the manipulated plot showed on average 1.7‰ and 0.7‰ higher δ^{15}N values in 2019 and 2020, than those from control plot. These results indicate that predators approached to prey in deeper organic layers. Collembola species sampled in manipulated plot showed up to 0.5‰ lower δ^{13}C values and up to 0.7‰ higher δ^{15}N values than controlled plot in 2019. The difference in the δ^{13}C value expanded up to 1.1 ‰in a surface-dwelling Collembola (*Tomocerus varius*). Based on the effect of litter removal on δ^{13}C of some Collembola species, phytophagous-oriented diet shift was

©2021. Japan Geoscience Union. All Right Reserved.

suggested. On the other hand, relative abundance of *Tomocerus varius* was higher in the litter exclusion plot, while relative abundance of *Folsomia octoculata* and *Isotoma carpenteli*, species inhabiting deeper organic-layer (Upper F, lower F), decreased. These results indicate that ecological plasticity both on food and habitat is a key to survive in a perturbed system.

Keywords: soil microarthropods, food web, ecology

©2021. Japan Geoscience Union. All Right Reserved.

Evaluation of air pollution stress in roadside trees using stable carbon isotope ratio

*Yuko T. Hanba[1], Mayu Matsumoto[1], Takashi Kiyomizu[1], Tomomitsu Kinoshita[1], Atsushi Kume[2]

1. Kyoto Institute of Technology, 2. Kyushu University

In Japan, the problem of air pollutants, especially nitrogen oxides, emitted from automobiles and other vehicles became apparent as "urban- and lifestyle-type" air pollution in the 1970s. In Japan in the year of 2021, the amount of nitrogen dioxide in the air has been steadily decreasing in general, but in areas with heavy traffic, the amount of nitrogen dioxide can exceed the environmental standard concentration. Therefore, air pollution in cities is not a problem of the past in Japan. On the other hand, since the 2000s, the amount of nitrogen oxides in the atmosphere has been dramatically increasing in the Asian region along with the remarkable economic growth of China and India, causing serious air pollution problems.

Roadside trees planted in cities have many benefits, such as absorption and trapping of air pollutants in the canopy, suppression of high temperatures through canopy shade formation, and absorption of carbon dioxide through photosynthesis. Since photosynthesis is a physiological function that supports the growth and survival of roadside trees, maintaining photosynthetic activity is essential for the survival of trees in urban areas, which are harsh environments. However, photosynthetic activity is extremely sensitive to various stresses, including air pollution. In particular, the stomata, which uptake carbon dioxide for photosynthesis, close quickly when stressed, resulting in reduced photosynthesis. In order to maintain the photosynthetic function of roadside trees, it is necessary to develop technology that can evaluate the function of the stomata of planted roadside trees in the field. Carbon stable isotope fractionation (Δ13C) of photosynthetic products in leaves has been found to reflect average stomatal openness and has been widely used to determine stress in plants in the natural environment, but there are limited examples of studies applying it to plants in urban areas.

In this presentation, we report the results of a survey conducted from 2007 to 2019 to evaluate the air pollution stress of roadside trees. *Rhododendron* x *pulchrum* (*R. pulchrum*) and *Ginkgo biloba* (*G. biloba*) were selected for the study. The *R. pulchrum* is the most widely used roadside shrub tree species in Japan. Since it is evergreen and often trimmed to within about one meter in height, it is very susceptible to the effects of automobile exhausts. *G. biloba* is the most widely used tree species in Japan as a tall roadside tree. *G. biloba* is a deciduous species, with its height is often trimmed to less than 20 meters in urban areas.

The study was conducted as follows:

(1) Twenty-one locations were selected in Kyoto City where traffic volumes and concentrations of nitrogen oxides in the air were different.

(2) Branches of *R. pulchrum* and *G. biloba* were collected, and the photosynthetic function of the leaves was analyzed in detail in 2016 and 2017.

For the calculation of Δ13C, the stable carbon isotope ratio of carbon dioxide in the atmosphere was used as a correction. For the amount of nitrogen oxides, we used values from a database provided by the National Institute of the Environmental Studies.

©2021. Japan Geoscience Union. All Right Reserved.

4) Using the data of traffic volume and 3), we mapped Δ13C of *R. pulchrum* in Kyoto City.

Photosynthesis data analysis for 2016-2017 revealed that the photosynthetic rate of *R. pulchrum* was lower at study sites with higher concentrations of air pollutants, while the rate of photosynthesis of *G. biloba* was higher at study sites with higher concentrations of air pollutants. The analysis of the annual data from 2007 to 2019 showed that the Δ13C of *R. pulchrum* was decreased with higher atmospheric nitrogen dioxide concentration. This indicates that the higher the nitrogen dioxide concentration in the air, the smaller the stomatal opening of the *R. pulchrum*, indicating that the high nitrogen dioxide concentration imposes a stress to *R. pulchrum*. On the other hand, the Δ13C of *G. biloba* was almost constant regardless of the nitrogen dioxide concentration, indicating that the effect of nitrogen dioxide on the stomatal behavior was small. Mapping of Δ13C for *R. pulchrum* showed that the stomatal opening of *R. pulchrum* was reduced mainly due to the effect of automobile exhaust at the area around Kyoto Station where the traffic volume was particularly high.

Keywords: photosynthesis, stomata, water use efficiency

©2021. Japan Geoscience Union. All Right Reserved.

Effects of Traffic Volume on Photosynthetic Function and Water Use Efficiency of Tall Street Trees in Kyoto City

*Takumi Matsuura[1], Yuko T. Hanba[1]

1. Kyoto Institute of Technology

Introduction

Urban trees play an important role in improving the urban environment by providing shade through their canopy, cooling effects through transpiration, capturing air pollutants, and absorbing carbon dioxide.

However, because street trees are planted in urban areas, they are susceptible to the air pollution caused by exhaust gases. The stress caused by air pollution is known to reduce physiological functions such as photosynthesis, which may prevent street trees from fulfilling their required role.

In this study, we focused on the environmental stress caused by air pollution and investigated the effect of different traffic levels on the photosynthetic function of tall street trees by measuring the photosynthetic function and stable carbon isotope ratios of three street tree species at four sites with different traffic levels in Kyoto City. Since traffic volume and air pollution levels are strongly related, we used traffic volume as an indicator to measure air pollution in Kyoto City.

Materials and methods

1. Tree species

Three species were used: ginkgo (*Ginkgo bioloba* L.), Japanese maple (*Acer buergerianum* Miq.), and Someiyoshino cherry (*Prunus×yedoensis* Matsum.). These are all deciduous tall trees. The top three most commonly planted tall trees in Japan and in Kyoto were selected for the study.

2.Study site

The four study sites were chosen to be near an air monitoring stations that was set up by the Kyoto city government, which constantly measures the concentration of air pollutants. he four study sites were selected to provide as much variability as possible in 12-hour vehicle traffic volumes on adjacent roads.

3.Photosynthesis measurements using the Li-6400 XT

The collected leaves were used to generate an A-Ci curve using a photosynthesis measurement system (Li-6400 XT, Li-Cor, USA). The maximum carboxylation rate (V_{cmax}) and the electron transport rate (J) of the thylakoid membrane were determined from the A-Ci curves.

Since the average CO_2 concentration in the environment where trees are actually planted is about 400 μ mol mol^{-1}, the photosynthetic rate (A) at a CO_2 concentration of 400 μmol mol^{-1} of CO_2 was calculated as A_{400}, and the stomatal conductance (g_s) at 400 μmol mol^{-1} was also determined. The water use efficiency (WUE) was calculated as A_{400}/g_s.

4.Stable carbon isotope ratio measurement of leaves

The dried leaves were powdered and sealed in tin foil at 1.0 ±0.05 mg each. The stable carbon isotope ratios (delta-^{13}C) were measured using a CN-IRMS mass spectrometer at the Research Institute for Humanity and Nature. Working standards CERKU-03 and CERKU-07 (03:Glycine, 07:STARCH-C4) were used for the correction of delta-^{13}C.

©2021. Japan Geoscience Union. All Right Reserved.

Results

The photosynthetic rate of *G. biloba* was lower at high traffic sites and higher at low traffic sites. For *P. yedoensis*, the photosynthetic rate was lower at the site that had second highest traffic volume, compared to the other three sites. For *A. buergerianum*, stomatal conductance decreased with increasing traffic volumes, but the maximum carboxylation rate increased, and as a result, there was no difference in photosynthetic rate between sites. Water use efficiency tended to increase with traffic volume in *P. yedoensis,* but did not correlate with traffic volume in *G. biloba* and *A. buergerianum*.

Discussion

Different air pollution levels had different effects on photosynthetic function in different tree species. High air pollution levels imposed negative impact on the photosynthetic rate for *G. biloba*, and it imposed positive impact on the water use efficiency for *P. yedoensis*. The photosynthetic rate of *P. yedoensis* was higher than that of the other two tree species at all study sites, and it may have a sensitive response to stress because its water use efficiency increased with the increase in traffic volumes. These results suggest that the leaves of *P. yedoensis* effectively absorbed CO_2 as a street tree in the year 2020.

Keywords: Stable carbon isotope ratio, Environmental stress, Photosynthesis

©2021. Japan Geoscience Union. All Right Reserved.

Effect of flooding stress on photosynthesis of aquatic plants

*Yutaro Yasui[1], Yuko T. Hanba[1]

1. Kyoto Institute of Technology

Introduction

How to efficiently take in CO_2 from the air through photosynthesis is an important issue for plants to grow and survive in various environments on earth. However, in the natural environment, there are various environmental stresses such as high light stress, low temperature stress, and water stress, which cause a decline in photosynthetic function. Among the water stresses is the flooding stress caused by floods. Aquatic plants are subjected to significant changes in the degree of flooding, and the area in contact with the air fluctuates, resulting in large fluctuations in the amount of CO_2 they can take up. Therefore, photosynthetic function is also expected to change significantly due to flooding stress. However, although many ecological studies have been conducted on aquatic plants in response to flooding stress, it is not well understood how photosynthetic function is affected. Therefore, the purpose of this study was to investigate how flooding stress affects the photosynthetic function of aquatic plants.

Material & Method

Two types of grasses were used as plant material: rice(*Oryza sativa*), a crop, and reeds(*Phragmites australis*), a wild plant that grows in colonies in lakes and marshes. The height of the grass is about 60 cm for rice and about 150 cm for reeds. Plant seedlings were planted in plastic pots and flooded to fix the water level at 60 cm, and the flooding response of photosynthetic function was investigated at three stages: 5, 10, and 15 days later.

The LI-7000 infrared gas analyzer was used to measure the following three parameters of leaf photosynthetic function: the saturation photosynthetic rate (A_{400}) at a CO_2 concentration of 400 ppm, the stomatal conductance (g_s), which indicates how open the stomata were, and the mesophyll conductance (g_m), which indicates how easily the CO_2 taken up through the stomata passed through the mesophyll cells. The leaf conductance is a measure of carbon stability. Leaf conductance was measured using the carbon stable isotope method. In addition, the number of pores per 1 mm^2 of leaf area (stomatal density) was measured using the secondary replica method.

Results

In both rice and reed species, all three parameters of photosynthetic function were significantly reduced by flooding. In other words, rice and reed showed strong responses to flooding stress, such as reduced photosynthetic rate, stomatal closure, and limited CO_2 diffusion in the mesophyll cells. The rate of decrease was higher in reed than in rice for all parameters. The stomatal density of reed was 661, which was about 16 times higher than that of rice.

Discussion

The reason for the significant decrease in the three parameters of photosynthetic function in plants subjected to flooding stress is that the exposure of the plant to water caused problems in the regulation of stomatal opening and closing, which inhibited CO_2 uptake. In addition, some morphological changes in the leaves may have restricted CO_2 diffusion in the mesophyll cells. The reason why each photosynthetic parameter was significantly reduced in reed than in rice was because the stomatal density was greater than that of rice, and thus the limitation of CO_2 uptake by flooding was greater. These results indicate that

©2021. Japan Geoscience Union. All Right Reserved.

flooding is a strong stress on aquatic plants and that the degree of response of photosynthetic functions varies among plant species.

Keywords: flooding stress, carbon stable isotope method, mesophyll conductance

©2021. Japan Geoscience Union. All Right Reserved.

The incubation method using ^{18}O-water and phosphate oxygen isotope for quantitative evaluation of bioavailable phosphate in soil.

*Takuya Ishida[1]

1. Hiroshima University

Phosphorus (P) is one of the main limiting factor for primary production and has a significant impact on biogeochemical processes and food production in ecosystems. The amount of bioavailable P in soils is about 1% of total phosphorus, and most of it exists in organic form or tightly bound to clay minerals (Pierzynski et al., 2005). Bioavailable P is formed by physicochemical processes such as adsorption/desorption and precipitation/dissolution, and biological processes such as absorption/release and mineralization of organic P by organisms. To understand bioavailable P dynamics, it is necessary to clarify the fluxes to bioavailable P pool through each processe and factors affecting the processes.
Recently, phosphate oxygen isotope ratio ($\delta^{18}O_{PO4}$) has been used as a promising tool to elucidate the P cycling (Paytan and McLaughlin, 2012). Because the P–O bonds in dissolved inorganic phosphate (DIP) do not easily hydrolyze at typical earth's surface temperatures and pressures, DIP movement through physicochemical processes maintain the $\delta^{18}O_{PO4}$ values in a reactant pool. In contrast, biological processes mediated by enzymes that cleave the P–O bonds cause large isotopic fractionation. For example, inorganic pyrophosphatase (PPase) associated with absorption/release and phosphatases associated with organic P mineralization can alter the $\delta^{18}O_{PO4}$ signatures. These isotopic fractionations are controlled by water oxygen isotope ratio and temperature. Equations have been proposed to estimate the fractionation (Paytan and McLaughlin, 2012). These facts indicate it is possible to control the $\delta^{18}O_{PO4}$ value of DIP generated by each process by controlling the water oxygen isotope ratio and temperature. The purpose of this study is to propose a soil incubation experiment using incubation water with two different water oxygen isotope ratios (e.g., +30‰ and -5‰) to quantitatively evaluate the flux of each process to the available P pool. The incubation experiment can simulate a two-isotope system like $\delta^{15}N\text{-}NO_3$ and $\delta^{18}O\text{-}NO_3$, and the fluxes of each process can be quantified by Bayesian mixing model. The poster will present the detailed theoretical background, hypothesis, and preliminary results of the study.

Reference

Paytan, A. and McLaughlin, K. (2012) 'Tracing the Sources and Biogeochemical Cycling of Phosphorus in Aquatic Systems Using Isotopes of Oxygen in Phosphate', in Baskaran, M. (ed.) *Handbook of Environmental Isotope Geochemistry*. Berlin, Heidelberg: Springer Berlin Heidelberg, pp. 419–436. doi: 10.1007/978-3-642-10637-8.
Pierzynski, G. M., McDowell, R. W. and Thomas Sims, J. (2005) 'Chemistry, Cycling, and Potential Movement of Inorganic Phosphorus in Soils', in, pp. 51–86. doi: 10.2134/agronmonogr46.c3.

Keywords: Phosphorus dynamics, Soil incubation, Bayesian mixing model

©2021. Japan Geoscience Union. All Right Reserved.

Trace element quantification in organic materials by low temperature plasma ashing

Taisuke Hino[1], Yuriko Umeda[1], Hibiki Shishime[1], Akane Ito[1], *Masaharu Tanimizu[1]

1. Kwansei Gakuin University

Inorganic chemical analysis of various environmental samples has been applied to clarify the elemental cycle on the earth's surface, and determination of elemental concentrations among biological samples and fossil fuels is sometimes necessary for the purpose. Instrumental analyses by Atomic absorption spectrometry, ICP optical emission spectrometry, and ICP mass spectrometry are frequently used for the determination, and decomposition of samples is usually required prior to the analysis. For the decomposition and removal of organic hydrocarbons, which are the main components of organic samples, pretreatment methods using the high-temperature ashing method and the microwave thermal decomposition method have been conventionally used. In the former method, the loss of volatile elements due to high temperature and contamination from the surrounding environments are concerned. In the latter case, there are potential spectral and non-spectral interferences due to a large amount of dissolved organic components remaining in the solution. In particular, a large amount of organic sample must be pretreated for the isotope analysis of trace inorganic elements, so the limitation of the decomposable sample amount is a fundamental problem in the latter method.
Our group has been working on the establishment of a low-temperature plasma ashing method using oxygen radicals as the pretreatment method to efficiently remove organic hydrocarbons in organic samples. Organic hydrocarbons are gradually oxidized in oxygen plasma generated by glow discharge under reduced pressure, and finally removing them into the gas phase. In this report, elemental recovery yields in the low-temperature ashing treatment were evaluated using a commercially available organometallic standard solution. As a result, the yield changed depending on factors such as volatility of element oxides, formation of insoluble compounds during ashing, and solubility of residual ash in various inorganic acids. This method was applied to crude oil, seaweed, and brown rice, and their elemental yields were evaluated.

Keywords: plasma ashing, isotopic analysis, organic material

©2021. Japan Geoscience Union. All Right Reserved.

Metal element isotope analysis for Environmental Reference Materials

*Ki-Cheol Shin[1]

1. Research Institute for Humanity and Nature

In recent years, the development of analytical technics has made it possible to detect a limited variation of stable isotope ratios in metal elements. After that, many researchers had challenged and produced excellent results in this field, but the supply of primary reference materials for isotope measurement is limited.

To promote a stable isotope study related to the environmental research fields, RIHN has carried out high-precision isotope analysis using MC-ICP-MS for relatively abundant secondary environmental reference materials (ERMs).

For this research, I purchased 30 types of ERMs from NIST (National Institute of standard and technology, U.S.), JRC (European Commission's Joint Research Centre), and NMIJ(National Metrology Institute of Japan). These materials are not for isotopic analysis but certification of metal element concentration.

This presentation reports a data set of Mg-Zn-Fe stable isotope values and Sr-Pb-Nd radiogenic isotope ratios. This data set is a final version of earlier reports related to the isotopic analysis of environmental reference materials.

Keywords: Reference materials, metal element, isotope analysis

©2021. Japan Geoscience Union. All Right Reserved.

[J] Poster | H (Human Geosciences)：H-TT Technology & Techniques

Thu. Jun 3, 2021 5:15 PM - 6:30 PM JST | Thu. Jun 3, 2021 8:15 AM - 9:30 AM UTC | Ch.08_3

[H-TT17] New Developments in Shallow Geophysics

convener:Kyosuke Onishi(Public Works Research Institute), Kunio Aoike(Oyo corporation), Tishiyuki Yokota(National Institute of Advanced Industrial Science and Technology), Toru Takahashi(Fukada Geological Institute)

The session of shallow geophysics calls various research topics to contribute on geophysical exploration techniques for the near surface. The shallow geophysics uses many types of methods to survey various targets. This session does not restrict any survey methods and targets of your research but restrict the target depth in the zones from 5 cm to 30 m (or from 2 in to 100 ft) below the surface of the ground. The shallow part under the ground may be the closest and unknown territory for human society, and advanced societies cannot have controlled it yet to avoid disasters caused by dynamics in the near surface. Peoples require techniques to manage levee, landslide and earth constructions and knowledge to control groundwater, liquefaction and soil pollution. The near surface faces many geotechnical, environmental and hydrogeologic problems. Major survey techniques are surface wave method, electric exploration, ground-penetrating radar and microtremor survey, but any methods can be discussed if your target is located in the shallow depths. This session also welcomes to discuss laboratory tests and rock physics for unconsolidated porous media in the vadose zone. Additionally, we will welcome not only cutting-edge technologies but also usual works, if the knowledge and skills is useful for human living. 3D will be one of main subjects in this year.

[HTT17-P01] **An Atempt to Estimate the Water Level Change of Non-confined Groundwater by Earthing Resistance (III) - Characteristics of the Anniversary Changes -**

*Kunihiro Ryoki[1] (1.Polytechnic University)

[HTT17-P02] Estimation of underground structure beneath the debris control dams constructed during the Edo era based on the microtremor measurements

*Atsushi Mukai[1] (1.Faculty of Urban Management, Fukuyama City University)

[HTT17-P03] Measuring the distribution of surface thickness of pavement using ground-penetrating radar

*Kyosuke Onishi[1], Kobayashi Takayuki[1] (1.Public Works Research Institute)

An Atempt to Estimate the Water Level Change of Non-confined Groundwater by Earthing Resistance (III) - Characteristics of the Anniversary Changes -

*Kunihiro Ryoki[1]

1. Polytechnic University

1. Introduction

In order to investigate the relationship between the water level of unconfined groundwater and the earthing resistance of the grounding electrode attached to electrical equipment, measurements of both have been conducted since April 2019. As a result, the relationship was confirmed on both. In addition to the variation of the groundwater level, it is considered that the variation of the ground resistance may be affected by the annual change of the distribution of the ground temperature (Ryoki, 2020). The results, which are measured up to now, are reported and the future measurement plan is described In this paper.

2. Measurement

The earthing resistance is expected to change considering the relationship between the thickness of the first layer and the equivalent earthing resistance in a horizontal two-layer structure (Ryoki, 2019b). Therefore, in order to investigate the relationship between the water level of unconfined groundwater and the earthding resistance, an observation well, WPTU, was installed in the area where the Kanto loam layer is widely distributed. The Specifications of WPTU and measuring instruments are shown in Table 1. At the same time, groundwater temperature and electrical conductivity are measured at 10-minute intervals in WPTU. In the vicinity of the observation wells, the earthing resistance of the grounding electrodes for the safety of electrical equipment was measured repeatedly.

3. Result

Fig. 1 shows groundwater level, water temperature, and electrical conductivity in WPTU from April 23, 2019 to January 25, 2021. It shows that the conductivity increases when the water level rises rapidly. And decreases when the water level decreases relatively slowly, except for the unstable period immediately after the excavation of the observation pit.

Fig. 2 shows the earthing resistance which connected to Class A earthing electrode under a concrete building near the WPTU. It shows the water level observed at the same time, and the air temperature directly above the WPTU, too.

Fig. 2 shows that as the water level rises, the earthing resistance decreases, and as the water level decreases, the ground resistance increases. The relationship with the water level and the earthing resistance is harmonious. On the other hand, when the annual change in the 10-day moving average curve of temperature is compared with the change in water level, the relationship is harmonious, but the phases are not coincident. In general, when the temperature rises, the ground resistance decreases, and when the temperature decreases, the ground resistance increases. The phase lag of the earthing resistance to the air temperature is about two months if we focus on these extreme values.

In areas where marine clay strata are outcropping, it has been reported that when spontaneous potential is formed by the sulphide minerals in marine clay strata, the annual change in spontaneous potential lags behind the temperature (Ryoki, 1990). In response to this, Ryoki (2020) suggested that since the ground resistance is also affected by the underground temperature, the annual variation of the earthing resistance would show a lagging phenomenon with respect to the surface temperature. The measurement

©2021. Japan Geoscience Union. All Right Reserved.

results shown in Fig. 2 are in harmony with this suggestion.

References

Ryoki, K. (1990): Annual Variation of Spontaneous Potential -Toward a Teaching Material for Familiar Geophysical Phenomena-, *Sci. Edu. in Osaka*, **4**, 25-32.
Ryoki, K. (2019a): An Attempt to Estimate the Level of Non-confind Groundwater by Earthing Resistance (I) -Outline of Theory-, *Proc. Jap. Geosci. U. 2019*, HTT22-03.
Ryoki, K. (2019b): A Theory of Water Level Estimation to Focus on the Change of Earthing Resistance for the Prediction of Flood Occurrence, *Jour. of Polytech. Sci.*, **35**, 30-35.
Ryoki, K. (2020): A Study on the Relationship between Earthing Resistance and Groundwater Level, *Pro. of Kansai Geo-Sym.*, **8**, 18-21.

Keywords: electrical equipment, Musashino district, loam layer, perchied water, flood damage, equivalent earthing resistance

©2021. Japan Geoscience Union. All Right Reserved.

表 1　観測井および測定機器の諸元

Table1 Shows the specifications of observation wells and measuring equipment

観測井	位置	35° 44' 19.2" N 139° 29' 41" E
	孔口標高	81.92m
	孔長	30.17m
	内径	50.0mm
水位計	応用地質社製	S&DL miniEC 10m計
接地抵抗計	横河製作所製	3235型

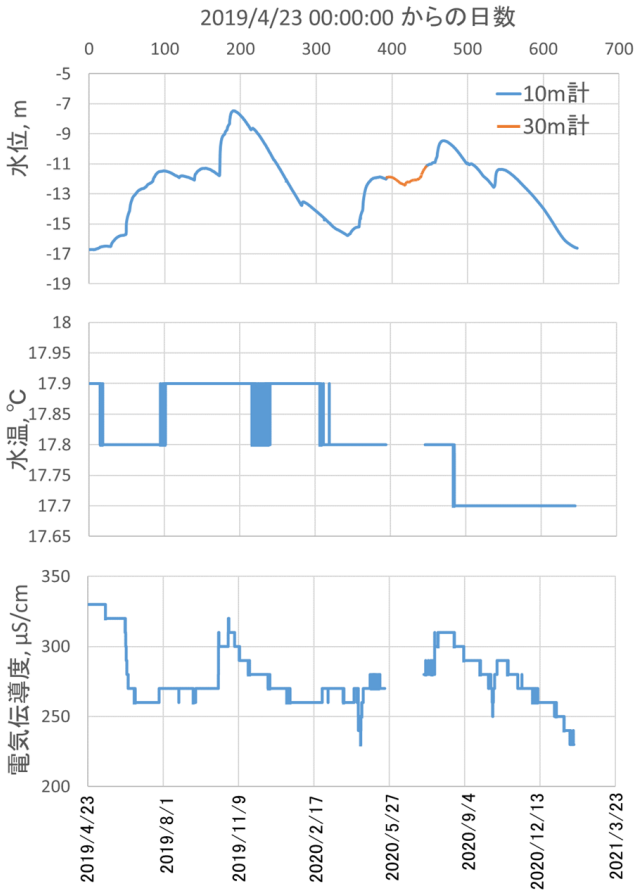


図1　観測井WPTUでの地下水の水位，水温及び電気伝導度の変化

Fig.1Observations of groundwater level, water temperature and al conductivity at WPTU.

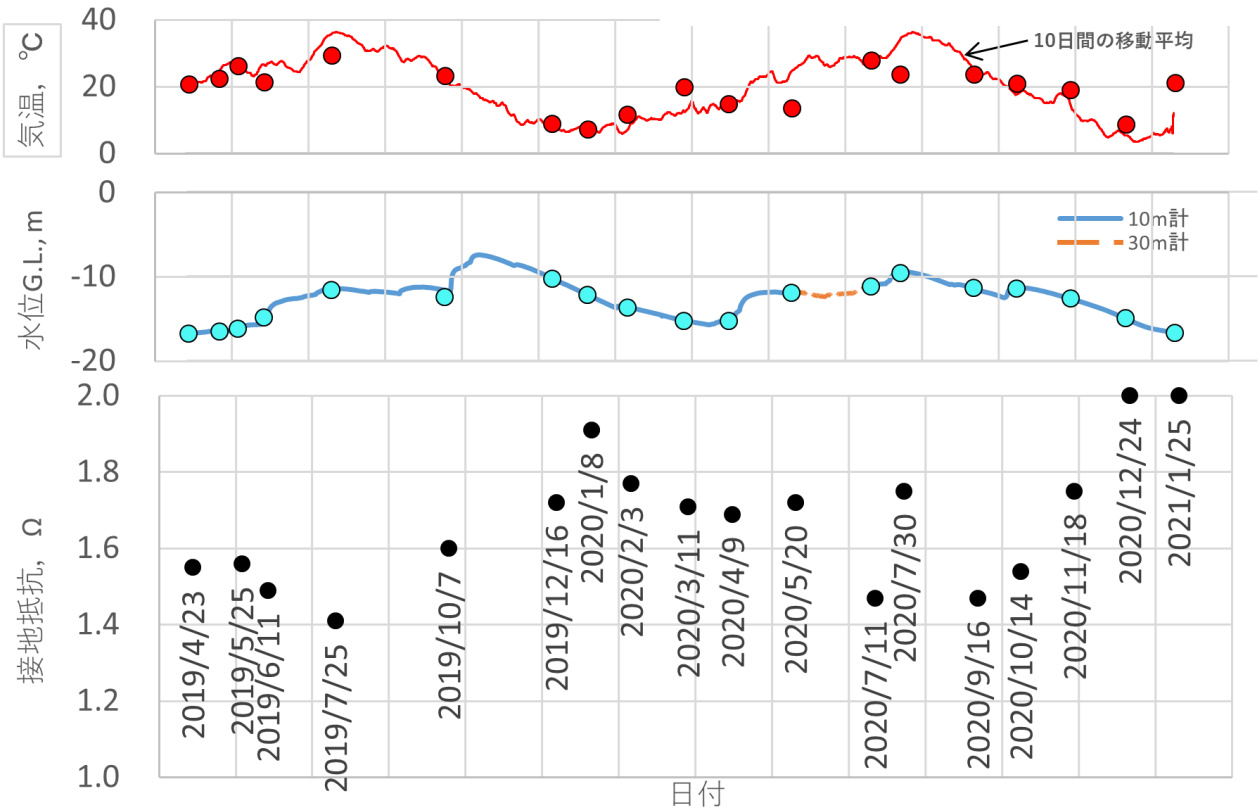


図 2　観測井WPTUでの地下水位と近傍における気温及び接地抵抗の変化

Fig. 2 Variation in groundwater level, temperature on the surface of the earth and earthing resistance, at the observation well WPTU

©2021. Japan Geoscience Union. All Right Reserved.

Estimation of underground structure beneath the debris control dams constructed during the Edo era based on the microtremor measurements

*Atsushi Mukai[1]

1. Faculty of Urban Management, Fukuyama City University

In Fukuyama city, Hiroshima, many debris control dams "Sunadome" had been constructed during the Edo era and have been left. The largest one in such dams is “Dodo-gawa Rokuban Sunadome”. I performed the microtremor measurements at Dodo park constructed on the sedimentation of Sunadome, and estimated the underground structure beneath the park by using the H/V spectral ratio. The soft surface layer was estimated to be thicker around the Dodo river flowing in the middle of the park and be thinner nearby the mountain slope. In this study, I estimated the underground structures in other debris control dams along the river by using the microtremor measurements in order to reproduce the topography before the constructions of Sunadome.

Major geology in Hiroshima prefecture is granite, which can be easily turned to the decomposed granite soil due to weathering. Therefore, the surface layer in this area tends to collapse into landslide disaster. Fukuyama city has suffered the serious landslide disasters repeatedly. In May, 1673, the large-scale debris flow occurred along the Dodo river due to the local heavy rainfall and swept away the Kokubunji, houses and farms. That was the reason that the Fukuyama domain started the construction of Sunadome and had installed many debris control dams in this city. “Dodo-gawa Rokuban Sunadome” with dam height of 8.8m started to be constructed in 18th century.

I have performed the microtremor measurements at Dodo park since 2017. This park is about 70m x 250m in size along the Dodo river. I recorded 5 minute microtremors measured by the three-component seismometer at 70 sites which were set up at intervals of about 15m. I applied FFT to the measurements to obtain the H/V spectral ratios, and estimated the dominant frequency at each site.

Two dominant frequencies could be found at every sites in this park. One is a low frequency 0.1-1 Hz, and the other is a high frequency of 1-10 Hz. The H/V spectral ratio is larger at the latter one and can be definitely extracted from the noise. I assumed two lateral layer as the underground structure and estimated P wave velocity and thickness of the surface layer by using the higher dominant frequency and its H/V spectral ratio. The other parameters such as density and S-wave velocity were assumed to be constant.
As a result of the estimation of underground structure, the surface layer was found to be thicker around the Dodo River flowing through the middle of the park, and be thinner near the mountain slopes on both sides of the river. In addition, I could see the surface layer tended to be thinner from the downstream to the upstream of the river. It might be indicated that the subsurface structure estimated in this study shows the topography of the valley before the construction of Sunadome. These results suggest that we can estimate a complicated underground structure in the lateral scale of 10m, even if a simple horizontally stratified structure is assumed for estimation of the underground structure. In this study, we have performed the microtremor measurements at other Sunadome along the river and tried to reproduce the past topography of the valley before the construction of Sunadome.

©2021. Japan Geoscience Union. All Right Reserved.

Keywords: microtremor measurement, debris control dam

©2021. Japan Geoscience Union. All Right Reserved.

Measuring the distribution of surface thickness of pavement using ground-penetrating radar

*Kyosuke Onishi[1], Kobayashi Takayuki[1]

1. Public Works Research Institute

Information of the structure of pavement is sometimes required to manage conditions of paved roads. In this report, we introduce to measure the thickness distribution of the surface layer constructing pavement with the accuracy about a centimeter using ground-penetrating radar. Structure Scan of the GSSI and Mini Pod of the Earth Radar were mainly used in this measuring test. The central frequencies are about 2.7 GHz and 800 MHz, respectively. The Structure Scan is developed to detect reinforcing steels in concrete structures and can survey the undulation of interfaces in pavements with high accuracy for its high vertical resolution. Meanwhile, the Mini Pod, which is a multi-channel radar system with 12 antennas, can measure wide area in short time.

The test data were acquired on a test pavement in our research institute. The propagation velocity of electromagnetic wave was decided to fit depths verified by collected cores for improving the accuracy of depths measured from reflection responses in a shallow zone. A series of processing including zero offset processing was applied to records based on the value of propagation velocity. The velocity of asphalt concrete mixture is decided to 0.135 m/ns. Acquired velocity distribution fits to the thickness of surface layer of the pavement. The reference thickness is estimated from measuring cores which was not used for deciding propagation velocity.

The asphalt concrete mixture has two layers of the surface and the basic layer. The depth distribution of interfaces between the surface and the basic layer was measured in the radar records. The upper surface of subgrade which is constructed with heavy machineries has a certain level of roughness. On the other hand, the upper surface of basic layer in the asphalt concrete mixture has fine flatness. Therefore, the thickness of the basic layer has large variations in locations. When the ground-penetrating radar can easily measure the distribution of thickness of the basic layer, it provides important information to analyze durability and health of pavement.

Keywords: ground-penetrating radar, pavement, asphalt concrete mixture

©2021. Japan Geoscience Union. All Right Reserved.

[J] Poster | H (Human Geosciences)：H-CG Complex & General

Thu. Jun 3, 2021 5:15 PM - 6:30 PM JST | Thu. Jun 3, 2021 8:15 AM - 9:30 AM UTC | Ch.09_3

[H-CG28] Earth surface processes related to deposition, erosion and sediment transport

convener:Koji Seike(Geological Survey of Japan, AIST), Masayuki Ikeda(University of Tokyo), Hajime Naruse(Department of Geology and Mineralogy, Graduate School of Science, Kyoto University), Hideko Takayanagi(Institute of Geology and Paleontology, Graduate School of Science, Tohoku University)

To understand landscape evolution and dynamics of erosion, transport and sedimentation of earth-surface materials, the latest results of multiple research fields including engineering and earth sciences will be presented. As well as any researches of sedimentology and sedimentary petrology, interaction between fluid, sediments and geomorphology is focused. Interdisciplinary discussions of science, disaster prevention and resource exploration will be expected.

[HCG28-P01] Preliminary study on the relationships between landform of coastal to alluvial plain and sediments supply from watershed

*Taku Komatsubara[1] (1.Institute of Geology and Geoinformation, Advanced Industrial Science and Technology)

[HCG28-P02] Relationship between magnetic anisotropy and hydraulic conditions in modern flood deposits

*Ryo Tateishi[1], Ichiro Kimura[1], Naoto Ishikawa[1] (1.University of Toyama)

[HCG28-P03] Flume experiment on crevasse-splay deposits formed by the 2019 flooding of the Chikuma River

*Taichi Kato[1], Masaki Yamada[1], Hajime Naruse[2], Sakai Yuichi[2] (1.Department of Geology, Faculty of Science, Shinshu University, 2.Graduate school of Science, Kyoto University)

[HCG28-P04] Sedimentary environments and fluctuations in lake levels as recorded in the latest Pleistocene and Holocene core from the Suwa Basin, central Japan

*Nozomi Hatano[1], Ritsuho Kawano[2], Kohki Yoshida[2] (1.Natural Environment Division, Nagano Environmental Conservation Research Institute, 2.Department of Geology, Faculty of Science, Shinshu University)

[HCG28-P05] Microcodization in a Kasimovian section of the Omi Limestone (Niigata Prefecture, central Japan), the Upper Carboniferous

*Yoshihiro Kakizaki[1], Yasuhiro Ota[2], Kenji Kashiwagi[3], Akihiro Kano[1] (1.Department of Earth and Planetary Science, Graduate School of Science, The University of Tokyo, 2.Kitakyushu Museum of Natural History & Human History, 3. Graduate School of Science and Engineering for Research, University of Toyama)

[HCG28-P06] Coastal transport process of pebble along the Seisho Coast, Kanagawa Prefecture, estimated from changes in lithological composition and form of pebble particles

*Masaaki Shirai[1], Tomomi Akiyama[1], Kiyokazu Kawajiri[2], Takako UTSUGAWA[3], Takayuki Takahashi[4] (1.Tokyo Metropolitan University, 2.Sagamihara Cuty Museum, 3.Rissho University, 4.Tohoku University)

[HCG28-P07] A consideration of the age of the higher terraces in the southeastern part of the Kashiwazaki plain, Niigata Prefecture, central Japan.

*Satoshi Kaneko[1], Toshimichi Kaneto[1], Akiko Miyawaki[2], Akira Fukuchi[2], Mitsugu Momose[2] (1.Tokyo Electric Power Company Holdings, Inc., 2.Hanshin Consultants Co., Ltd.)

[HCG28-P08] Linear stability analysis of plane beds with active suspended load

Koji Ohata[1], *Hajime Naruse[1], Norihiro Izumi[2] (1.Department of Geology and Mineralogy, Graduate School of Science, Kyoto University, 2.Graduate School of Engineering)

Preliminary study on the relationships between landform of coastal to alluvial plain and sediments supply from watershed

*Taku Komatsubara[1]

1. Institute of Geology and Geoinformation, Advanced Industrial Science and Technology

1. Introduction
Sedimentation data in water reservoirs became to be accumulated and annually published (e.g. Water Management and Land Conservation Bureau, MLIT, 2012), we are able to concretely discuss on the relationships between sediment production in upper course of watershed and sedimentation in the lower course of it. The presenter tried to make roughly clear some relationships among volume of the Holocene alluvium deposits, estimated duration of its sedimentation (temporary fill-up duration: estimated from sediment supply and volume of the Holocene alluvium) and geomorphological features especially river-channel landform, taking the case of seven coastal to alluvial plain which have different rate of sediment supply and geomorphological shape of sedimentary basin of the Holocene deposits.
2. Subject
ATST have continued a research project named “Investigation on Geology and Active Faults in the Coastal Zone of Japan” since 2007, its purpose is to make clear continuity of sedimentary bodies and geological structures. Subjects of this study are 7 areas (Table 1) of this AIST project except for Noto area (which do not accompany with alluvial plain).
3. Data
The author used deposition rates measured in water reservoir after Hasegawa et al. (2005) as basic data and Water Management and Land Conservation Bureau MLIT (2012) as supplementary data for estimating denudation rates in the upper course of the watershed (D), and roughly estimated sediment supply rates (S) by multiplying the area of watershed except for depositional area (Aw) and denudation rate (D). Volume of the Holocene alluvium and coastal deposits (Aa) is roughly estimated by multiplying mean thickness of the Holocene deposits (Ta) and total area of the Holocene alluvial and coastal plain (Aa). However, denudation rate (D) is short periods’ one (during only several ten years) when artificial action has done, so it may be larger than natural and long-term rate. And volume of the Holocene deposits (Aa) includes large errors (The author did not use GIS calculation).
4. Results
Va, S, temporary fill-up duration (F = Va / S), distance between recent river mouth and outer edge of the continental shelf (breadth of continental shelf), and so on in each district are shown in Table 1. This table indicates as follows. 1) The meandering channel and branching channel zones do not develop and only braided channel zone is dominant in the Sagami and Shizuoka Plains which F is less than several thousand years and less than several kilo-meters in breadth of continental shelf. 2) The braided, meandering and branching channel zones develop in the Niigata, Nobi and Tokusima Plains where F is several thousand years, breadth of continental shelf is several tens kilo meters. 3) The braided and meandering channel zone do not develop in the Yufutsu and Fukuoka Plains where F is larger than ten thousand years.
5. Discussion
F values of the Sagami and Shizuoka Plains are significantly shorter than actual duration of the Holocene deposits (several thousand to ten thousand years) and both plains directly face to deep sea. Much of sediments supplied to these plains should removed to deep sea bottom in short period. The other hand, F values of the Yufutsu and Fukuoka Plains are longer than ten thousand years, and these plains’ deposits include large amount of organic materials and they accompanies beach ridges. This investigation is no

©2021. Japan Geoscience Union. All Right Reserved.

doubtfully loose one, however the author think it also have some values for discussion on sediment linkage from mountain, plain and sea.

Refference
Hasegawa, K., Wakamastu, K. and Matsuoka, M. (2005) Mapping of potential erosion-rate evaluated from reserboir sedimentation in Japan. Jouranal of Japan Society of Natural Disaster Science, 24, 287-301.
Water Management and Land Conservation Bureau, MLIT (2012) Situation of the reservoir sedimentation in whole Japan (at end of the 2008 fiscal year)
(http://suigenren.jp/wp-content/uploads/2012/09/H20zenkokutaisade-ta.pdf)

Keywords: Geomorphology, Denudation, Sedimentation, Watershd, On-going earth processes

地域	主要河川名・山地流域面積 Aw(㎢)	山地流域の削剥速度 D（㎜/年）	土砂流入速度 S（㎢/年） S=Aw×D	沖積平野の面積 Aa（㎢）	沖積層の平均厚さ Ta（m）	沖積層の体積 Va（㎢） Va=Aa×Ta	計算上満砂時間 F（年） F=Va／S	河道形態・平野地形*	盆地形態・海底地形**	陸棚幅*** （km）
勇払平野	安平川 400	±0.1	±4×10-5	80	±10	±0.8	±2×104	A+S	外洋・陸棚	21
新潟平野（新潟市以南）	*信濃川* 10000	±0.5	±5×10-3	800	±40	±30	±6×103	B+M+A+S	内湾・陸棚	33
相模平野	相模川 1500	±2	±3×10-3	80	±30	±2	±7×102	B+(M)+(S)	狭い入り江・深海	2
静岡平野	安倍川 500	±2	±1×10-3	40	±20	±0.8	±8×102	B	狭い入り江・深海	4
濃尾平野	木曽三川 8000	±1	±8×10-3	1100	±30	±30	±4×103	B+M+D	内湾	85
徳島平野	吉野川 3000	±0.5	±2×10-3	200	±20	±4	±2×103	B+M+D	内湾・陸棚	48
福岡平野	那珂川など 300	±0.1	±3×10-5	60	±5	±0.3	±1×104	D+(S)	多島海・内湾	210

斜字：中流に構造盆地をもつ河川

＊：河道形態・平野地形　B：網状河川(扇状地)　M：蛇行河川(蛇行原)　D：分岐河道(三角州)　A：アナストモージング河道(湿地帯)　S：浜堤列

＊＊：沖積層の受け皿の形態を特徴的に示す地形

＊＊＊：現河口から最も近い陸棚外縁までの距離

©2021. Japan Geoscience Union. All Right Reserved.

Relationship between magnetic anisotropy and hydraulic conditions in modern flood deposits

*Ryo Tateishi[1], Ichiro Kimura[1], Naoto Ishikawa[1]

1. University of Toyama

Introduction: The magnetic susceptibility measurement is widely used in paleocurrent reconstruction because of its high efficiency, but the relationship between the magnetic anisotropy and hydraulic conditions has not been well studied. In this paper, we discuss the relationship between magnetic anisoropy and paleocurrent / hydraulic conditions, based on the comparison of these analysis; observation of the modern flood sediments, the magnetic susceptibility measurement of each unit, and the particle orientation analyze using X-ray CT images.

Subject / Method: The location of the outcrop was at the east end of Toyama O-hashi on the right bank of the Jinzu River, Toyama Prefecture. The outcrop of mound-like deposits found here is 1.6 m high and 6.3 m wide, and distributed along a slope that dips 15˚ west toward the river channel. A 7cc plastic cube was used to collect samples in a fixed position, and magnetic susceptibility measurements, X-ray CT imaging, and particle analysis were performed to compare the results. ImageJ and R were used to analyze the particle orientation.

Results of field observation: The beds can be divided into three main units. The lowest unit, Unit A, consists of a 20cm thick, alternating layer of well-sorted very fine sand and fine sand, including plant fragments. The sand layer forms a foreset lamination along the slope. The upper unit, Unit B, consists of 22cm thick, well-sorted fine sand that eroding the Unit A. The sand layer has planar-cross lamination that is parallel to the channel associated with current ripple movement. The uppermost unit, Unit C, consists of 18cm thick, well-sorted fine sand with foreset lamination along the slope as in Unit A. Unit C contains no plant fragments.
Results of X-ray CT image analysis: The maximum axis of unit A is mainly towerd to the left bank or upstream direction with low angle (about 15˚), showing a radial distribution with large dispersion. The maximum axis of unit B is dominated by the upstream to downstream direction with low angle (about 15˚), and the dispersion is the largest. The maximum axis of unit C is towerd to the left bank with low angle (about 15˚), and the dispersion is the narrowest.
Results of magnetic susceptibility measurement: The shape of the anisotropy was all closer to oblate. The direction of the minimum axis of the anisotropy showed good concentration in each unit. In Unit A, the minimum axis is almost vertical, and the maximum axis has little variation and points to a very low angle (less than 10˚) on the left or right bank. In Unit B, the minimum axis is inclined by 30˚to 44˚ in the direction between the upstream and the left bank, and the maximum axis is highly variable and refers to the lower angle (less than 26˚) than the left bank. In Unit C, the minimum axis is almost vertical, the maximum axis is highly variable, and refers to the upstream, downstream right bank, and the very low angle (less than 8˚) of the right bank.

Discussion: Since the components of the particles do not change significantly with each unit and are not intercalated by temporal gaps such as mud drapes or organic thickening layers, this formation is considered to have been deposited in a single flood. The direction of deposition is basically lateral accretion along the slope. Considering the sedimentary structure and the upward coarsening of the units, the hydraulic conditions can be regarded as a lower flow regime for Units A / B and an upper flow regime

©2021. Japan Geoscience Union. All Right Reserved.

for Unit C. X-ray CT image analysis of the particle orientation is consistent with this interpretation. When Unit A was deposited, the maximum axis was oriented toward the left bank due to down-slope gravity, and when Unit B was deposited, the downstream flow at the water level lowering was dominant, and the maximum axis was oriented in the upstream-downstream direction. When Unit C was deposited, the down-slope flow was more dominant than the downstream flow, and the maximum axis was concentrated in the left bank direction. The results of the magnetic susceptibility measurement indicate that it is difficult to completely reconstruct the paleocurrent direction and particle orientation from magnetic anisotropy alone, and that at least a detailed description and analysis of the facies is necessary. On the other hand, the increase in the dispersion of the maximum axis from unit A to unit C may reflect the increase in the traction force from the lower flow regime to the upper flow regime, suggesting that the magnetic anisotropy and hydraulic conditions correspond to some extent.

Acknowledgemnt: This work was supported by JSPS KAKENHI Grant Number 20K21055.

Keywords: magnetic anisotropy, modern deposits, X-ray CT analysis

©2021. Japan Geoscience Union. All Right Reserved.

Flume experiment on crevasse-splay deposits formed by the 2019 flooding of the Chikuma River

*Taichi Kato[1], Masaki Yamada[1], Hajime Naruse[2], Sakai Yuichi[2]

1. Department of Geology, Faculty of Science, Shinshu University, 2. Graduate school of Science, Kyoto University

On October 13, 2019, flooding of the Chikuma River was caused by heavy rain in central Japan. The 30 m wide levee revetment of the left bank of the river was breached over a length of 70 m in Hoyasu, Nagano City. As a result, gravelly and sandy piles were formed at upstream and downstream sides of the crevasse channel perpendicular to the river. This study aims to obtain a better understanding of the processes involved in transport and deposition during the flooding by flume experiments to reproduce the distribution and sedimentary characteristics of the surveyed crevasse-splay deposits.

In the flume experiments, we first mixed two types of sand grains with water, and flow it into the acrylic experimental flume which was a simplified scale model of the Chikuma River (about 2 m long and 8 cm wide). We used green-colored sand (150–250 μm in diameter) and red-colored sand (40–100 μm in diameter) as analogs of gravels and sand grains in field scale respectively. The flow depth in the main channel was controlled by narrowing the flume width at the downstream end with the board. After the flow reached the steady condition, we removed 2 cm high boards piled to compose the sluice gate (35 cm) at the middle part of the water way, causing levee breach on the floodplain (100×150 cm) adjacent to the water way. We conducted ten runs of the experiment with different conditions. Sediment sampling and analysis were conducted on Run 10 because of its highest reproducibility of the actual levee breach.

On Run 10, we first removed the top of four small boards to cause overspilling of the flow at the time of 59 s after the start of experiment. At the time of 28 s after overspilling, we removed two boards to cause the successive levee breaching while the last board was left until the time of 132 s after levee breach. Based on the video observation, a crevasse channel was formed the side sluice gate with deposition of piles composed of red sands on both sides of the channel during overflow stage. The direction of the crevasse channel was inclined downstream by 24° measured from the direction perpendicular to the main channel. Immediately after levee breach, the flooding flow swept away the sediment initially deposited on the bottom, and a pile of sediment was deposited instantly in the upstream region of the crevasse channel. As a result, the channel shifted its direction toward downstream (32° at 30 s after levee breach) because the sediment pile interrupted the flow. At the time of 90 s after the onset of levee breach, the depositional area in the upstream region of the channel expanded, and the channel consequently shifted to downstream direction furthermore (38°).

The measurement of the flooding flow indicated that the flow velocity immediately after levee breach was the highest during the experimental period. The flow in the overbank area was about 41 cm/s before levee breach and was about 83 cm/s at the timing when levee breach occurred. Then, it became about 53 cm/s at 60 s after levee breach. The pile deposited in the upstream side of the crevasse channel was formed from the bedload of the flooding flow in the initial stage of levee breach, and thus it presumably exhibited high bed shear stress. Subsequently, the pile was isolated at the upstream side by the shift of the crevasse channel to downstream region with waning of the flow velocity.
The feature of the coarse-grained pile in the upstream side of the crevasse channel quite resemble that of the gravel pile formed in the 2019 Chikuma River flooding. Thus, it can be interpreted that the crevasse splay deposits at the study site were formed in the similar process in which the shift of crevasse channel

©2021. Japan Geoscience Union. All Right Reserved.

occurred with waning the flow. Further experimental and field surveys are needed to reveal whether the feature of the coarse-grained sediment pile examined in this study is a general characteristics of the crevasse splay deposits or it can be only formed at a specific hydraulic condition.

©2021. Japan Geoscience Union. All Right Reserved.

Sedimentary environments and fluctuations in lake levels as recorded in the latest Pleistocene and Holocene core from the Suwa Basin, central Japan

*Nozomi Hatano[1], Ritsuho Kawano[2], Kohki Yoshida[2]

1. Natural Environment Division, Nagano Environmental Conservation Research Institute, 2. Department of Geology, Faculty of Science, Shinshu University

Introduction: The Suwa Basin is an inland basin located at a high altitude in central Japan. The sedimentation processes and sediment production in such a basin are regulated by a balance between the paleoclimate and tectonics (e.g., Shanley and McCabe, 1994; Miall, 1996). Furthermore, this basin, which has long daylight hours, can be expected to have archived paleoclimatic conditions. In this study, the sedimentary facies analysis, paleosol description, major elemental analysis, and CN elemental analysis were conducted for the late Pleistocene and Holocene boring core obtained at a site on the southern coast of Lake Suwa, to clarify the sedimentary processes occurring there and fluctuations in the lake water level.

Sedimentary facies and paleosols: The succession in the core can be divided into three sedimentological units based on the sedimentary facies, paleosols, TOC, TN, and C/N ratios. In ascending order, they are as follows: meandering fluvial, lacustrine, and delta units. The meandering fluvial unit is composed of inversely graded sand beds (crevasse splay deposits), alternating beds between sand and carbonaceous mud (fluvial and back-swamp deposits), and normally graded gravel–sand beds (channel deposits). The C/N ratios of this unit are relatively higher (10.25 on average) than those of the other units. Some paleosols are developed in this unit. These paleosols can be recognized by fine rootlet fossils, fecal pellets, illuviated clay, and brownish-reddish soil colors. Some of these paleosols underwent groundwater and surface-water gleizations. The lacustrine unit is composed of carbonaceous mud beds (pond deposits) and silt-clay beds (lake deposits) and has a low C/N ratios (8.19 on average). In this unit, some paleosols can be recognized by fine rootlet fossils and illuviated clay. The paleosol and lacustrine mud bed which has a high content of SiO_2 crowded with diatoms alternated between the depths of 14.5 and 18.0 m. The delta unit is dominated by gravel–sand and exhibits upward-coarsening successions.

Discussion: The accumulation curve constructed based on the calendar dates calculated from the ^{14}C ages provides the period of environmental changes in the Suwa Basin. Meandering fluvial depositions were laid from the last glacial maximum to ca. 15,000 cal years BP. The lacustrine (pond and marsh) environment expanded onto the study site from ca. 15,000 cal years BP. The primary productivity in the lake is considered to have been higher during the period ca. 12,000–6,000 cal years BP, based on the lower and static C/N ratios and higher TN. Delta progradation occurred at ca. 4,000–3,000 cal years BP. The repetition of paleosols and diatom-rich mud beds in the lacustrine unit suggests short-term fluctuations in the lake-level during the period between 12,000–7,000 cal years BP. The lake-level underwent declines in the period ca. 12,000–11,000 cal years BP and ca. 9,000–8,200 cal years BP. The high lake-level developing during the period ca. 7,000–4,000 cal years BP coincides with the middle Holocene climatic optimum (e.g., Wanner et al., 2008). These fluctuations of the sedimentary environments and the lake-level could have been caused by climate change and/or basement subsidence.

©2021. Japan Geoscience Union. All Right Reserved.

This study was carried out under an ordinary research project (Research on the medium to long term management and maintenance of lakes, ponds, and their catchment areas in Nagano Prefecture) at the Nagano Environmental Conservation Research Institute.

References: Miall, A.D., 1996. Springer-Verlag, Berlin Heidelberg, p. 598. Shanley, K.W., McCabe, P.J., 1994. Am. Assoc. Petrol. Geol. Bull. 78, 544–568. Wanner, H. et al., 2008. Quat. Sci. Rev., 27, 1791–1828.

Keywords: late Pleistocene to Holocene, sedimentary facies, paleosol, lake-level, lacustrine deposits, Lake Suwa

©2021. Japan Geoscience Union. All Right Reserved.

Microcodization in a Kasimovian section of the Omi Limestone (Niigata Prefecture, central Japan), the Upper Carboniferous

*Yoshihiro Kakizaki[1], Yasuhiro Ota[2], Kenji Kashiwagi[3], Akihiro Kano[1]

1. Department of Earth and Planetary Science, Graduate School of Science, The University of Tokyo, 2. Kitakyushu Museum of Natural History & Human History, 3. Graduate School of Science and Engineering for Research, University of Toyama

INTRODUCTION

Microcodium is structure consisting of carbonate minerals, which are biologically induced via decomposition of organic matter (plant roots, fungi, corroded organic matter) by microorganisms in Ca-rich soil (Kabanov et al., 2008). Therefore, occurrence of *microcodium* from marine limestone is a powerful indicator of subaerial exposure.

Here, we report the occurrence of *microcodium* from the Gongen section of the Omi Limestone, a Caeboniferous–Permian seamount-type limestone in Niigata Prefecture, central Japan. In Japan, *microcodium* had been known as "*blackish brown sparry calcite*" (Machiyama, 1994). Hasegawa and Goto (1990) reported *blackish brown sparry calcite* is laterally and continuously occurred from the lower part of the *Triticites* zone (Kasimovian, the Upper Carboniferous) in the Omi Limestone. Takeuchi and Nakazawa (2010) also reported the occurrence of *microcodium* from the Upper Carboniferous in the Gongen section. However, they did not show the mode of occurrence and horizon.

AGE OF GONGEN SECTION

Schwagerinids (Fusuliniod foraminifer) are occurred from the middle (11 m horizon) and the uppermost part (28 m horizon) of the Gongen section, which exposes about 30 m–thick shallow marine limestone. They are identified as *Montiparus* sp., based on the following characters: 1) Small (about 2 to 3 mm diameter) and oval test with massive chomata and the relative primitive forms in the genus *Triticites* (s. l.) in the axial section, 2) Coiling tight in the early stage and gradually coiled with growth, and the dark colored secondary deposits near the septa and at the bottom of the chambers in the sagittal section. Hence, the middle to the uppermost horizons of the Gongen section can be correlated to the middle Kasimovian, the Upper Carboniferous (Davydov, 1990).

OCCURRENCE & CHARACTERISTICS OF MICROCODIUM

Microcodium is occurred in the upper horizon (~ 27 m horizon) of the Gongen section. The host rock of the microcodium is the Bioclastic Pack–wackestone, which is rich in fragments of crinoids and peloids. On the surface of the outcrop, the microcodium agglutination shows amorphous to gathering clouds–shape, and the gathering clouds–shaped agglutination partly extends to the direction of the bedding plane. In the microscopic views, *microcodium* shows a “corn-cob texture” with a diameter of ~2 mm, and is frequently occurred with solution voids filled with blocky cement.

ISOTOPIC RATIO OF MICROCODIUM

The bulk carbon isotope ratios (the $\delta^{13}C$ values) of Bioclastic Pack–wackestone, the host rock of microcodium, range from +0.8 to +3.5 ‰(Ave. +1.94 ‰), and the bulk oxygen isotope ratios (the $\delta^{18}O$ values) range from -6.9 to -5.5 ‰(Ave. -6.05). Meanwhile, the $\delta^{13}C$ values of microcodium range from +0.9 to +2.5 ‰(Ave. +1.68 ‰), and the $\delta^{18}O$ values range from -6.6 to -2.6 ‰(Ave. -4.40 ‰). On average, the microcodium has a lower $\delta^{13}C$ value (-0.26 ‰lower) and a higher $\delta^{18}O$ value (+1.65 ‰higher). The $\delta^{13}C$ values of *microcodium* are lower than those of host rock, probably because more ^{12}C were fixed in *microcodium* via microbial corrosion and decomposition process (Kabanov, 2008).

MICROCODIUM FROM OTHER SEAMOUNT-TYPE LIMESTONE IN JAPAN

From the above, it is interpreted that the Gongen section was subaerially exposed just after the middle

©2021. Japan Geoscience Union. All Right Reserved.

Kasimovian, and then pedogenesis and microcodization were progressed on the surface of the limestone. *Microcodium* is also occurred from the Moscovian to the Kasimovian sections of the Akiyoshidai Limestone (Hasegawa, 1988; Machiyama, 1994; Sano et al., 2004). In particular, Sano et al. (2004) suggested that the Akiyoshidai Limestone was subaerially exposed during the late Kasimovian, based on the lack of the upper Kasimovian fusuline biozone. The *microcodium* has also been reported from seamount-type limestone in the Ashio Belt, which is thought to be the Kasimovian (Uchiyama et al., 2010). As the future works, it will be necessary to discuss about synchronism of the subaerial exposure and the microcodization of seamount-type limestone, including sea-level changes and the paleogeographic position of seamounts, comprehensively.

REFERENCES

Davydov, 1990, *Paleontol. Jour.* 2, 13-25; Hasegawa, 1988, Reports of KAKENHI Grants-in-Aid for Scientific Research (C) by JSPS, 14pp. 3 figs., 3pls.; Hasegawa & Goto, 1990, Guidebook for geol. excurs. of 97th Annual Meet. of Geol. Soc. Japan, Toyama, pp. 227 –260; Kabanov et al., 2008, *Sediment. Geol.* 205, 79–99; Takeuchi & Nakazawa, 2010, In: Nagamori et al. (eds.), Explan. booklet 1:50,000 Geol. Map ”Kotaki”, pp. 15–28; Sano et al., 2004, *Palaeogeogr., Palaeoclimatol., Palaeoecol.* 213, 187–206; Uchino et al., 2010, *Jour. Geol. Soc. Japan* 116, 118-123.

Keywords: Microcodium, Carboniferous, Kasimovian, Omi Limestone, subaerial exposure, sea-level change

©2021. Japan Geoscience Union. All Right Reserved.

Coastal transport process of pebble along the Seisho Coast, Kanagawa Prefecture, estimated from changes in lithological composition and form of pebble particles

*Masaaki Shirai[1], Tomomi Akiyama[1], Kiyokazu Kawajiri[2], Takako UTSUGAWA[3], Takayuki Takahashi[4]

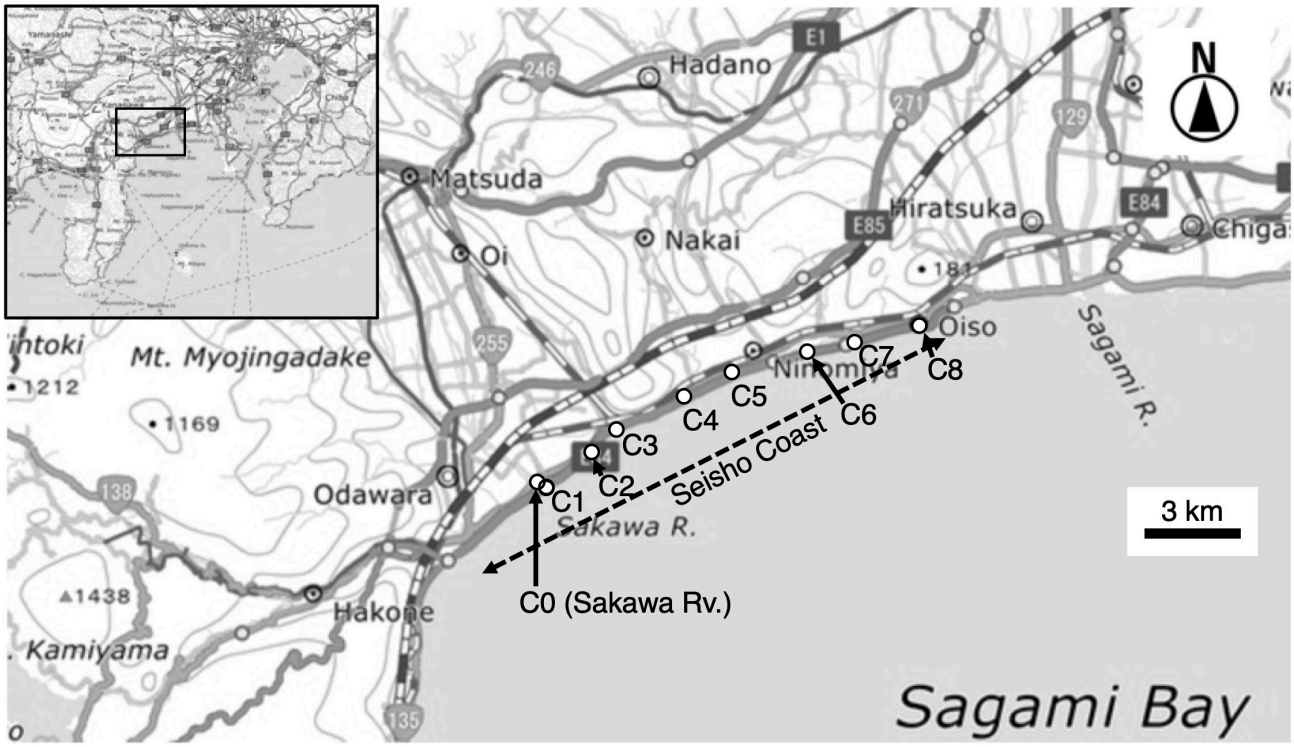
1. Tokyo Metropolitan University, 2. Sagamihara Cuty Museum, 3. Rissho University, 4. Tohoku University

Coastal erosion along the Seisho Coast, Kanagawa Prefecture has been one of the severe social problems on infrastructure. As a countermeasure to the coastal erosion of the Seisho Coast, artificial beach nourishment has been carried out since 1995. We estimate alongshore transport rate of pebble along the Seisho Coast using classical evaluation method of lithologic composition and flatness of pebble particles. Gravel beach of the Seisho coast is maintained by sediment supply from the Sakawa River which is rich in tuff and diorite gravels derived from the Tanzawa Mountains (e.g., Aramaki and Suzuki, 1962). Based on a temporal change of coast line on old topographic maps, spatial change of lithological composition and flatness of pebble particles along the coast, coastal transport of pebble along the Seisho Coast is estimated as below.
(1) Temporal seaward shift of shoreline occurred during 1916 to 1933. It might have been caused by increase in sediment supply due to the Taisho Kanto Earthquake slope failures at the Tanzawa mountains on 1923.
(2) An abundance of flat tuff gravels at site C5 ca. 7 km east from the Sakawa river-mouth imply that pebbles may have been transported along the Seisho Coast from the river mouth since 1923–1933. Therefore, eastward average transport rate of 16-32 mm size pebbles is estimated as 70–80 m/y.
(3) Tuff gravels with low average flatness at site C6 may be brought directly from the lower reaches of the Sakawa River by artificial beach nourishment since 1995. Site C6 locating 0.6 km east from the beach nourishment site is near enough to the site. Whereas, tuff gravels having been brought the beach nourishment site do not reach site C7 2.0 km east from the site yet.

References
Aramaki, M. and Suzuki, T. (1962) Geographical Review, 35, 17-34.

Keywords: pebble, transport process, flatness, beach nourishment, Seisho Coast

©2021. Japan Geoscience Union. All Right Reserved.



©2021. Japan Geoscience Union. All Right Reserved.

A consideration of the age of the higher terraces in the southeastern part of the Kashiwazaki plain, Niigata Prefecture, central Japan.

*Satoshi Kaneko[1], Toshimichi Kaneto[1], Akiko Miyawaki[2], Akira Fukuchi[2], Mitsugu Momose[2]

1. Tokyo Electric Power Company Holdings, Inc., 2. Hanshin Consultants Co., Ltd.

1.Introduction
The Kashiwazaki plain (15 km in length and 4 –7 km in width) locating in the middle part of Niigata Prefecture, central Japan is surrounded by Chuo Hills and Mt. Yoneyama.
The upper Pleistocene in this plain is described by Kashiwazaki plain Quaternary Formation Research Group (“KRG” , here in after) (1965) and Kishi et al. (1996), whereas the middle Pleistocene in this area has not been well studied, so far.
Our study implemented boring survey drilled to basement rock in order to grasp stratigraphy of the higher and middle terraces in the southeastern part of the Kashiwazaki plain.

2.Location of drilling
Kishi et al. (1996) classified terraces in the Kashiwazaki plain into the lower, middle and higher ones. The middle terrace is subdivided to M_{II} surface, M_I surface and M_I^+ surface from the lower, however several levels of higher terraces are lumped together as H surface. M_I and M_I^+ surface and H surface are correlated to Yasuda surface and Oumigawa surface that are defined by KRG (1965), respectively.
The middle and higher terraces are present in study area. The higher terrace in this area is higher than M_I surface by a level. Each three boring cores were drilled on M_I and H surfaces.

3.Stratigraphy in the southeastern part of the Kashiwazaki plain
Boring survey results showed that sediments in study area can be divided into three layers based on fining-upward cycle. These three layers are M_I terrace deposit, H terrace deposit and layer overlain by H terrace deposit, from the upper.
M_I terrace deposit under M_I surface is correlated to Yasuda Formation defined by KRG (1965), and this formation is subdivided into the lower and upper parts. Base of this formation shows coarse clastics consisting of gravels and coarse-grained sands, and silt or clay overlays them. Visible volcanic ash layer is absent in this formation.
H terrace deposit under H surface shows coarse clastics consisting of gravels at the base, and silt or clay overlying them. White-colored gravel layer consisting of well-rounded white-colored gravels is present in the lower part of this deposit. The combination of this white-colored gravel layer and overlying humic layer continues under Yasuda Formation. White fine vitric ash is present in the base of this layer.
Layer overlain by H terrace deposit is distributed only in the middle part of study area. Base of this layer shows coarse clastics consisting of gravels, and silt or clay overlays them. Visible volcanic ash layer is absent in this layer.

4.Analysis of tephra
White fine vitric ash in the base of H terrace deposit is correlated to Ata-Toihama tephra based on major chemical composition of glass shards. Presence or absence of volcanic ash in Yasuda Formation and loam overlying H terrace deposit is examined by particle composition analysis. This analysis revealed that cummingtonite is accumulated in the lower part of Yasuda Formation and in the base of loam. Cummingtonites are correlated to Iiduna Kamitaru c tephra based on their major chemical composition.

©2021. Japan Geoscience Union. All Right Reserved.

5.Summary

Our study results are summarized as follows.

・M_I terrace deposit (Yasuda Formation) under M_I surface is correlated to MIS5e based on Iiduna Kamitaru c tephra.

・H terrace deposit under H surface is correlated to MIS7 based on Ata-Toihama tephra. It continues under M_I terrace deposit based on combination of characteristic facies.

・H terrace deposit under H terrace and layer overlain by H terrace deposits are present under M_I deposits (Yasuda Formation) and both are called “paleo-Yasuda Formation”, herein.

References

Kashiwazaki plain Quaternary Formation Research Group. 1965. A study of the Quaternary formation at the Kashiwazaki Plain, Niigata Prefecture, Japan. Memoir of Niigata University. 10. 145-185.

Kishi, K., Miyawaki, R. and Miyawaki, A. 1996. The stratigraphy and paleoenvironmental reconstruction of the late Pleistocene deposits in Kashiwazaki plain, Niigata Prefecture. Quaternary Research. 35(1). 1-16.

Keywords: middle Pleistocene, upper Pleistocene, tephra, Niigata Prefecture

©2021. Japan Geoscience Union. All Right Reserved.

Linear stability analysis of plane beds with active suspended load

Koji Ohata[1], *Hajime Naruse[1], Norihiro Izumi[2]

1. Department of Geology and Mineralogy, Graduate School of Science, Kyoto University, 2. Graduate School of Engineering

Plane beds develop under riverine and marine environments and can be recorded as parallel lamination in sandstone beds, such as those found in turbidites. However, whereas turbidites typically exhibit parallel lamination, they rarely feature dunescale cross lamination. Although the reason for the scarcity of dune-scale crosslamination in turbidites is still debated, the formation of dunes may be dampened by suspended load. Here, I perform linear stability analysis to show that flows with suspended load facilitate the formation of plane beds. For a fine-grained bed, suspended load can promote the formation of plane beds anddampen the formation of dunes. These results of theoretical analysiswere verified with observational data of plane beds under open-channel flows. In the case of coarse-grained beds, the stability diagrams do not coincide with the experimental data of plane beds under sheet flows. Further analytical studies of bedforms should consider sheet flows, one of the transport modes associated with open-channel flows and sediment-laden gravity currents.

Keywords: bedform, turbidite, plane bed, dune, stability analysis

©2021. Japan Geoscience Union. All Right Reserved.

[J] Poster | S (Solid Earth Sciences)：S-SS Seismology

Thu. Jun 3, 2021 5:15 PM - 6:30 PM JST | Thu. Jun 3, 2021 8:15 AM - 9:30 AM UTC | Ch.10_1

[S-SS05] Crustal Deformation

convener:Masayuki Kano(Graduate school of science, Tohoku University), Tadafumi Ochi(Institute of Earthquake and Volcano Geology, Geological Survey of Japan, The National Institute of Advanced Industrial Science and Technology), Fumiaki Tomita(Japan Agency for Marine-Earth Science and Technology)

Study of crustal deformation plays an extremely important role in the investigation of wide scale earth dynamics those are earthquake and volcanic activity, plate motion and so on. In our session, we discuss the study related to crustal deformation, such as development of observation instrument, observed crustal deformation, analysis method, and simulation study.

[SSS05-P01] Estimation of Afterslip Distribution and Viscoelastic Deformation by MCMC Method

*Ryoji Kawabata[1], Hiroshi Munekane[1] (1.GSI of Japan)

[SSS05-P02] Application of a slow slip objective detection method to GNSS 6-hour coordinates

*Akio Kobayashi[1] (1.Meteorological Research Institute, Japan Meteorological Agency)

[SSS05-P03] Long-term SSE along the Nankai trough detected by Geonet

*Shinzaburo Ozawa[1], Ryoji Kawabata[1], Hiroshi Munekane[1] (1.Geographical Survey Institute of Japan)

[SSS05-P04] Estimation of strain-rate field in the Japanese Islands using optimized distance-decaying constants

*Issei Kosugi[1], Yuta Mitsui[2] (1.Graduate School Of Science and Technology, Shizuoka University , 2.Faculty of Science, Shizuoka University)

[SSS05-P05] **Evaluation of inland seismic potential in southwest Japan using GNSS data and seismic catalog**

*Hiroki Sato[1], Takeo Ito[1] (1.Graduate School of Environmental Studies, Nagoya University)

[SSS05-P06] Re-evaluation of earthquake swarm activity in the offshore region to the northeast of Izu Peninsula focusing on crustal deformation for several months (1990-2011)

Keisuke Takeshita[1], *Kazuhiro Kimura[1], Takeshi Kimura[2] (1.Meteorological College, 2.National Research Institute for Earth Science and Disaster Resilience)

[SSS05-P07] Evaluation earthquake potential using a kinematic block motion model in Indonesia based on GNSS Observation

*Rio Raharja[1], Takeo Ito[1], Hiroshi Kimura[1], Irwan Meilano[2] (1.Graduate School of Environmental Studies, Nagoya University, Japan, 2.Faculty of Earth Sciences and Technology, Bandung Institute of Technology, Indonesia)

[SSS05-P08] **A recent example of active intraplate deformation in the Central Anatolia: Obruk-Bor (Nigde) earthquakes, Turkey**

*Dogan Kalafat[1] (1.Bogazici University Kandilli Observatory and Earthquake Research Institute Cengelkoy, Istanbul Turkey)

[SSS05-P09] Modification of computer program GOTIC2 for calculation of the ocean tidal loading effect
- Application of Green's function to calculate theoretical strain at depth of borehole observation near coasts -

Osamu Kamigaichi[1,2], *Norio Matsumoto[2], Fuyuki Hirose[3] (1.Japan Meteorological Business Support Center, 2.Geological Survey of Japan, National Institute of Advanced Industrial Science and Technology (AIST), 3.Seismology and Tsunami Research Department, Meteorological Research Institute)

[SSS05-P10] Crustal deformation observed with Tenryu-Funagira laser strainmeter

*Takahiro Tsuyuki[1] (1.Meteorological Research Institute)

[SSS05-P11] Crustal movements due to the seismic motions observed in Kobe

*Atsushi Mukai[1] (1.Faculty of Urban Management, Fukuyama City University)

Estimation of Afterslip Distribution and Viscoelastic Deformation by MCMC Method

*Ryoji Kawabata[1], Hiroshi Munekane[1]

1. GSI of Japan

Summary

Postseismic deformation of the 2011 off the Pacific coast of Tohoku Earthquake is still observed about ten years after the main rupture. Afterslip and viscoelastic deformation triggered by the main rupture are considered to be the mechanisms of the postseismic deformation. In this study, following Tomita et al. (2020), we estimate contributions of the afterslip and viscoelastic deformation including viscosity value simultaneously from the spatial pattern of the postseismic deformation obtained by the geodetic observation.

Calculation method

The displacements by afterslip and Viscoelastic are given by:

$d_0 = G_e\, s_0$
$d_1 = G_{v,10}\, s_0 + G_e\, s_1$

where d_0 and d_1 are coseismic (t=0) and postseismic ($t=t_1$) displacements, s_0 and s_1 are the coseismic slip and afterslip at $t=t_1$, and G_e, $G_{e,10}$ are the elastic Green's functions and viscoelastic Green's functions at $t=t_1$ by cosesimic slip. In this study, we use only two timesteps (t=0, t_1), and do not consider the viscoelastic deformation induced by the afterslip.

We calculate elastic and viscoelastic Green's functions of 600 fault patches, which are aligned with the Pacific Plate interface, using the code of Fukahata and Matsu'ura (2005). We assume a half-space consisting of an elastic surface layer with thickness of 50 km and a Maxwell viscoelastic substratum.

Inland postseismic displacements are derived from the F3 solutions of the 448 GEONET sites, by removing linear velocities and annual/semi-annual signals estimated from preseismic data. We also use seafloor observation data of Japan Coast Guard by removing the linear velocities estimated from preseismic data and fitting the timeseries by logarithm functions (Yokota et al. 2018). In addition, coseismic deformation data of three seafloor observation points of the Tohoku University are also used (Sato et al. 2011, Kido et al. 2011, Ito et al. 2011).

We use Markov Chain Monte Carlo (MCMC) method to estimate the fault slip parameters as well as hyperparameters for the smoothness of the slip distributions (Fukuda and Johnson 2008).

Results

Fig. 1 shows estimated slip distribution five years after the main rupture. The contribution of the afterslip dominates that of the viscoelastic deformation in the coastal region near the rupture area, where the sites show eastward and upward deformation. Far from the rupture area, the contribution of viscoelastic deformation becomes relatively larger. On the other hand, on the seafloor near the rupture area, the afterslip and viscoelastic deformation contribute in opposite sense, making moderate deformation on the seafloor observation points.

©2021. Japan Geoscience Union. All Right Reserved.

The effect of the viscoelastic deformation can be canceled by the afterslip for a wide range of viscosity in the coastal region near the rupture area. However, it is difficult to explain the deformation on the seafloor and far inland area for too large or small viscosity. As the result, the optimal viscosity, which makes smallest residuals between observed and calculated displacements, is estimated to be around 10^{19} Pa s (Fig. 2).

Note that our estimated slip distributions would not include the effect of plate interface coupling, since the preseismic velocities are subtracted from the data. This could be the reason why our estimated slip shows slightly larger seaward compared with the result of Tomita et al. (2020), in which they used the velocities relative to the continental plate. Nevertheless, the optimal viscosity in our result is very close to that of Tomita et al. (2020).
In our presentation, we will also show the results using different observation periods.

<Fig. 1> Estimated slip distribution five years after the 2011 off the Pacific coast of Tohoku Earthquake. Upper left and lower left figure respectively shows the horizontal and vertical displacements of observation (black) and calculation (white). Upper right and lower right figure respectively shows the contribution of the afterslip (magenta) and viscoelastic deformation (green) to the calculated displacements. In this calculation, the viscosity of 10^{19} Pa s is used. The estimated slip distribution of the main rupture (black contour), epicenter (star), and CMT solutions of the main shock and large aftershocks by JMA are also plotted.
<Fig. 2> Mean values of the residuals with respect to the viscosity.

Keywords: The 2011 off the Pacific coast of Tohoku Earthquake, Postseismic deformation, Markov Chain Monte Carlo method

©2021. Japan Geoscience Union. All Right Reserved.

Figure 1

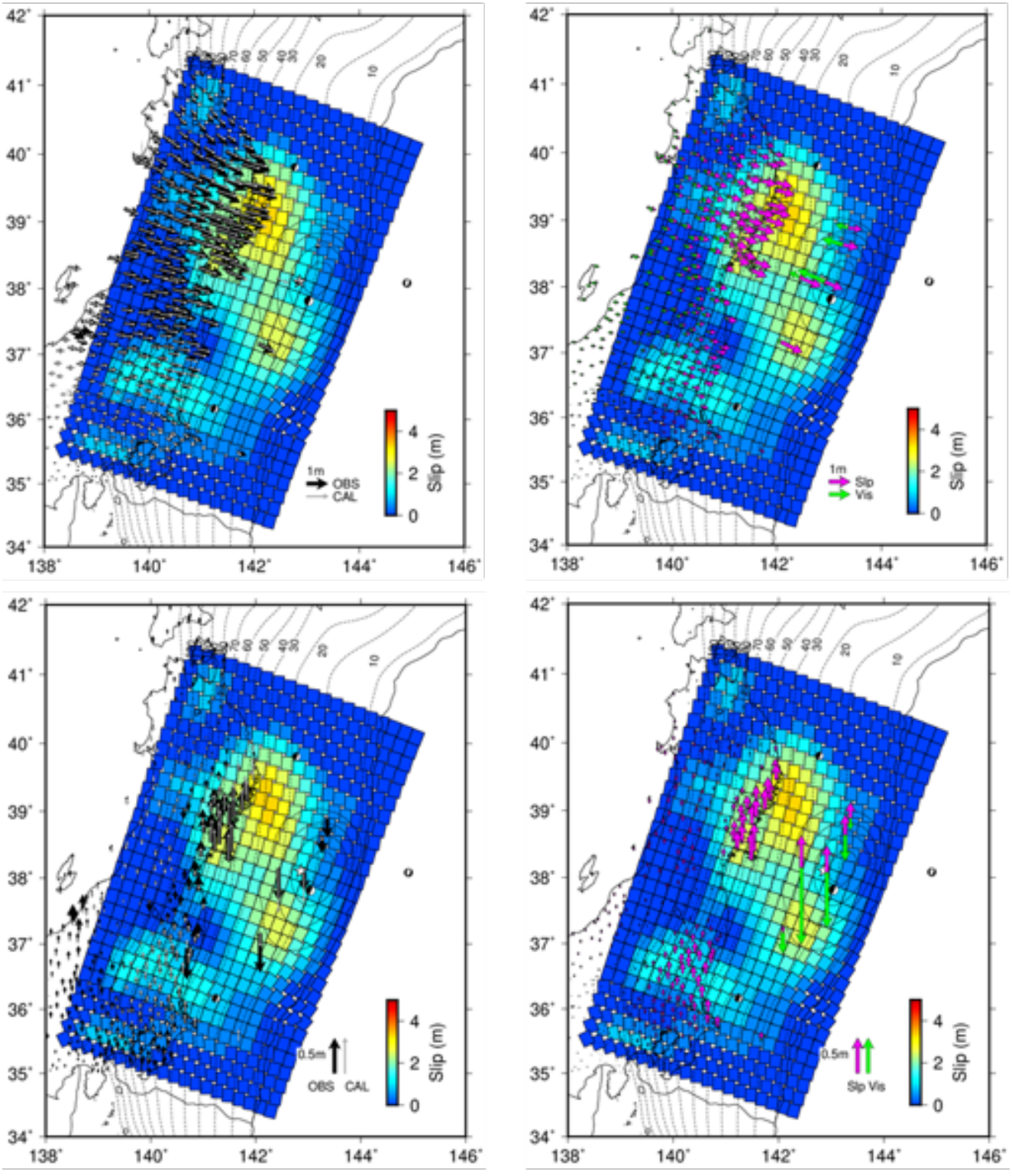
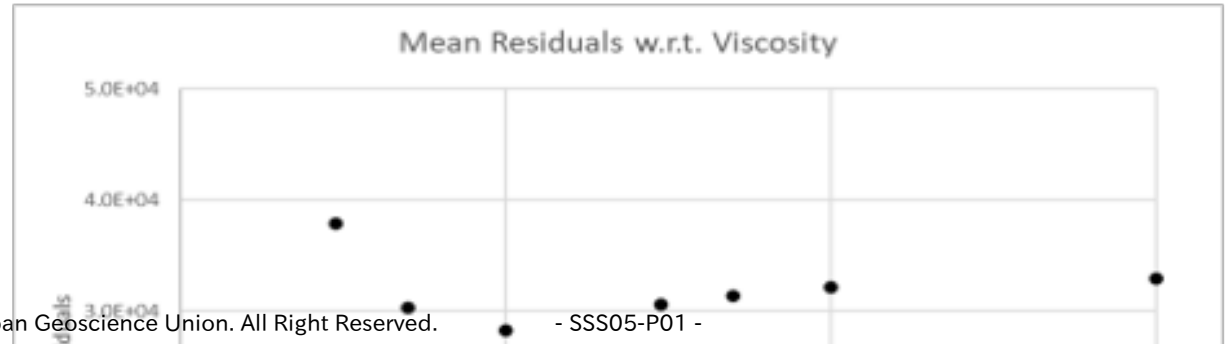


Figure 2



©2021. Japan Geoscience Union. All Right Reserved.

©2021. Japan Geoscience Union. All Right Reserved.

Application of a slow slip objective detection method to GNSS 6-hour coordinates

*Akio Kobayashi[1]

1. Meteorological Research Institute, Japan Meteorological Agency

In the Nankai Trough, slow earthquakes such as short-term slow slip events (SSEs) and long-term SSEs have been observed. Kobayashi (2017) developed a method for objective detection of long-term SSEs and revealed their spatiotemporal distribution. Kobayashi (2021) applied the method to short-term SSEs and extracted the crustal deformations associated with short-term SSEs. Here we tried the same detection method using 6-hour GNSS coordinates.

From November 15 to December 5, 2017, deep low-frequency earthquakes and strain changes were observed from Nara Prefecture to near the Aichi-Nagano border. The short-term SSE objective detection method using GNSS daily coordinates showed a high correlation associated with this phenomenon. The correlation values with the ramp function with a 7-day slope at November 25 were 0.74 for the daily coordinates, 0.44 for the 6-hour coordinates, and 0.72 for the median of the past 24 hours for the 6-hour coordinates. The 6-hour coordinates had a low correlation value, probably due to its high variability, but the change in the median value over the past 24 hours was similar to the daily coordinates, and the correlation value was also similar to the daily coordinates. Monitoring by 6-hour coordinates may detect the phenomenon earlier than daily coordinates.

Keywords: slow slip event, Nankai Trough, GNSS

©2021. Japan Geoscience Union. All Right Reserved.

Long-term SSE along the Nankai trough detected by Geonet

*Shinzaburo Ozawa[1], Ryoji Kawabata[1], Hiroshi Munekane[1]

1. Geographical Survey Institute of Japan

GNSS network has revealed transitional crustal movements in the Kyushu, Shikoku, Kii Channel, and Shima Peninsula areas since 2018. The interplate slip in the Nankai Trough area was estimated from the observed transient. As a result, from June 2018 to August 2019, SSE has occurred in the northern part of Hyuga Nada and Bungo Channel, and from early 2019 to late 2020, SSE has occurred in central Shikoku. It was estimated that SSE occurred in Kii Channel from around April 2019 to late 2020, and SSE occurred in the Shima Peninsula from around early 2019 to around April 2020. Northern and southern Hyuga-nada SSE occurred from mid 2020.

Introduction

In Bungo Channel, long-term SSE has repeatedly occurred in a cycle of 5 to 6 years. In central Shikoku, long-term SSE is estimated in 1977-1980, 1998, 2004, 2010, 2012, and 2015. The long-term SSE of Kii Channel occurred in 1996, 2000 and 2016. The Shima Peninsula SSE occurred during 2017-2018. Transitional crustal movements have occurred in northern Kyushu from around June 2018, and from around October 2018, in the Bungo Channel. Transient have been observed around Kii Channel since April 2019, and in the Shima Peninsula area since early 2019. In this study, we estimated the spatiotemporal variation of interplate slip in the Shikoku, Kyushu, Kii Channel, and Shima Peninsula from the data of crustal deformation detected by GNSS.

Analytical Procedure

From the position time series, the annual and semi-annual components for 2013-2019 were estimated and removed from the original position time series. The 2017-2018 trend is subtracted from the analysis for the Kyushu, Shikoku and the Kii channel areas, and the primary trend from March 2016 to March 2017 is subtracted from the Shima Peninsula analysis. Time-dependent inversion analysis was performed using the east-west, north-south, and top-bottom coordinate time-series data at 250 observation points. The shape of the Philippine Sea plate compiled by Hirose et al. (2008) is represented by triangular elements and used for analysis. The grid interval is about 20-40km. The slip direction on the plate boundary was constrained to be the plate converging direction.

Results and discussion

From around June 2018 to around August 2019, SSE occurred in Bungo Channel and in northern Hinata Nada. SSE occurred in central Shikoku from early 2019 to late 2020. The SSE of Kii-channel occurred around April 2019 and ended in late 2020. The Shima Peninsula SSE occurred from early 2019 and ended around April 2020. It was estimated that Bungo channel SSE was Mw 6.9, central Shikoku SSE was Mw 6.1, Kii channel SSE was Mw 6.1, and Shima Peninsula SSE was Mw 6.2. The Bungo channel SSE is

©2021. Japan Geoscience Union. All Right Reserved.

roughly in harmony with the 5-6 year cycle. The repeating intervals of central Shikoku SSE do not seem to be periodic. The Kii Channel SSE does not appear to have a periodic interval. It is not clear whether Shima peninsula SSE is a series of SSEs or separate SSEs, which started from 2017. Northern Hyuga-nada SSE started from 2018 and subsided in early 2020 and started from the middle of 2020, whose rupture history seems to be different from those of the past events.

Keywords: long-term SSE, Nankai trough, GNSS

©2021. Japan Geoscience Union. All Right Reserved.

Estimation of strain-rate field in the Japanese Islands using optimized distance-decaying constants

*Issei Kosugi[1], Yuta Mitsui[2]

1. Graduate School Of Science and Technology, Shizuoka University , 2. Faculty of Science, Shizuoka University

Estimation of strain-rate field based on Global Navigation Satellite System (GNSS) data has been performed to extract local crustal deformation (e.g., Meneses-Gutierreza and Sagiya, 2016; Nishimura et al., 2018). The method of Shen et al. (1996) has been frequently used to estimate the strain rate. In this method, a distance-decaying constant is assumed and used for Gaussian weighting of the observation point data. The accuracy of the strain rates at grid points should depend on the coarseness of the observation points. Therefore, Shen et al. (2015) proposed a method to optimize the distance-decaying constant for each grid point using the sum of the Gaussian weightings as a constraint.

In this study, we use horizontal displacement components from the F3 solution (Nakagawa et al., 2009) of GEONET, the GNSS array by the Geospatial Information Authority of Japan (GSI), with removing offsets due to major earthquakes and antenna replacement from February 1997 to February 2020. The optimal distance-decaying constant and strain-rate fields are estimated for each grid point divided by 0.3 degrees of latitude and longitude respectively, before and after the 2011 Tohoku megathrust earthquake. The constraint is set so that the estimation errors at the observation points are the smallest.

With respect to the estimation results before the 2011 Tohoku earthquake, the maximum shear strain rate and the dilatation rate are negatively correlated as a whole (correlation coefficient is about -0.5). The areas with high shear strain rate and high compressive rate (negative dilatation rate) are located around Shikoku, Shizuoka, Tokyo, and Niigata, which may indicate the plate coupling associated with the subduction of the Philippine Sea Plate and the existence of the Niigata-Kobe tectonic zone. By contrast, the above correlation collapses in the estimated results after the 2011 Tohoku earthquake. In particular, both the shear strain rate and the expansion rate (positive dilatation rate) are higher on the Japan Sea side from Akita to Aomori in the northern Tohoku region. This relationship is not observed in the southern Tohoku region. In addition, rotational components estimated simultaneously with the strain rates show opposite directions in the northern and southern parts of the Pacific coast of the Tohoku region. Our results suggest that there was a notable north-south difference in the postseismic deformation of the 2011 Tohoku earthquake.

©2021. Japan Geoscience Union. All Right Reserved.

Evaluation of inland seismic potential in southwest Japan using GNSS data and seismic catalog

*Hiroki Sato[1], Takeo Ito[1]

1. Graduate School of Environmental Studies, Nagoya University

Major earthquakes have repeatedly caused massive damage in Japan. The Headquarters for Earthquake Research Promotion (HERP) evaluates the seismic potential for major earthquakes. Although the HERP had only assessed damaging earthquakes at major active faults, several major earthquakes occurred along non-target faults recently. Against this background, some previous research estimated inland seismic potential regionally based on strain rates estimated from GNSS observation and Japan Metrological Agency (JMA) seismic catalog. However, they ignore the effects of interplate coupling and postseismic deformations on strain rates (Takahashi & Shinohara, 2015), and use a relatively shorter period of seismic catalog for calculating the seismic moment's release rate (Kimura *et al.*, 2018). We evaluated inland seismic potential at each crustal block of southwest Japan using internal strain rates at each crustal block and a relatively longer seismic catalog.

Inland earthquakes release accumulated internal strain in the crustal block. Based on this relation, we focused on accumulation and release rates of the seismic moment at each crustal block, and evaluated inland seismic potential using the balance between both rates. To evaluate the seismic potential, we used the crustal block model and internal strain rates at each crustal block (Kimura *et al.*, 2018), and seismic catalogs by JMA and Utsu (1982, 1985). The seismic moment's accumulation rate is equivalent to the average seismic moment rate due to plate motion and interaction between crustal blocks It is calculated from internal strain rates, thickness of seismogenic layer (D90 in this research), and the equation proposed by Savage & Simpson (1997). On the other hand, the seismic moment's release rate corresponds to the released average seismic moment rate due to earthquakes. It is obtained from seismic moment integration assuming that inland earthquakes occur according to cumulative GR-law. Then, we regarded the difference of accumulation and release rates as the energy released by future earthquakes. The evaluated inland seismic potential in 30 years assumed the occurrence of M_w7.0 earthquakes using the Poisson process.

We evaluated inland seismic potential at six crustal blocks. In Kinki and Setouchi blocks, the estimated seismic potentials from combined geodetic data are 2.16±0.01% and 9.07±0.25%, respectively. We compared the results with the seismicity at each crustal block. As a result, the seismic potentials estimated from the seismicity are 0.08±0.001% and 3.25±0.02%, respectively, and are close to the seismic potentials from combined geodetic data. Therefore, the estimated seismic potentials are consistent with the seismicity. In the Forearc block, while the estimated seismic potential from combined geodetic data is 62.06±0.16%, the seismic potential from the seismicity is 3.69±0.02%. It is significantly smaller than the estimated seismic potential from combined geodetic data. However, since internal strain rates at the Forearc block are relatively larger than other crustal blocks, this discrepancy reflects the relatively higher risk for major earthquakes. In the Okinawa block, the estimated seismic potential from combined geodetic data is 99.87±0.002%. The crustal block has a significantly wide area covering from Kagoshima to Taiwan and significantly large internal strain rates due to a single crustal block, including the interaction between crustal blocks. Therefore, the significantly high seismic potential may reflect both effects. In the Chubu block and Izu microplate, the seismic potentials from combined geodetic data cannot be evaluated because the release rates are larger than the accumulation rates. In both crustal

©2021. Japan Geoscience Union. All Right Reserved.

blocks, the release rates may be overestimated due to the various effects of active volcanoes. In the future, we need to improve our methods, such as removing the earthquakes near active volcanoes and the boundaries of crustal blocks.

Keywords: seismic potential, GNSS observation, seismic catalog, seismic moment

©2021. Japan Geoscience Union. All Right Reserved.

Re-evaluation of earthquake swarm activity in the offshore region to the northeast of Izu Peninsula focusing on crustal deformation for several months (1990-2011)

Keisuke Takeshita[1], *Kazuhiro Kimura[1], Takeshi Kimura[2]

1. Meteorological College, 2. National Research Institute for Earth Science and Disaster Resilience

From 1978 to 2011, earthquake swarm activity had occured frequently in the offshore region to the northeast of Izu Peninsula. Previous studies had shown that volcanic activity is the cause of this earthquake swarm activity, and that crustal deformation can be explained by dike intrusion. This earthquake swarm activity caused by dike intrusion coutinuesd for a week.

We have found five different crustal deformation phenomenon that coutinuesd for several months since 1990. Four of them are sources of variation at almost the same location as the sill expansion in the inland area of the Izu Peninsula, estimated by Nishimura and Murakami (2007) after the 1930 earthquake swarm activity. In addition, our result show that the volume change of this sill is about 30% compared to the dyke intrusion at the same time, and the dike intrusion did not occur during the expansion period of the sill inland area of the Izu Peninsula.

Keywords: crustal deformation , tiltmeter, strainmeter, GNSS, volume change

©2021. Japan Geoscience Union. All Right Reserved.

Evaluation earthquake potential using a kinematic block motion model in Indonesia based on GNSS Observation

*Rio Raharja[1], Takeo Ito[1], Hiroshi Kimura[1], Irwan Meilano[2]

1. Graduate School of Environmental Studies, Nagoya University, Japan, 2. Faculty of Earth Sciences and Technology, Bandung Institute of Technology, Indonesia

Indonesia is located in a tectonically complex region and lies in the interaction of four major plates. This interaction resulted in seismic activity in Indonesia and is one of the highest in the world. With this condition, research on evaluating the earthquake potential in Indonesia becomes urgent. Previous geology and geodesy studies have been done to describe the crustal block boundaries and also crustal block motion in Indonesia (e.g. Bird, 2003; Koulali et al., 2016; Koulali et al., 2017). However, some inland faults are still not well described, and used few GNSS data in previous studies. This research would provide an improved crustal block motion model for Indonesia to evaluate the interaction among these blocks and estimate the earthquake potential in research area and also to identify which regions are more vulnerable to the earthquake.

In this research, we use GNSS data derived from Indonesia CORS Network (InaCORS), Sumatran GPS Array (SuGAR), and International GNSS Service (IGS). The total number of GNSS sites is 205 during 2008 to 2018. To get the velocity field, we utilize Bernese 5.2 software package (Dach et al., 2015) and VISCO1D (Pollitz et al, 1997) for analyzing the GNSS data and removing the deformation due to earthquakes that occurred before 2008, respectively. We employ the MCMC (Markov Chain Monte Carlo) method to generate many kinematic block motion models and choose the optimum model based on AIC (Akaike’ s Information Criterion).

By using the optimum model, MODEL12, our results of coupling show that the strong coupling is estimated mostly at the depth of 0-30km and mostly weak coupling for more than lower than 30km depth. Our results also show a possible recovery from the 2006 Java earthquake. For the earthquake potential, our results show 4 areas with high coupling which possible to generate big earthquakes. Area 1 has enough seismic moment deficit to produce a Mw8.3 earthquake every 119±15 years. Area 2, Area 3, and Area 4 have enough seismic moment deficit to produce a Mw8.6 earthquake every 182±24 years, 186± 27 years, and 169±24 years, respectively. A Mw8.9 earthquake can be produced every 261±35 years if Area 2 and Area 3 rupture together at the same time.

©2021. Japan Geoscience Union. All Right Reserved.

A recent example of active intraplate deformation in the Central Anatolia: Obruk-Bor (Nigde) earthquakes, Turkey

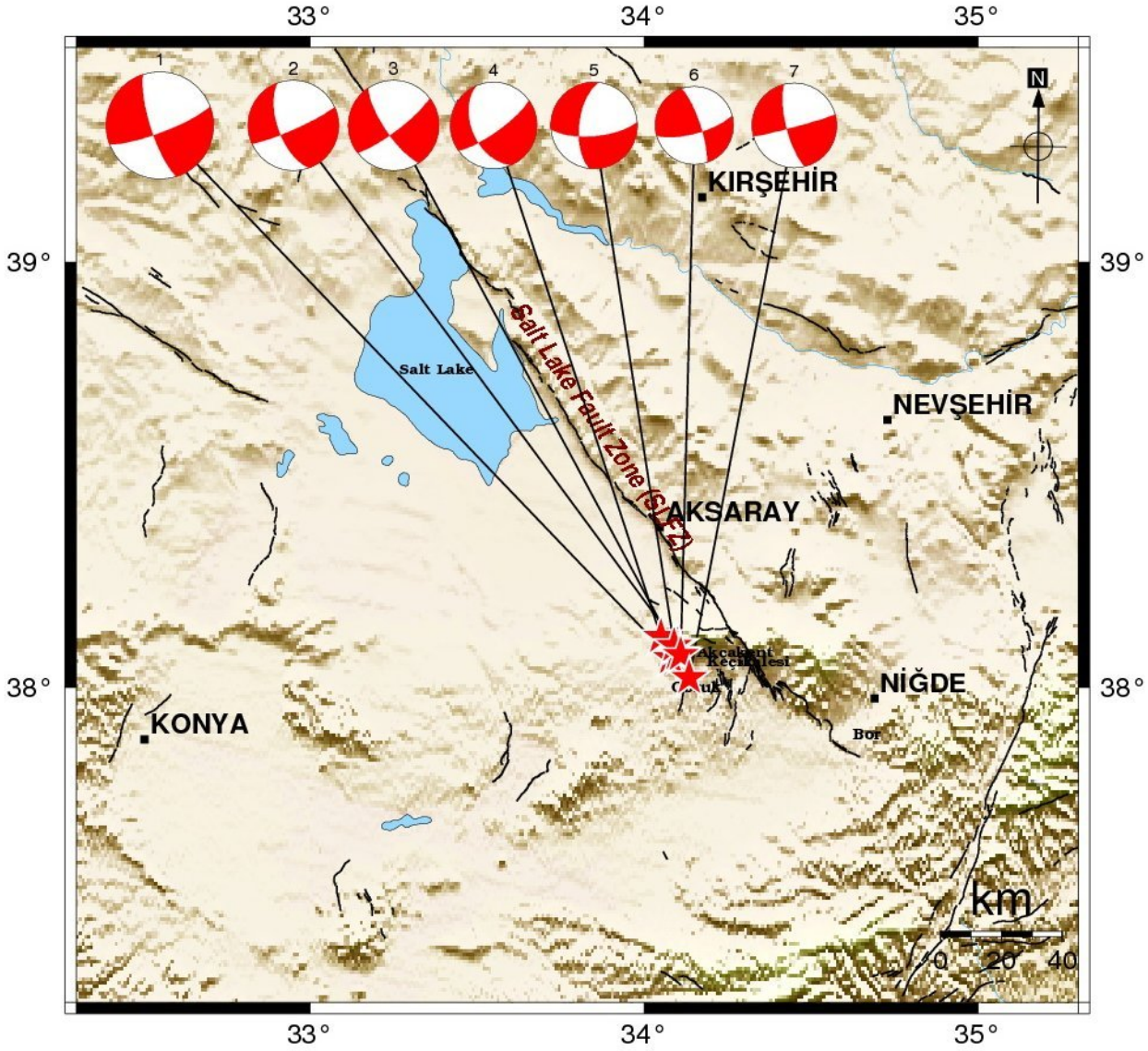
*Dogan Kalafat[1]

1. Bogazici University Kandilli Observatory and Earthquake Research Institute Cengelkoy, Istanbul Turkey

Salt Lake (Tuz Golu) basin is evident morphological trace in the Central Anatolia which is one of the biggest tectonic lakes in Turkey. Salt Lake Basin is NW-SE trending sediment basin and generally restricted by NW-SE trending strike-slip faults which is called the Salt Lake Fault zone (SLFZ). SLFZ is the biggest faulting zone with 200 km length in the Central Anatolia. Also, SLFZ is a kind of intraplate zone of active deformation characterized by oblique right lateral strike-slip faulting. SLFZ did not produce strong earthquakes last a couple of hundred years. Salt Lake is surrounded by Aksaray Fault and Hasandagi volcanic rise. Seismicity in Salt Lake and surrounding region is quite low, because of intraplate deformation of Anatolian microplate. However recent years several moderate earthquakes (M>5) and aftershocks in the region showed that the rim of the northwest of the SLFZ and especially secondary faults in Bala-Kulu were active parts of the SLFZ. Due to these activities along the SLFZ it is decided to monitor micro-seismic activity (M<2.5) by establishing low-magnitude threshold seismic network. For this purpose, six broadband seismic stations have been established since 2010 to control the entire region.
On Sunday 20 September 2020 moderate sized (Mw=5.1) earthquake occurred at the locality approximately 4 km NE of Obruk Village (Bor-Nigde), Central Turkey. 143 masonry-adobe houses were damaged in village of Obruk of Bor district. In this study, focal mechanisms of earthquakes (M>4) are calculated using moment tensor inversion from broadband stations. Moment tensor solutions show that mainshock and important aftershocks obviously revealed that the SLFZ is being dominated by NW-SE trending dextral strike-slip faulting. Aftershock locations are correlated with fault plane orientations. Recent earthquakes have revealed the presence and activity of small fault segments parallel to the main fault segment in the SLFZ in the region. The results of the stress tensor analysis conducted within the scope of the study show that the main stress T_{max} axis is in the NW-SE direction and the maximum stress P_{max} axes are in the NE-SW direction.
This work is supported by Bogazici University BAP/SRP Project No: 16403. On this occasion, we would like to thank the Bogazici University Research Fund Commission and its valuable members. Also I would like to gratefully thanks to Prof. Dr. Nafi Toksoz from MIT/USA.

Keywords: Central Anatolia, Obruk-Bor , Intraplate deformation , Salt Lake Fault Zone , Moment tensor inversion , Dextral strike-slip faulting

©2021. Japan Geoscience Union. All Right Reserved.



Moment tensor solutions of important earthquakes which occurred in 2020 in the Obruk-Bor (Nigde), Central Turkey region

©2021. Japan Geoscience Union. All Right Reserved.

Modification of computer program GOTIC2 for calculation of the ocean tidal loading effect
- Application of Green's function to calculate theoretical strain at depth of borehole observation near coasts -

Osamu Kamigaichi[1,2], *Norio Matsumoto[2], Fuyuki Hirose[3]

1. Japan Meteorological Business Support Center, 2. Geological Survey of Japan, National Institute of Advanced Industrial Science and Technology (AIST), 3. Seismology and Tsunami Research Department, Meteorological Research Institute

We modified computer software GOTIC2 (Matsumoto et al., 2001) for estimating the crustal deformation caused by ocean tidal loading to enable calculation of the loading effect not only at the surface but also in subsurface observations using the PREM Earth model. To modify the software, we (i) revised the eigenfunctions using the PREM Earth model and (ii) calculated Green's functions of displacements and strains caused by a surface load in surface and subsurface observations by applying the eigenfunction. Green's functions of displacements and strains at depth became different from those at the surface for a range of angular distance less than 0.01 –0.1°. These Green's functions closely agree with the corresponding Boussinesq approximations for tidal loading at angular distances of less than about 0.01 –0.001°, which supports the adequacy of these Green's functions. We examined the difference between the ocean tidal loading effect estimated by Green's functions at the surface and the effect for subsurface observations based on very simple and realistic conditions, and found a non-negligible difference when the ratio of deployment depth to distance between the coast and observatory is larger than 0.05. We compared amplitudes and phase shifts of areal and shear strains in M_2 and O_1 tidal constituents observed by borehole strainmeters at 11 observatories with the theoretical strains using the Green's functions at the deployment depth and those at the surface. The theoretical strains using Green's function at the deployment depth are much closer to the observed strains than theoretical strains at the surface at four observatories where the ratios of deployment depth to distance from the coast to the observatories are large. These results suggest that Green's functions at the deployment depth are needed to estimate theoretical strains precisely near the coast. The computer program modified GOTIC2 with the Green's functions of gravity, displacement, tilt, and strain at depth was published in GSJ Open-File Report (https://www.gsj.jp/publications/pub/openfile/openfile0705.html).

Keywords: GOTIC2, oceanic tidal loading, Green's function, strain, subsurface observation

©2021. Japan Geoscience Union. All Right Reserved.

Crustal deformation observed with Tenryu-Funagira laser strainmeter

*Takahiro Tsuyuki[1]

1. Meteorological Research Institute

Meteorological Research Institute installed a long-baseline laser strainmeter (north-south direction, baseline length 400 m) at the Tenryu-Funagira station (34 ˚53.2'N, 137 ˚49.1' E) in Hamamatsu, Shizuoka Prefecture to detect wideband crustal movements including slow slips in the Tokai region (Katsumata et al., 2010). From March, 2017, the stabilized laser was replaced with the YAG laser (Araya et al., 2002).

It has been shown that the laser strainmeter has higher resolution than GNSS observation and has lower noise level with respect to the long-period deformation than borehole type strainmeter. It is expected as a measuring instrument that can detect not only short-term SSEs but also long-term SSEs. There have been no long-term SSEs that occurred during the period when the laser strainmeter was in operation, but some short-term SSE records have been detected.

This research examined the records of such slow slip after 2020. There was change that was thought to be due to short-term SSE near Aichi Prefecture occurred around January 2020. Change is almost consistent with the calculated from a fault model obtained by the Japan Meteorological Agency. Katsumata et al. (2020) detected a slow slip with a duration of 1 hour from the correlation analysis between the laser strainmeter recording and the borehole type strainmeter recording. No such slow slip could be detected from January 2020 record.

A slow slip with a duration of 1 hour (Katsumata et al., 2020) was detected during the SSE in January, 2019. I examined the effects of tidal changes during the event on faults modeled by JMA using the program used in Hirose et al. (2019). However, no siginificant correlation was found.

Keywords: Laser strainmeter, Slow slip

©2021. Japan Geoscience Union. All Right Reserved.

Crustal movements due to the seismic motions observed in Kobe

*Atsushi Mukai[1]

1. Faculty of Urban Management, Fukuyama City University

Strain changes due to the source processes of the 2011 off the Pacific coast of Tohoku earthquake (M9.0) and the 2018 northern Osaka earthquake (M6.1) were observed by using the Ishii-type three-component strainmeter at Rokko-Takao station of Kyoto University in Kobe (Mukai et al., 2020). This station is equipped with the extensometers as well as the strainmeter, and one extensometer is installed at the nearby Rokko-Futatabi station. Strain changes observed by those extensometers significantly contained the changes due to the source processes as well. We can get some information about a source process by investigating the observational data of strainmeters and extensometers installed in an underground tunnel away from the focal region.

Rokko-Takao station passes through the fracture zone of Manpukuji fault. In this station, the continuous observation of crustal movements have been performed by using the Ishii-type three-component strainmeter, the extensometers, the water-tube tiltmeters, the pore pressure meters and so on. The maximum principal strain of extension in the east-northeast direction increased at nearly constant rate for about 30 seconds just after the arrival of the seismic waves of the 2011 earthquake. In addition, just after the arrival of the seismic waves of the 2018 earthquake, the maximum principal strain in the east-northeast direction increased for about one second and kept constant for the following two seconds. These principal strain changes agreed with the calculated ones based on the source processes reported by the Meteorological Agency and Disaster Prevention Research Institute, Kyoto University (Mukai et al., 2020). It is considered that we could detect the strain changes due to the time development of co-seismic fault slips, that is, the source process by using the strainmeter.

Three extensometers in the direction of N69^{o}E are installed in Rokko-Takao station. Rokko-Futtabi station about 0.5km south of Rokko-Takao station is equipped with one extensometer in the direction of N9^{o}W. These extensometers observed the increase of the strain changes at nearly constant rate just after the arrival of the seismic waves of the above earthquakes as the case of the strainmeter, and the observed strain changes agreed with the calculated ones based on the source processes. This shows that we can confirm a source process by using the crustal movements observed by strainmeters and extensometers installed in the underground tunnel.
Rokko-Takao station and Rokko-Futatabi station are equipped with some water-tube tiltmeters as well. Although these tiltmeters respond slowly to the inclined ground, the tilt changes at nearly constant rate could be observed with the water-tube tiltmeters for several 10 seconds just after the 2011 earthquake as a result of the long source process. In this study, I investigated the crustal movements due to the source processes observed by the water-tube tiltmeters as well as the strainmeter and the extensometers.

Keywords: crustal movements, source process

©2021. Japan Geoscience Union. All Right Reserved.

[J] Poster | S (Solid Earth Sciences)：S-SS Seismology

Thu. Jun 3, 2021 5:15 PM - 6:30 PM JST | Thu. Jun 3, 2021 8:15 AM - 9:30 AM UTC | Ch.10_2

[S-SS06] Statistical seismology and underlying physical processes

convener:Yasuhiro Yoshida(Meteorological Research Institute, Japan Meteorological Agency)

This session aims to improve our understanding on seismicity. Any contribution on behavior of earthquakes as a cluster, such as regional seismicity and aftershocks, are welcomed. We also welcome contribution on temporal and spatial interactions that control seismicity, and tectonic processes, and geological and thermal structures that regulate seismicity.

[SSS06-P01] Accuracy improvement of DONET seismometer orientations estimated from seismic waveforms

*Shuichiro Yada[1], Takehiro Nishiyama[1], Keisuke Ariyoshi[1], Yojiro Yamamoto[1], Masaru Nakano[1], Kentaro Sueki[1], Takane Hori[1], Narumi Takahashi[2,1] (1.Japan Agency for Marine-Earth Science and Technology, 2.National Research Institute for Earth Science and Disaster Resilience)

[SSS06-P02] A preliminary study on data quality characterization for the DONET seismic catalogue

*Kazuyoshi Nanjo[1,2,3], Keisuke Ariyoshi[4], Narumi Takahashi[4,5], Shuichiro Yada[4], Yojiro Yamamoto[4], Takane Hori[4] (1.University of Shizuoka, 2.Shizuoka University, 3.Institute of Statistical Mathematics, 4.Japan Agency for Marine-Earth Science and Technology, 5.National Research Institute for Earth Science and Disaster Resilience)

[SSS06-P03] Aftershock activity of the 2015 M7.1 earthquake and back-arc rifting in the northern Okinawa Trough

*Hirotsugu Yanagida[1], Yukihiro Nakatani[2], Hiroshi Yakiwara[2], Shuichiro Hirano[1], Reiji Kobayashi[1], Yusuke Yamashita[3], Takeshi Matsushima[4], Hiroshi Shimizu[4], Kodo Umakoshi[5], Masanao Shinohara[6] (1.Graduate School of Science and Engineering, Kagoshima University, 2.Nansei-Toko Observatory for Earthquakes and Volcanoes, Kagoshima University, 3.Disaster Prevention Research Institute, Kyoto University, 4.Institute of Seismology and Volcanology, Faculty of Science, Kyushu University, 5.Graduate School of Fisheries and Environmental Sciences, Nagasaki University, 6.Earthquake Research Institute, the University of Tokyo)

[SSS06-P04] Microseismic Monitoring and Stress Inversion: before the 2018 Mw 6.4 Hualien earthquake and 2019 M_L 6.0 Ilan earthquake

*Wei-Jhe Wu[1], Chein-Min Su[1], Strong Wen[1], Yi-Heng Li[2], Chun-Rong Chen[2], Chau-Huei Chen[1] (1.National Chung Cheng University, 2.Industrial Technology Research Institute)

[SSS06-P05] Aftershock activity and its duration following inland earthquakes in Japan

*Taichi Honda[1], Takuji Yamada[2] (1.Ibaraki University, 2.Faculty of Science, Graduate School of Science and Technology, Ibaraki University)

[SSS06-P06] Whether the change in shear strain energy causes change in *b* value? Case study for the 2016 Kumamoto Earthquakes and the interplate coupling along the Nankai Trough

*Kohei Nagata[1], Akemi Noda[1], Koji Tamaribuchi[1], Fuyuki Hirose[1] (1.Meteorological Research Institute)

[SSS06-P07] Inter-plate aseismic slip determined from teleseismic similar earthquakes recorded by the Japanese seismic network

*Toshihiro Igarashi[1], Aitaro Kato[1] (1.Earthquake Research Institute, University of Tokyo)

[SSS06-P08] Seasonal variations in crustal seismicity and surface load

*Taku Ueda[1], Aitaro Kato[1] (1.Earthquake Research Institute, the University of Tokyo)

Accuracy improvement of DONET seismometer orientations estimated from seismic waveforms

*Shuichiro Yada[1], Takehiro Nishiyama[1], Keisuke Ariyoshi[1], Yojiro Yamamoto[1], Masaru Nakano[1], Kentaro Sueki[1], Takane Hori[1], Narumi Takahashi[2,1]

1. Japan Agency for Marine-Earth Science and Technology, 2. National Research Institute for Earth Science and Disaster Resilience

We re-estimated DONET seismometer orientations with 9 years of seismic observation data during the year between 2011 and 2020. With this study, we obtained one digit smaller standard errors of estimated seismometer orientations compared to the former study, thanks to the longer analysis period.

In 2012, Nakano et al. have firstly estimated DONET1 seismometer orientations by the 3 types of analysis method as follows: [1]
correlations of long-period seismic waveforms with land seismometer observation direction of P-wave first motion for distant earthquakes particle motions of airgun signals
This study shows that the orientation difference compared to the measurement data of ROV video is up to 10 degrees for the most seismometers, while the difference comes up about 50 degrees for some others.

Further, Nakano reinforced the information of estimated orientations of seismometers after the construction of DONET2 in 2017 using the method (1) and (2) described in Nakano et al. (2012) as above. Nakano also re-estimated the seismometer orientations of DONET1 with this study. [2]

In this study, Nakano shows that the obtained standard errors of estimated seismometer orientations is around 1 to 2 degrees. However, for some seismometers, estimated orientation figures are considered to have a few degrees of error, because of insufficient distant earthquake event that were available during the study. Since DONET2 construction completed in the middle of this study, enough observation period could not be available for these seismometers.

Therefore, it has been expected to re-estimate the DONET seismometer orientations with longer observation period and with sufficient distant earthquake events that can be used for the analysis.
We re-estimated DONET seismometer orientations by the method (2) described in Nakano et al. (2012) with 9 years of DONET data and obtained the latest figures of estimated orientation after the replacement of seismometer at observation point KMC11 in June 2018. We confirmed that the obtained orientations are basically consistent with the previous studies, e.g. Nakano et al. (2012) and Nakano (2017). Also, 9 years of DONET data enables us to obtain the standard errors of estimated orientation with the order of 0.1 degree for most seismometers. We hope that the most up to date and more accurate figures of estimated DONET seismometer orientations will help the concerned scientists and researchers for their studies.

[1] Masaru Nakano, Takashi Tonegawa, and Yoshiyuki Kaneda. Orientations of DONET seismometers estimated from seismic waveforms. JAMSTEC Rep. Res. Dev., Volume 15, September 2012, 77-89

[2] Masaru Nakano, Orientations of DONET2 seismometers estimated from seismic waveforms, JpGU-AGU Joint Meeting 2017, STT59-P03

©2021. Japan Geoscience Union. All Right Reserved.

Keywords: Ocean-bottom seismometer, Nankai trough, DONET, Seismometer orientation

©2021. Japan Geoscience Union. All Right Reserved.

A preliminary study on data quality characterization for the DONET seismic catalogue

*Kazuyoshi Nanjo[1,2,3], Keisuke Ariyoshi[4], Narumi Takahashi[4,5], Shuichiro Yada[4], Yojiro Yamamoto[4], Takane Hori[4]

1. University of Shizuoka, 2. Shizuoka University, 3. Institute of Statistical Mathematics, 4. Japan Agency for Marine-Earth Science and Technology, 5. National Research Institute for Earth Science and Disaster Resilience

To understand the characteristics of seismicity occurring in the source area of the Nankai Trough earthquake, research based on past observation data is indispensable, and a seismic catalogue that includes earthquakes in and around this area, if available, becomes one of them. It is also necessary to examine whether or not the data in such catalogue can be used for this research, and the results of evaluating the data quality will be the basic information for establishing the research direction. In this presentation, we report preliminary results from a study to evaluate qualities of the seismic catalogue including earthquakes observed by the DONET (Dense Oceanfloor Network system for Earthquakes and Tsunamis).

In this study, quality evaluation was carried out, using three techniques that utilize statistical properties of earthquakes. The first is based on the frequency-magnitude distribution of earthquakes. Using this technique, it is confirmed that larger earthquakes tend to have fewer numbers and smaller ones tend to have more numbers, and that this tendency is well correlated with the Gutenberg-Richter's law. The second approach is to plot the frequency of earthquakes as a function of hour. Natural earthquakes should occur day and night, and it is suggested that if the frequency of earthquake occurrence changes depending on time, it originates from anthropogenic causes (e.g., human activities and artificial earthquakes). The frequency was found to be approximately constant, which is considered to be due to few anthropogenic effects because the DONET is installed offshore. The third approach is based on the assumptions that the smaller magnitude is, the harder earthquake detection is, and that earthquakes with magnitudes, above a certain threshold value, are observed without missing. The threshold is called completeness magnitude, M_c, above which all earthquakes consider to be detected. This is an indicator of the quality assessment of seismic catalogues. As a result of the completeness analysis, we observed spatiotemporal variability of M_c, as observed for other seismic networks such as the ones used to create the catalogue maintained by the Japan Meteorological Agency.

This study on data quality characterization for the DONET catalogue is currently underway. Our results in the presentation will include the most recent findings.

Keywords: Seismicity, Statistical analysis, Data quality characterization, DONET, Nankai Trough

©2021. Japan Geoscience Union. All Right Reserved.

Aftershock activity of the 2015 M7.1 earthquake and back-arc rifting in the northern Okinawa Trough

*Hirotsugu Yanagida[1], Yukihiro Nakatani[2], Hiroshi Yakiwara[2], Shuichiro Hirano[1], Reiji Kobayashi[1], Yusuke Yamashita[3], Takeshi Matsushima[4], Hiroshi Shimizu[4], Kodo Umakoshi[5], Masanao Shinohara[6]

1. Graduate School of Science and Engineering, Kagoshima University, 2. Nansei-Toko Observatory for Earthquakes and Volcanoes, Kagoshima University, 3. Disaster Prevention Research Institute, Kyoto University, 4. Institute of Seismology and Volcanology, Faculty of Science, Kyushu University, 5. Graduate School of Fisheries and Environmental Sciences, Nagasaki University, 6. Earthquake Research Institute, the University of Tokyo

A magnitude (M) 7.1 earthquake occurred on November 14, 2015 at the western margin of the northern Okinawa Trough (OT). The northern OT is assumed to be in an incipient stage of the back-arc spreading [e.g., Iwasaki et al., 1990; Nakahigashi et al., 2004] and the mainshock–aftershock sequence of the 2015 event might be caused by the back-arc rifting. Although the aftershock activity seems to be distributed along the transition area from the East China Sea shelf to the OT [Nishizawa et al., 2019], their focal depths were not well constrained because of the onshore seismic station coverage. In order to better understand the tectonic process which controls the aftershock sequences, we precisely relocated their hypocenters and determined focal mechanisms using long-term ocean bottom seismometer (LOBS) data. We used data from seven onshore stations operated by Kagoshima University and Kyushu University and five LOBSs. We selected the aftershocks equal to or larger than M2.0 (M2.5 in part) in the Japan Meteorological Agency (JMA) catalog data from April 12, 2016 to April 16, 2017. Initial hypocenters were determined by HYPOMH program [Hirata and Matsu’ura, 1987] with manual picks of the P and S phases. Station corrections for the LOBSs were calculated using a time difference between P- and PS-converted wave arrivals for intermediate-deep earthquakes which occurred around Satsuma Peninsula at depths of 80–180 km. We applied the station correction values for all stations to both P and S arrivals, and then obtained the 453 final hypocenters. Due to the station correction, the mean of median values of travel-time residuals for P and S waves decreased from -43 msec to -1 msec and from 421 msec to -158 msec, respectively. We also determined 122 focal mechanisms based on estimating the strike and dip of the two nodal planes satisfying P-wave first-motion polarities.

Final relocated hypocenter distribution shows sharp linear trends, while the JMA one shows two broad clusters. From our results, we can clearly recognize the aftershock activity as three earthquake alignments: a 70-km-long trend along the NNE-SSW direction (Segment A), a 30-km-long trend along the WNW-ESE direction (Segment B) located on the north of Segment A, and a 20-km-long trend along the NNE-SSW trend (Segment C). The relocated focal depths are mainly distributed around 10 km in Segments A and B, and in the range of 0–15 km in Segment C, while the JMA ones are widely distributed within the range of 0–20 km. In Segment A, the spatiotemporal variation of seismicity indicates that the aftershocks seem to migrate from south to north, and most of the focal mechanisms show normal-fault types with NW-SE tension axes. In Segment B, the seismicity is relatively steady during the observation period, and left-lateral strike-slip-fault types with NW-SE tension axes are largely confirmed. In Segment C, an earthquake swarm activity started about half a year after the mainshock and lasted for about two months, and normal-fault types with NW-SE tension axes are dominant.

The activities in Segments A and C are mainly concentrated in the upper crust. These aftershocks might be caused by crustal extension related to the back-arc rifting in the northern OT because their focal mechanisms and the directions of the alignments are consistent with the existing normal faults imaged by the MCS survey [Nishizawa et al., 2019]. The left-lateral strike-slip faulting type events in Segment B could

©2021. Japan Geoscience Union. All Right Reserved.

be explained by along-axis variation in the back-arc spreading rate and presence of a transcurrent fault [Kakuta and Goto, 2002].

Keywords: OBS observation, the northern Okinawa Trough, back-arc rifting, aftershock activity

©2021. Japan Geoscience Union. All Right Reserved.

Microseismic Monitoring and Stress Inversion: before the 2018 Mw 6.4 Hualien earthquake and 2019 M_L 6.0 Ilan earthquake<gdiv></gdiv>

*Wei-Jhe Wu[1], Chein-Min Su[1], Strong Wen[1], Yi-Heng Li[2], Chun-Rong Chen[2], Chau-Huei Chen[1]

1. National Chung Cheng University, 2. Industrial Technology Research Institute

In 2020, we have been in difficulty at applying traditional research methods of Earth Science because of the COVID-19 outbreak. This study aims to make the most of the microseismic events, which are often excluded in stress-optical studies in the past, to gain extra information that was not able to measure in the past. Therefore, we will be able to acquire more detailed information on seismogenic structure and stress state in specific areas. Through 3D velocity structure re-location, ray-tracing technique, and stress inversion method of the entire event, this study will be able to apply seismic data more objectively and more accurately. This way will ensure the result more credibility due to the fact that the study avoids the influence of subjective consciousness and introduce the concept of confidence limits. The result shows that the seismogenic structure of Northeast Taiwan is under complex influences of Philippine Sea Plate subduction and Okinawa Trough open. The seismic activity is complicated. Through increasing microseismic data and microzonation, we will be able to understand thoroughly the distribution of the space in the seismogenic structure of that area. Furthermore, this will offer the background stress information that the study needs when we study stress-transfer in the future.<gdiv></gdiv>

Keywords: Northeast Taiwan, stress inversion, microseismic

©2021. Japan Geoscience Union. All Right Reserved.

Aftershock activity and its duration following inland earthquakes in Japan

*Taichi Honda[1], Takuji Yamada[2]

1. Ibaraki University, 2. Faculty of Science, Graduate School of Science and Technology, Ibaraki University

A major earthquake (main shock) will be followed by many smaller earthquakes, which are called aftershocks, around its source area. Aftershock activity of a large earthquake is clearly detectable even in the number of earthquakes in all over Japan as a function of their size (magnitude). The analysis of aftershock activity is also important for disaster mitigation. In this study, we analyzed the number and duration of aftershocks for inland earthquakes in Japan and investigated their relationships to the size of major earthquakes.
In order to distinguish aftershocks from the steady seismic activity, it is necessary to define aftershocks in space and time. We first picked up earthquakes shallower than 30 km in the circular area from the epicenter of a large earthquake with a radius of 10^(0.5Mw-2) km as aftershock candidates, where Mw indicates the moment magnitude of the large main shock. We then define the seismic activity within 180 days before the main shock as the regular activity and investigated the period until the earthquake activity becomes lower than n times of the regular one, which is regarded as the aftershock duration. We analyzed three values of n=3, 5, 7 and confirmed that the conclusion is independent of the n value. Earthquakes with Mj equal to 3 and greater were investigated in this study for confirming the detection completeness, especially immediately after the 2011 Tohoku earthquake, where Mj stands for the magnitude value determined by Japan Meteorological Agency.
Although the temporal aftershock activity seems not to have a clear relationship to the size of main shocks, we detected a strong correlation between the size of main shocks and the number of aftershocks. We also found a weak correlation of the aftershock duration to the size of main shocks. We also investigated the effect of the regular earthquake rate to the results of aftershock duration. Earthquakes in a high seismic rate were likely to have a shorter aftershock duration, but we found no clear correlation between activities of regular earthquakes and aftershocks. These results suggest that the aftershock activity will be affected by other factors in addition to the main shock size, including the complexity of the rupture characteristics and the depth of the fault plane.

Keywords: inland earthquakes, aftershock activity, duration of aftershock activity

©2021. Japan Geoscience Union. All Right Reserved.

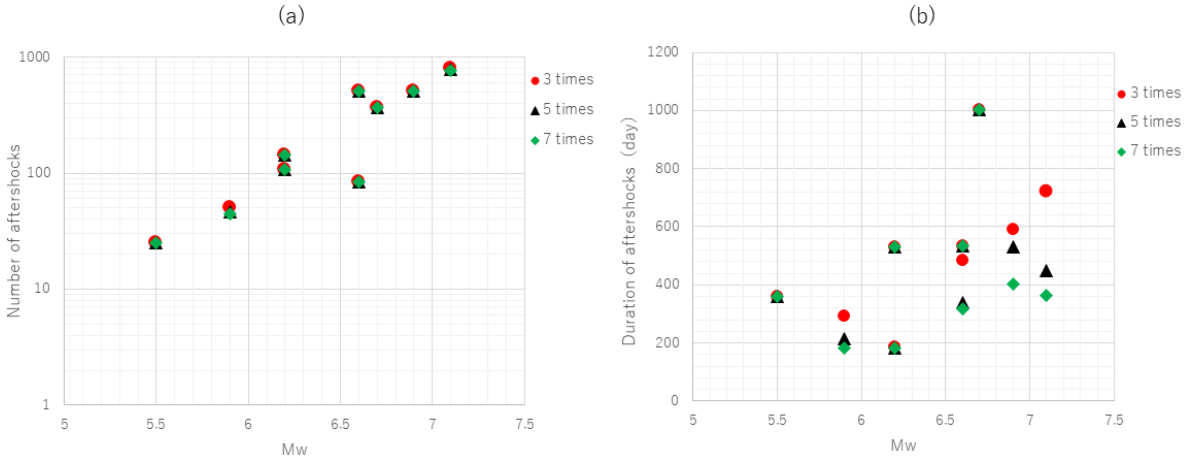


Figure1.
(a) Relationship between the magnitude of the main shock (Mw) and the number of aftershocks (magnitude 3.0 or higher). The symbols indicate results for three different values of n (refer to the main text).
(b) Duration of aftershocks as a function of the main shock size.

©2021. Japan Geoscience Union. All Right Reserved.

Whether the change in shear strain energy causes change in *b* value? Case study for the 2016 Kumamoto Earthquakes and the interplate coupling along the Nankai Trough

*Kohei Nagata[1], Akemi Noda[1], Koji Tamaribuchi[1], Fuyuki Hirose[1]

1. Meteorological Research Institute

The *b* value in the Gutenberg–Richter law, one of the typical parameters representing the characteristics of seismic activity, is often considered to depend on the differential stress from observations in laboratory experiments and regional differences in seismic activity (Scholz, 2015). Regarding the physical background of the stress dependence, it is reasonable to think that the larger the differential stress, the higher the probability of crack growth and the number of relatively large-scale earthquakes increase, as proposed by Scholz (1968). However, estimating the stress field including its absolute value involves great uncertainty, and it is difficult to estimate the differential stress on a scale corresponding to actual seismic activity. Therefore, when considering the use for real-time monitoring of earthquakes or earthquake forecasts, it would be unrealistic to discuss the change in *b* value focusing only on the relationship with the differential stress.

On the other hand, in recent years, changes in shear strain energy (ΔSSE, hereafter) have been proposed to be used as an index that quantitatively evaluates the degree of shear stress accumulation from relative changes in the stress field without assuming a fault plane (Saito et al., 2018; Matsu'ura et al., 2019; Terakawa et al., 2020; Noda et al., 2020). An increase in shear strain energy means an average increase in shear stress when fault planes are randomly oriented in the crust, and a relationship with an increase in the number of earthquakes has already been reported. If the increase in shear strain energy contributes the growth of rupture in earthquake faults, it is expected that the *b* value will decrease correspondingly.

Based on this view, we investigated the difference in the size distribution of seismic activity corresponding to ΔSSE due to the 2016 Kumamoto earthquakes (Noda et al., 2020). Estimates of shear strain energy have uncertainty mainly due to the uncertainty of the assumed effective friction coefficient. However, unless the effective friction coefficient is 0, the spatial distribution of increase and decrease of shear strain energy is almost constant except in the very vicinity of the fault. Therefore, we first, identified the region where the shear strain energy increased/decreased (positive/negative ΔSSE) in any case with the effective friction coefficient of 0.1 to 0.4. Then, for each region, the earthquakes that occurred in the region were extracted from the Japan Meteorological Agency unified seismic catalog. Using the extracted hypocenter data, *b* values before the Kumamoto earthquakes (January 2000-April 13, 2016), and those after the decrease of detectability due to the largest earthquake has almost recovered (April 16, 2016, 8:00 to August 2020) were estimated with some different lower limit of M(M_{th}, hereafter) in the range from 2.0 to 3.0.

As a result, in the positive ΔSSE region, the *b* value decreased after the Kumamoto earthquakes compared to before the earthquakes. The amount of decrease exceeded the standard error for almost all M_{th}. After the Kumamoto earthquake, the *b* value in the positive ΔSSE region was lower than the *b* value in the negative ΔSSE region for all M_{th}. This difference was slightly smaller than the standard error for most M_{th}. In the negative ΔSSE region, no clear change in *b* value was observed before and after the Kumamoto earthquake. There is no significant difference in the distribution of focal depths in each of

©2021. Japan Geoscience Union. All Right Reserved.

these comparison targets.

In addition to the above results, we investigate the relationship between ΔSSE due to interplate coupling along Nankai Trough (Saito et al., 2018) and the *b* value. Comparing the size distributions of seismic activity corresponding to the positive and negative of the shear strain energy change in the entire analysis region, the estimated *b* values tend to be slightly higher in the region where the shear strain energy change is negative. Though there are some parts that cannot be simply compared since the comparison is made over a wide area where the regional differences in *b* value can be affected not only by ΔSSE considered here but also by various causes such as focal depth and effective normal stress, on average, the results are consistent with the expectations. We would like to discuss these results together in the presentation.

Keywords: seismicity, shear strain energy, b value

©2021. Japan Geoscience Union. All Right Reserved.

Inter-plate aseismic slip determined from teleseismic similar earthquakes recorded by the Japanese seismic network

*Toshihiro Igarashi[1], Aitaro Kato[1]

1. Earthquake Research Institute, University of Tokyo

Similar earthquakes that occur in approximately the same location at different times have the potential to reveal the spatio-temporal changes in aseismic slip rate along plate boundaries. In this study, we identified similar earthquakes with moderate magnitudes in worldwide by calculating the cross-correlations of bandpass-filtered seismograms recorded by the Japanese dense seismic network. As a result, many similar earthquakes were detected along subduction plate boundaries, including the Japan–Kuril–Kamchatka–Aleutian, the Andaman–Sumatra–Java, and the Solomon–Vanuatu–Tonga region. Based on the spatio-temporal evolutions of similar earthquakes, we investigated the spatial distribution and temporal characteristics of inter-plate aseismic slip around the Pacific and Indian oceans. The estimated slip rates in several areas are higher than the relative velocity of the two converging plates. These areas correspond to regions where similar earthquakes with relatively short recurrence intervals were identified following megathrust earthquakes. We infer that these similar earthquakes were induced by postseismic slip along the plate boundary. In other regions, similar earthquake sequences have a constant recurrence interval of several years to several decades. Estimated slip rates are equal to or less than the relative velocities of plate motion, including the back-arc spreading rate. These observations indicate that the plate boundary faults in these regions are strongly locked. These results suggest that spatio-temporal changes in inter-plate aseismic slip around the world can be estimated by analyzing similar earthquake sequences. We believe that additional similar earthquakes will be detected by extending the analysis periods in areas where similar earthquakes were not identified in this study, resulting in slip rates with higher spatio-temporal resolution. A time series of stacked slip rates against the elapsed time since megathrust earthquakes initially increased rapidly following the rupture of each earthquake and then gradually decayed over periods of ~10 years, which correlates with after-slip progressing around the source areas. Around 30 years after megathrust earthquakes, the slip rate begins to increase with approaching the next megathrust rupture. This gradual increase in slip rate during the middle and later stages of the earthquake cycle may be due to an increase in stress levels that accumulate during tectonic loading. A similar earthquake catalog provides a valuable framework for understanding the long-term evolution of slip-rate during megathrust earthquake cycles.

©2021. Japan Geoscience Union. All Right Reserved.

Seasonal variations in crustal seismicity and surface load

*Taku Ueda[1], Aitaro Kato[1]

1. Earthquake Research Institute, the University of Tokyo

It has been reported that seismicity rate correlates with phenomena cause temporal changes of stress and fault strength at the surface and shallow subsurface, such as precipitation and irrigation (e.g., Heki, 2003: Amos et al., 2014). For example, in California, previous studies have indicated that seismicity rate varies seasonally in response to stress changes due to annual variations in hydrological loading (e.g., Amos et al., 2014; Johnson et al., 2017). Johnson et al. (2017) calculated the stress change which hydrological loading imposes on the fault plane based on GPS vertical displacement. They showed that seismicity in California is more likely to occur when shear stress increases. The seasonal variations in seismicity in Japan have also been pointed out, and its relationship to snow loading and precipitation has been discussed as the plausible cause (e.g., Heki, 2003; Ueda and Kato, 2019). However, few studies have directly compared the seasonal variations in seismicity with the stress changes brought by surface loading.

In this study, we estimate the spatial and temporal distribution of surface load from the vertical displacement data in the inland Tohoku region and investigate the relationship between the stress change by the surface load and the timing of earthquake occurrence. First, we extract the seasonal variation component from the vertical displacement of the GEONET F5 solution (2017/1/29-2020/5/2) by excluding transient changes such as earthquakes and postseismic deformation using the method proposed by Bedford and Bevis (2018). Then, we calculate the spatial and temporal distribution of surface load using the extracted seasonal variation components according to Johnson et al. (2017). Then, we compute the stress changes at the earthquake occurrence using the observed focal mechanism to quantitatively evaluate the relationship between earthquake occurrence and seasonal stress changes.

©2021. Japan Geoscience Union. All Right Reserved.

[J] Poster | S (Solid Earth Sciences)：S-SS Seismology

Thu. Jun 3, 2021 5:15 PM - 6:30 PM JST | Thu. Jun 3, 2021 8:15 AM - 9:30 AM UTC | Ch.11_1

[S-SS07] Crustal Structure

convener:Mikiya Yamashita(National Institute of Advanced Industrial Science and Technology)

The aim of this session is to cover seismological and geophysical studies on the Earth's crust and uppermost mantle. Contribution on seismological and geophysical structure of the crust, processes that develop in the crust which include earthquakes, volcanoes and geological descriptions of the crust are welcomed. We also welcome theoretical and methodological studies that will serve as basics in such explorations.

[SSS07-P01] Local variations of seismic scattering-attenuation structure around the volcanic front in Hokkaido

*Kiyoshi Yomogida[1], Hidekatsu Masuda[2], Takahiro Shiina[3], Kei Katsumata[4] (1.Department of Earth and Planetary Dynamics, Graduate School of Science, Hokkaido University, 2.Earth and Planetary Dynamics, Faculty of Natural History Sciences, Graduate School of Science, Hokkaido University, 3.National Institute of Advanced Industrial Science and Technology, 4.Institute of Seismology and Volcanology, Hokkaido University)

[SSS07-P02] Study of the delamination structure at the southern end of the Hidaka collision zone-Examination using numerical calculation-

*Masahiro Shimazaki[1], Noriko Tsumura[2] (1.Graduate School of Science and Engineering, Chiba University, 2.Graduate School of Science, Chiba University)

[SSS07-P03] Three-dimensional resistivity modeling in the eastern Iburi district, Hokkaido

*Ryo Ito[1], Takeshi Hashimoto[1], Tomohiro Inoue[1], Makoto Uyeshima[2], Hiroshi Ichihara[3], Yusuke Yamaya[4] (1.Graduate School of Science, Hokkaido University, 2.Earthquake Research Institute, The University of Tokyo, 3.Graduate school of environmental studies, Nagoya University, 4.National Institute of Advanced Industrial Science and Technology)

[SSS07-P04] Measurement of seismic velocity anisotropy in the Tohoku region, NE Japan by shear wave splitting analysis (3)

*Tatsuya Mizuta[1], Tomomi Okada[1], Martha Savage[2], Ryota Takagi[1], Keisuke Yoshida[1], Shin'ichi Sakai[3], Mako Ohzono[3,9], Masahiro Kosuga[4], Yoshiko Yamanaka[5], Hiroshi Katao[6], Takeshi Matsushima[7], Hiroshi Yakiwara[8], Takashi NAKAYAMA[1], Satoshi Hirahara[1], Toshio Kono[1], Toru Matsuzawa[1], _ Group for the aftershock observations of the 2011 off the Pacific coast of Tohoku Earthquake (1.Tohoku Univ., 2.Victoria University of Wellington, 3.Tokyo Univ., 4.Hirosaki Univ., 5.Nagoya Univ., 6.kyoto univ., 7.kyushu Univ., 8.Kagoshima Univ., 9.Hokkaido Univ.)

[SSS07-P05] Velocity structure of the uppermost mantle beneath central Japan

*Akio Katsumata[1] (1.Faculty of Sustainable Design, University of Toyama)

[SSS07-P06] Seismological structure revealed by regional deep-event records beneath the Kii peninsula

*Yasunori Sawaki[1], Takuo Shibutani[2], Yihuan Ruan[1], Yoshihiro Ito[2] (1.Graduate School of Science, Kyoto University , 2.Disaster Prevention Research Institute, Kyoto University)

[SSS07-P07] Deep crustal seismicity in Hiroshima Prefecture

*Azusa Shito[1] (1.Okayama University of Science)

[SSS07-P08] Seismic imaging of the subducting Kyushu-Palau ridge in relation to the distribution of tectonic tremors

*Yanxue Ma[1], Kimihiro Mochizuki[1], Rie Nakata[1], Seiichi Miura[2], Yasuyuki Nakamura[2], Ryuta Arai[2], Gou Fujie[2], Yuka Kaiho[2], Shuichi Kodaira[2] (1.Earthquake Research Institute, University of Tokyo, 2.Japan Agency for Marine-Earth Science and Technology)

[SSS07-P09] **Analysis of JAMSTEC Seismic Survey Database site**

*Yuka Kaiho[1], Seiichi Miura[1], Ayako Nakanishi[1], Tetsuo No[1], Kaoru Takizawa[1], Yasuyuki Nakamura[1], Gou Fujie[1], Koichiro Obana[1], Shuichi Kodaira[1] (1.Japan Agency for Marine-Earth Science and Technology)

Local variations of seismic scattering-attenuation structure around the volcanic front in Hokkaido

*Kiyoshi Yomogida[1], Hidekatsu Masuda[2], Takahiro Shiina[3], Kei Katsumata[4]

1. Department of Earth and Planetary Dynamics, Graduate School of Science, Hokkaido University, 2. Earth and Planetary Dynamics, Faculty of Natural History Sciences, Graduate School of Science, Hokkaido University, 3. National Institute of Advanced Industrial Science and Technology, 4. Institute of Seismology and Volcanology, Hokkaido University

Inhomogeneous seismic structures of various scales exist in and above a subducting plate. Especially for S waves in a frequency range of higher than 1 Hz, the observed waveforms are affected by scattering and attenuation by small-scale inhomogeneous structures. As a result, a wavepacket, generally called coda wave, is formed after the direct S wave, but their features are far from the standard of monotonically decaying in time. The envelope of an S waveform passing through the strong heterogeneous region in the subduction zone has its peak time delayed relative to the expected time of the direct wave, and its duration is generally long, forming a spindle-shaped waveform. Peculiar waveforms are observed especially near the volcanic front. In Kanto and Tohoku regions of Japan, large difference in waveform characteristics has been clearly detected at their volcanic front as a sharp vertical boundary. The characteristics of their fine heterogeneous structures have been studied. For example, characteristic S coda waves are observed with a high frequency component of 8 Hz or higher (Shiina et al., 2021).

In this study, we analyzed S waveforms recorded at stations in Hokkaido, Japan, for deep intraplate earthquakes. The frequency dependency of their S wave envelopes is strong on the north side of volcanic front but weak on its vicinity. We also investigated the spatial variation of S wave envelopes along the volcanic front, in addition to across the front. The arrival delays of envelope peaks are generally small in the central Hokkaido area including the Hidaka mountains while those in the eastern area of Shiretoko Peninsula shows similar characteristics to the Tohoku region. In contrast, the volcanic front near Lake Akan appears to be a sharper discontinuity than in the other regions, that is, there exist highly complex structures with small scales together with a distinctive volumetric body of intensive seismic attenuation.

Keywords: small-scale heterogeneities, scattering, attenuation, volcanic front

©2021. Japan Geoscience Union. All Right Reserved.

Study of the delamination structure at the southern end of the Hidaka collision zone -Examination using numerical calculation-

*Masahiro Shimazaki[1], Noriko Tsumura[2]

1. Graduate School of Science and Engineering, Chiba University, 2. Graduate School of Science, Chiba University

Hidaka Collision Zone (HCZ) is located in the central and southern part of Hokkaido where the Kuril forearc dragged by oblique subduction of the Pacific plate has collided with the Northeastern Japan arc. From upper to upper part of the Kuril’s arc lower crust have been thrusted up along the Hidaka Main Thrust (HMT) and are exposed to the surface. Various seismic surveys have been conducted for the purpose of investigating the subsurface structure of this region.

Reflection survey was carried out across the collision zone at the south end of the HCZ. From obtained depth section, Ito et al. (2013) showed that the lower crust of the Kuril arc is divided into a northeast-dipping ascending layer and a southwest-dipping descending layer at a depth of 23km. Meanwhile, Kita et al. (2012) estimated the three-dimensional P wave velocity structure in the same region by travel time tomography. They interpreted that crustal material of the Northeastern Japan arc has subdected under the thrusting Kuril arc.

In order to understand that how mass excess due to the collision between island arcs will be resolved, it is necessary to know the structure of the deep part of the collision zone. In this study, based on the two interpretations, we prepared two kind of structure models and compared the features of the actual seismic profiles and synthetic seismic profile, and examined which model is appropriate. One of models is a Delami model in which delamination occurs and delaminated lower part of the Kuril arc’s lower crust is continuously subducting to the Pacific plate and the other model is a Non-delami model in which the crustal material of the Northeastern Japan arc is subducting under the thrusting Kuril arc. Numerical calculation was performed using the two models under the similar conditions as in the actual survey, and a synthetic seismic profiles was created by applying the reflection method to the calculated waveforms. As a result, synthetic seismic profile for the Delami model, the features of the descending and thrusting reflectors are almost the same as the actual seismic profile. However, the depth of the reflector that can be traced by the reflected wave from the upper surface of the lower crust below the Kuril arc in the synthetic seismic profile appears deeper than the actual seismic profile. On the other hand, synthetic seismic profile for the Non-Delami model, it was found that only the feature of the thrusting reflector is matched. From this result, it is considered that the delaminated structure of the Kuril arc is needed to explain the result of the actual seismic profile. However, the reflected wave from the deeper extension of the Kuril’s arc subducting lower crust does not reach the receivers within the recording length and can not be imaged on the synthetic seismic profile.

Next, we performed another numerical calculation to know the location where we shot to confirm it if the deeper extension of the subducting Kuril’s arc crust is present. As a result, if we shot at the southwestern point of 45 km from the southwestern end of the actual reflection survey line, the reflected wave from the deeper extension of the Kuril’s arc subducting lower crust will reach about 24 seconds after the shooting to the recievers of the previous reflection survey settled on the land area.

Keywords: collision zone, Hidaka, reflection survey

©2021. Japan Geoscience Union. All Right Reserved.

©2021. Japan Geoscience Union. All Right Reserved.

Three-dimensional resistivity modeling in the eastern Iburi district, Hokkaido

*Ryo Ito[1], Takeshi Hashimoto[1], Tomohiro Inoue[1], Makoto Uyeshima[2], Hiroshi Ichihara[3], Yusuke Yamaya[4]

1. Graduate School of Science, Hokkaido University, 2. Earthquake Research Institute, The University of Tokyo, 3. Graduate school of environmental studies, Nagoya University, 4. National Institute of Advanced Industrial Science and Technology

A magnetotelluric (MT) survey was carried out in October to November in 2018 at 14 sites around the epicenter of the 2018 Hokkaido Eastern Iburi earthquake (September 6, 2018: Mw 6.6). We inverted full components of the MT impedance and tippers to estimate a three-dimensional (3-D) electrical resistivity model of this area by using the BIRRP (Chave and Thomson, 2004) and ModEM programs (Egbert & Kelbert, 2012). The main shock was located at a depth of nearly 40 km, and its aftershocks were concentrated in a depth range from 20 to 40 km. It is important to investigate the subsurface structure of the seismogenic zone of such an unusually deep intraplate earthquake. Previous studies have suggested that the low resistivity regions in the mid-crust under active faults are saturated with aqueous fluid, and that pore water pressure increases as the fluid migrates to the surroundings, driving earthquakes (e.g., Ogawa et al., 2001). A distinct low resistivity body was also found by Yamaya et al. (2017) at the depth of Ishikari-teichi-toen fault zone (ITFZ), the western neighbor of the target area of our study. They presumed that the pore space created by ductile deformation of the lower part of the thick sediment layer was saturated with fluid. In our 3-D model a low-resistivity layer of about 10 Ωm was found at a depth from the surface down to c.a. 10 km. Similar conductive thick sediments were reported in the previous studies that dealt with the MT data across the Hidaka collision zone (Ichihara et al., 2019), and that investigated the ITFZ (Yamaya et al., 2017). On the other hand, our 3-D model at present is not well constrained for the deeper part including the hypocenter region. In the next step, we are going to incorporate the data from the previous studies into our inversion model to better image an electrical structure in the deeper part.

Acknowledgments: M. Takada, K. Saito (HU), and M. Masuda (ERI, UT) contributed to the fieldwork and data acquisition in 2018. This study was supported by ERI JURP 2018-F2-04 for the MT instruments, and financially supported by MEXT KAKENHI Grant-in-Aid for Special Purposes #18K19952.

©2021. Japan Geoscience Union. All Right Reserved.

Measurement of seismic velocity anisotropy in the Tohoku region, NE Japan by shear wave splitting analysis (3)

*Tatsuya Mizuta[1], Tomomi Okada[1], Martha Savage[2], Ryota Takagi[1], Keisuke Yoshida[1], Shin'ichi Sakai[3], Mako Ohzono[3,9], Masahiro Kosuga[4], Yoshiko Yamanaka[5], Hiroshi Katao[6], Takeshi Matsushima[7], Hiroshi Yakiwara[8], Takashi NAKAYAMA[1], Satoshi Hirahara[1], Toshio Kono[1], Toru Matsuzawa[1], _ Group for the aftershock observations of the 2011 off the Pacific coast of Tohoku Earthquake

1. Tohoku Univ., 2. Victoria University of Wellington, 3. Tokyo Univ., 4. Hirosaki Univ., 5. Nagoya Univ., 6. kyoto univ., 7. kyushu Univ., 8. Kagoshima Univ., 9. Hokkaido Univ.

Shear wave polarization anisotropy in the Tohoku region was measured using shear wave splitting, in which shear wave splits into fast and slow shear waves when a seismic wave passes through an anisotropic elastic medium in the crust. The method used was the Multiple Filter Automatic Splitting Technique (MFAST; Savage et al., 2010). In this method, by inputting the three components of the seismic waveform, the optimum filter is selected from 14 prepared filters, and the orientation and magnitude of the anisotropy in multiple time windows are measured by the method of SC91 (Silver and Chan, 1991). Then, quality evaluation is performed using cluster analysis (Teanby et al., 2004) from values measured from multiple time windows. MFAST is a program that automates this sequence, so it can process large amounts of data automatically, and can obtain objective and reliable measurements.

The analysis was carried out throughout the Tohoku region, and further detailed analysis was performed in the area where earthquakes are swarming in Akita Prefecture. We used temporary earthquake observation data from the Group for the aftershock observations of the 2011 off the Pacific coast of Tohoku Earthquake (the Tohoku-oki earthquake) and others. After the 2011 off the Pacific coast of Tohoku Earthquake, the orientations of anisotropy measured at each station in the whole Tohoku region can be seen as either N-S orientation or E-W orientation. In the Pacific coast from Iwate to Miyagi, the N-S orientation dominated, and in the central inland area, the E-W orientation had a stronger tendency. In addition, at some stations, the observed orientations were different for the deep earthquakes in the subducting plate and for the shallow earthquakes in the crust. The delay time, which indicates the magnitude of anisotropy, tended to increase in the regions where earthquake swarms occurred.

In the inland area of Akita prefecture, the analysis was performed before and after the 2011 Tohoku-oki earthquake. Overall, NE-SW to N-S orientation was predominant, and the orientation did not change much before and after the Tohoku-oki earthquake. Especially around the region where earthquakes swarms occurred, the tendency of the orientation differs for each station, suggesting that the anisotropy changes on a small scale. The delay time was larger overall before and after the Tohoku-oki earthquake than in the whole Tohoku region. In comparison before and after the Tohoku-oki earthquake, both areas with increased delay time and with decreased were observed.

Keywords: anisotropy

©2021. Japan Geoscience Union. All Right Reserved.

Velocity structure of the uppermost mantle beneath central Japan

*Akio Katsumata[1]

1. Faculty of Sustainable Design, University of Toyama

In the central Japan area, complicated tectonic structure is recognized due to the interaction between the Pacific plate and the Philippine Sea plate. The volcanic front bends sharply in this area. There are many volcanoes with wide distribution such as Mt. Asama, those in northern Nagano Prefecture, and Hida mountain range. We estimated velocity structure of the uppermost mantle beneath this area with the tomography method. We used a method by Katsumata (2010), in which velocity structure was estimated from shallower parts to the deeper including depth distributions of discontinuities sequentially.

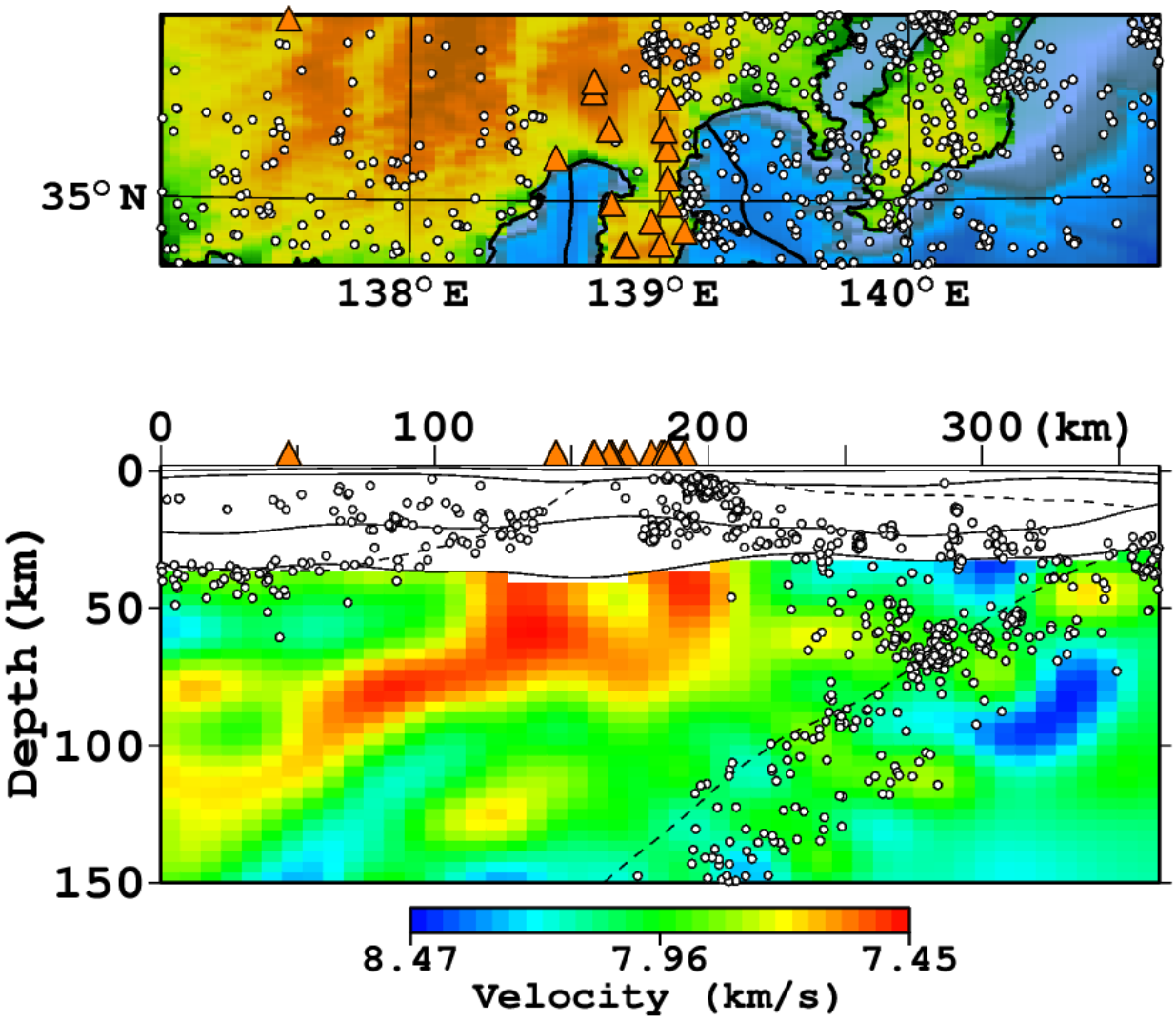
We describe the low velocity areas seen in the result of the tomographic analysis. Low velocity area is recognized beneath Niijima island. The low velocity area is distributed beneath the Philippine Sea plate rather than extending toward the Pacific Plate. In northeastern Japan, characteristic low velocity areas are recognized beneath the volcanic front which is considered to be related to the Pacific plate subduction. It is natural that the low velocity area beneath Izu Islands extends toward the Pacific plate. However, the appearance of the low velocity area is different from the expectation. Beneath the Izu Peninsula, the low velocity area seems to connect to the low velocity area beneath the western area of Shizuoka Prefecture down to about 100 km. It is similar to the low velocity area beneath Mt. Fuji (Figure). We recognize a large low velocity area beneath Yamanashi Prefecture at depth of about 100 km. Low velocity area is recognized beneath Mt. Yakedake above the Philippine Sea plate. Whereas it seems that low velocity area beneath Mt. Nasu extends toward the Pacific plate, low velocity areas beneath Mt. Myoko and Mt. Tateyama seems to extend downward to the west.

These low velocity distributions are just appearance seen in the result of a tomographic analysis, and interpretation on them are an unresolved problem.

Acknowledgements: We used the data provided by the Japan Meteorological Agency with the cooperation of the Ministry of Education, Culture, Sports, Science and Technology of Japan based on data from NIED, Hokkaido University, Hirosaki University, Tohoku University, The University of Tokyo, Nagoya University, Kyoto University, Kochi University, Kyushu University, Kagoshima University, the National Institute of Advanced Industrial Science and Technology, the Geospatial Information Authority of Japan, the Japan Agency for Marine-Earth Science and Technology, the Association for the Development of Earthquake Prediction, the Incorporated Research Institutes for Seismology, the Japan Meteorological Agency, and the governments of Aomori Prefecture, the Tokyo Metropolitan Government, Shizuoka Prefecture, and Kanagawa Prefecture.

Keywords: velocity structure of upper most mantle, volcanic front, Chubu district, Japan

©2021. Japan Geoscience Union. All Right Reserved.



©2021. Japan Geoscience Union. All Right Reserved.

Seismological structure revealed by regional deep-event records beneath the Kii peninsula

*Yasunori Sawaki[1], Takuo Shibutani[2], Yihuan Ruan[1], Yoshihiro Ito[2]

1. Graduate School of Science, Kyoto University , 2. Disaster Prevention Research Institute, Kyoto University

Elucidating seismological structure around subducting interfaces is essential to understand physical processes on slow earthquakes. Shibutani & Hirahara (2018, SSJ Fall Meeting) showed lateral variations on receiver function (RF) images beneath the Kii peninsula, southwestern Japan. We, here, calculate high-frequency RFs from seismic data recorded at temporary high-dense observation in the whole Kii peninsula from 2004 to 2013, especially using regional deep-focus earthquakes to image the Philippine Sea plate (PHS) around bimodal tremor sources: episodic tremor at the updip portion and continual tremor activity at the downdip portions.

Deep slow earthquakes such as tectonic tremor (tremor; Obara, 2002), low-frequency earthquakes (LFE; e.g., Katsumata & Kamaya, 2003), very-low-frequency earthquakes (VLFE; Ito et al., 2009) have occurred at the transition zone from the shallow brittle region to the deep stable slip region (e.g., Hirose & Obara, 2006) in southwestern Japan. Seismological structures from RFs have configured the shapes of the oceanic plate (e.g., Shiomi et al., 2008; Ueno et al., 2008), and constrained source regions of slow earthquakes; LFEs were located at the mantle wedge corner in the Tokai (Kato et al., 2010) and the western Shikoku (Shiomi et al, 2020). RF phases from the subducting interface become weak at downdip portions due to the entry to hydrous mantle wedge (Akuhara & Mochizuki, 2015; Kato et al., 2014).

Some clusters of continual tremors with minor bursts of shorter durations were also found at downdip portions of the tremor zone (Obara et al., 2010). Sawaki et al. (under review) estimated seismological structures of the subducting slab beneath the northeastern Kii peninsula from high-frequency RFs, and showed that the bimodal tremor source areas are under different seismological structures; the updip episodic tremor occurs beneath the forearc crust on near-lithostatic pore-fluid pressures and the downdip continual tremor occurs at the mantle wedge corner. However, the relationship between the lateral variation of seismological structures and the bimodal distribution of tremor has not been well examined. In this study, we investigate detailed seismic structures by multi-band RF analysis, using records of regional deep-focus earthquakes and teleseisms from the dense seismic observations in the Kii Peninsula from March 2004 to March 2013 (Nishimura et al., 2005, 2006).

For the calculation of RFs, we use the extended-time multitaper method (Shibutani et al., 2008) and the iterative deconvolution method (e.g., Ligorria & Ammon, 1999). Following Sawaki et al. (under review), we select records of the deep earthquakes within about 10˚ of epicentral distance, and remove traces that include direct *S* waves or converted *sP* waves. As result, cross-section RFs along the PHS subduction show structures of the PHS slab and the mantle wedge. The amplitudes of the PHS Moho decrease around the mantle wedge corner on the western survey lines. This may support the eclogitation of the basaltic oceanic crust, which increases the speed of the oceanic crust (e.g., Bostock et al., 2002), or indicate a fluid pathway of dehydrated fluid from the further deep Pacific slab (Kato et al., 2014; Umeda et al., 2012).

Keywords: Receiver function, Slow earthquake, Kii Peninsula, Fluid

©2021. Japan Geoscience Union. All Right Reserved.

©2021. Japan Geoscience Union. All Right Reserved.

Deep crustal seismicity in Hiroshima Prefecture

*Azusa Shito[1]

1. Okayama University of Science

The thickness of the seismogenic layer and the lateral variation are important parameters for understanding the generation mechanism of crustal seismicity and earthquake hazard analysis [e.g., Iio et al., 2002].

The spatial distribution of D90, which corresponds to the cutoff depth for shallow earthquakes is obtained for the entire Japan by Omuralieva et al. [2012]. They showed that the lateral variation of D90 ranges from about 5 km to 40 km. Some remarkably deep D90 areas are found in the fore-arc side of east Japan along the Pacific coast. In the study, the causes of these locally deep D90 are explained by cooling effect of the subducting oceanic plate. There is another locally deep D90 area found in Hiroshima Prefecture, in the southwest part of the Chugoku region in southwestern Japan. The locally deep D90 in Hiroshima Prefecture is also considered to be caused by the cooling effect of the subducting Philippine Sea plate. Beneath this area, the Philippine Sea plate subducts at a very shallow angle, which may effectively cool the above inland crust [Omuralieva et al., 2012].

In this study, we analyze the characteristics of the locally deep seismicity in Hiroshima Prefecture. The seismicity distributes in the area with radius 10 km, centered at 34.5N, 132.7E. The deepest earthquakes occurred at ~ 30 km depths. The most magnitudes of the earthquakes are smaller than 3.0. We also investigate seismic wave velocities in the source region and the surroundings of the locally deep seismicity. The Vp and Vs are relatively high in the southern part of the seismicity area. This may give additional insight to the cause of the locally deep seismicity.

Keywords: crust, seismicity , D90

©2021. Japan Geoscience Union. All Right Reserved.

Seismic imaging of the subducting Kyushu-Palau ridge in relation to the distribution of tectonic tremors

*Yanxue Ma[1], Kimihiro Mochizuki[1], Rie Nakata[1], Seiichi Miura[2], Yasuyuki Nakamura[2], Ryuta Arai[2], Gou Fujie[2], Yuka Kaiho[2], Shuichi Kodaira[2]

1. Earthquake Research Institute, University of Tokyo, 2. Japan Agency for Marine-Earth Science and Technology

Various types of slow earthquakes including slow slip events (SSEs), very low frequency earthquakes (VLFEs) and tectonic tremors occur around the boundary in the region off the Bungo-Channel located between the Kyushu and Shikoku Islands and their distributions appear to vary along depth of the subduction of the Philippine Sea Plate. Such variations are considered to reflect the frictional properties of the interface between the subducting and overriding plates. The morphology and the physical properties of the materials along the plate interface are the major controlling factors of the frictional properties. A subducted seamount has been identified from existing seismic reflection profiles and the magnetic anomaly map as a part of the Kyushu Palau Ridge. The VLFE and tremor activities have been found to occur around this subducted seamount (Yamashita et al., 2015; Tonegawa et al., 2020; Nakata et al., 2020). We conducted a marine active-source seismic survey in August-September, 2020 along four survey lines over the tremor activity region, NE-SW (HYU01), WNW-ESE (HYU02), and two NW-SE (HYU18 and 22) directions, using ocean bottom seismometers (OBSs) and a multi-channel seismic (MCS) hydrophone streamer. The HYU01 profile runs along the strike of the Nankai Trough, and the HYU02 runs over the subducting Kyushu-Palau Ridge in the along-dip direction of the Philippine Sea plate. We analyze and image seismic structures of the along-dip profile (HYU02) as well as the previously acquired KR0114-8 profile (Park et al., 2008) that intersects with HYU02 over the tremor activity region.

For wide-angle reflection / refraction analyses, we deployed 50 OBSs at a 2 km interval, and the 10,600-cubic-inch air gun array was fired at 50 and 200 m intervals along the line HYU02 during the KM20-05 research cruise using R/V *Kaimei* operated by Japan Agency for Marine-Earth Science and Technology (JAMSTEC). The data quality of the OBS records is good. We can trace the refraction first arrivals up to ~70 km offset, and some wide-angle reflections are identified. We will first apply the travel time inversion to reveal a 2D P-wave velocity structure along the subduction of the Kyushu-Palau Ridge. The reflection data were recorded by using 444-channel streamer (5.6 km long) with 12.5 m interval for HYU02 and a 156-channel streamer (4 km long) with 25 m interval for KR0114-8. The HYU02 reflection data are being processed using broadband techniques and pre-stack time/depth migration to generate detailed reflectivity images as deep as the plate interface (Nakata et al., 2021). We reprocess the KR0114-8 line using the same modern methodology and aim to derive the high-resolution image with the focus on the subducted seamount and associated deformation within the overriding plate. By combining the OBS velocity, reflection data and magnetic data, we discuss the relationships between the distribution of the tremor activity, the morphology and physical properties along the plate interface.

Keywords: Kyushu-Palau ridge, Nankai Trough, ocean bottom seismometers, multi-channel seismic, reflection profile

©2021. Japan Geoscience Union. All Right Reserved.

Analysis of JAMSTEC Seismic Survey Database site

*Yuka Kaiho[1], Seiichi Miura[1], Ayako Nakanishi[1], Tetsuo No[1], Kaoru Takizawa[1], Yasuyuki Nakamura[1], Gou Fujie[1], Koichiro Obana[1], Shuichi Kodaira[1]

1. Japan Agency for Marine-Earth Science and Technology

JAMSTEC provide seismic survey data and outcome through JAMSTEC Seismic Survey Database Website. We introduce database feature and trend of data request.This Website have two major rolls. One is data providing system and the other is publicity of research results.
We can provide survey data by using this website systematically after two years data moratorium. Besides, processed data, published results and derivative data such as seismic velocity model are available. Furthermore, analysis software download page and references list with survey area and cruise ID are in this Website. It is useful for publicity of research results.URL and DOI are follows.
http://www.jamstec.go.jp/obsmcs_db/e/
JAMSTEC (2004) JAMSTEC Seismic Survey Database. JAMSTEC. doi:10.17596/0002069
Our providing data is marine seismic survey data. Multi-Channel Seismic reflection (MCS) data and Ocean Bottom Seismograph (OBS) data can be requested from this Website. Data format of MCS data are SEG-D and SEG-Y. Data format of OBS are SEG-Y format about seismic survey, and SAC and WIN in earthquake observation. As a peculiarity of providing, huge size of survey dataset requires off-line data providing. Metadata about survey cruise and data image are available in Website.
During 17 years, we have over 150 case of data providing. About 15 % case are proposal by student. Number of data request by overseas users is gradually increasing after 2010. Seasonal trend of request number is not remarkable. Popular uses of data are reprocessing of raw data, test-data of analysis technique development, and utilization of continuous raw data are.Popular uses of processed MCS data and MCS profile image are seismic disaster field and preparation of IODP proposal. Derivative data, such as seismic velocity model, are use with various field of earth science.
Though analysis of data providing needs, trends of research project and site management, we will continue GUI maintenance and review of web system.

Keywords: MCS, OBS, Database

©2021. Japan Geoscience Union. All Right Reserved.

[J] Poster | S (Solid Earth Sciences)：S-EM Earth's Electromagnetism

Thu. Jun 3, 2021 5:15 PM - 6:30 PM JST | Thu. Jun 3, 2021 8:15 AM - 9:30 AM UTC | Ch.11_3

[S-EM14] Electromagnetic Induction in the Earth and Planetary Interiors, and Tectono-Electromagnetism

convener:Maki Hata(Earthquake Research Institute, the University of Tokyo), Mitsuru Utsugi(Aso Volcanological Laboratory, Institute for Geothermal Sciences, Graduate School of Science, Kyoto University)

This session welcomes papers on electromagnetism in the Earth and planetary interiors. The topics include but not limited to electromagnetic phenomena associated with earthquakes and volcanism, electrical conductivity structure, laboratory experiments, results of simulations, new equipment for observation, and methods of data analysis.

[SEM14-P01] A research report on the fundamental investigations of an electrical resistivity structure beneath Chugoku and Shikoku regions, southwestern Japan(2020)

*Ichiro Shiozaki[1], Tomofumi Uto[1], Makoto Uyeshima[2], Hideki Murakami[3], Naoto Oshiman[4], Yoshihisa Iio[4] (1.Graduate School of Engineering, Tottori University, 2.Earthquake Research Institute, The University of Tokyo, 3.Research and Education Faculty, Kochi University, 4.Disaster Prevention Research Institute, Kyoto University)

[SEM14-P02] 1-D forward calculation of tidally-induced magnetic variation in the Lau Basin: Comparison of calculation and seafloor magnetic data and sensitivity analysis

*Nakaya Tokuma[1], Takuto Minami[1], Nobukazu Seama[1] (1.Kobe University)

[SEM14-P03] Detection of magnetic field variation induced by tsunami

*Ai Kataoka[1], Ikuko Fujii[1] (1.Japan Meteorological Agency)

[SEM14-P04] Repeated aeromagnetic survey of Tarumae volcano using an unmanned autonomous helicopter

*Keiichi Shibuya[1], Takeshi Hashimoto[2], Tomoya Hayakawa[3], Keitaro Yoshikawa[4] (1.Graduate School of Science, Hokkaido University, 2.Faculty of Science, Hokkaido University, 3.Nippon Koei Co., Ltd., 4.Hokkaido Regional Development Bureau)

[SEM14-P05] A magnetic inversion method to recover the subsurface block structures based on L1-TV1 regularization

*Mitsuru Utsugi[1] (1.Aso Volcanological Laboratory, Institute for Geothermal Sciences, Graduate School of Science, Kyoto University)

A research report on the fundamental investigations of an electrical resistivity structure beneath Chugoku and Shikoku regions, southwestern Japan(2020)

*Ichiro Shiozaki[1], Tomofumi Uto[1], Makoto Uyeshima[2], Hideki Murakami[3], Naoto Oshiman[4], Yoshihisa Iio[4]

1. Graduate School of Engineering, Tottori University, 2. Earthquake Research Institute, The University of Tokyo, 3. Research and Education Faculty, Kochi University, 4. Disaster Prevention Research Institute, Kyoto University

The purpose of this study is to investigate the spatial and structural heterogeneity of the crust and upper mantle by conducting basic resistivity surveys in Chugoku and Shikoku regions in order to contribute to the mitigation of disasters due to earthquakes and volcanic eruptions.

So far, our research group has shown that there is a close relationship between resistivity structure and seismic activity in the San'in and Shikoku regions. For example, in the eastern part of the Sanin region, there are prominent earthquake occurrence areas and belt-shaped seismic activities along the coast of the Sea of Japan, including the Shikano-Yoshioka fault, which is the Tottori earthquake (1943, M = 7.2). MT surveys were conducted on survey lines that cross the active area, and the existence of conductive regions were clarified in the deep part of the crust under the seismogenic layer, which is resistive region, along the seismic active zone extending in the almost east-west direction. If an inland earthquake is caused by local stress concentration caused by an inhomogeneous structure directly under the seismic active zone (Iio, 2009), it is important to carefully examine the homogeneous structure and consider seismic activity and stress concentration / relaxation.

On the other hand, in the Shikoku region, the survey results mainly in the outer zone indicate that there is a remarkable conductive region in the upper crust, and that it is clearly related to aseismic region in the central and western regions. For a unified understanding of seismic phenomena, it is important to elucidate not only the activity pattern of slow earthquakes but also the environment and principle of occurrence (Ohara (2017)), so the regional characteristics of the overall resistivity structure must be deternmined. Fundamental investigation of resistivity structure for this purpose is required.

MT observation point surveys were conducted in the central and northern regions of the Chugoku region, taking into consideration the electromagnetic noise environment, topography, roads and land use conditions. In addition, the existing two survey line data in this area (for example, acquired in the area around Mt. Sanbe and the seismic gap in the eastern part of Shimane Prefecture) were examined. In particular, in the area around Mt. Sanbe, we reevaluated the data obtained from past observations and introduced Phase Tensor (PT) analysis (Caldwell et al. (2004)), which was not included in the previous analysis, to examine the 3-dimensionality of the structure and to compare the findings in the seismic gap area of eastern Shimane to investigate the spatial and electrical characteristics of these areas.

As a result, in the area around Mt. Sanbe, three-dimensional nature was implied for the some period bands, and it is pointed out that further investigation is necessary for the structure elucidation. At present, paying attention to this periodic zone, the strike of the resistivyty structure was estimated to be N50E from the direction of the PT and induction vector analysis, and Groom and Bailey (1989) decomposition was performed to try to extract the two-dimensional structure. From the results of structural analysis obtained

©2021. Japan Geoscience Union. All Right Reserved.

using the code of Ogawa and Uchida (1996), the crust was generally estimated as a high resistivity region.

The characteristics of this resistivity structure are in harmony with the research results of Shiozaki (1993). The estimated northern conduvtive / resistive boundary may be related to the 2018 Western Shimane Earthquake (M6.1) that occurred around the intersection of the two seismic zones pointed out by Asano et al. (1986). In addition, the seismic activity from around Mt. Sanbe to the southeast direction corresponds to the resistive region.

For the 3D resistivity structure analysis of the Shikoku region, we created the input data according to the format of the 3D analysis program code (Siripinvaraporn and Egbert (2009)) by utilizing and integrating the existing wideband MT observation data. In addition, ETOPO1 Ice Surface data published by NOAA was used for the land and sea distribution information of the created initial model.

Keywords: electrical resistivity, fundamental investigations, Chugoku and Shikoku regions

©2021. Japan Geoscience Union. All Right Reserved.

1-D forward calculation of tidally-induced magnetic variation in the Lau Basin: Comparison of calculation and seafloor magnetic data and sensitivity analysis

*Nakaya Tokuma[1], Takuto Minami[1], Nobukazu Seama[1]

1. Kobe University

Electrically conductive seawater moving in the geomagnetic main field causes electric currents in the ocean. In recent years, researches aiming at using this phenomenon to infer resistivity structures (Schnepf et al. 2014; 2015, Zhang et al. 2019) attract interests of researchers. It is known that the conventional MT method reduces estimation accuracy of its response function over periods around half a day to a day. The periods of ocean tides can complement this period band and the sounding depth corresponds to the upper mantle. Therefore, combination of MT and subseafloor sounding by the tidally induced magnetic variation possibly improves accuracy of resistivity values of the upper mantle compared to previous studies. Although Grayver et al. (2016) performed inversions of satellite tidally-induced magnetic data observed at the satellite altitude, there have been no reports of inversions of tidally-induced magnetic data observed at the seafloor. At the satellite altitude, one can observe only the poloidal component of the tidal magnetic variation. On the other hand, the seafloor magnetic data can observe both toroidal and poloidal components with shorter horizontal wave lengths compared to the satellite altitude. This implies that the usage of seafloor tidal magnetic variation may provide more accurate resistivity images with higher spatial resolution.

In this study, we developed a one-dimensional (1-D) forward calculation code for the tidally-induced magnetic variation, compared calculation results with seafloor magnetic data observed at the Lau Basin, and further investigated the sensitivity of the tidal magnetic variation to the resistivity structure, toward future inversions of seafloor tidal magnetic data. We focus only on the M2 component in this study. The tidal components of magnetic data were estimated by the least square method for sinusoidal functions. In our 1-D forward calculation, we used the analytical solution from Chave and Luther (1990), the tidal current model from Egbert and Erofeeva (2002), and the geomagnetic main field from IGRF-13 (Alken et al. in print). We prepared a 1-D resistivity structure from the two-dimensional structure in the Lau Basin inferred by Matsukura (2014, Master thesis of Kobe University). Comparison of the vertical component of the tidal magnetic field between the numerical and observation results shows discrepancy apparently correlated with the bathymetry, which implies the effect of bathymetry neglected in our 1-D calculation. On the other hand, the comparison of the horizontal components shows significantly larger amplitudes of the observed magnetic variation compared to the 1-D calculation. This could be due to toroidal magnetic component excited by the baroclinic current due to the internal tidal wave, which was not included in the adopted barotropic tidal model. We further investigated the sensitivity of the seafloor tidal magnetic variation in the Lau Basin to changes of the adopted 1-D resistivity structure. From shallow to deep part, we multiplied the original resistivity values by three within a 50 km thick zone and checked the change of amplitude of the vertical component of the tidal magnetic variation at the seafloor. As a result, we found that tidal magnetic variation in the Lau Basin is most sensitive to the depth of 250 to 300 km, where the amplitude enhanced by 2.5 %. In the presentation, we will explain details of our 1-D forward calculation, and report the results of comparison between the observation and numerical calculation and those of sensitivity analysis mentioned above.

©2021. Japan Geoscience Union. All Right Reserved.

Keywords: ocean tide, resistivity

©2021. Japan Geoscience Union. All Right Reserved.

Detection of magnetic field variation induced by tsunami

*Ai Kataoka[1], Ikuko Fujii[1]

1. Japan Meteorological Agency

1. Introduction

When a tsunami moves in the geomagnetic field, an electromagnetic field is induced by the dynamo effect (tsunami induced electromagnetic field, hereafter TIEM). Tyler (2005) shows that the vertical component of TIM is approximately linearly correlated with sea level. TIM appears in the vertical component before tsunami arrive (Tatehata et al., 2015) which shows a possibility to contribute to the tsunami warning. However, there are few reports on TIEM, and their characteristics are known little. Therefore, in this study, we try to investigate the characteristics of TIM at magnetic stations in the Pacific.

2. Analysis

We compared 1-minute values of the vertical geomagnetic field at a seaside station with 1-minute values of the tide level nearby. There are 9 pairs of those stations whose data are available online. Magnetic field data was provided by the JMA, GIS, EIR, and WDC, and tide level data was provided by the JMA, GIS, IOC, and NOAA for the 14 earthquakes which tsunamis have been observed in Japan since 2006.

The trend was removed by 60-minute moving average. Geomagnetic changes originating from the ionosphere and magnetosphere in the vertical component were estimated and removed using the horizontal magnetic field of the same observatory with a Kalman filter.

The significance of the correlation between the vertical geomagnetic field and the sea level change was judged by statistics. The criteria are (1) that both the first-order correlation coefficient in the time domain and the squared coherence in the frequency meets the 95% confidence limit of the uncorrelated test, and (2) that the first-order correlation coefficient has periodic change due to the predominant period of the tsunami.

3. Results

Significant correlation between vertical geomagnetic field and sea level were confirmed in 44 cases out of 98. When the maximum sea level change is 20 cm or less, the correlation tends to be insignificant. That suggests that 20 cm for the maximum wave height is a thresh hold to stably observe TIM. In 19 significant cases whose maximum sea level change are larger than 20 cm the amplitude of the vertical magnetic field is approximately proportional to the amplitude of the sea level change. Furthermore, there are regional differences in the stability of the correlation between geomagnetic field and sea level changes. The significant correlation is often seen on isolated islands in the ocean.

4. Calculation of TIM using tsunami numerical model

To explain causes of regional differences in the correlation, we theoretically calculate TIM from the sea level change and flow velocity obtained from a tsunami numerical model. In this study, we calculated for the 2010 Chile earthquake, which tsunami was observed at many stations.

©2021. Japan Geoscience Union. All Right Reserved.

One-minute values of the sea level change and flow velocity at every 0.025 degree throughout the Pacific were provided by a two-dimensional plane tsunami calculation model (Minami, personal communication).

Then, TIM were computed around 9 magnetic stations by using Biot-Savart’ s law (Tatehata et al., 2015).

The computed vertical magnetic field was correlated to the modeled sea level change at 7 stations, except 2 in the Southern Hemisphere.
At the 7 stations, the correlation is high for changes at periods longer than 20 minutes and for the tsunami arrival time. The amplitude ratio of TIM to sea level change was large at isolated islands in the Pacific, probably because the current density was available on many grid points, and the tsunami flow around the island tend to be a simple long wave. These imply that topography and land-sea distribution affect the regional differences in correlation. The amplitude ratio is larger than that of the observation. Imposed conditions and assumptions may cause the difference.

©2021. Japan Geoscience Union. All Right Reserved.

Repeated aeromagnetic survey of Tarumae volcano using an unmanned autonomous helicopter

*Keiichi Shibuya[1], Takeshi Hashimoto[2], Tomoya Hayakawa[3], Keitaro Yoshikawa[4]

1. Graduate School of Science, Hokkaido University, 2. Faculty of Science, Hokkaido University, 3. Nippon Koei Co., Ltd., 4. Hokkaido Regional Development Bureau

Aeromagnetic surveys using an unmanned autonomous helicopter have been conducted at active volcanoes in Hokkaido. In October 2020, we performed the fourth survey at Mt. Tarumae following the previous ones in 2011, 2012 and 2013. In this study, we analyzed the aeromagnetic data in 2020 and compared to the previous surveys in 2011 and 2013. Following the manual correction of the time stamp of the magnetometer for the 2020 data to maximize the correlation with the 2013 data, we obtained the temporal changes between them. The accuracy of the repeated flight was satisfactory as gaps between the actual flight trajectories were mostly within 5m. Then we obtained the temporal changes in the total magnetic field by taking the simple differences of the selected nearest points between the two surveys. We also calculated the temporal changes for the pair between 2011 and 2013 through the same procedure. Both the pairs showed a systematic field pattern suggesting a magnetizing trend beneath the summit lava dome. We accounted for the magnetic field changes in terms of a single dipole source beneath the lave dome with magnetic moment changes of 7.9×10^{6} Am^{2} and 8.0×10^{6} Am^{2}, respectively for the 2011-2013 and the 2013-2020 pairs. The source depth was almost the same (c.a. 400 m deep from the lava dome surface), but the horizontal location of the latter source shifted slightly southeast from the former. The almost same amount of the magnetic moment for the two periods suggested a slowdown in the magnetization rate after 2013. This result was consistent with the ground-based monitoring that was annually performed by the Japan Meteorological Agency and Hokkaido University (Hashimoto et al., 2018).

©2021. Japan Geoscience Union. All Right Reserved.

A magnetic inversion method to recover the subsurface block structures based on L1-TV1 regularization

*Mitsuru Utsugi[1]

1. Aso Volcanological Laboratory, Institute for Geothermal Sciences, Graduate School of Science, Kyoto University

Magnetic inversion is a popular method to obtain information about subsurface structures. However, this method has a serious limitation in that the linear equations to be solved become ill-posed and under-determined, and therefore, the uniqueness of the solution is not guaranteed. Consequently, several different models fit the observed data with the same accuracy. Conventional studies introduced a regularization technique based on a quadratic solution norm to reduce this non-uniqueness of the problem. However, these regularization methods impose a certain level of smoothness into the model, which cause the resultant model to be blurred. Sparse regularization was introduced in many recent magnetic inversion studies to obtain a focused model; some studies investigated methods to recover the blocky feature of subsurface structures with their sharp boundaries to facilitate model interpretation. To this end, this study attempts to use the combination of the L1 norm and total variation (TV) penalty. The TV penalty is widely used in geophysical inversion studies. Although this penalty is written by the L1 norm of the model differentiation, most conventional studies replace this penalty with an alternative quadratic penalty to make it easy to solve the penalized inversion problem. However, in this study, TV1, the original TV penalty written by the L1 norm, is directly incorporated into the inversion method to derive a model that emphasizes the structural boundaries [1]. To solve this L1-TV1 penalized problem, alternating direction method of multipliers (ADMM) is used, which is one of the simple, and efficient algorithm to solve a problem with multi-type L1 penalty terms. In this paper, a scheme of this L1-TV1 penalized magnetic inversion method is proposed, and its effectiveness and the improvements to computational efficiency are discussed. Further, the proposed inversion scheme was applied to a real aeromagnetic data aquired over the Sakainokami pluton of the North Kitakami belt in Tohoku area, northeast Japan, which is a granite plutonic body intruded on Early Cretaceous, and attempted to obtain subsurface magnetic susceptibility model. For this real data test, a part of the aeromagnetic data of the aeromagnetic survey database (AMSurvDB) [2], was used.

[1] Utsugi, M., 2021. Magnetic inversion method to recover the subsurface block structures based on L1-TV1 regularization, G.J.I.(submitted)
[2] Okuma, S. & Nakatsuka, T., 2005. Aeromagnetic Anomalies Database of Japan, Digital Geoscience Maps, 6, Geological Survey of Japan, AIST.

Keywords: 3D magnetic sparse inversion, L1 norm regularization and total variation, ADMM

©2021. Japan Geoscience Union. All Right Reserved.

[J] Poster | S (Solid Earth Sciences)：S-IT Science of the Earth's Interior & Techtonophysics

Thu. Jun 3, 2021 5:15 PM - 6:30 PM JST | Thu. Jun 3, 2021 8:15 AM - 9:30 AM UTC | Ch.12_2

[S-IT21] Innovation through the Integration of Solid Earth Science and Materials Science

convener:Kenji Kawai(Department of Earth and Planetary Science, School of Science, University of Tokyo), Jun Tsuchiya(Geodynamics Research Center, Ehime University), Ryuichi Nomura(Kyoto University), Satoshi Ohmura(Hiroshima Institute of Technology)

In recent years, collaborative studies on the physical and chemical properties of the Earth's interior, at depths from the mantle to the Earth's core, and on the formation and evolution of the Earth, have led to the elucidation of the dynamic behavior of deep Earth materials, such as core-mantle interaction and coevolution. This session will bring together researchers in Earth science and materials science to exchange information on the development of new technologies, which have the potential to revolutionize studies of the deep Earth's interior. These technologies include high-resolution electron microscopy, large-scale multi-scale computation, and machine-learning methods that allow us to design materials at an atomic scale.

[SIT21-P01] Theoretical approach to the pattern formation in spin systems via the time-dependent Ginzburg-Landau equation

*Ryoji Anzaki[1], Shin-ichi Ito[1,2], Hiromichi Nagao[1,2], Masaichiro Mizumaki[3], Masato Okada[4], Ichiro Akai[5] (1.ERI/UTokyo, 2.IST/UTokyo, 3.JASRI, 4.GSFS/UTokyo, 5.IINa, Kumamoto Univ.)

[SIT21-P02] Waveform inversion for localized 3-D transversely isotropic structure in the lowermost mantle beneath the western Pacific using Thai Seismic Array (TSAR) data

*Yuki Suzuki[1], Kenji Kawai[2], Robert J. Geller[2], Satoru Tanaka[3], Weerachai Siripunvaraporn[4], Songkhun Boonchaisuku[4], Noisagool Sutthipong[4], Yasushi Ishihara[3], Taweoon Kim[3] (1.Department of Earth and Planetary Science School of Science Tokyo Institute of Technology, 2.Department of Earth and Planetary Science School of Science University of Tokyo, 3.Japan Agency for Marine-Earth Science and Technology, 4.Faculty of Science, Mahidol University)

[SIT21-P03] Measurements of local stress using TEM in-situ obserbation

*Akira Miyake[1], Satoko Motai[1], Yohei Igami[1], Ryuichi Nomura[1] (1.Kyoto University)

[SIT21-P04] Measurements of local strain in minerals using electron nanoprobe

★Invited Papers

*Yohei Igami[1], Akira Miyake[1] (1.Kyoto University)

[SIT21-P05] Elastic properties of fine-grained polycrystalline clinopyroxene under high *P-T* conditions

*Yumiko Tsubokawa[1,2], Masahiro Ishikawa[2] (1.Kyushu University, 2.Yokohama National University)

[SIT21-P06] Effect of Al on stability and crystal strucutre of superhydrous phase B

*Sho Kakizawa[1,2], Toru Inoue[1,2], Hiroto Nakano[3], Minami Kuroda[4], Takahiro Kuribayashi[5], Naoya Sakamoto[6], Hisayoshi Yurimoto[7] (1.Graduate School of Advanced Science and Engineering, Hiroshima University, 2.Hiroshima Institute of Plate Convergence Region Research (HiPeR), 3.Geodynamics Research Center, Ehime University, 4.Graduate School of Sciences, Hokkaido University, 5.Department of Earth Science, Graduate School of Science, Tohoku University, 6.Creative Research Institution, Hokkaido University, 7.Department of Natural History Sciences, Hokkaido University)

Theoretical approach to the pattern formation in spin systems via the time-dependent Ginzburg-Landau equation

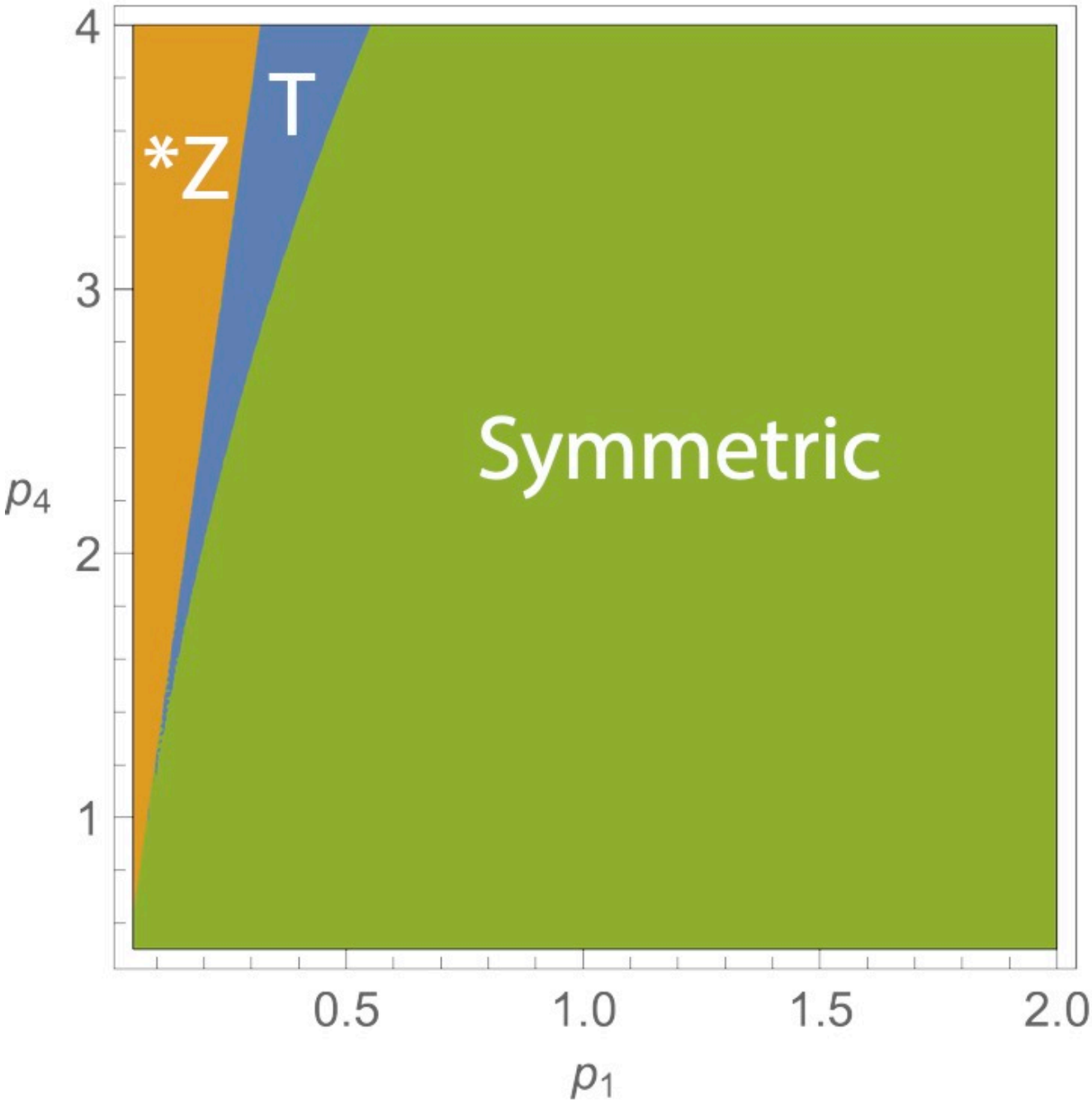
*Ryoji Anzaki[1], Shin-ichi Ito[1,2], Hiromichi Nagao[1,2], Masaichiro Mizumaki[3], Masato Okada[4], Ichiro Akai[5]

1. ERI/UTokyo, 2. IST/UTokyo, 3. JASRI, 4. GSFS/UTokyo, 5. IINa, Kumamoto Univ.

In this research, we study the two-dimensional classical spin model with the time-dependent Ginzburg-Landau equation as a model for magnetic thin materials. We classify the spatial patterns at the equilibrium (i.e., phases) using the spin $\mathbf{Z}_2$ and spatial symmetries. We approximate the equilibrium equation of the system using the RPSA [R. Anzaki *et al., Ann. Phys.* **353** 107 (2015)] and developed a method to predict the type of phases that are realized for each set of model parameters. The figure shows the phase diagram of the system for the system thickness (p_4) and dipole-dipole interaction intensity (p_1). In this figure, 'Symmetric', 'T', and '*Z' indecate the phases with no magnetization, no *total* magnetization but spatial patterns, and others, respectively. The quantities are normalized via coordinate-scale transformations. The finding of this research is accepted as a Regular Article in *Physical Review B*.

Keywords: magnetic materials, pattern formation, symmetry

©2021. Japan Geoscience Union. All Right Reserved.



©2021. Japan Geoscience Union. All Right Reserved.

Waveform inversion for localized 3-D transversely isotropic structure in the lowermost mantle beneath the western Pacific using Thai Seismic Array (TSAR) data

*Yuki Suzuki[1], Kenji Kawai[2], Robert J. Geller[2], Satoru Tanaka[3], Weerachai Siripunvaraporn[4], Songkhun Boonchaisuku[4], Noisagool Sutthipong[4], Yasushi Ishihara[3], Taweoon Kim[3]

1. Department of Earth and Planetary Science School of Science Tokyo Institute of Technology, 2. Department of Earth and Planetary Science School of Science University of Tokyo, 3. Japan Agency for Marine-Earth Science and Technology, 4. Faculty of Science, Mahidol University

Previous tomographic studies found a large-scale low S-velocity province (LLSVP) in the lowermost mantle beneath the Pacific. However, due to a lack of resolution it remained unclear whether the LLSVP consists of clusters of small-scale low-velocity anomalies or large-scale anomalies. In a previous study (Suzuki et al., PEPI, 2020) we inverted a new dataset from the Thai Seismic Array (TSAR; Tanaka et al., BERI, 2019) to infer the isotropic 3-D S-velocity structure beneath the western Pacific. We found a high-velocity anomaly extending vertically to 400 km above the core-mantle boundary (CMB) beneath the Philippine Sea and small-scale low-velocity patches with a diameter of ~300 km at the CMB beneath New Guinea. We hypothesized that a vertically continuous high-velocity anomaly could be the sinking Izanagi paleoslab, which subducted ~200 Ma, and interpreted small-scale low-velocity anomalies as a plume cluster that forms at the western margin of the Pacific LLSVP.
To obtain further geodynamical information, in this study we conduct waveform inversion for transversely isotropic structure. We infer high-resolution 3-D models of the S-velocity perturbation δVs and the anisotropy parameter $\delta \xi$ in the lowermost 400 km of the mantle. The inferred anisotropic structure is due to the deformation-induced alignment of the crystal caused by mantle flow for either Mg-perovskite, Mg-post-perovskite, ferropericlase, or a combination thereof because of the high-stress condition in the boundary layer of the mantle convection. When we assume the dominant glide system of each mineral under the lowermost mantle conditions given by previous experimental results, the inferred anisotropic structure shows that vertical flow (upwelling plumes and downwelling of paleoslabs) is dominant in the lowermost mantle beneath the western Pacific.

Keywords: Lowermost mantle, Anisotropy, Waveform inversion, Pacific LLSVP, Plume cluster, D″ region

©2021. Japan Geoscience Union. All Right Reserved.

Measurements of local stress using TEM in-situ obserbation

*Akira Miyake[1], Satoko Motai[1], Yohei Igami[1], Ryuichi Nomura[1]

1. Kyoto University

[Introduction] Extensive in-situ loading/ indentation experiments have been conducted inside a transmission electron microscope (TEM) to understand the nanomechanical properties of materials (e.g., Wang et al., 2015). In these studies, the stress on the sample were estimated just by dividing the applied load by the area loaded on and/or analyzed by the finite element method. In this study, we succeeded in measuring the stress state within a sample directly from the electron diffraction patterns of a deformed sample.

[Materials and Methods] A thin film of monocrystalline silicon with 100 nm thickness was prepared by a focused ion beam (FIB, Helios NanoLab G3 CX, Thermo Fisher Scientific). In-situ indentation/ compression tests were performed with a diamond indenter inside the chamber of TEM at Kyoto University (JEM-2100F, JEOL), under the load-controlled mode up to 40, 100, 200, and 500 μN (Hysitron PI95 TEM PicoIndenter, Bruker). The film with the crystal zone axis of approximately [01-1] was compressed on the (001) plane along the [001] direction. Diffraction patterns were taken before, during, and after the compression. Digital Microgarph (Gatan, Inc.) and ReciPro (developed by Y. Seto, http://pmsl.planet.sci.kobe-u.ac.jp/~seto/) were used for data analysis. The equation of state of Si by Pandya et al. (2012) was used to calculate the stress from the lattice strain.

[Results and Discussion] The results show that the lattice spacing parallel to the loading axis [001] reduced on compression. On the other hand, the lattice spacing of the [110] direction, perpendicular to the compression axis, did not change during compression. Calculated stresses along the compression axis were ~1.7 GPa at 40 μN, ~2.4 GPa at 100 μN, ~3.7 GPa at 200 μN and ~7.1 GPa at 500 μN, respectively. The lattice parameter along the [110] direction changed negligibly or expanded slightly. The pressure was estimated from the change of a cell volume as ~1.1 GPa at 200 μN, and ~1.4 GPa at 500 μN, assuming that there was no strain along the direction of incident electron beam. The local stress became small with the increase of the distance from the contact point of the indenter. Clarifying the detailed geometry of the contacting point is needed for more accurate analysis.

Wang et al., (2015) Scripta Materialia, 98, 40; Pandya et al. (2012) J. Phys.: Conf. Ser. 377 012097

Keywords: electron microscope, in-situ experiment, nano-deformation

©2021. Japan Geoscience Union. All Right Reserved.

Measurements of local strain in minerals using electron nanoprobe

*Yohei Igami[1], Akira Miyake[1]

1. Kyoto University

Interface/surface of minerals having complex textures frequently shows local strain, which more or less affects phase transitions and/or relevant micro-texture formations. In addition, strain locally remained in natural minerals may be key information to understand various geophysical events such as tectonics or meteorite impacts. There exist some measurement methods to determine strain in minerals, for example, X-ray diffraction or micro-laser Raman spectroscopy [e.g., 1,2], but higher spatial resolution/selectivity is required to precisely analyze specific regions in nanometer order. The high spatial resolution analysis would become also important for future challenging experiments to simulate extreme environments in the Earth because amount of such experimental products is frequently very small.
As for semiconductor devices of which miniaturization rapidly progresses, local strain is utilized to control electric function, thus some strain measurements with nanometric order have already been performed [e.g., 3]. In particular, diffraction imaging method which uses scanning electron nanoprobe to obtain many diffraction patterns from nanometric regions should be able to measure local strain precisely with corresponding high magnification images [4]. This would be effective to study mineral samples, but minerals have large diversity in phase, size, morphology and/or crystal orientation, whereas experimental conditions to study the semiconductor devices can be relatively limited. Because appearance of electron diffraction pattern varies sensitively to sample conditions, it would be important to establish experimental/analytical procedures of the method adequate for mineral samples.
In this study, we obtained and analyzed diffraction imaging datasets from mineral samples by scripting control of a transmission electron microscope (TEM) and a CCD camera. Illumination electron beam was adjusted to be mostly parallel with its spot size smaller than 10 nm in diameter, which gives spotty diffraction patterns and allows us to easily determine reciprocal basis of each illuminated point. Sample damage could be reduced because electron dose in the illumination condition is much smaller than that of the convergence beam generally used in STEM (scanning TEM) method. No damage textures or contaminations due to the experiments were observed in TEM images. The obtained datasets were analyzed to construct strain maps and diffraction-contrast images by virtual objective apertures with arbitrary shapes.

References

[1] Seto, Y. (2012) *Rev. High Press. Sci. Tech.* 22, 144–152.
[2] Enami, M., Nishiyama, T. and Mouri, T. (2007) *Am. Mineral.* 92, 1303-1315.
[3] Cooper, D., Denneulin, T., Bernier, N., Béché, A. and Rouvière, J. L. (2016) *Micron*, 80, 145-165.
[4] Ophus, C. (2019) *Microsc. Microanal.* 25, 563-582.

Keywords: electron microscopy, strain analysis

©2021. Japan Geoscience Union. All Right Reserved.

Elastic properties of fine-grained polycrystalline clinopyroxene under high *P-T* conditions

*Yumiko Tsubokawa[1,2], Masahiro Ishikawa[2]

1. Kyushu University, 2. Yokohama National University

Grain size may play an important role in determining the physical properties of rock-forming minerals under some conditions. Even though the occurrences of minerals with grain size of < 1 μm are limited, they might have a significant effect on geophysical processes due to its high surface area to volume ratio; for example, nanocrystalline forsterite is more compressible than forsterite with micron-scale grains due to the weakening of elastic properties of grain boundary and triple junction (Couvy et al., 2010; *PCM*). In this study, we demonstrated ultrasonic wave velocity measurements of polycrystalline clinopyroxene with submicron grain sizes under high *P-T* conditions, and compared its elastic properties with those reported from samples with much larger grain size.
Fine-grained polycrystalline clinopyroxene with average grain size of ~400 nm were sintered from pulverized clinopyroxene crystals ($Ca_{0.92}Na_{0.07}Mg_{0.93}$ $Fe_{0.01}Al_{0.06}Mn_{0.01}Si_2O_6$). The V_p and V_s values of the fine-grained clinopyroxene were measured up to 1.0 GPa and 640 ˚C for V_p and 750 ˚C for V_s with a piston-cylinder type high-pressure apparatus. At room temperature, V_p increases rapidly with increasing pressure up to 0.5 GPa, whereas it exhibit a gradual increase between 0.5 and 1.0 GPa, suggesting closure of porosity at > 0.5 GPa. The velocity increase at pressures from 0.5 to 1.0 GPa is ~1 %, and the velocity reduction at temperatures from 25 to 640 ˚C at 1.0 GPa is ~3-5 %. At 1.0 GPa and 640 ˚C, V_p of fine-grained polycrystalline is ~7.6 km/s, which is smaller than those of polycrystalline clinopyroxene with grain size of < 100 μm (Liebermann and Mayson, 1976; *PEPI*). The calculated bulk modulus for fine-grained clinopyroxene is relatively small, and this V_p difference may be attributed to this small value of bulk modulus in this study. This decrease of bulk modulus for fine-grained clinopyroxene is consistent with the grain-size-sensitive elastic behavior of nanocrystalline forsterite. According to our results, we found that fine-grained polycrystalline clinopyroxene exhibit low bulk modulus, causing the decrease in V_p and V_p/V_s, and this might be associated with the decrease of grain size to submicron scale.

Keywords: clinopyroxene, submicron, elastic velocity, piston-cylinder type high-pressure apparatus

©2021. Japan Geoscience Union. All Right Reserved.

Effect of Al on stability and crystal strucutre of superhydrous phase B

*Sho Kakizawa[1,2], Toru Inoue[1,2], Hiroto Nakano[3], Minami Kuroda[4], Takahiro Kuribayashi[5], Naoya Sakamoto[6], Hisayoshi Yurimoto[7]

1. Graduate School of Advanced Science and Engineering, Hiroshima University, 2. Hiroshima Institute of Plate Convergence Region Research (HiPeR), 3. Geodynamics Research Center, Ehime University, 4. Graduate School of Sciences, Hokkaido University, 5. Department of Earth Science, Graduate School of Science, Tohoku University, 6. Creative Research Institution, Hokkaido University, 7. Department of Natural History Sciences, Hokkaido University

We determined the stability and chemical composition of Al-bearing superhydrous phase B at 20–24 GPa and 1400–2000 ˚C to discuss the mechanism of water transport in the mantle transition zone and uppermost lower mantle at temperatures close to the mantle geotherm. Superhydrous phase B[$Mg_{10}Si_4O_{14}(OH)_4$] is one of the important dense hydrous magnesium silicates (DHMSs) in hydrous peridotite system for understanding the deep water cycle in the Earth’ s interior. It contained significant amounts of Al_2O_3, from 14 to 32 wt%, and Al-bearing superhydrous phase B remained stable, even at 2000 ˚C and pressures of approximately 20–24 GPa. Moreover, two types of superhydrous phase B with different chemical compositions coexisted at 20–24 GPa and 1600 ˚C. The Al_2O_3 and H_2O contents increased, and the MgO and SiO_2 contents decreased as the pressure and temperature increased up to 1600 ˚C. Above 1600 ˚C, the MgO and Al_2O_3 contents increased, and the SiO_2 and H_2O contents decreased as the temperature increased. We found two substitution mechanisms: (1) $2Mg^{2+} + Si^{4+} = 2Al^{3+} + 2H^+ + V_{Mg}$ (Mg site vacancy) $(2Mg^{2+} = Al^{3+} + H^+ + V_{Mg}):(Si^{4+} = Al^{3+} + H^+) = 1:1$, (2) $Si^{4+} + 16H^+ = 4Mg^{2+} + 4Al^{3+}$. The maximum H_2O content of Al-bearing superhydrous phase B is 11.1(3) wt%, which is ~1.9 times larger than that of the Mg-end-member. The crystal structures of the two coexisting superhydrous phase B values are expected to be slightly different from each other. The present results indicate that Al-bearing superhydrous phase B can be stable in a subducted slab with a high Al content compared to pyrolite (e.g, chlorite) at temperatures typical of the mantle transition zone and the lower mantle. Thus, water can be transported to the lower mantle by Al-bearing superhydrous phase B in the subducting slab, even at the typical mantle geotherm.

In addtion, we investigated the crystal structure of Al-bearing superhydrous phase B ($Mg_{8.1}Si_{2.0}Al_{1.9}H_{5.9}O_{18}$) by single crystal X-ray diffraction (XRD), Raman and Fourier Transform infrared spectroscopy (FT-IR) to determine the Al positions and to predict the H positions in Al-bearing superhydrous phase B. As a result of the crystal structure refinement, Al was clarified to be located in octahedral Mg1, Mg2, and Si1 sites in superhydrous phase B with *Pnnm* space group. The result is consistent with $2Mg^{2+} + Si^{4+} = 2Al^{3+} + 2H^+ + V_{Mg}$ substitution. The obtained FT-IR spectra, difference Fourier maps, and bond-valence considerations leaded to new H positions. They are located at (1) O6-H···O4, which is a part of AlO_6 octahedron, (2) O5-H···O3, which is the same as Mg-endmember superhydrous phase B, and (3) O4-H···O1, which is share edge of $Mg2O_6$ and $Mg4O_6$ octahedra.

Keywords: Earth's deep mantle, water, hydrous mineral, superhydrous phase B

©2021. Japan Geoscience Union. All Right Reserved.

[J] Poster | S (Solid Earth Sciences)：S-VC Volcanology

Thu. Jun 3, 2021 5:15 PM - 6:30 PM JST | Thu. Jun 3, 2021 8:15 AM - 9:30 AM UTC | Ch.13_1

[S-VC30] Volcanic and igneous activities, and these long-term forecasting

convener:Takeshi Hasegawa(Department of Earth Sciences, College of Science, Ibaraki University), Teruki Oikawa(GSJ, National Institute of Advanced Industrial Science and Technology), Daisuke MIURA(Department of Physical Science, Graduate School of Science, Osaka Prefecture University), Nobuo Geshi(Geological Survey of Japan, The National Institute of Advanced Industrial Science and Technology)

This session focuses on generation and accumulation processes of magmas, magma-crust interaction and degassing, and modes of eruption, long-term forecast of eruption, dispersal and emplacement of the volcanic products. The discussion spans petrological, geochemical, geophysical, and geological processes related with volcanic activity and products in the past, the present and the future.

[SVC30-P01] Yield strength obtained from lava flow and lava tube cave of Undara volcano

*Tsutomu Honda[1] (1.Vulcano-speleological Society)

[SVC30-P02] Survey on Fissure Cave and Lava Tube Cave in Kansuyama Lava Flow of Mt.Fuji

*Tsutomu Honda[1], Masaru Hatanaka[1], Takayoshi Katumata[1] (1.Vulcano-speleological Society)

[SVC30-P03] The origin of bimodal magmatism in the Okinawa Trough, Japan

*Arran Peter Murch[1], Kenichiro Tani[1], Takashi Sano[1], Shigekazu Yoneda[1] (1.National Museum of Nature and Science, Tsukuba, Ibaraki, Japan)

[SVC30-P04] Reinvestigation of Holocene eruption history of Nikko-Shirane Volcano, central Japan

*Yuki Kusano[1], Yoshihiro Ishizuka[1], Teruki Oikawa[1], Osamu Ishizuka[1] (1.Geological Survey of Japan, AIST)

[SVC30-P05] Construction of Geochemical database of Kikai Caldera magmas for understanding the magmatic evolution prior to caldera-forming eruptions

*Satoru Haraguchi[1,2], Kenta Ueki[2], Kenta Yoshida[2], Tatsu Kuwatani[2], Morihisa Hamada[2], Iona McIntosh[2], Takashi Miyazaki[2], Takeshi Hanyu[2] (1.Earthquake Research Institute, University of Tokyo, 2.JAMSTEC)

[SVC30-P06] Reconstruction of the volcanic history of Nakadake volcano in Kirishima volcano group, Kyushu, Japan (1)

*Yasuhisa Tajima[1], Atsushi Yasuda[2], Mitsuru Okuno[3] (1.Research & Development Center, Nippon Koei Co.,LTD., 2.Earthquake Research Institute, University of Tokyo, 3.Faculty of Science Department of Earth System Science, Fukuoka University)

[SVC30-P07] The effect of dissolved water induced by lithostatic pressure on lava migration

*Akio Goto[1] (1.Center for Northeast Asian Studies, Tohoku University)

[SVC30-P08] An attempt to detect volcanic materials of Ogasawara Ioto (Iwojima) Volcano from the core sample of the turbidite layers deposited in the Palace Bella Basin

*Masashi NAGAI[1], Takahiro Miwa[1] (1. Volcano Research Department, National Research Institute for Earth Science and Disaster Resilience)

Yield strength obtained from lava flow and lava tube cave of Undara volcano

*Tsutomu Honda[1]

1. Vulcano-speleological Society

[Introduction]

The Undara Cave is a huge lava tube system with a maximum height of 20 m and a maximum width of 32 m, formed on a gentle slope with an average inclination angle of 0.3 °,in a lava flow length of 160 km(Fig.1) which was erupted by Undara volcano 190,000 years ago[1,2]. The lava eruption temperature of Undara volcano is said to be 1170-1220 ℃, and the silicic acid weight fraction is 48.9wt% [1,2]. By using the published data of Atkinson et al.[1,2,3], the lava yield strength is estimated by two methods [4]: the lava flow stop condition and the lava tube formation limit condition.

[Yield strength obtained from the thickness of the Undara volcanic lava flow]

Table 1 shows the lava flow thickness, slope angle and yield strength obtained for each lava flow section. The column ① to ③ in Table1 are based on reference [1]. ④ is yield strength obtained from the values of column ② and ③. The yield strength was obtained from the lava flow stop condition [4]: $f_B = H (\rho g \sin\alpha)$. The high apparent yield strength f_B = 4.3 to 6.4x10^3 Pa may be due to lava inflation and/or lava superposition. The true lava yield strength is considered to be the lower yield strength f_B = 1.5 ~ 2.1x10^3 Pa.

[Yield strength obtained from the height of the cavity in Undara Cave]

Table 2 shows the cavity height, width, and slope angle of representative parts of the Undara cave system [3]. The columns ① to ⑤ in Table2 are based on the reference [3]. The column ⑥ is yield strength obtained from the values of ③ and ⑤. The longest among these caves, Bayliss cave and Barkers cave, clearly show the tube like structure[1]. Others are fragmentary caves that occupy a small part of the lava cave system due to the burial of the floor. As shown in ⑥ of Table 2, the yield strength by using the limit condition for lava tube cave formation [4]:$f_B = H (\rho g \sin\alpha) / 4$ is obtained from this cavity height and slope angle. Tayler cave, Bayliss cave, and Barkers cave show high yield strength, on the other hand, other small caves show low yield strength due to low cavity height with buried floor. It is considered that several layers of lava flow have accumulated and the cavity height has decreased, showing a low apparent yield value f_B = 272 to 834 Pa. High lava yield strength obtained from Tayler cave, Bayliss cave, and Barkers cave:f_B = 1.4 ~ 3.4x10^3 Pa is considered to be close to the true yield strength. This yield strength is also consistent with the lava yield strength f_B = 1.5 ~ 2.1x103 Pa obtained from the lava flow stop condition.

[Conclusion]

The lava yield strength f_B = 1.4 ~ 3.4x10^3 Pa obtained from Tayler cave, Bayliss cave, and Barkers cave is a reasonable value for basalt with a silicic acid weight fraction of 48.9 wt%. For other small fragmentary caves with low apparent yield values, the floor is buried and the cavity height is decreased. It is necessary to judge whether the estimated yield strength is a reasonable value or not by observing the structure inside the cave in detail.

References:

[1] Anne Atkinson (2010): Undara Volcano, North Queensland, Australia and its Lava Field –Lava Caves, Depressions and The Wall –a Possible Lunar Analogue, Proceedings 14th International Symposium on Vulcanospeleology, 2010. www.vulcanospeleology.org/sym14 /papers/Atkinson.pdf

[2] Anne and Vernon Atkinson (1995): Undara Volcano and its Lava tubes, A geological Wonder of Australia in Undara Volcanic National Park, North Queensland

[3] Graeme P. Melville (1994): Lava tubes and channels of the Earth, Venus, Moon and Mars, Master of

©2021. Japan Geoscience Union. All Right Reserved.

Science (Hons.) Thesis, Department of Physics, University of Wollongong, 1994.
http://ro.uow.edu.au/theses/2859
[4]Tsutomu Honda, Takayoshi Katsumata, Yutaka Ito, Masaru Hatanaka(2017): B3-06 Examination of Mt. Fuji and Suyama womb lava flow by lava tube cave and lava tree type, 2017 Proceedings of the Autumn Meeting of the Volcanic Society of Japan
https://www.jstage.jst.go.jp/article/vsj/2017/0/2017_96/_pdf/-char/ja

Keywords: Lava tube, Yield strength, Lava flow, Undara volcano

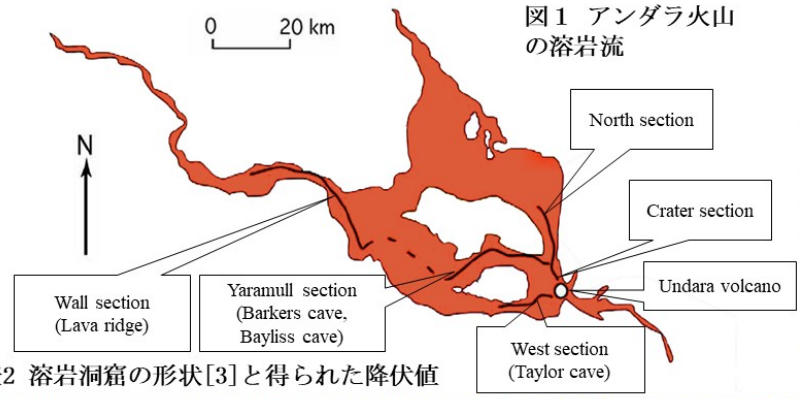


図１ アンダラ火山の溶岩流

表1 溶岩流の厚さ・傾斜度[1]と得られた降伏値

①溶岩流領域	②溶岩厚さH	③傾斜角度α	④ 降 伏 値f_B
Crater section	~5m	1°	2138 Pa
West section	~20m	0.75°	6414 Pa
North section	~20m	0.5°	4276 Pa
Yaramull section	~20m	0.7°	5986 Pa
Wall section	~40m	0.09°	1540 Pa

表2 溶岩洞窟の形状[3]と得られた降伏値

①洞窟名	②洞窟長さ	③最大空洞高さH	④最大空洞幅	⑤平均傾斜角度α	⑥溶岩降伏値f_B
Taylor cave	108m	10.8m	16.3m	2.92°	3367 Pa
Ollier cave	49.4m	3.2m	10.4m	0°	-
Greeley cave	103m	3.8m	12.4m	1.75°	711 Pa
Peterson cave	102m	3.7m	17.1m	0.67°	272 Pa
Stevens cave	70.4m	3.0m	8.8m	1.33°	427 Pa
Pinwill cave	150m	8.8m	21.0m	0.83°	781 Pa
Road cave	220m	9.4m	21.2m	0.83°	834 Pa
Bayliss cave	901m	11.5m	18.9m	1.17°	1438 Pa
Darcy cave	99m	6.3m	16.3m	0°	-
Barkers cave	561m	13.5m	19.8m	2.17°	3131 Pa

©2021. Japan Geoscience Union. All Right Reserved.

Survey on Fissure Cave and Lava Tube Cave in Kansuyama Lava Flow of Mt.Fuji

*Tsutomu Honda[1], Masaru Hatanaka[1], Takayoshi Katumata[1]

1. Vulcano-speleological Society

[Introduction]

Kansuyama lava flow (Juriki marubi lava flow) is a low-viscosity lava flow of SiO2 50.9 wt% ejected around AD710-800 and covers Kurozuka lava flow[1)]. The length of Kansuyama lava flow is about 5 km, and the existence of Kaminari-ana cave, Jurigi koori ana, Suzumi fuketu, and Jurigi tree mold groups are known in the lava flow[2,3,4)]. Recent investigations have revealed that Kaminari-ana cave is a fissure cave located in the channel-like flow path from Kansu yama pyroclastic cone , and that there are several small lava tube caves in the upstream and downstream on the channel-like flow path surface. We estimate the yield strength and lava temperature from surface lava tube cave. Figures 1 shows the locations of Kaminari-ana cave and surface lava tube caves.

[Kaminari ana cave located in lava channel structure]

Kaminari ana cave shown in Fig. 2 and Table1 is a cave with horizontal hole cavity that communicates with the deep vertical hole openings (Photo 1 and 2). The deep vertical hole opening of Kaminari ana cave is traditionally called the gas ejection hole [2,4)], and it is one of the fissure vent because it is on the extension of the fissure vent row according to a survey by Hiroshi Tachihara and Osamu Ohshima in 2010. It is pointed out that the horizontal hole cavity at the bottom has no characteristics as a lava tube cave (roopy lava on the floor, lava shelf on the wall, arched ceiling, etc.), and the fissure wall is covered by lava. It can be clearly regarded as a fissure cave created by draining back of magma. The cavity is sandwiched by parallel walls on both sides, and a scoria layer can be seen behind the collapsed side wall.

[Lava tube cave on the surface of lava channel]

On the surface layer just in the upstream and downstream of Kaminari ana cave, there is a small rectangular lava tube caves (for large one, cavity height: 1 m, width: 4.8 m, length: 5.8 m) shown in Table 1 and Photo 3. Judging from the contour lines, the downstream one has an inclination angle of about $\alpha =$ 8 degrees ($\sin \alpha = 0.143$), and with the tube cavity height H = 1m, g = 9.8m / sec^2, $\rho = 2500kg / m^3$, the lava yield strength[5)] can be obtained as f_B = 1168 Pa from $f_B = (H\ g\ \rho \sin \alpha) / 3$. This yield strength is a reasonable value for basalt. Here, the temperature was calculated as 1068 ˚C by using the temperature-dependent equation [7)] based on the data created by Ishibashi & Sato[6)]from Mt. Fuji 1707 eruption basalt.

[Conclusion]

Several surface lava tube caves are formed on the surface of a channel-shaped depression with Kaminari an fissure cave extending from Kansu yama to the south. The yield strength of 1168 Pa obtained from the surface lava tube cave is a reasonable value for basalt. The temperature at which the surface lava tube cave was formed was estimated from this yield value as 1068 ˚C.

References:

1) Akira Takada, Takahiro Yamamoto, Yoshihiro Ishizuka, Shun Nakano (2016): Geological Map of Fuji Volcano (2nd Edition) Manual, National Institute of Advanced Industrial Science and Technology
2) Takanori Ogawa (1980): Geological observation of lava caves and lava tree molds on Mt. Fuji, Dojin,

©2021. Japan Geoscience Union. All Right Reserved.

Vol. 2, No. 3, Japan Cave Association
3) Hideo Endo (1983): Bizarre and Legendary Cave Exploration of Mt. Fuji, published June 1, 1983, Ryokuseisha
4) Takanori Ogawa (1991): Susono City Cultural Monument Survey Report Vol. 5, Lava Cave at the South Foot of Fuji, Susono City Board of Education
5) Tsutomu Honda (2017): Lava tube formation and application of lava tube cave formation model to the Moon and Mars, Proceedings of the 61st Meeting of the Japan Society for Aeronautical and Space Sciences 1B11
6)H.Ishibashi,H.Sato(2010):Journal of Mineralogical and Petrological Science,volume105,pp334-339
7) Tsutomu Honda (2018): Estimating the yield value of Mt. Fuji and lava flow by lava tube cave and lava tree mold, Japan Geoscience Union Meeting 2018 Proceedings SVC43-02

Keywords: Mt.Fuji, Lava flow, Lava tube, Lava cave, Fissure vent

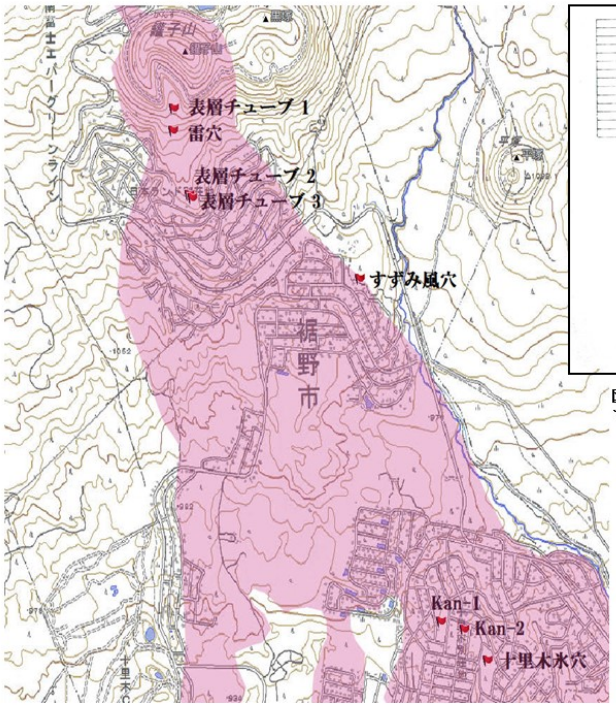


図1 鐘子山と雷穴及び表層溶岩チューブ洞窟及び調査した樹型の位置(カシミール3Dを使用)

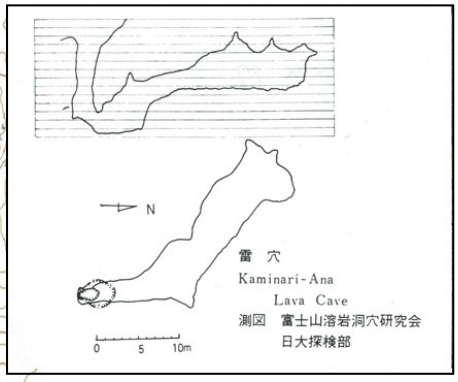


図2 雷穴の測量図(内部の横穴は鐘子山の方向に向いている)

表1 鐘子山溶岩流の洞窟に関するデータ

上流部洞窟	洞窟の形状と寸法	傾斜度
表層チューブ1	矩形断面チューブ,約1.0m(高さ)x3.7m(長さ)	-
雷穴	竪穴+横穴(文献2,4),竪穴深さ:13m,横穴長さ:35m	-
表層チューブ2	矩形断面チューブ,約0.5m(高さ)x3m(長さ)	-
表層チューブ3	矩形断面チューブ,1m(高さ)x4.8m(幅)x5.3m(長さ)	8°



写真1 雷穴の竪穴





写真2 雷穴の横穴

写真3 表層チューブ3の内部

©NPO法人 火山洞窟学会

©2021. Japan Geoscience Union. All Right Reserved.

The origin of bimodal magmatism in the Okinawa Trough, Japan

*Arran Peter Murch[1], Kenichiro Tani[1], Takashi Sano[1], Shigekazu Yoneda[1]

1. National Museum of Nature and Science, Tsukuba, Ibaraki, Japan

The Okinawa Trough (OT) is an incipient continental back-arc basin that extends ~1200 km south from Kyushu to Taiwan, and can be split in to three segments, the Northern (NOT), Middle (MOT), and Southern (SOT). Back-arc volcanism in the OT is bimodal (basaltic to rhyolitic) and restricted to volcanic centres located in en-echelon grabens the MOT and SOT.

Here we present petrological descriptions, along with major, trace element and Sr–Nd isotopic data for a bimodal sample suite collected during the R/V Sonne HYDROMIN1 and 2 cruises in 1988 and 1990, respectively. Samples were recovered as lavas and pumice dredged from various seafloor knolls and ridges located in the Io and Iheya grabens and from Izena Hole in the MOT, and from a single volcanic ridge in the Yaeyama graben and a single isolated knoll in the SOT.

The mafic end member ranges from ~50 to 56 wt% SiO_2. Samples from the SOT show a fractionation trend with an initial enrichment of FeO indicating a tholeiitic trend, while MOT samples are characterised by a calc-alkaline trend. Major and trace element data also suggests at least two groups of basalt in the MOT defined by the relative depletion in incompatible elements (K, Na, Si, Zr, Nb, Rb, Ba, Th, Ce, etc.), and enrichment in Al_2O_3, V, Cr, Sr of one group vs the other. However, the entire mafic end member sample suite records a strong subduction signature with MORB normalised spider plot patterns showing enrichment of incompatible elements, especially LIL, and Pb, along with the depletion of Nb and Ta. Chondrite normalised REE trends also show enrichment in LREE.

The silica end member ranges from ~71 to 77 wt% SiO2. However, major and trace element data shows the silica end member is highly diverse with at least four identifiable groups based on differences in the degree of enrichment in incompatible elements (K, Rb, Ba, Nb, Zr, Y, Th). Chondrite normalised REE diagrams indicate the same diversity with variable $(La/Sm)^N$ ratios. While MORD normalised spider diagrams show the same subduction signature present in the mafic end member. Each group contains at least one dense lava sample suggesting the chemical diversity is a primary feature of magmatism in the Okinawa Trough rather than a result of the floating in of pumiceous material from various locations.

Using petrological descriptions and the chemistry of samples along with MELTS modelling we plan to evaluate the conditions and processes of magma formation and evolution. In doing so we hope to provide a model to explain the magma chemistry in the MOT and SOT.

Keywords: Okinawa Trough, Bimodal volcanism, Magma Formation

©2021. Japan Geoscience Union. All Right Reserved.

Reinvestigation of Holocene eruption history of Nikko-Shirane Volcano, central Japan

*Yuki Kusano[1], Yoshihiro Ishizuka[1], Teruki Oikawa[1], Osamu Ishizuka[1]

1. Geological Survey of Japan, AIST

Holocene eruption history of Nikko-Shirane Volcano was reinvestigated, based on the geological mapping, 5–10 m digital elevation model reading, and 14C ages, and correlated with the tephra stratigraphy. Nikko-Shirane Volcano (peak Mt. Shirane: 2578 m) is located on the border of Gunma and Tochigi prefecture, central Japan. It has three crater area, located at Mt. Shirane, Chinoikejigoku and Mt. Zazen (2317 m). The oldest Marunuma Lava is overlying Miocene basement, Kinugawa Rhyolites, and covered with thin soil and Asama-Itahana yellow (As-YP) tephra of 17 ka suggesting that Nikko-Shirane Volcano has been started eruption around 17 ka. Mt. Zazen is composed of Zazen Lava and Zazen'yama Pyroclastic Cone which has a 200 m-long crater on top. Eruption age of Zazen Lava is estimated to 7.6–5.7 ka (cal: calendar age).

There are seven tephra layers on Zazen Lava, from the lowest to the upper layers, Nks-G, Nks-F, Nks-E, Nks-D (defined in this study), Haruna-Futatsudake-Ikaho (Hr-FP: 6th century: Machida and Arai, 2003), Nks-C and Nks-A (Kusano and Ishizuka, 2020). Eruption age of Nks-G and Nks-D are estimated to 5.7–5.5 ka (cal) and 3.1–2.9 ka (cal). These ^{14}C ages and soil sedimentary rate between these tephra suggest that Nks-F was erupted in 5.2 ka, and Nks-E was erupted in 4.7 ka. Based on the volcanic stratigraphy, modal composition of tephra, petrography and geochemistry, Nks-F, Nks-E and Nks-D are correlated with Goshikinuma Pyroclastic Cone, Shirane-gongen Pyroclastic Cone and Shiranesan Lava, respectively.

We described Jigokunagi Pyroclastic Flow Deposit along a western valley of Mt. Shirane. It has more than 7 m in thickness, and consists of unwelded, block and ash flow deposit. It composed of volcanic blocks with fresh, dense and weakly vesiculated andesite with cooling joints, ash matrix of the same composition, and some charcoals. The pyroclastic flow deposit is covered with soil and Hr-FP. Petrographic feature and bulk-rock composition of these volcanic blocks is similar to that of Shiranesan Lava. Charcoal in the pyroclastic flow deposit show 3.3–3.2 ka. These lines of evidence indicate that the latest Shiranesan Lava was erupted around 3 ka and the crumbling of the lava formed Jigokunagi Pyroclastic Flow Deposit.
We conclude that magmatic eruption in Nikko-shirane Volcano occurs once in 300–1,500 years in recent 7,500 years.

Keywords: Nikko-Shirane Volcano, Eruption history, Geology, Active volcano, Volcanic stratigraphy, Radio carbon age

©2021. Japan Geoscience Union. All Right Reserved.

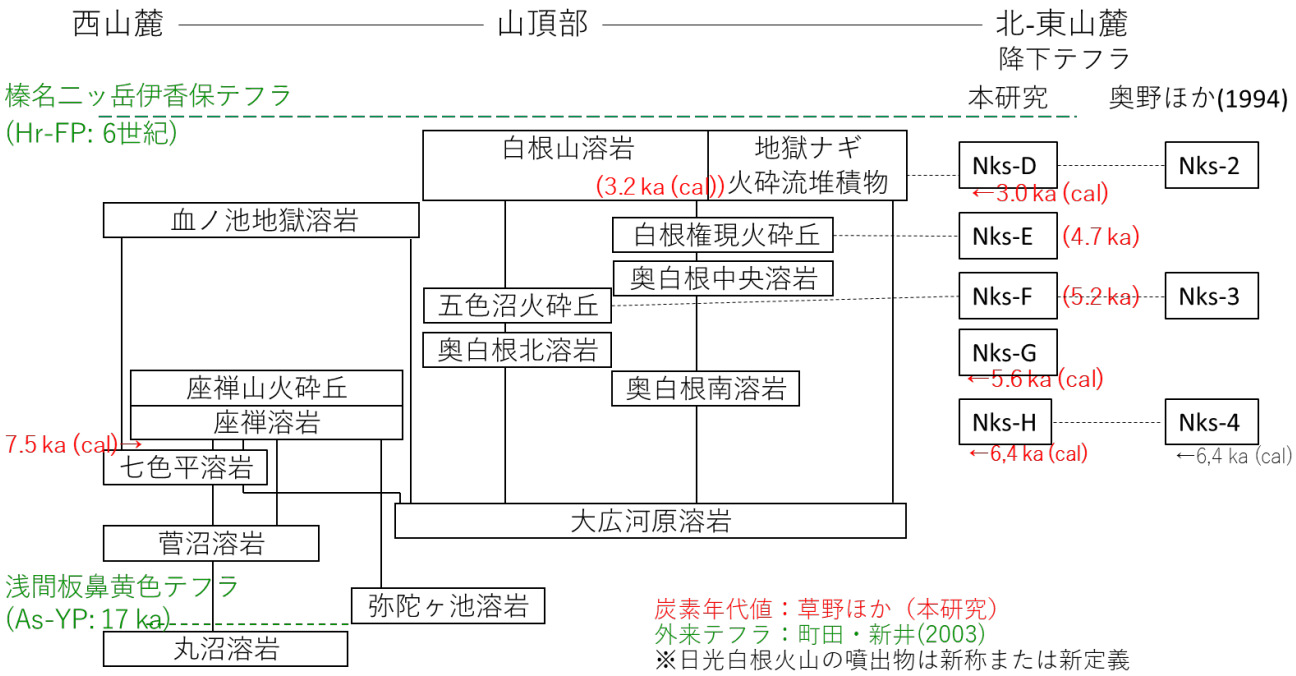


図1　日光白根火山の層序関係図
Fig. 1 Stratigraphic relationships of geologic units of Nikko-Shirane Volcano

©2021. Japan Geoscience Union. All Right Reserved.

Construction of Geochemical database of Kikai Caldera magmas for understanding the magmatic evolution prior to caldera-forming eruptions

*Satoru Haraguchi[1,2], Kenta Ueki[2], Kenta Yoshida[2], Tatsu Kuwatani[2], Morihisa Hamada[2], Iona McIntosh[2], Takashi Miyazaki[2], Takeshi Hanyu[2]

1. Earthquake Research Institute, University of Tokyo, 2. JAMSTEC

The Kikai Caldera, located in southern Kyushu, experienced a caldera-forming eruption at 7.3 ka, which was the youngest and largest one on Earth during the Holocene, and caused voluminous deposits of pyroclastic flow and tephra (known as the Akahoya ash). In order to evaluate such past supereruptions and prepare for future eruptions, we compile a database that integrates available geochemical data from throughout the eruptive history of the Kikai Caldera. Based on the database, we will discuss the evolution and diversity of magmas responsible for past activities of the Kikai Caldera.
To track and correlate the widespread tephra from past Kikai eruptions, it is necessary to collate and compare information on volcanic ash collected from various parts of Japan. Recent advances in analytical techniques have allowed us to conduct microanalyses of various major and trace elements and multiple isotope ratios of glass and minerals in volcanic ash. To date, geochemical data of eruption products derived from the Kikai Caldera are; (1) whole-rock analytical data of proximal lavas and pyroclastic flows around the Kikai Caldera, such as those on Satsuma-Iwojima and Takeshima islands, using wet analysis or XRF, and (2) microanalytical data of volcanic glass of widespread tephra such as Kikai-Akahoya from a wide area ranging from Kyushu to Kanto, using EPMA and LA-ICP-MS. The former covers a wide range of ages, from pre-caldera activities to the eruptions during 1934-1935 that formed Showa-Iwojima, although available data are limited to major elements and specific trace elements. On the other hand, detailed geochemical data of eruption products including multiple trace element data for the widespread tephra from the Kikai Caldera, have been reported and become available over the past decade.
We will introduce the outline of the constructed database and the characteristics of available geochemical data related to the Kikai Caldera. Based on analysis using the database, the compositional variation of magmas throughout the period of Kikai Caldera activity will be evaluated. The database will be provided on a publicly available website.

Keywords: Kikai Caldera, Caldera-forming eruption, Wide-spread tephra, Database, Analytical Technique, Magma genesis

©2021. Japan Geoscience Union. All Right Reserved.

Reconstruction of the volcanic history of Nakadake volcano in Kirishima volcano group, Kyushu, Japan (1)

*Yasuhisa Tajima[1], Atsushi Yasuda[2], Mitsuru Okuno[3]

1. Research & Development Center, Nippon Koei Co.,LTD., 2. Earthquake Research Institute, University of Tokyo, 3. Faculty of Science Department of Earth System Science, Fukuoka University

The long-term eruption histories of Ohachi, Shinmoedake, and Ebinokogen-Ioyama volcanoes in Kirishima volcano group were revealed through recent geologic observations (Tsustui et al., 2007; Tajima et al., 2013, 2014). However, detailed eruption histories of the Nakadake and Ohatayama volcanoes, which erupted during the Holocene, remain unknown. It was found that Nd1 and Nd2 lava were covered by the K-Ah tephra, whereas for Nd3 and Nd4 lava, the key tephra relationship has not been investigated. Nd7 lava is likely newer than Nd6 lava, while Nd8–Nd11 lava were the youngest Nakadake lava (Inoue, 1993). Based on ^{14}C ages and the key tephra layer relationship, the earlier 10 tephra layers of the Nakadake volcano are known to originate from eruptions occurring from 4700 to 2200 cal BP (Tsutsui et al., 2005, 2007). However, the beginning ^{14}C age of the Nakadake lava above the K-Ah tephra is unknown.

We investigated the lava and tephra layers around Nakadake volcano by using chronology and geochemical techniques. The earlier stage of the Nakadake volcano likely originated from Nd3 lava, as it sits at the bottom layer of the earlier Nakadake tephra layers above the Miike tephra. Additionally, the ^{14}C ages of 3680±40 BP (JAT-14,003) and 3500±40 BP (JAT-14,002) in the earlier Nakadake tephra layers above the Sm-Sy tephra (4.5 cal BP) were measured for humic soils. The AMS^{14}C dating was carried out at Tono Geoscience Center of Japan Atomic Energy Agency (JAEA).

Keywords: Kirishima volcano group, Nakadake volcano, volcanic history

©2021. Japan Geoscience Union. All Right Reserved.

The effect of dissolved water induced by lithostatic pressure on lava migration

*Akio Goto[1]

1. Center for Northeast Asian Studies, Tohoku University

The apparent viscosity of Unzen lobe lava had been estimated to be 0.9–4.2×10^{10} Pa s from the observed lava surface velocity (2~5 m/h) in 1991, using Jeffreys model with lava density 2300 kg/m^3, lava thickness 40~70 m and slope angle 25~30 °, based on the assumption that the lava was a Newtonian or Bingham fluid (Fukui et al., 1991; Suto et al., 1993). In contrast, the viscosity of synthetic groundmass glass derived from Unzen lava (~79 wt.% SiO_2) had been measured in the laboratory at expected lava temperatures (780°C–880°C: Nakada and Motomura, 1999) to be 10^{11}–10^{13} Pa s (Goto, 1999). On the basis of Einstein–Roscoe equation, Goto (1999) concluded that ~50 vol.% crystallized Unzen lava lobes probably did have a few orders of magnitude higher viscosity than was observed, and he speculated that the lava-migration mechanism was different from that of Newtonian flow. On the other hand, Cordonnier et al. (2009), who obtained higher viscosity values from laboratory experiments than the field-based values for Unzen natural-lava samples, pointed out that, based on Hess and Dingwell's (1996) hydrous-melt viscosity model, 0.2 wt.% water in the groundmass glass (Nakada and Motomura, 1999) compensates for the gap between observed and experimental viscosity. In the present study the effect of dissolved water on lava migration was numerically investigated, based on synthetic dry Unzen groundmass glass viscosity data by Goto (1999), with the aids of water solubility model by Liu et al. (2005) and the degree of viscosity decrease by dissolved water derived from hydrous rhyolitic melt viscosity by Goto et al. (2005). In the following we fix the lava temperature to be 825°C.

Liu et al. (2005) provided empirical water solubility model for rhyolitic melt as functions of pressure and temperature. Using this model water solubility in rhyolitic groundmass glass was calculated for the interior of 70 m-thick Unzen dacite lava at each depth: e.g., 0.44 wt.% at the base of lava (1.71 MPa), 0.29 wt.% at 30 m form the surface (0.79 MPa) and 0.10 wt.% at the surface under atmospheric pressure (0.1 MPa). Empirical viscosity from hydrous rhyolitic melt (~77 wt.% SiO_2) by Goto et al. (2005) was fitted well as a function of water content at fixed temperature, expressing exponential decrease in logarithmic viscosity with increasing water content: -1.89, -1.62 and -0.83 by 0.44, 0.29 and 0.10 wt.% dissolved water, respectively. Supposing that the effect of dissolved water on the degree of rhyolitic melt viscosity decrease is identical, hydrous Unzen groundmass glass viscosity is estimated from dry melt viscosity by Goto (1999) to be 1.4×10^{10} Pa s at the base of lava, 2.7×10^{10} Pa s at 30 m from the surface and 1.7×10^{11} Pa s at the surface. These values are similar to or higher than the field-based viscosity, but integrated shear velocity at each depth gives surface velocity ~5 m/h, similar to the highest end of the observed velocity, mainly from the contribution of low viscosity zone on the bottom. These are the cases if the lava is crystal-free, but Unzen lava contains ~50 vol.% crystals. It is difficult to evaluate the effect of crystals on Unzen lava viscosity correctly because there is no universal viscosity model applicable to differing suspensions of crystals of various size and shape distributions, but simple Einstein–Roscoe equation expects a few order increase in viscosity by suspended crystals. The highest end of estimated effusion temperature (880°C) gives one order lower groundmass glass viscosity than the above evaluations, but insufficient to compensate for the viscosity increase by suspended crystals.

The present study indicates the importance of dissolved water induced by lava lithostatic pressure and resultant viscosity decrease, but insufficient to compensates for the gap between observed and experimentally-predicted viscosity of Unzen lava.

©2021. Japan Geoscience Union. All Right Reserved.

Keywords: Unzen volcano, lava viscosity, dissolved water

©2021. Japan Geoscience Union. All Right Reserved.

An attempt to detect volcanic materials of Ogasawara Ioto (Iwojima) Volcano from the core sample of the turbidite layers deposited in the Palace Bella Basin

*Masashi NAGAI[1], Takahiro Miwa[1]

1. Volcano Research Department, National Research Institute for Earth Science and Disaster Resilience

Ogasawara Ioto (Iwojima) Volcano is a volcanic Island with a 10 km-width caldera, and intense post-caldera volcanic activity ongoing. There are many unclear points about the products deposited on the surrounding seafloor, and little is known about the entire history of volcanic development. Therefore, not so much information is available on the timing, scale, eruption style, and impact on the surrounding environment, which is necessary for evaluating the disaster potential of Ioto volcano.
We focused on existing seafloor core samples and examined whether products from Ioto could be confirmed. The subject is the piston core KR98-01 P1 collected in the Palace Bella Basin. This core sample was analyzed in detail by Ikehara et al.(1998) and Kawamura et al.(1999 ; 2002), and considered to alternating layers of the turbidite layer and the pelagic clay layer. The depositional age was estimated to be younger than 460,000 years ago by microfossil analysis. Since the turbidite layer contains large amounts of volcanic glass particles and calcareous microfossils even though it was a core sample located deeper than CCD, it was probable that pyroclastic materials and microfossils once deposited shallower than the CCD were reworked by turbidity current. From the examination of paleocurrent direction and the seafloor topography, it was considered that the source was the relatively shallower seafloor around Ioto volcano at the southern end of the Izu-Ogasawara arc, which is more than 300 km away from the core site. However, the origin of pyroclastic material particles has not been investigated in detail. On the other hand, volcanoes in Ioto and surrounding submarine volcanoes are known to produce more alkaline rocks than adjacent areas, and have properties that are advantageous for identifying source volcanoes based on petrological characteristics.
This time, we mainly report the results of the major element composition analysis of volcanic glass particles by SEM-EDS using the core samples stored in the Kochi Core Center, Kochi University / JAMSTEC. According to the analysis results, most of the particles are rich in alkali elements and range from trachyandesite to trachydacite. In all the SiO_2 variation diagram of the measured elements, there is a part that overlaps with the composition range of the known Ioto volcanic products, and it is considered that particles originating from Ioto volcano are included in core samples. On the SiO_2-Na_2O diagram, there are two major composition trends. On the SiO_2-Na_2O diagram, there are two major composition trends. The Na_2O-rich composition trend is more consistent with Ioto volcano, and the Na_2O-poor trend is in the position slightly poorer in Na_2O than the whole rock composition of Fukutoku-Okanoba volcano (Kato, 1988 ; Ossaka et al., 1990 ; Nakano and Kawanabe, 1992 etc.), and the corresponding volcano is unknown at present. Because each turbidite layers always contain particles that match both trends, it is thought that the direct origin is mixture of the products from Ioto and unknown volcanoes. In addition to the above, trace amounts of high-silica rhyolite glass particles similar to AT tephra have been confirmed from the pelagic clay layer, and there is a possibility that the depositional age can be further narrowed down.
The results of this study support the estimation of the source area by Ikehara et al.(1998) and suggest that large-scale mass transport were repeated in seafloor around Ioto area. It is considered that the components of each turbidite layer reflected the surface deposits in the area around the volcanoes at the time of the turbidity current had occurred, so by analyzing each layer in detail, temporal changes such as

©2021. Japan Geoscience Union. All Right Reserved.

eruption magma properties might be obtained.
Acknowledgment : We thank JAMSTEC for permitting the use of the piston core samples. We also thank Dr. Toshio Hisamitsu and other staff members of the Kochi Core Center for support of collection of analytical samples.

©2021. Japan Geoscience Union. All Right Reserved.

[J] Poster | S (Solid Earth Sciences)：S-TT Technology & Techniques

Thu. Jun 3, 2021 5:15 PM - 6:30 PM JST | Thu. Jun 3, 2021 8:15 AM - 9:30 AM UTC | Ch.14_1

[S-TT34] Airborne surveys and monitoring of the Earth

convener:Shigekazu Kusumoto(Institute for Geothermal Sciences, Graduate School of Science, Kyoto University), Shigeo Okuma(Geological Survey of Japan, AIST), Takao Koyama(Earthquake Research Institute, The University of Tokyo), Yuji Mitsuhata(AdvancedIndustrial Science and Technology)

Airborne surveys are useful to better understand the whole and/or the detailed structures of the Earth and their variations. They can be implemented from a traditional manned and newly-developed unmanned aircraft to efficiently map very large or remote areas with difficult access. We invite studies on theory, instrumentation, processing, modeling or inversion and applications of airborne surveys.

[STT34-P01] Geological structure survey by drone airborne electromagnetic survey method

*Youichi Yuuki[1], Akira Shinsei[1], Zenshiro Saito[1], Satoshi Tomimori[1], Akiyo Yamaguti[1], Akira Jomori[2], Atsuyoshi Jomori[2], Tatsuya Toyama[2] (1.Oyo corporation, 2.Neo Science)

[STT34-P02] Development of a Portable Infrared Camera system for Measuring Volcanic Surface Phenomena

*Tetsuya Jitsufuchi[1] (1.National Research Institute for Earth Science and Disaster Resilience)

Geological structure survey by drone airborne electromagnetic survey method

*Youichi Yuuki[1], Akira Shinsei[1], Zenshiro Saito[1], Satoshi Tomimori[1], Akiyo Yamaguti[1], Akira Jomori[2], Atsuyoshi Jomori[2], Tatsuya Toyama[2]

1. Oyo corporation, 2. Neo Science

The drone airborne electromagnetic survey method (D-GREATEM) has been in practical use for several years, and has been used for tunnel route surveys and landslide surveys. We have developed a new transmission device that can be mounted on a drone, and obtained the resistivity structure by using a method called D-TEM, in which two drones towing a transmission device and a reception device are flown simultaneously to measure the resistivity structure. The survey was carried out in the Seino region to understand the structure and hydraulic properties of fan-shaped sand and gravel, which are the recharge sources of groundwater in the Nobi Plain, alluvial clay that causes groundwater to be pressurized, and faults that can regulate groundwater flow. In order to capture seasonal changes in groundwater, the study was conducted twice, during the high rainfall season (September-October 2019) and the low rainfall season (December 2019), and these results were reported at the Japan Geoscience Union 2020 Conference (Yuki et al., 2020).
In this paper, we report on the results of the D-GREATEM and D-TEM expeditions conducted in 2020, following last year's report. Two surveys were carried out in September and December 2020 on the same survey line. The results of D-GREATEM were compared with the results of the previous exploration to confirm the reproducibility of the exploration technique and to examine the geological and hydraulic structures by differentiating the two periods. The D-TEM was conducted on the same survey line as the D-GREATEM, and the depth and resolution of the D-TEM were verified by comparing the results.
The survey area was a non-dense populated area with a lot of farmland, but it was also dotted with private houses and factories, and the roads were lined with power distribution lines. In some areas, underground lines for high-voltage power transmission were buried, and the influence of these measurement environments on the exploration results was also examined.
This paper reports the results of the comparison of the results of the two surveys, D-GREATEM and D-TEM, and discusses the characteristics and limitations of each method, estimation of geological and hydraulic structures, and the effects of measurement conditions.
This survey was conducted by the Strategic Innovation Program (SIP) "Strengthening National Resilience (Disaster Prevention and Mitigation)" of the Council for Science, Technology and Innovation (CSTI), Cabinet Office, Government of Japan (administrator: Disaster Prevention Research Institute).

Keywords: drone, Airborne electromagnetic survey, Drone airborne electromagnetic survey, D-GREATEM, D-TEM

©2021. Japan Geoscience Union. All Right Reserved.

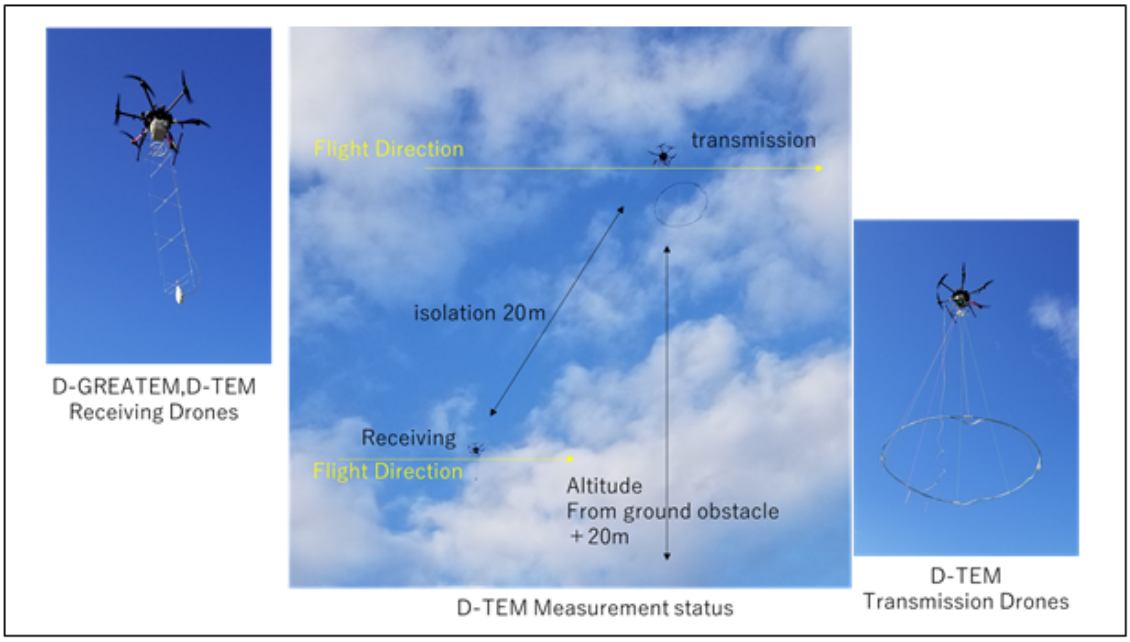


Figure 1: Drone airborne electromagnetic survey measurement

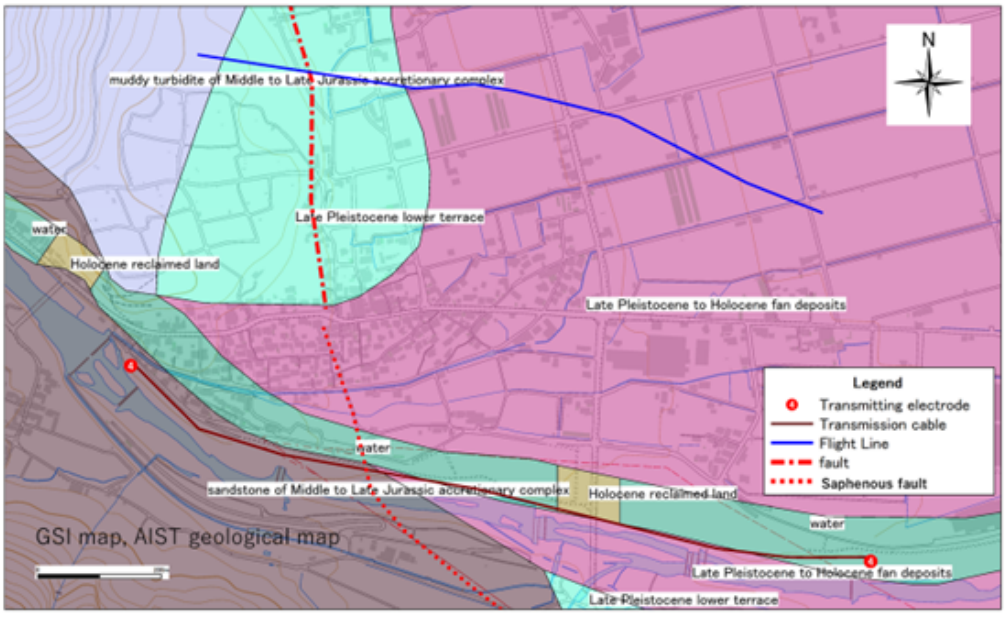
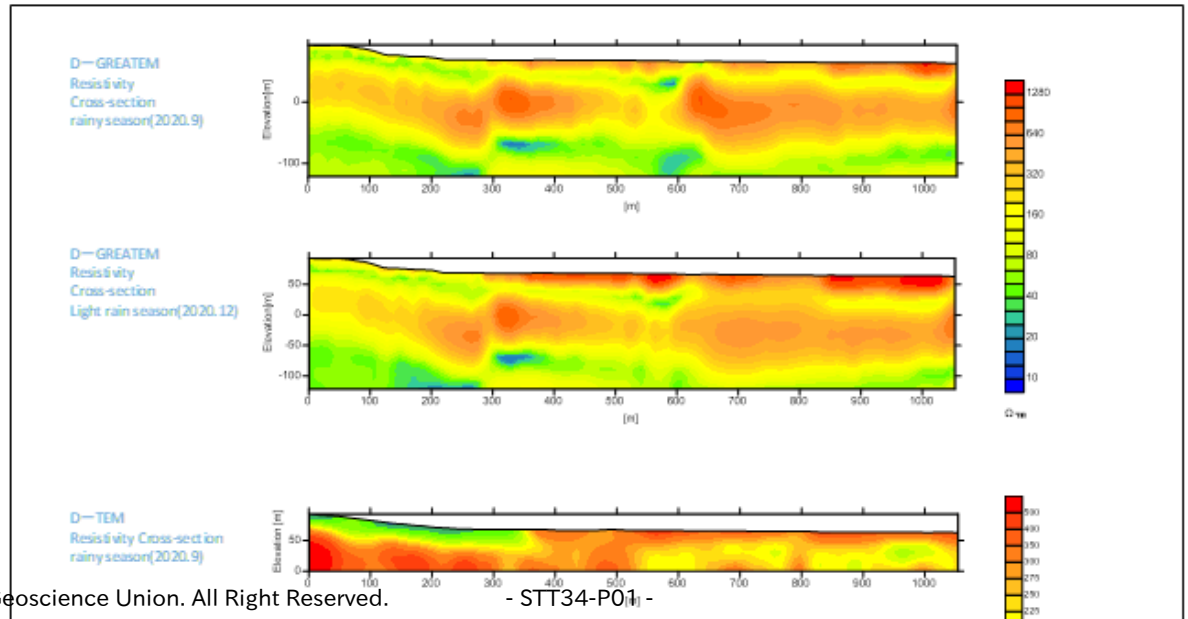


Fig. 2 Geological map



©2021. Japan Geoscience Union. All Right Reserved.

©2021. Japan Geoscience Union. All Right Reserved.

Development of a Portable Infrared Camera system for Measuring Volcanic Surface Phenomena

*Tetsuya Jitsufuchi[1]

1. National Research Institute for Earth Science and Disaster Resilience

The National Research Institute for Earth Science and Disaster Resilience (NIED) developed a portable infrared camera system, Structure and Thermal Information Capture-Portable (STIC-P) for volcano observations in March of 2020. STIC-P is a handheld portable system that can be used for observations on the ground and for handheld observations from an aircraft.

NIED has been conducting research, development and utilization of their own airborne remote sensing system for volcano observation since 1988. The first airborne spectral imaging system, the VAM-90A, was developed in 1990. In 2006, the second airborne hyperspectral sensor, the ARTS, was developed. In June 2015, the ARTS was remodeled into the ARTS-SE. ARTS-SE consists of a modified system of push-broom imaging spectrometer (ARTS) and a newly developed camera system, the Structure and Thermal Information Capture (STIC). The STIC consists of four cameras. These cameras are the two visible cameras and the two uncooled infrared cameras. The STIC specifications provide images data sets for the Structure from Motion (SfM) technique for operational volcanic observations to assess volcanic activity. In November and December 2015, we conducted observations with the ARTS-SE at the Hakone volcanoes and Asama volcanoes. These results indicated that the structure from motion (SfM) processing of image data (framed images) captured by the newly developed STIC can derive digital surface models (DSMs) and ortho-corrected images of the ground surface. We also demonstrated that the uncooled infrared camera can measure brightness temperature distributions under installed on a moving platform at approximately 270 km/h (groundspeed: 75 m/s).

Based on these results, we developed a new device that realizes the functions of STIC as a portable device, and in March 2020, a portable infrared camera system: Structure and Thermal Information Capture-Portable (STIC-P) was developed. The SPIC-P consists of three cameras. These cameras are the two visible cameras and the one uncooled infrared camera. All cameras can measure frame images or videos (30Hz) images. The STIC-P is a portable system and can realize ground-based observations and oblique observations from the sky. NIED is conducting experimental flight of mountain topography (Gifu prefecture) and experimental volcano observations (Mt. Hakone (Owakudani)) for performance evaluation of STIC-P using a helicopter. From these observation results, a geothermal distribution analysis and SfM processing will be performed to assess its accuracy.

Keywords: a portable cameras system, airborne remote sensing, volcano observations, infrared camera, visible camera

©2021. Japan Geoscience Union. All Right Reserved.

[J] Poster | S (Solid Earth Sciences)：S-TT Technology & Techniques

Thu. Jun 3, 2021 5:15 PM - 6:30 PM JST | Thu. Jun 3, 2021 8:15 AM - 9:30 AM UTC | Ch.14_2

[S-TT37] Seismic Big Data Analysis Based on the State-of-the-Art of Bayesian Statistics

convener:Hiromichi Nagao(Earthquake Research Institute, The University of Tokyo), Aitaro Kato(Earthquake Research Institute, the University of Tokyo), Keisuke Yano(The Institute of Statistical Mathematics), Takahiro Shiina(National Institute of Advanced Industrial Science and Technology)

Recently, a big seismic database has been being constructed that collects data of vibrators implemented in such as buildings, lifelines and smartphones, in addition to seismic data of the conventional continuous/temporal dense seismic observation arrays. Development of methodologies and algorithms, which are inadequate at this moment, optimized to comprehensively analyze the seismic big data is essential in order to utilize the big database as much as possible for prevention/mitigation of earthquake disasters and clarification of earthquake phenomena. On the other hand, recent progress of Bayesian statistics is significant, which is the mathematical basis of various methodologies, such as machine learning, especially deep learning, to extract valuable information from big data. The state-of-the-art of Bayesian statistics is expected to substantially advance seismic big data analyses.
This session mainly accepts presentations that focus on analyses of seismic big data, especially related to analysis methods based on Bayesian statistics such as machine learning, sparse modeling and data assimilation, and their applications to real seismic data. Presentations related to mathematical or statistical theories beneficial to data analyses, feasibility studies of algorithms eventually applicable to real seismic data, and the current status of seismic observations and analysis results are also highly welcome.

[STT37-P01] Clustering seismic noises using semi-supervised learning

*Kotaro Sato[1], Keisuke Yano[2], Komaki Fumiyasu[1] (1.The University of Tokyo, 2.The Institute of Statistical Mathematics)

[STT37-P02] Convolutional Neural Network to Detect Deep Low-Frequency Tremors from Seismic Waveform Images

*Ryosuke Kaneko[1,2], Hiromichi Nagao[2,1], Shin-ichi Ito[2,1], Kazushige Obara[2], Hiroshi Tsuruoka[2] (1.Graduate School of Information Science and Technology, The University of Tokyo, 2.Earthquake Research Institute, The University of Tokyo)

[STT37-P03] A Convolutional Neural Network based classification of local earthquakes and tectonic tremors in Sanriku-oki using a single station S-net data and its generalization ability

*Masayuki Kano[1], Hidenobu Takahashi[1], Kazuya Tateiwa[1], Keisuke Yano[2] (1.Graduate school of science, Tohoku University, 2.The Institute of Statistical Mathematics)

[STT37-P04] Forecasting temporal variation of aftershocks immediately after a main shock using Gaussian process regression

*Kosuke Morikawa[1], Hiromichi Nagao[2,3], Shin-ichi Ito[2,3], Yoshikazu Terada[1,4], Shin'ichi Sakai[2,5], Naoshi Hirata[2,6] (1.Osaka University, 2.Earthquake Research Institute, The University of Tokyo,, 3.Graduate School of Information Science and Technology, 4.Center for Advanced Intelligence Project, 5.Interfaculty Initiative in Information Studies, The University of Tokyo, 6.National Research Institute for Earth Science and Disaster Resilience)

[STT37-P05] Detection of deep low-frequency earthquakes based on matched filter technique using mutual information

*Ryo Kurihara[1], Aitaro Kato[1], Hiromichi Nagao[1,2], Sumito Kurata[2] (1.Earthquake Research Institute, The University of Tokyo, 2.Graduate School of Information Science and Technology, The University of Tokyo)

[STT37-P06] Adjoint-based uncertainty quantification of frictional inhomogeneity on slow-slipping fault

*Shin-ichi Ito[1], Masayuki Kano[2], Hiromichi Nagao[1] (1.The University of Tokyo, 2.Tohoku University)

[STT37-P07] Sensor selection for seismic wavefield reconstruction based on sparse observation (Part II: Preliminary study on method based on data-driven low-dimensional model)

*Takayuki Nagata[1], Kumi Nakai[1], Yuji Saito[1], Taku Nonomura[1], Masayuki Kano[1], Shin-ichi Ito[2], Hiromichi Nagao[2] (1.Tohoku University, 2.Earthquake Research Institute, The University of Tokyo)

Clustering seismic noises using semi-supervised learning

*Kotaro Sato[1], Keisuke Yano[2], Komaki Fumiyasu[1]

1. The University of Tokyo, 2. The Institute of Statistical Mathematics

Seismic records contain various kinds of seismic activity (such as normal and weak tectonic tremors) and noise signals. An example of noise signals is ambient noise signals caused by atmospheric pressure fluctuation[1], temperature change[2], waves and wind[3]. Another example is noise signals due to human activities such as automobiles, trains, air-planes, and wind power generation[3]. Appropriate classification of a wide variety of seismic activities and noises leads to not only the improvement of seismic detection accuracy but also the understanding of surrounding ground and site characteristics[4].

Noise is usually classified by unsupervised learning because it is difficult to label noise signals. Johnson et al.[5] used the K-means method to cluster the noise signals after removing obvious earthquake signals. Complete earthquake detection is difficult so noise signals contain earthquake signals that have been manually missed [6]. However, we found that regular earthquake signals are uniformly distributed when we apply the model trained by Johnson et al.'s method to regular earthquake signals.

In this study, we propose a semi-supervised learning method that uses known seismic records as labeled data to appropriately cluster other weak noise waveforms while organizing labeled seismic data into a cluster. We first employ t-Distributed Stochastic Neighbor Embedding(t-SNE) to reduce the dimensionality. We next use a semi-supervised mixed Gaussian model and perform classification using its likelihood.

The accuracy of the proposed method is verified using the vertical acceleration waveform records acquired by the seismograph array of the Metropolitan Area Seismic Observing Network (MeSO-net). As a result, we confirmed that the seismic waveforms are clustered more tightly in terms of the log-likelihood. The characteristics of the frequency and amplitude of the data belonging to each cluster will be reported.

References

[1] Lei Qin, Frank L. Vernon, Christopher W. Johnson, and Yehuda Ben-Zion. Spectral characteristics of daily to seasonal ground motion at the Pi˜non Flats Observatory from coherence of seismic data. Bulletin of the Seismological Society of America, Vol. 109, No. 5, pp. 1948–1967, 2019.
[2] Gregor Hillers and Y. Ben-Zion. Seasonal variations of observed noise amplitudes at 2–18 hz in southern California. Geophysical Journal International, Vol. 184, No. 2, pp. 860–868, 2011.
[3] Kawakita, Y., Sakai, S., Various Types of Noise in MeSO-net. Earthquake Res. Inst. Lec., Vol. 84, No. 2, pp. 127–139, 2009.
[4] Qingkai Kong, Daniel T. Trugman, Zachary E. Ross, Michael J. Bianco, Brendan J. Meade, and Peter Gerstoft. Machine learning in seismology: Turning data into insights. Seismological Research Letters, Vol. 90, No. 1, pp. 3–14, 2019.
[5] Christopher W. Johnson, Yehuda Ben-Zion, Haoran Meng, and Frank Vernon. Identifying different classes of seismic noise signals using unsupervised learning. Geophysical Research Letters, Vol. 47, No. 15, p. e2020GL088353, 2020.
[6] Zachary E Ross, Daniel T Trugman, Egill Hauksson, and Peter M Shearer. Searching for hidden earthquakes in southern california. Science, Vol. 364, No. 6442, pp. 767–771, 2019.

©2021. Japan Geoscience Union. All Right Reserved.

Keywords: seismic noise, semi-supervised learning, classification

©2021. Japan Geoscience Union. All Right Reserved.

Convolutional Neural Network to Detect Deep Low-Frequency Tremors from Seismic Waveform Images

*Ryosuke Kaneko[1,2], Hiromichi Nagao[2,1], Shin-ichi Ito[2,1], Kazushige Obara[2], Hiroshi Tsuruoka[2]

1. Graduate School of Information Science and Technology, The University of Tokyo, 2. Earthquake Research Institute, The University of Tokyo

The establishment of Hi-net [1, 2] led to the discovery of deep low-frequency tremors [3]. Considering the expected relations between tremors and large earthquakes (*e.g.*, [4]), it is important to investigate tremors that occurred before establishing the dense seismometer arrays. Past seismometers used more than 50 years ago drew waveforms continuously on paper wrapped on a drum. The digitization of seismograph paper records by tracing the waveforms is effective for investigating large earthquakes because such waveforms are distinctive and consequently extractable given the low frequencies and large amplitudes. In contrast, tremors have much smaller amplitudes and higher frequencies than large earthquakes, so their digitization is much more difficult due to overlapping waveforms. Therefore, we use a convolutional neural network (CNN) aiming to detect evidence of tremors from seismograph paper records. The CNN is a representative deep learning method that exhibits high performance in tasks such as image recognition and handwriting recognition. A CNN can automatically tune its internal parameters by learning the characteristics of tremors from input images without requiring prior knowledge of tremors or manually adjusting the parameters. Training a CNN from scratch with real data polluted by a variety of noises may hinder the model construction and hyperparameter tuning. Thus, we conducted numerical experiments to train a CNN with synthetic images generated according to seismograph paper records. We constructed the CNN based on the ResNet [5] architecture for better performance. The results show that the trained model can learn tremor features and correctly determine the presence of tremors in the seismic waveforms. In addition, heatmaps generated based on gradient-weighted class activation mapping (Grad-CAM) [6] clearly indicate the tremor location on each image. These suggest that a CNN can be a promising alternative for effective tremor detection compared to individual waveform extraction through digitization. Based on the finding from the experiments, we will conduct CNN training with real data and apply the trained model to seismograph paper records.

References

[1] Obara, K., Kasahara, K., Hori, S., Okada, Y.: A densely distributed high-sensitivity seismograph network in Japan: Hi-net by National Research Institute for Earth Science and Disaster Prevention. Review of Scientific Instruments 76(2), 021301 (2005). doi: 10.1063/1.1854197

[2] Okada, Y., Kasahara, K., Hori, S., Obara, K., Sekiguchi, S., Fujiwara, H., Yamamoto, A.: Recent progress of seismic observation networks in Japan —Hi-net, F-net, K-NET and KiK-net—. Earth, Planets and Space 56(8), xv–xxviii (2004). doi: 10.1186/BF03353076

[3] Obara, K.: Nonvolcanic deep tremor associated with subduction in southwest Japan. Science 296(5573), 1679–1681 (2002). doi: 10.1126/science.1070378

[4] Obara, K., Kato, A.: Connecting slow earthquakes to huge earthquakes. Science 353(6296), 253–257 (2016). doi: 10.1126/science.aaf1512

[5] He, K., Zhang, X., Ren, S., Sun, J.: Deep residual learning for image recognition. In: 2016 IEEE Conference on Computer Vision and Pattern Recognition (CVPR). pp. 770–778 (2016). doi: 10.1109/CVPR.2016.90

[6] Selvaraju, R.R., Cogswell, M., Das, A., Vedantam, R., Parikh, D., Batra, D.: Grad-CAM: visual explanations from deep networks via gradient-based localization. In: 2017 IEEE International Conference

©2021. Japan Geoscience Union. All Right Reserved.

on Computer Vision (ICCV). pp. 618–626 (2017). doi: 10.1109/ICCV.2017.74

Keywords: Deep low-frequency tremor, Convolutional neural network, ResNet, Grad-CAM

©2021. Japan Geoscience Union. All Right Reserved.

A Convolutional Neural Network based classification of local earthquakes and tectonic tremors in Sanriku-oki using a single station S-net data and its generalization ability

*Masayuki Kano[1], Hidenobu Takahashi[1], Kazuya Tateiwa[1], Keisuke Yano[2]

1. Graduate school of science, Tohoku University, 2. The Institute of Statistical Mathematics

Slow earthquakes characterized by a longer duration compared to regular earthquakes in the same magnitude have been widely detected in many tectonic zones (e.g., Obara and Kato, 2016). Tectonic tremors are a kind of slow earthquakes and have been often located in the adjacent areas of megathrust zones. Therefore, monitoring spatio-temporal activities of tremors provides important clues to slow fault slips.

Envelope correlation method (ECM) has been widely used to detect tremors. Although the ECM is a powerful tool for tremor detections, it principally detects signals of earthquakes as well. To classify local earthquakes, tremors and noise, Nakano et al. (2019) developed a supervised, convolutional neural network (CNN)-based method. They adopted spectrograms obtained by DONET ocean seismometers deployed in the Nankai subduction zone as input images for the CNN and attained 99.5% accuracy of classifications.

Here, we attempt to classify local earthquakes, tremors, and noise observed by S-net in northeast Japan following the approach developed by Nakano et al. (2019). However, S-net seismometers have a characteristic period of 15 Hz and thus are less sensitive to the dominant frequencies of tremors (2-10 Hz) compared to the DONET seismometers. Therefore, we modify the structures and retrain the parameters in the CNN developed by Nakano et al. (2019) to adjust the S-net data. As a first step, this study attempts to classify the known local earthquakes, tremors, and noise by the CNN using a single station to investigate how our CNN works for our final purpose of monitoring tremor activities.

We used spectrograms of three component velocity waveforms for 2 minutes in the time domain and for 2-10 Hz in the frequency domain that are obtained from 16 August 2016 to 14 August 2018, at N. S4N21, located off-Sanriku. As training data for CNN, we utilized JMA unified catalog for local earthquakes with epicentral distances smaller than 80 km, and tremor catalog (Nishikawa et al. 2019). We divided the whole data periods into two data sets; waveforms from 16 August 2016–2 December 2017 were used for training and those December 2017–14 August 2018 were used for validation.

As a result, the CNN truly classified 100, 96 and 98 % of local earthquakes, tectonic tremors and noise, respectively. The output probabilities for the true classification of earthquakes and tremors have become smaller with an increasing epicentral distance and that for the true classification of earthquakes with a smaller magnitude. This indicates that the probabilities to be judged as a true classification depend on the signal to noise ratio of the original record.

In this presentation, we will also show the classification results when applying the CNN trained at N.S4N21 to the untrained surrounding S-net stations and discuss the generalization ability of the CNN.

©2021. Japan Geoscience Union. All Right Reserved.

Keywords: Slow earthquakes, S-net, CNN

©2021. Japan Geoscience Union. All Right Reserved.

Forecasting temporal variation of aftershocks immediately after a main shock using Gaussian process regression

*Kosuke Morikawa[1], Hiromichi Nagao[2,3], Shin-ichi Ito[2,3], Yoshikazu Terada[1,4], Shin'ichi Sakai[2,5], Naoshi Hirata[2,6]

1. Osaka University, 2. Earthquake Research Institute, The University of Tokyo,, 3. Graduate School of Information Science and Technology, 4. Center for Advanced Intelligence Project, 5. Interfaculty Initiative in Information Studies, The University of Tokyo, 6. National Research Institute for Earth Science and Disaster Resilience

Uncovering the distribution of magnitudes and arrival times of aftershocks is a key to comprehending the characteristics of earthquake sequences, which enables us to predict seismic activities and conduct hazard assessments. However, identifying the number of aftershocks immediately after the main shock is practically difficult due to contaminations of arriving seismic waves. To overcome this difficulty, we construct a likelihood based on the detected data, incorporating a detection function to which Gaussian process regression (GPR) is applied. The GPR is capable of estimating not only the parameters of the distribution of aftershocks together with the detection function, but also credible intervals for both the parameters and the detection function. The property that the distributions of both the Gaussian process and aftershocks are exponential functions leads to an efficient Bayesian computational algorithm to estimate hyperparameters. After its validation through numerical tests, the proposed method is retrospectively applied to the catalog data related to the 2004 Chuetsu earthquake for the early forecasting of the aftershocks. The results show that the proposed method stably and simultaneously estimates distribution parameters and credible intervals, even within 3hours after the main shock.

Keywords: Statistical seismology, Time series analysis, Gaussian Process Regression

©2021. Japan Geoscience Union. All Right Reserved.

Detection of deep low-frequency earthquakes based on matched filter technique using mutual information

*Ryo Kurihara[1], Aitaro Kato[1], Hiromichi Nagao[1,2], Sumito Kurata[2]

1. Earthquake Research Institute, The University of Tokyo, 2. Graduate School of Information Science and Technology, The University of Tokyo

Matched filter technique is often used to detect microearthquakes such as deep low-frequency(DLF) earthquakes occurred in plate subduction zones or volcanic regions. Matched filter technique is usually based on the summed correlation coefficients between the template waveform and the observed data at multiple observation stations. However, the detection accuracy decreases when there are not enough observation stations or enough templates. Then, matched filter technique is able to be applied to only limited cases. In this study, we developed a new method of the matched filter technique using only one station data to evaluate the similarity of waveforms by calculating not only the correlation coefficient but also mutual information.

In the method, waveforms in a wide frequency band were used and the product of mutual information and correlation coefficient was used as an index for detection. Mutual information is an index which show relationships between two variables including non-linear relationship. Mutual information was calculated by normalizing the amplitude of the template waveform and the amplitude of the continuous waveform for all time steps in the time window. The normalized amplitudes were divided into a cell out of 5×5 cells.

First, we tested the new method on a dataset of artificial noise waveforms in which a waveform of DLF earthquakes is added to. As a result, it was confirmed that for both cases of white noise and sinusoidal noise of 1.25 Hz which corresponds to the dominant frequency of DLF earthquakes, the product of mutual information and correlation coefficient has a clear peak corresponding to the signal of the earthquake, compared to the case which only correlation coefficient is used.

Next, we used 200 template waveforms and applied the method to the data of Kirishima volcano in December 2010 before the eruptions of 2011. We detected 354 DLF earthquakes using the new matched filter technique using the product of mutual information and correlation coefficient at one station, while only two earthquakes were detected in the catalog of Japan Meteorological Agency in this term. Compared to the results of the matched filter technique using summed correlation coefficient of six stations, we missed only 8 events out of 88 events that had a high probability of DLF earthquakes, and 302 out of 354 events were events to be regarded as events with low probability of false detection.

In the case of using six stations, only small peaks which is not over a threshold value were obtained for some templates because the correlation coefficient changes due to slight differences in the source location and waveform characteristics of the templates. Therefore, it is necessary to use a large number of templates for the matched filter technique of multiple stations. On the other hand, in the case of one-station matched filter technique, even such template had a clear peak over the threshold value of detection.
In conclusion, it is considered that even when using data of only one station, it is possible to create an accurate catalog of DLF earthquakes by using the matched filter technique using the product of the correlation coefficient and the mutual information as the index of detection.

©2021. Japan Geoscience Union. All Right Reserved.

Keywords: Matched filter technique, Deep low-frequency earthquake, Mutual information

©2021. Japan Geoscience Union. All Right Reserved.

Adjoint-based uncertainty quantification of frictional inhomogeneity on slow-slipping fault

*Shin-ichi Ito[1], Masayuki Kano[2], Hiromichi Nagao[1]

1. The University of Tokyo, 2. Tohoku University

Slip motion along a fault largely depends on the inhomogeneity of friction that occurs between the fault interfaces. Thus, it is a crucial task to estimate the spatial-dependent frictional features from the observations of the slip motion and then to identify essential parts that contribute to the principal slip motion by quantifying uncertainties involved in the estimates. This study considers an uncertainty quantification problem of the spatially-dependent frictional features based on a fault motion model that mimics the slow-slipping region along the Bungo Channel in the southwestern part of Japan. The fault motion model employs a rate-and-state dependent friction law, in which the frictional parameters are spatially dependent. Although uncertainty quantification in high-resolution is needed to attain the above task, such quantification based on the conventional statistical ways is computationally hard since the complexity exponentially increases with the spatial resolution. This study employs a variational data assimilation method based on a second-order adjoint method to avoid such complexity. Since the data assimilation method enables a selective extraction of the uncertainty of interest, we can attain a fast uncertainty quantification of the frictional parameters in high-resolution. The application of the data assimilation to the fault motion model together with the synthetic observational data of the slip velocity quantifies the spatial dependency of the uncertainty involved in the frictional parameters in high-resolution and reveals how the amount or quality of the observational data of the slip motion influences to the spatial distribution of the frictional parameters. Such quantification provides valuable information to the observational design.

Keywords: Uncertainty quantification, Frictional feature

©2021. Japan Geoscience Union. All Right Reserved.

Sensor selection for seismic wavefield reconstruction based on sparse observation (Part II: Preliminary study on method based on data-driven low-dimensional model)

*Takayuki Nagata[1], Kumi Nakai[1], Yuji Saito[1], Taku Nonomura[1], Masayuki Kano[1], Shin-ichi Ito[2], Hiromichi Nagao[2]

1. Tohoku University, 2. Earthquake Research Institute, The University of Tokyo

In the present study, we conducted a preliminary study on data-driven sensor selection for seismic wavefield reconstruction based on sparse observation. Simulations of the seismic wavefield with the horizontally layered subsurface structure model were performed under various conditions and were extracted the modes of the seismic wavefield. Sensors suitable for accurate seismic wavefield reconstruction were selected based on the modes of the extracted seismic wave.

Keywords: data-driven science, low-dimensional model, sparse sensing

©2021. Japan Geoscience Union. All Right Reserved.

[J] Poster | S (Solid Earth Sciences)：S-CG Complex & General

Thu. Jun 3, 2021 5:15 PM - 6:30 PM JST | Thu. Jun 3, 2021 8:15 AM - 9:30 AM UTC | Ch.15_2

[S-CG50] Dynamics in mobile belts

convener:Yukitoshi Fukahata(Disaster Prevention Research Institute, Kyoto University), Hikaru Iwamori(Earthquake Research Institute, The University of Tokyo), Kiyokazu Oohashi(Graduate School of Sciences and Technology for Innovation, Yamaguchi University)

The dynamic behaviors of mobile belts are expressed across a wide range of time scales, from the seismic and volcanic events that impact society during our lifetimes, to orogeny and the formation of large-scale fault systems which can take place over millions of years. Deformation occurs on length scales from microscopic fracture and flow to macroscopic deformation to plate-scale tectonics. To gain a physical understanding of the dynamics of mobile belts, we must determine the relationships between deformation and the driving stresses associated with plate motion and other causes, which are connected through the rheological properties of the materials. To understand the full physical system, an integration of geophysics, geomorphology, geology, petrology, and geochemistry is necessary, as is the integration of observational, theoretical and experimental approaches. In particular, rheological properties, which are physically affected by fluids in the crust and chemical reactions assisted by fluids, can be resolved only through such an interdisciplinary approach. After the 2011 great Tohoku-oki earthquake, large-scale changes in seismic activity and regional scale crustal deformation were observed, making present-day Japan a unique natural laboratory for the study of the dynamics of mobile belts. This session welcomes presentations from different disciplines, such as seismology, geodesy, tectonic geomorphology, structural geology, petrology, geochemistry and hydrology, as well as interdisciplinary studies, that relate to the dynamic behaviors of mobile belts.

[SCG50-P01] Seismic anisotropy of the dipping Pacific slab and adjacent mantle

*Dapeng Zhao[1], Zewei Wang[1] (1.Department of Geophysics, Tohoku University)

[SCG50-P02] Magnitude of east-west contraction forces acting to Japanese Islands since 3Ma estimated from altitude changes

*Ryohei Sasajima[1], Yukitoshi Fukahata[1] (1.Research Center For Earthquake Prediction, Disaster Prevention Research Institute, Kyoto University)

[SCG50-P03] Earthquake simulation based on Coulomb stress change on inland faults during megathrust earthquake cycles in southwest Japan

*Tsukasa MITOGAWA[1], Takuya NISHIMURA[2] (1.Graduate School of Science, Kyoto University, 2.Disaster Prevention Research Institute, Kyoto University)

[SCG50-P04] GNSS observation around the shear zone in southern Kyushu, southwest Japan (5)

*Tsuyoshi Watanabe[1], Koichi Asamori[1], Akiomi Shimada[1], Atsushi Saiga[1], Hiroki Ogawa[1], Umeda Koji[2], Akira Goto[1], Koji Shimada[1], Tsuneari Ishimaru[1] (1.Japan Atomic Energy Agency, 2.Graduate School of Science and Technology, Hirosaki University)

[SCG50-P05] Classification of faults using vertical gravity gradient data by machine learning

*Yuya Honda[1], Kohei Hotta[1] (1.University of Toyama)

[SCG50-P06] Hierarchical clustering of reduced stress tensors based on angular stress distance

*Noriaki Abe[1], Katsushi Sato[1] (1.Kyoto University)

[SCG50-P07] Characteristic of fault geometry and the subducting plate boundary in the focal area of the 2016 Mw7.8 Kaikoura earthquake, New Zealand inferred from high precision aftershock distribution

*Yuta Kawamura[1], Satoshi Matsumoto[1], Tomomi Okada[2], Miu Matsuno[2], Yoshihisa Iio[3], Tadashi Sato[2], Stephen Bannister[4], John Ristau[4], Martha Savage[5], Richard Sibson[6] (1.Kyushu University, 2.Tohoku University, 3.Kyoto University, 4.GNS Science, 5.Victoria University of Wellington, 6.University of Otago)

[SCG50-P08] Analysis of fault kinematics and internal structure of fracture zone at ISTL

*HIBIKI CHIBA[1], Kenta Kobayashi[1], Keita Takahashi[1] (1.Gradate School of Science and Technology Niigata University)

[SCG50-P09] Non-double-couple earthquake in the focal area of the 2000 Western Tottori earthquake by “0.1 manten” hyperdense seismic observation

*Takumi Motokoshi[1], Satoshi Matsumoto[2], Yoshihisa Iio[3], Shin'ichi Sakai[4], Aitaro Kato[4] (1.Department of Earth and Planetary Sciences, Graduate School of Science, Kyushu University, 2.Institute of Seismology and Volcanology, Faculty of Science, Kyushu University, 3.Disaster Prevention Research Institute, Kyoto University, 4.Earthquake Research Institute , the University of Tokyo)

[SCG50-P10] Transition from radial to parallel dike swarm in Amakusa, Japan and their paleostress analyses

*Kentaro Ushimaru[1], Atsushi Yamaji[1] (1.Division of Earth and Planetary Sciences, Graduate School of Science, Kyoto University)

[SCG50-P11] **Electrical conductivity in a brine-saturated granite under uni-axial compression**

*Yui Aikawa[1], Tohru Watanabe[1] (1.University of Toyama)

[SCG50-P12] Lithologic and thermal controls of seismicity in the northwestern Kii Peninsula, southern Honshu, Japan

*Sumire Maeda[1], Shinji Toda[2], Toru Matsuzawa[3], Makoto Otsubo[4] (1.National Research Institute for Earth Science and Disaster Resilience, 2.International Research Institute of Disaster Science, Tohoku University, 3.Graduate School of Science, Tohoku University, 4.Geological Survey of Japan, National Institute of Advanced Industrial Science and Technology)

[SCG50-P13] On approximations of EASY%R_o model to estimate maximum experienced temperature from vitrinite reflectance in rocks

*Shunya Kaneki[1], Hiroyuki Noda[1] (1.Disaster Prevention Research Institute, Kyoto University)

Seismic anisotropy of the dipping Pacific slab and adjacent mantle

*Dapeng Zhao[1], Zewei Wang[1]

1. Department of Geophysics, Tohoku University

With the increasing number of seismic stations deployed and high-quality seismic data accumulated, body-wave anisotropic tomography has shown its power in revealing the 3-D anisotropic structure of subduction zones (e.g., *Wang & Zhao*, 2008, 2013; *Zhao*, 2015; *Liu & Zhao*, 2016, 2017; *Ishise et al.*, 2018). To simplify the calculation, the previous studies often assume an anisotropy with a hexagonal symmetry for materials in the modeling space. This assumption is a good approximation for typical mantle minerals such as olivine. For a further simplification, the previous studies assumed the symmetry axis to be either horizontal or vertical for investigating azimuthal anisotropy or radial anisotropy. However, the assumption of horizontal or vertical symmetry axis is not reasonable at least in two cases that are common in subduction zones: (1) complex mantle flow with a flow direction neither parallel nor perpendicular to any of the modeling axes, and (2) intra-slab anisotropy affected by the geometric inclining of a subducting slab. Therefore, the horizontal or vertical symmetry axis assumption should be released for better revealing the intra-slab fabric alignment and the 3-D mantle flow field in subduction zones. Under a general hexagonal symmetry anisotropy assumption, we developed a new tomographic method (*Wang & Zhao*, 2021) to determine a high-resolution 3-D P-wave anisotropic model of the Japan subduction zone by inverting a great number of travel-time data of local and teleseismic events. As a result, the 3-D anisotropic structure in and around the dipping Pacific slab is firstly revealed. Significant anisotropy with a dipping symmetry axis also occurs in the mantle wedge and the sub-slab mantle associated with the slab subduction. Our results show that slab deformation plays an important role in both mantle flow and intra-slab fabric, and the widely observed trench-parallel anisotropy in the forearc from shear-wave splitting measurements is related to the intra-slab deformation during the outer-rise yielding of the subducting plate.

References

Ishise, M. et al. (2018). *Geophys. Res. Lett.* 45, 3923–3931.
Liu, X., D. Zhao (2016). *J. Geophys. Res.* 121, 5086-5115.
Liu, X., D. Zhao (2017). *Earth Planet. Sci. Lett.* 473, 33-43.
Wang, J., D. Zhao (2008). *Phys. Earth Planet. Inter.* 170, 115-133.
Wang, J., D. Zhao (2013). *Geophys. J. Int.* 193, 1166-1181.
Wang, Z.W., D. Zhao (2021). *Science Advances* 7, eabc9620.
Zhao, D. (2015). *Multiscale seismic tomography.* Springer, 304 pp.

Keywords: subduction zones, seismic anisotropy, seismic tomography

©2021. Japan Geoscience Union. All Right Reserved.

Magnitude of east-west contraction forces acting to Japanese Islands since 3Ma estimated from altitude changes

*Ryohei Sasajima[1], Yukitoshi Fukahata[1]

1. Research Center For Earthquake Prediction, Disaster Prevention Research Institute, Kyoto University

Rapid east-west contraction accompanied by uplift of mountain ranges has been occurred on the Central and North-Eastern Japan since 3 Ma. Takahashi (2006, 2017) proposed a hypothesis that these are caused by the east-ward migration of the TTT-triple junction and the Japan Trench arising from the motion direction change of the Philippine Sea plate. This hypothesis is consistent with several geological observations, while no validation from a view point of mechanics has been done.

Therefore, this study attempts to estimate the magnitude and distribution of the east-west contraction forces acting to Japanese Island since 3 Ma. Based on the estimation, we validate the hypothesis from a view point of mechanics and discuss the origin of the forces.

Horizontal contraction forces that cause uplift of a mountain range and extensional forces arising from an increment of lithospheric body forces associated with the uplift are nearly equilibrium (e.g, Molnar and Lyon-Caen, 1988). Therefore, we can estimate a magnitude of an increment of contraction forces from altitude changes of mountain ranges. This study estimated the magnitude and distribution of the increment of the east-west contraction forces acting to Japanese Island since 3 Ma from the altitude change of the five mountain ranges: Kiso, Akaishi, Hida, Echigo, and Ou.

We obtain the following results. For Kiso, Akaishi, and Hida mountain ranges, ~2×10^{12} [N/m] of the contraction forces per unit length has been added along 200 km of the length of the mountain ranges. For Echigo and Ou mountain ranges, they are ~0.4×10^{12} [N/m] along 300 km. In total, 5.2×10^{17} [N] of the east-west contraction forces has been added to the Japanese Island since 3 Ma.

If the east-west contraction is caused by the east-ward migration of the triple junction and the Japan Trench arise from the motion direction change of the Philippine Sea plate, the magnitude of the contraction forces should be consistent with the magnitude of the force that caused the motion direction change of the Philippine Sea plate. The candidate of the force caused the motion direction change is the slab-pull arising from the west-ward subduction from the Philippine Trench initiated at 5-8 Ma. Seno (2000) estimated that the magnitude of the slab-pull force along the Philippine Trench is 3×10^{18} [N]. From the analysis of global plate motion, Forsyth and Uyeda [1975] estimated that around 90% of a slab-pull force balances to a slab viscous resistance force and the rest 10 % of it balances to the forces acting to the surface part of plates. Therefore, 5.2×10^{17} [N] of the east-west contraction forces estimated by this study are consistent with the slab-pull force although both of the magnitude of the forces are rough estimation. This result indicates that the east-west contraction of the Japanese Island can be explained by the motion direction change of the Philippine Sea plate from a view point of mechanics. In addition, the estimated east-west contraction forces take a maximum value for Central Japan. This implies that the largest east-west contraction force acting from around the TTT-triple junction. This is also consistent with the hypothesis.

©2021. Japan Geoscience Union. All Right Reserved.

Forsyth, D. and Uyeda, S. (1975), Geophys. J. Int., 43(1), 163-200.

Molnar, P. and Lyon-Caen, H. (1988), Geol. Soc. Am. Special Paper, 218.

Takahashi, M. (2006), Journal of Geography, 114, 116–123.

Takahashi, M. (2017), Bull. Geol. Surv. Japan, 68(4), 155–161.

Seno, T. (2000), *J. Geol. Soc. Phillip., 55*, 105–107.

Keywords: Japanese Islands, East-west contraction, Quaternary, Tectonics, Lithospheric body force, Gravitational potential energy

©2021. Japan Geoscience Union. All Right Reserved.

Earthquake simulation based on Coulomb stress change on inland faults during megathrust earthquake cycles in southwest Japan

*Tsukasa MITOGAWA[1], Takuya NISHIMURA[2]

1. Graduate School of Science, Kyoto University, 2. Disaster Prevention Research Institute, Kyoto University

In the subduction zone, the stress changes due to megathrust earthquakes may modulate the shallow crustal seismicity in the overriding plate. Historical documents indicate the frequent occurrence of large shallow crustal earthquakes in the overriding continental plate 50 years before and 10 years after the megathrust earthquakes along the Nankai trough in southwest Japan (i.e., active period). We performed the earthquake simulation based on Coulomb failure stress (CFS) change assuming the strength of inland block boundary faults using the locking distribution of the megathrust fault and the relative motion rate of block boundary faults (hereafter "inland faults") estimated using geodetic data. The stress change is computed using numerical code by Fukahata and Matsu'ura (2006), assuming the medium composed of an elastic layer overlying a Maxwell viscoelastic half-space. The stress sources of inland faults are the slip (i.e., earthquake) and locking on the megathrust fault and inland faults. The stress change due to megathrust fault locking is calculated using geodetic backslip rates. On the other hand, the backslip rate of the inland faults is assumed by multiplying the geodetic rate of relative block motion by an arbitrary coupling ratio uniformly for all the inland faults. The megathrust earthquake releases backslip accumulated during the interseismic period every 120 years. The inland earthquake occurs when the CFS exceeds the assumed fault strength of an inland fault. As a result of the simulation, the "active period" of the past seismic activity in southwest Japan could be explained when the apparent friction coefficient and the coupling ratio of inland faults were about 0 and 0.1, respectively. The tendency of simulated long-term seismic activity is consistent with the past seismic activity at the low apparent friction coefficient. It suggests that the fault strength hardly changes over time. Furthermore, the small coupling ratio indicating low loading rates of the inland faults suggests that most part of geodetic observed deformations are inelastic deformations. Another interpretation is also possible that the low loading rates imply that the geodetic relative block motion is distributed among slips on not only major faults but also minor faults along the block boundary.

Keywords: Megathrust Earthquake Cycles, Southwest Japan, Inland Earthquake, Earthquake Simulation, Active Period

©2021. Japan Geoscience Union. All Right Reserved.

GNSS observation around the shear zone in southern Kyushu, southwest Japan (5)

*Tsuyoshi Watanabe[1], Koichi Asamori[1], Akiomi Shimada[1], Atsushi Saiga[1], Hiroki Ogawa[1], Umeda Koji[2], Akira Goto[1], Koji Shimada[1], Tsuneari Ishimaru[1]

1. Japan Atomic Energy Agency, 2. Graduate School of Science and Technology, Hirosaki University

GNSS observation (Ref.1; Ref.2) illustrates an active left-lateral shear zone with high shear strain rate (>10^{-7}/yr) in southern Kyushu (hereafter SKSZ), where M5-6 earthquakes have occurred frequently (Ref.3). However, the surface topography does not have the traces of obvious active faults. In order to explore the crustal deformation in more detail, we established 10 GNSS sites across the SKSZ and started observation from March 2016. From the observation up to November 17, 2019, the slip rate and locking depth were estimated to be 13 mm/yr and 22 km (Ref.4) using a vertical strike-slip fault model (Ref.5). On the other hand, block fault modeling using GNSS data (e.g., Ref.6) shows the slip rate of 7-8 mm/yr at the SKSZ and our estimated locking depth seems to be slightly deeper than the average thickness of the earth's crust. To solve the discrepancies, we added another year of GNSS data and examined other deformation factors such as after slip of the 2016 Kumamoto earthquake (hereafter KEQ2016) and re-estimated the slip rate and locking depth of the SKSZ.

Daily site coordinates at our sites from April 19, 2016 to November 30, 2020 were estimated using Bernese GNSS Software (ver.5.2). Subsequently, we corrected those by removing the following factors: 1) common mode bias, 2) viscoelastic deformation due to the KEQ2016, 3) volcanic deformation at Kirishima and Sakurajima volcanoes, 4) slow slip event in the Bungo Channel, 5) coseismic displacement of a M6.3 earthquake in the Hyuganada on May 10, 2019, 6) subduction of the Philippine Sea plate, 7) after slip of the KEQ2016, and 8) annual and semi-annual variations in coordinates time series. After the processes, site velocities relative to the Amur plate were estimated. Additionally, we also applied the Ref.5 fault model to the site velocities of a target area. The area was assumed to be a width of 25 km in the EW direction and a length of 90 km in the NS direction from the tentative center of the SKSZ (E130.5˚, N32.0˚), and its strike was assumed to be N104.8˚E (Ref.4). However, we obtain only the solutions that the locking depth exceeded average crustal thickness in the case of single strike-slip zone. Therefore, we introduced the case of double strike-slip zones. As a result, we found that the first and second deformations occur at 13.83±6.75 km north and 40.98±7.23 km south from the tentative center of the SKSZ with left-lateral slip rates of 10.06±4.13 mm/yr and 6.43±4.24 mm/yr and locking depths of 8.13±11.26 km and 5.23±13.36 km.

For the first deformation, our slip rate is consistent with that derived from block fault modeling and our locking depth is close to the hypocentral depths of the 1997 Northwestern Kagoshima earthquakes. For the second deformation, it is not known for the geodetic observation and our dense GNSS observation detects it for the first time. From the seismological study, the hypocenters with left-lateral strike-slip mechanisms lead from Kagoshima city to Koshikijima (Ref.7), and its strike and slip sense agree with our observation. This suggests that aseismic slip at a deep part of the earth's crust contributes to the strain accumulation and at least two deformation centers with left-lateral strike-slip are in the SKSZ.

This study was carried out by a contract with the Agency of Natural Resources and Energy, part of the Ministry of Economy, Trade and Industry of Japan as part of its R&D program supporting development of technology for geological disposal of high-level radioactive waste.

Reference

©2021. Japan Geoscience Union. All Right Reserved.

1) Wallace et al. (2009): Geology, 37(2), 143-146, 2009.
2) Nishimura et al. (2018): Geosphere, 14(2), 535-551, 2018.
3) Takayama and Yoshida (2007): J. Geophys. Res., 112, B06413, 2007.
4) Watanabe et al. (2020): JpGU-AGU Joint Meeting 2020, SSS14-P23, 2020.
5) Savage and Burford (1973): J. Geophys. Res., 78, 832-845, 1973.
6) Kimura et al. (2019): J. Geophys. Res., 124, 6140-6164, 2019.
7) Kakuta and Goto (2002): J. Seismol. Soc. Japan, 55, 317-336, 2002.

Keywords: shear zone in southern Kyushu, left-lateral strike slip fault, dense GNSS observation, the 2016 Kumamoto earthquake, post-seismic crustal deformation

©2021. Japan Geoscience Union. All Right Reserved.

Classification of faults using vertical gravity gradient data by machine learning

*Yuya Honda[1], Kohei Hotta[1]

1. University of Toyama

Changes in the density structure of the subsurface due to fault movement have been observed as gravity anomalies or gravity gradients. Gravity gradients are more sensitive to the change in the subsurface density structure compare to gravity anomalies, and are therefore widely used to estimate subsurface structures such as faults (e.g., Thompson, 1982; Copper and Cowan, 2006). Subsurface normal faults can be seen because the low-density layer is the upper plate. On the other hand, subsurface reverse faults are difficult to determine their structures such as their dips because the high-density layer is the upper plate.

Machine learning is one of the artificial intelligence (AI) techniques, which is used to filter out spam mail and automated driving technology, for example. It can classify data or pictures which are difficult to judge visually. In this study, we applied the machine learning method to classify faults, which have been done by researchers' visual judgements or roadside surveys, from vertical gravity gradients data obtained from fault models. For machine learning, we used Convolutional Neural Network (CNN), which is useful for image classification. The gravity gradient data was obtained by assuming fault models using the Talwani's method (Talwani, 1965), and the data were subjected to random noise with 0-50 Eötvös. The data was imaged and the image size was unified as 256×256 pixel for supervised learning. Here, we classified normal and reverse faults with different fault dips. At first, the normal faults were classified by fault dips of *45°*, *60°* and *75°*. 200 images with a fault dip of *60°* were classified. The value of the loss function was approximately 0.10, which yields the accuracy of 97%. Next, the reverse faults were classified by fault dips of *15°*, *30°*, *45°* and *60°*. 200 images with a fault dip of *30°* were classified. The value of the loss function was approximately 0.15, which yields the accuracy of 88.5%. The values of the loss functions were approximately 0.10 and 0.15, indicating that classifications of the fault dip were done with high accuracy. This indicates that the classification of normal and reverse fault using the machine learning method is possible. However, the accuracy of the reverse faults was 10% lower than that of the normal faults. This indicates that the classification of reverse faults is more difficult than that of normal faults. We will apply this method to actually observed data in the future study. However, since our method is based on linear fault model, we need to use actual data that can be approximated to be linear faults.

Keywords: machine learning, gravity gradient, fault

©2021. Japan Geoscience Union. All Right Reserved.

Hierarchical clustering of reduced stress tensors based on angular stress distance

*Noriaki Abe[1], Katsushi Sato[1]

1. Kyoto University

To reveal the crustal stress state is essential to elucidate mechanism and driving force of tectonics. In the field of geology, mesoscale structures such as faults, mineral veins and dikes are used to detect paleostresses through stress tensor inversion techniques. The techniques usually determine so-called reduced stress tensors which carry three principal stress axes and a stress ratio. Since the crustal stress state changes temporally and spatially, plural different stresses can be recorded in a set of mesoscale structures. Sometimes we meet a difficulty in inferring the tectonic origins of stresses because of a large number of and a wide variety of stress tensors detected from a study area. In such case we need a statistical approach to find out the characteristics of a group of stress tensors. In order to meet such requirement, this study proposes to utilize the hierarchical clustering method.
The hierarchical clustering method needs to define the differences between elements. In this study, angular stress distance (Yamaji and Sato, 2006) is used as the measure of difference between two reduced stress tensors. Once the tensors are grouped to form a cluster, we also need to define the distances between clusters. There are several methods to define the distances between clusters. Among them the group average method was found to be optimal through a Monte Carlo calculation to compare the methods with evaluations of the cophenetic correlation coefficients (Sokal and Rohlf, 1962).
We applied the hierarchical clustering method to stresses detected from the mesoscale structures in the Tanabe Group, SW Japan. The Tanabe Group is the middle Miocene paleoforearc basin fill, exposed in the southwest of the Kii Peninsula. A total of 1148 clastic dikes and 303 calcite veins have been analyzed by the mixed Bingham distribution method (Yamaji and Sato, 2011), and 327 faults have been analyzed by the Hough transform method (Sato, 2006). As the result of analyses, 21 stresses have been detected. The hierarchical clustering with group average method gave five clusters of stresses. In this clustering analysis, two clusters were distinguished when their angular stress distance is larger than 59.26° (Yamaji and Sato, 2019). Two of the clusters consist solely of the stresses detected in the southern sites. Plural different clusters detected in the same area suggest a temporal stress change. Another cluster comprises the stresses detected in the northern and the central sites. These three clusters appear to reflect a spatial change of the paleostress. Another cluster is composed of the stresses detected from clastic dikes. Clastic dikes observed in the Tanabe Group are considered to have intruded at the time during or soon after deposition (Miyata et al., 2009; Nakaya and Hamada, 2009). This cluster, therefore, shows the stress at the time of middle Miocene. The other cluster include only two stresses, and angular stress distance between them is near 59.26° of the threshold value. This cluster may not reflect the tectonic stress. In this way, hierarchical clustering of the detected stresses has indicated a spatio-temporal change of paleostress.

References

Miyata, Y., Miyake, K. and Tanaka, K., 2009, *The Journal of the Geological Society of Japan*, **115**, 470-482.
Nakaya, S. and Hamada, Y., 2009, *Journal of Geography*, **118**, 472-491.
Sato, K., 2006, *Tectonophysics*, **421**, 319-330.
Sokal, R.R. and Rohlf, F.J., 1962, *Taxon*, **11**, 33-40.
Yamaji, A. and Sato, K., 2006, *Geophysical Journal International*, **167**, 933-942.

©2021. Japan Geoscience Union. All Right Reserved.

Yamaji, A. and Sato, K., 2011, *Journal of Structural Geology*, **33**,1148-1157.
Yamaji, A. and Sato, K., 2019, *Journal of Structural Geology*, **125**, 296-310.

Keywords: paleostress analysis, hierarchical clustering, angular stress distance, Tanabe Group

©2021. Japan Geoscience Union. All Right Reserved.

Characteristic of fault geometry and the subducting plate boundary in the focal area of the 2016 Mw7.8 Kaikoura earthquake, New Zealand inferred from high precision aftershock distribution

*Yuta Kawamura[1], Satoshi Matsumoto[1], Tomomi Okada[2], Miu Matsuno[2], Yoshihisa Iio[3], Tadashi Sato[2], Stephen Bannister[4], John Ristau[4], Martha Savage[5], Richard Sibson[6]

1. Kyushu University, 2. Tohoku University, 3. Kyoto University, 4. GNS Science, 5. Victoria University of Wellington, 6. University of Otago

On 14 November 2016, in the northeast region of South Island, New Zealand, the Kaikoura earthquake (Mw 7.8) occurred. One of the main characteristics of this event, which is pointed out by previous studies, is the complexity of the rupture process involved with several faults. Our temporary observation group had installed more than 70 sites surrounding the target area before the mainshock and it has successfully recorded the mainshock and the aftershocks. In this study, we applied a double-difference relocation algorithm (Waldhauser and Ellsworth, 2000) to the dense observations and we determined fault geometries based on the high precision hypocenter distribution.
In order to evaluate the fault structure quantitatively, we employed multivariate analysis and a statistical method used in Yukutake and Iio (2017). As a result, we identified 11 fault planes in total. In particular, one of them is the fault where the rupture of the Kaikoura earthquake initiated, which is consistent with the structure shown by other studies and the nodal plane of the mainshock focal mechanism.
Furthermore, the bottom of the aftershock distribution in the northern area reveals a curved surface deepening towards the northwest direction. The result is almost parallel to, but approximately 3 km above, the slab interface determined by Williams et al. (2013). We detected many aftershocks in reverse fault type above this interface, which showed similarity in dip angle of the events to the interface. We consider whether the curved surface could represent the top of the subducting slab, or another type of interface.

Keywords: Kaikoura Earthquake, New Zealand, high precision aftershock distribution, fault geometry, plate boundary

©2021. Japan Geoscience Union. All Right Reserved.

Analysis of fault kinematics and internal structure of fracture zone at ISTL

*HIBIKI CHIBA[1], Kenta Kobayashi[1], Keita Takahashi[1]

1. Gradate School of Science and Technology Niigata University

Purpose of this study is to elucidate the activity history of the Yokokawa fault in FMP, And we carried out geological reconnaissance, structure observation of fault rocks, X-ray diffraction measurement and Rf/ ϕ strain analysis.

From the above results and considerations, we estimated formation process of Yokokawa fault and displacement of fault gouge. We used numerical expressions of displacement (Scholz, 1987). As a result, the amount of displacement was 4.7-470m. This result was smaller than displacement of Nechi-Ono Belt which was estimated by Shiraishi (2003). For this reason, we estimated that Yokokawa fault is connected to Nechi-Ono Belt.

Reference

Nagamori, H., Takeuchi, M., Furukawa, R., Nakazawa, T. and Nakano, S., 2010, Geology of the Kotaki district, Quadrangle Series, 1:50,000, Geological Survey of Japan, AIST, p.31-35, 66-69, 130

Scholz, C.H., 1987, Wear and gouge formation in brittle faulting, Geology, 15, p.493-495

Shiraishi, S., 2003, Geology of Itoigawa Spa and Itoigawa-Shizuoka Tectonic Line, Bulletin of the Fossa Magna Museum, No. 2, p.1-13

Keywords: Itoigawa Shizuoka Tectonic Line, Fault rock, Yokokawa Fault

©2021. Japan Geoscience Union. All Right Reserved.

Non-double-couple earthquake in the focal area of the 2000 Western Tottori earthquake by “0.1 manten” hyperdense seismic observation

*Takumi Motokoshi[1], Satoshi Matsumoto[2], Yoshihisa Iio[3], Shin'ichi Sakai[4], Aitaro Kato[4]

1. Department of Earth and Planetary Sciences, Graduate School of Science, Kyushu University, 2. Institute of Seismology and Volcanology, Faculty of Science, Kyushu University, 3. Disaster Prevention Research Institute, Kyoto University, 4. Earthquake Research Institute , the University of Tokyo

Non-double-couple (NDC) earthquakes are defined as a faulting of ordinary double-couple (DC) earthquake on a fault associated with additional rupture at the hypocenter. They have been mainly observed in volcanic zones and interpreted as faulting related to fluid effects in the hypocentral region. Study on NDC earthquakes is important for understanding the faulting process and provides an opportunity to obtain new information on stress and strength of the Earth’s crust.

In the focal area of the 2000 Western Tottori earthquake (M7.3), Yukutake et al. (2017) showed 8 best fit fault planes, suggesting the aftershock sequence was attributed to complex fault system. In order to investigate states of stress and strength in the large earthquake in detail, we have deployed 1,000 temporary seismic stations in and around the source region of the earthquake during the period from April 2017 to April 2018. This observation is called “0.1 manten” hyperdense seismic observation. We determined hypocenters and focal mechanisms using the data of the seismic network of both the “0.1 manten” and Hi-net by NIED. The data we analyze is both manually and automatically picked the arrival times and polarities of first P wave onset. Hayashida et al. (2020) found that the observational polarity distribution was slightly different from that expected by a DC source model at certain areas. In this study, we attempted to obtain spatial characteristic of the NDC events from the precise moment tensor solution. By following the processing in the previous study, we adopted the tensile-shear model and searched optimal model by performing a grid search and correlation analysis of S/P wave amplitude ratio. In addition, we introduced a weighting factor to homogenize the distribution of polarities on a focal sphere of an event in the NDC detection.
We found a trend that magnitude of NDC component become small as hypocenter was distant from the fault plan and located at edges of the faults plane. In addition, few earthquakes with large NDC components have large magnitude.

Keywords: inland earthquake, Non-double-couple earthquakes

©2021. Japan Geoscience Union. All Right Reserved.

Transition from radial to parallel dike swarm in Amakusa, Japan and their paleostress analyses

*Kentaro Ushimaru[1], Atsushi Yamaji[1]

1. Division of Earth and Planetary Sciences, Graduate School of Science, Kyoto University

Dikes in the Amakusa Islands were believed to have NNE trends, suggesting their intrusion accompanied by the initial rifting of the Okinawa Trough (Yamamoto, 1991). The sheet intrusions intruded to the Cretaceous and Paleogene sedimentary rocks, and the timing of intrusion was constrained to be 14–19 Ma depending on the radiometric ages of the intrusive rocks (Shibata and Togashi, 1975; Nagao et al., 1992; Hamasaki, 1996; Ohira et al., 2012). We observed 243 sheet intrusions in the islands and found that the NNE trending dikes were parts of a radial dike swarm. We also found that the radial pattern transformed laterally to a parallel one.

We took two approaches to estimate the paleostress(es) during the intrusion. First, to estimate the direction of σ_{Hmax}-axis during intrusion, a two-dimensional elastic model which involved the transition (e.g., Odé, 1957) was fitted to the distribution and trends of the sheet intrusions. The model assumed an elastic body with an internally pressured circular hole subjected to a bi-axial far field stress. This analysis showed the regional E-W trending σ_{Hmax}-axis.

Second, orientation data from the sheet intrusions were analyzed by the method of Yamaji and Sato (2011), which fits a mixed Bingham distribution to the orientations. This method was applied to the data set that consisted of 26 data taken from an area at the distances from 30 to 40 km form the center of the radiating system. The area existed within the parallel system. As a result, we obtained Stresses A and B of normal and strike-slip faulting regimes. Their σ_3-axes had N-S and ENE trends, respectively. Since the latter was obtained from sills in steeply dipping, well stratified sedimentary rock, we interpreted that Stress B was an artifact resulted from the mechanical weakness of the bedding. On the other hand, the principal axes of Stress A were approximately parallel to those determined by the two-dimensional elastic model. Therefore, Stress A was probably the regional stress at the time of dike intrusion. Stress A had the stress ratio of 0.40.

Magma pressure may have had temporal and spatial variations. The stress analysis yielded the DPI of 0.09: DPI (driving pressure index) is the 95th percentile of driving pressure ratios of the magmas (Faye et al., 2018). The orientation data of intrusions in an area from 2 to 10 km from the radiating center had two clusters indicating DPIs of 0.38 and 0.60 (Ushimaru and Yamaji, 2020), a few times larger than the DPI determined from the dikes far from the center. This difference is consistent with the picture that magma pressure declines with the distance from the center of a radiating dike system.

Keywords: stress, dike, sill

©2021. Japan Geoscience Union. All Right Reserved.

Electrical conductivity in a brine-saturated granite under uni-axial compression

*Yui Aikawa[1], Tohru Watanabe[1]

1. University of Toyama

Measurements of elastic wave velocity and electrical conductivity have been made on a brine-saturated rock (Aji granite) under uni-axial compression (< 20 MPa) in order to understand the influence of differential stress on electrical conductivity in fluid-bearing rocks. Microcracks perpendicular to the compression axis were preferentially closed to show anisotropic change in elastic wave velocity. Velocity significantly increased in the direction parallel to the compression axis, while it showed little change in the direction perpendicular to the compression axis. On the contrary, electrical conductivity showed no anisotropic change: conductivity decreased similarly in directions parallel and perpendicular to the compression axis. Cracks perpendicular to the compression axis, which were closed under compression, must contribute to electrical conduction in directions parallel and perpendicular to the compression axis. In order to understand the observed change in conductivity, the orientation distribution of cracks must be evaluated.

The orientation distribution of cracks can be evaluated by the crack density tenor (e.g., Sayers and Kachanov., 1995), which is calculated from elastic compliance tenor. In order to determine full compliance tensor, velocity must be measured in a direction oblique to the sample surface. Velocity measurement at an oblique angle was successfully made by attaching small (~10 mm) Aji granite prisms on sample surfaces. In a preliminary experiment on the dry sample, crack density tensor showed the closure of cracks perpendicular to the compression axis. We will next determine crack density tensor and aspect ratio in the wet sample and construct a quantitative model of electrical conduction to reproduce the observed conductivity change in both directions.

Keywords: electrical conductivity, crack, fluid, stress

©2021. Japan Geoscience Union. All Right Reserved.

Lithologic and thermal controls of seismicity in the northwestern Kii Peninsula, southern Honshu, Japan

*Sumire Maeda[1], Shinji Toda[2], Toru Matsuzawa[3], Makoto Otsubo[4]

1. National Research Institute for Earth Science and Disaster Resilience, 2. International Research Institute of Disaster Science, Tohoku University, 3. Graduate School of Science, Tohoku University, 4. Geological Survey of Japan, National Institute of Advanced Industrial Science and Technology

A spatial similarity of the distributions between inland earthquakes and the lithotectonic belts, which is considered to be controlled by the mechanical properties of the lithosphere such as rheology of minerals, has been reported by several papers (e.g., Huzita et al. 1973). Particularly, the relationship between the deeper limit of earthquakes (seismicity cut-off) and the depth to the brittle-ductile transitions in the crust has been extensively investigated (e.g., Albaric et al. 2009; Hauksson and Meier 2019). However, these studies have compared the vertical distribution of the seismicity only with the rocks consisting of the lithotectonic belts at the ground surface, but not with the subsurface geological structure. In order to understand the relationship between the earthquake occurrence and the rheological properties at depth in detail, we attempted to quantitatively interpret the horizontal variety in the vertical extent of the shallow inland seismicity related to the difference of the lithotectonic belts, based on the temperature-dependent rock friction.

The study area is the northwestern Kii Peninsula, southern Honshu, Japan. We first relocated the earthquake hypocenters in this area, based on the double-difference location method (Waldhauser and Ellsworth 2000). We then estimated the density distribution (Talwani et al. 1959) in the study area by analyzing gravity data (Geological Survey of Japan 2013) to clarify how deep the surficial lithotectonic belts vertically extend. We finally compared the horizontal and vertical relationship between the seismicity and the geological structure based on these results.

From the density analysis, we confirmed that the surface rock bodies in the tectonic belts are likely to extend from the surface to at least 7 km depth, although the lower limit of the subsurface tectonic structure can be deeper. Based on the results of the relocated hypocenters, we found that the earthquakes are concentrated mainly in the shallow part (approximately 4.5–6.0 km) within the pelitic rock belts. Within the mafic rock belts, on the other hand, the seismicity rate is low in the shallow part but high in the deep part (approximately 5.5–7.5 km).

In order to interpret the difference in the vertical extents of the seismicity depending on the lithology, we compare the frictional properties of pelitic and mafic rocks obtained by rock experiments with the earthquake depths within the lithotectonic belts composed of respective rocks in the study area. The rock experiments have shown that gouges of the pelitic and mafic (metabasalt) rocks exhibit the velocity-weakening at 250℃ to 400℃ (Den Hartog et al. 2012) and at 300℃ to 600℃ (Zhang et al. 2017), respectively. Based on the heat flow of 130 mW/m^2 in the Wakayama region estimated by Matsumoto (2007) and thermal conductivity of 2.5 $Wm^{-1}K^{-1}$ (Fowler 2005; Tanaka 2009), these temperature ranges in which the velocity-weakening occurs are converted to the depth ranges of approximately 4.7–7.7 km for the pelitic belt and 5.7–11.8 km for the mafic belt. The depth ranges of high-seismicity areas within representative pelitic and mafic rock belts are consistent with these vertical ranges of the velocity-weakening found from the experiments. These good consistencies strongly suggest that the occurrence of shallow intraplate earthquakes is controlled by the temperature-dependent and

©2021. Japan Geoscience Union. All Right Reserved.

lithology-dependent friction.

©2021. Japan Geoscience Union. All Right Reserved.

On approximations of EASY%R_o model to estimate maximum experienced temperature from vitrinite reflectance in rocks

*Shunya Kaneki[1], Hiroyuki Noda[1]

1. Disaster Prevention Research Institute, Kyoto University

Vitrinite reflectance is one of the most popular thermal indices for rocks. Among various models to estimate paleothermal histories, EASY%R_o has been widely used since proposed by Sweeney & Burnham (1990). Approximations of EASY%R_o solutions employing specific paleothermal histories have been used in the field of structural geology to estimate maximum experienced temperatures from vitrinite reflectance. However, comparisons of those approximations with results obtained with EASY%Ro itself have not been reported in scientific literatures, and the errors of approximations and the limitations of their use to determine maximum temperature remain undocumented. In this study, we performed such comparisons and found that the use of some approximations proposed in the previous studies can lead to considerable deviations from the results obtained with EASY%R_o. We then derived new approximations of EASY%R_o solutions for four representative paleothermal histories that provided estimates of the maximum temperatures within 3 ˚C of those obtained with EASY%R_o. We also describe the Jacobian of EASY%Ro for each specific paleothermal history, which can be used to propagate errors from vitrinite reflectance to maximum temperatures. We expect that four approximations derived in this study will be useful because of their smaller approximation errors and wider application ranges compared to the previous approximations, although we recommend to calculate EASY%R_o itself if greater precision or particular paleothermal histories other than those assumed in this study are required.

Keywords: Vitrinite reflectance, Paleothermal history, EASY%Ro, Approximation

©2021. Japan Geoscience Union. All Right Reserved.

[J] Poster | S (Solid Earth Sciences)：S-CG Complex & General

Thu. Jun 3, 2021 5:15 PM - 6:30 PM JST | Thu. Jun 3, 2021 8:15 AM - 9:30 AM UTC | Ch.12_3

[S-CG51] New perspectives of subduction zone earthquake dynamics through experiments across-scales

convener:Masataka Kinoshita(Earthquake Research Institute, University of Tokyo)

Knowledge on subduction zone earthquake phenomena has considerably increased in the last decade. On the other hand, there are limits to seismological approach alone to comprehensively elucidate the earthquake mechanism in which phenomena that differ by 10 orders of magnitude in space and time, from earthquake nucleation/growth processes to its driving force. Steps to enable scientific earthquake forecasting should include; monitoring regional seismic/tectonic activity using networked observatories, sampling of and insitu measurement in seismogenic faults and plate materials through ultra-deep drilling, and reproduction/insitu-observation of fracture nucleation processes by high-pressure quantum-beam experiments. Through a close collaboration, we challenge a dynamic imaging of earthquake processes. Based on the proposal approved as a Large Research Master Plan 2020 of the Science Council of Japan, we will deepen the interdisciplinary discussion on subduction-zone earthquakes and the state & property of lithosphere. We welcome, but not limited to, presentations from fields of ocean and land networks observation, seismogenic zone drilling, rock mechanical & quantum beam experiments, fracture process
theory, etc.

[SCG51-P01] For examining steady-state solution for pore pressure distribution in a plate-subduction zone incorporating fluid release by chemical reaction

*Shunya Kaneki[1], Hiroyuki Noda[1] (1.Disaster Prevention Research Institute, Kyoto University)

[SCG51-P02] A new method for large number of core sample CT scanning and preliminary results of Nankai Trough DSDP and ODP core samples

*Satoshi Tonai[1], Yusuke Kubo[2], Masataka Kinoshita[3], Keishi Okazaki[2] (1.Faculty of Science and Technology, Kochi University, 2.Kochi Institute for Core Sample Research, JAMSTEC, 3.Earthquake Research Institute, University of Tokyo)

For examining steady-state solution for pore pressure distribution in a plate-subduction zone incorporating fluid release by chemical reaction

*Shunya Kaneki[1], Hiroyuki Noda[1]

1. Disaster Prevention Research Institute, Kyoto University

Progressive compaction and dehydration of subducting sediments in a plate-subduction zone have been considered to affect its pore pressure condition. Representative dehydration reactions include smectite-illite-muscovite conversion and amorphous silica-Opal CT-quartz conversion reactions. Some previous studies modelled quantitative effects of compaction and these dehydration reactions on steady-state pore pressure and permeability. However, these studies ignore the volumetric change in solid phase by reaction, and thus the steady-state solutions incorporating the spatial heterogeneity of such volumetric change should be examined.

The ultimate goal of this study is to examine the steady-state solutions for pore pressure distribution incorporating progressive compaction and dehydration reactions based on a reasonable physical model. Because the permeability of fault rocks is generally much higher than that of surrounding intact rocks, we consider the very simple model in which fluid flows only along a fault zone. Dirichlet boundary conditions of pore pressure were postulated at a surface and a down-dip limit of seismogenic crust. We focus on Kumano Basin in Nankai Trough as an example of plate-subduction zones, and various physical properties were set according to the previous studies examined in this area. Amorphous silica content in the core samples is reported to be less than 1 wt%, so we focus only on the transformation reactions of smectite. As we could not find any literatures reporting kinetics of illite-muscovite conversion, only illitization of smectite is considered here.

The qualitative effect of fluid release due to chemical reaction on pore pressure depends on the balance between the rates of fluid release and pore volume created by reaction. On the basis of some reaction equations reported in previous studies, illitization of smectite can have both positive and negative effects on pore pressure. However, if we consider the constraints on the reaction equation such that the mole number of reacted smectite and generated illite must be equivalent, illitization of smectite may have positive effect on pore pressure. The preliminarily calculation shows that smectite dehydration can decrease pore pressure by up to ~10 MPa. In this presentation, we would like to discuss the calculation results obtained before the conference, in addition to these preliminarily results.

Keywords: Plate-subduction zone, Dehydration reaction, Smectite, Pore pressure, Steady-state solution

©2021. Japan Geoscience Union. All Right Reserved.

A new method for large number of core sample CT scanning and preliminary results of Nankai Trough DSDP and ODP core samples

*Satoshi Tonai[1], Yusuke Kubo[2], Masataka Kinoshita[3], Keishi Okazaki[2]

1. Faculty of Science and Technology, Kochi University, 2. Kochi Institute for Core Sample Research, JAMSTEC, 3. Earthquake Research Institute, University of Tokyo

X-ray CT scan (hereafter referred to as CT) can obtain the three-dimensional internal structure of an object with non-destructive and high spatial resolution by using the difference in the degree of X-ray absorption depending on the density and/or element. Since it is highly valuable as basic information for geological core samples, geological core samples drilled by D/V *Chikyu* are taken CT data on board. However, other core samples are basically not collected CT data. One of the issues when collecting CT data for a large number of core samples is working time, and we report a new method for acquiring efficiently CT data at Kochi Core Center, Japan (hereafter referred to as KCC).
At KCC, core samples are usually scanned one by one using CT scanner. In the reporting method, 12 core samples were scanned at one time and divided into CT data for each core using an image processing program. With these improvements, work efficiency has increased about 10 times. For example, CT data can be acquired in about 1 or 2 days for core samples from one site of ODP or IODP (several hundred meters long). The spatial resolution of the CT image from the new method is about 0.5 mm/pixel, which is slightly inferior to the resolution of 0.2 mm/pixel when taken with a one by one image. Nevertheless, they can be fully utilized for analysis of geological structure, crack distribution, or downhole profiles of mean CT values of core samples.
As a preliminary study, the method of this study was applied to some DSDP and ODP core samples around the Nankai Trough. In the Nankai Trough, a hydrothermal mineralization was reported from the drilling core at Site C0023 of IODP Expedition 370 located at the toe of the Nankai accretionary complex (Tsang et al., 2020). In order to clarify the scale and origin of the hydrothermal mineralization, CT data of other sites excavated around the Nankai Trough are considered to be effective, and mainly the Nankai Trough off the coast of Ashizuri, Kochi Prefecture. CT data were obtained for the core samples from seven sites. As a result, sections showing high CT values were confirmed at multiple intervals. In particular, high CT value intervals were found in the lower part of the Shikoku Basin sediments at site 1177. At least in some of these high CT value intervals, no corresponding description or physical property data was confirmed by previous studies using the same samples. Thus, it is considered that there is a possibility that new geological information of core samples can be extracted by acquiring a large amount of CT data.

Keywords: Nankai Trough, Hydrothermal alternation, X-ray CT

©2021. Japan Geoscience Union. All Right Reserved.

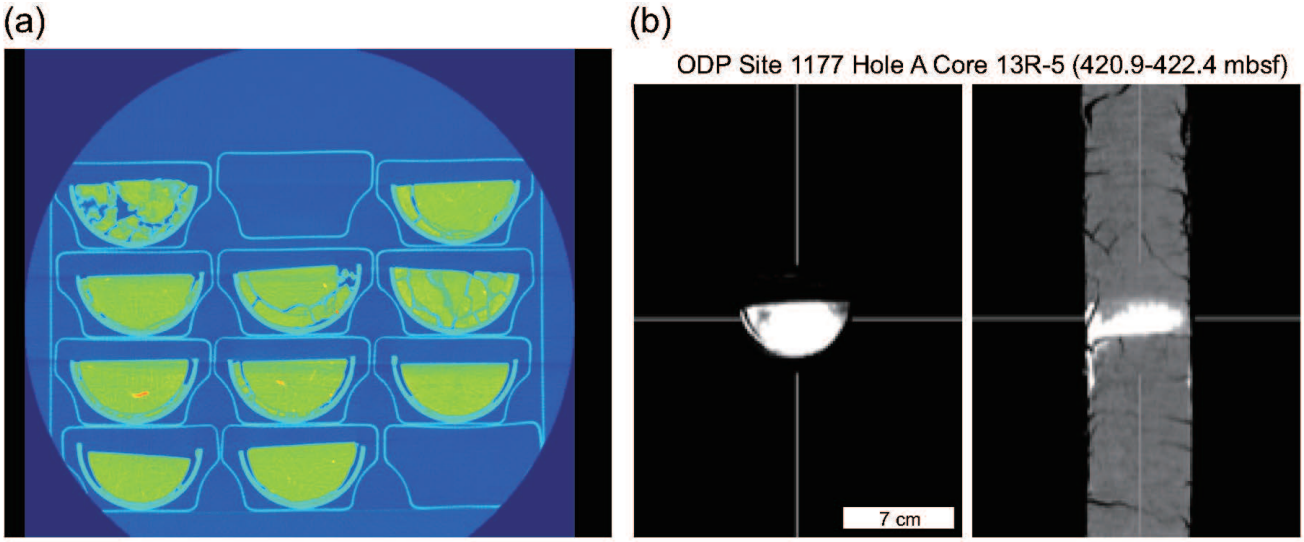


Fig.1. (a) 12 CT slice images scanning one time. (b) Typical high CT value interval of core sample (white area).

©2021. Japan Geoscience Union. All Right Reserved.

[J] Poster | S (Solid Earth Sciences)：S-CG Complex & General

Thu. Jun 3, 2021 5:15 PM - 6:30 PM JST | Thu. Jun 3, 2021 8:15 AM - 9:30 AM UTC | Ch.14_3

[S-CG52] Driving Solid Earth Science through Machine Learning

convener:Hisahiko Kubo(National Research Institute for Earth Science and Disaster Resilience), Yuki Kodera(Meteorological Research Institute, Japan Meteorological Agency), Makoto Naoi(Kyoto University), Keisuke Yano(The Institute of Statistical Mathematics)

The development of machine learning techniques, such as deep learning, has led to innovations in various fields and is gaining ground in the solid earth sciences. This session provides an opportunity to inspire each other for future developments by bringing studies of machine learning applications in various fields including solid earth science. We especially welcome researches that have led to the discovery of phenomena and theories in solid earth science. We also look forward to studies on the black box problem of deep learning and efforts toward explainable AI.

[SCG52-P01] Automatic hypocenter determination by deep learning for microseismic networks in geothermal areas

*Kyosuke Okamoto[1], Yusuke Mukuhira[2], Hiroshi Asanuma[1], Markus Häring[3] (1.National Institute of Advanced Industrial Science and Technology, 2.Tohoku University, 3.Häring GeoProject)

[SCG52-P02] Toward development of dense low cost citizen seismic network: Performance comparison of different types of neural network architectures

*Ahyi KIM[1], Hiroki Uematsu[1], Yuji Nakamura[1], Yuta Takahashi[1], Momoko Nakamura[1] (1.Yokohama City University)

[SCG52-P03] Unsupervised automatic classification of seismic records based on a hierarchical clustering

*Yuki Kodera[1], Shin'ichi Sakai[2] (1.Meteorological Research Institute, Japan Meteorological Agency, 2.Earthquake Research Institute, the University of Tokyo)

[SCG52-P04] Hierarchical cluster analysis of F-net moment-tensor-solution catalogue in Japan

*Hisahiko Kubo[1], Takeshi Kimura[1], Katsuhiko Shiomi[1] (1.National Research Institute for Earth Science and Disaster Resilience)

Automatic hypocenter determination by deep learning for microseismic networks in geothermal areas

*Kyosuke Okamoto[1], Yusuke Mukuhira[2], Hiroshi Asanuma[1], Markus Häring[3]

1. National Institute of Advanced Industrial Science and Technology, 2. Tohoku University, 3. Häring GeoProject

A dense seismic network including deep borehole sensors is ordinally employed in developing geothermal areas to detect a change in seismicity regarding the geothermal developments. It is possible that illuminating subsurface fluid flows in detail by tracking the microseismic clouds in high-resolution. However, hypocenter determinations based on manual phase picks are sometimes difficult due to lack of manpower as well as cost. Moreover, automatic event picks based on STA/LTA still need manual corrections of the picks for high-resolution hypocenter determinations,

In this study, we aimed to develop an automatic event pick method based on deep learning that could substitute for manual picks especially for microseismic networks in geothermal areas. We developed the method by using seismic data observed by a dense seismic network (five borehole sensors, four surface sensors) employed in Okuaizu Geothermal Field (Fukushima, Japan) since May 2015. We also examined applicability of this method to another geothermal field by using seismic data observed by a dense seismic network (six borehole sensors) in Basel geothermal field (Switzerland).

Deep learning was conducted by “teachers”: manual picks of 33,008 P-waves and 65,925 S-waves from microseismic events (local magnitude range: -1.5 –2.5) observed in the Okuaizu Geothermal Field. Then, the accuracy of the learning was evaluated by 3,344 P-waves and 3,310 S-waves. As the result, the accuracy for P-waves was average = ˜0.03 s and standard deviation = ˜0.46 s and that for S-waves average = ˜0.01 s and standard deviation = ˜0.30 s. We applied this deep learning phase picker to the seismic events detected from continuous seismic waves by STA/LTA in Okuaizu Geothermal Field, and found that the hypocenter distribution based on the deep learning pick showed a shape similar to that based on the manual pick. When applying to this deep learning phase picker to 3,069 seismic events in the Basel geothermal field (17,138 P-waves, 13,702 S-waves), the accuracy for P-waves was average = ˜0.15 s and standard deviation = ˜0.58 s and that for S-waves average = ˜0.16 s and standard deviation = ˜0.65 s.

For further applying this method to other seismic networks in geothermal areas, it is needed to consider transfer learning and optimization of the structure of hidden layers.

This study was performed as a part of the “Technology to evaluate and manage geothermal reservoirs” sponsored by Japan Oil, Gas and Metals National Corporation (JOGMEC).

Keywords: Deep learning, Phase pick, Microseismic monitoring, Geothermal development, Fluid flow

©2021. Japan Geoscience Union. All Right Reserved.

Toward development of dense low cost citizen seismic network: Performance comparison of different types of neural network architectures

*Ahyi KIM[1], Hiroki Uematsu[1], Yuji Nakamura[1], Yuta Takahashi[1], Momoko Nakamura[1]

1. Yokohama City University

We have developed a community based low cost seismic network in Yokohama, Japan, called Citizen Seismic Network (CSN), to monitor local scale strong motion which is closely linked to community’ s life. Each sensor unit composed of 12 bit MEMS accelerometer and Raspberry Pi.
Since the units are supposed to be installed under high-noise condition such as inside of house where spiky noise made by human activities often misinterpreted as seismic signal, it is difficult to discriminate the seismic signals from other noises. In such condition, applying conventional detection method using amplitude ratio (e.g. STA/LTA) is problematic. To overcome the issue, we employed an artificial neural network that utilizes pattern recognition to retrieve seismic signals. In this study, we compared the 3 different types of neural networks, namely, 3 layered shallow network (ANN), convolutional neural network, and recurrent neural network. For the training and validation, we prepared numerical data set produced by seismic records obtained from K-net adding CSN sensor noise (~90000 for training and ~40000 for validation). Since it is possible the amount of the data is not enough for CNN and RNN, we also tested transfer learning using pre-trained model open to public. As preliminary results, we found that using pre-trained ANN on the Raspberry Pi in real time and making final decision using deep neural network pre-trained by transfer learning on server is the most effective.

Keywords: Neural network, Machine Learning, Seismic signal, Seismometer, Strong motion, CNN

©2021. Japan Geoscience Union. All Right Reserved.

Unsupervised automatic classification of seismic records based on a hierarchical clustering

*Yuki Kodera[1], Shin'ichi Sakai[2]

1. Meteorological Research Institute, Japan Meteorological Agency, 2. Earthquake Research Institute, the University of Tokyo

Introduction

Continuous seismic waveforms recorded in a seismometer include various signals such as earthquakes, human activities, and instrumental noises. If the automatic classification of continuous records is possible, that enables us to understand geophysical phenomena around a target seismometer and to monitor the instrumental condition of a seismometer used in a real-time system such as earthquake early warning. We have been developing an unsupervised automatic classification algorithm for continuous records that is applicable to various seismometers deployed in different observation environments.
Kodera and Sakai (2020, SSJ Fall Meeting) proposed a classification algorithm that calculates running spectra as features and then clusters a dataset in the frequency and time domains using clustering methods based on the k-means and spectral clustering algorithms, respectively. However, the algorithm has a weak point in that the algorithm needs a hyperparameter that defines the number of clusters output by the spectral clustering algorithm, which is difficult to determine appropriately in advance. In this study, we propose a new algorithm based on a hierarchical clustering that does not require the hyperparameter for the number of output clusters and therefore can classify a dataset in a more flexible way.

Proposed algorithm

The proposed algorithm is divided into three parts as Kodera and Sakai (2020): (1) feature extraction, (2) clustering in the frequency domain, and (3) clustering in the time domain.
(1) Feature extraction: Running spectra are used as features, calculated with a 4-s time window every 0.1 s. Then, running spectra are converted into 10-dimensional vectors through a filter bank with 10 separated frequency bands.
(2) Clustering in the frequency domain: A dataset is clustered in the frequency domain by selecting 2000 representative points (RPs) and assigning each data point to the nearest RP. We determine the RPs by a random sampling, after dividing the dataset into several groups based on distances between data points to deal with the imbalanced data problem (i.e., the data amount of stationary noise signals is the largest).
(3) Clustering in the time domain: In the spectral clustering, the kernel principal component analysis (kPCA) is performed based on the adjacent matrix of a graph, and then the k-means algorithm is used to determine the clusters; in this study, the k-means algorithm is replaced with the Ward hierarchical clustering algorithm. The adjacent matrix is constructed from a transition matrix assuming the Markov chain. The dimension of the kPCA is set to 10.

Application to test data

We applied the proposed algorithm to continuous records from March 1 to 7, 2017, at station E.JDJM, a MeSO-net station located near a subway (Kawakita and Sakai, 2009). The figure shows a dendrogram obtained from the hierarchical clustering algorithm and classification results for a certain 30-minute record. At a high level in the dendrogram, there were two groups separated with small and large clusters; the former and latter may correspond to groups related to earthquake and noise signals, respectively. When the dendrogram was cut at 1/2 of the maximum height, frequent noise signals were classified into high- and low-level noise classes. With the dendrogram cut at 1/3, the high-level noise class was divided

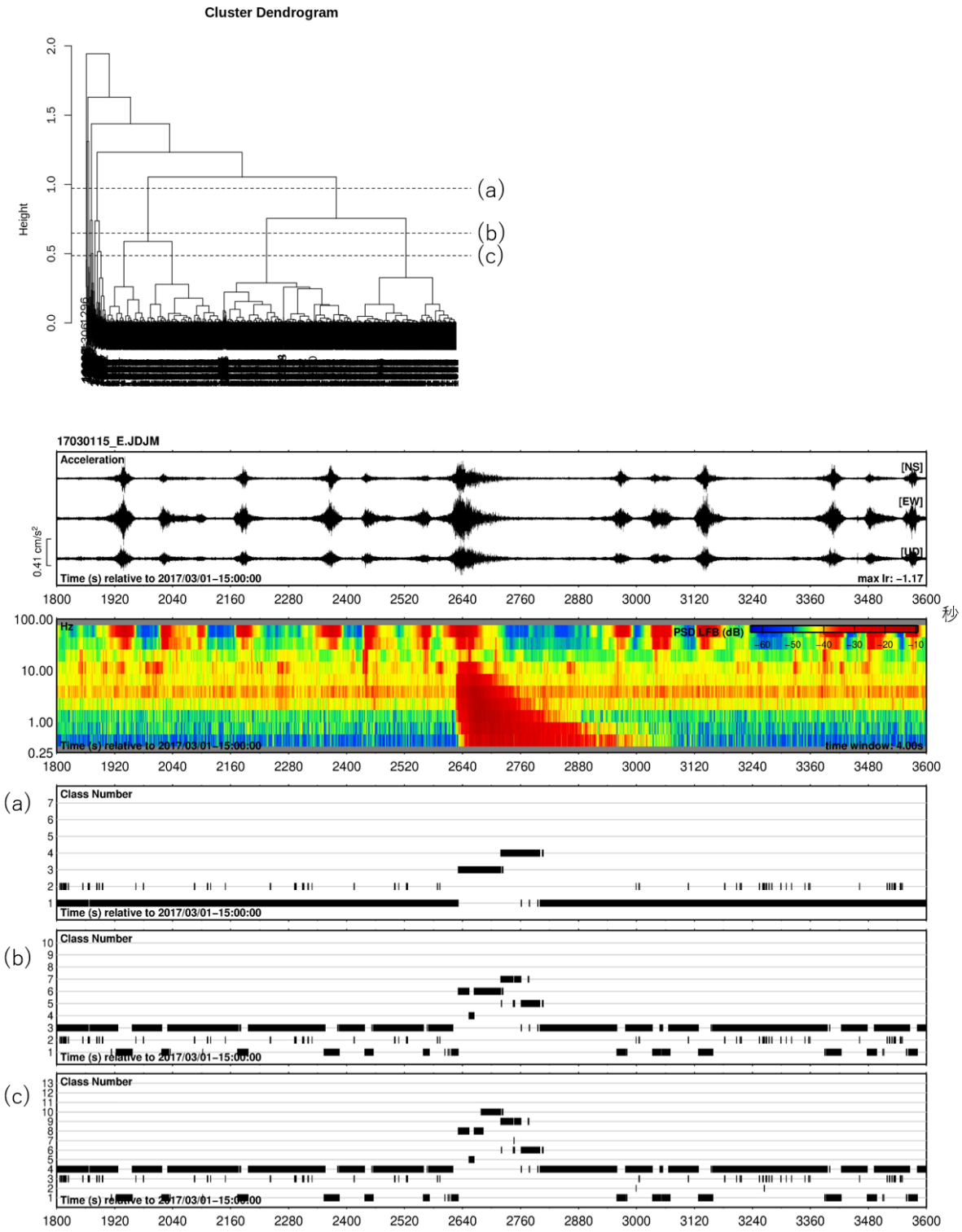
©2021. Japan Geoscience Union. All Right Reserved.

into two sub-classes, one of which corresponded to train noises.
Those results indicate that, although there remains an issue of how to cut the dendrogram appropriately, signals on continuous records could be classified and extracted by the hierarchical clustering algorithm.

Acknowledgment: We used seismic records of MeSO-net maintained by the Earthquake Research Institute, the University of Tokyo.

Keywords: Machine learning, Unsupervised learning, Automatic classification, Seismic waveform record

©2021. Japan Geoscience Union. All Right Reserved.



図：階層的クラスタリングにより得られたデンドログラムとクラス分類結果．(a), (b), (c)はデンドログラムをそれぞれ最大高さの1/2, 1/3, 1/4でカットしたときの分類結果に対応する．

Figure: A dendrogram obtained from the hierarchical clustering algorithm and classification results for a certain 30-minute record. (a), (b), and (c) correspond to classification results with the dendrogram cut at 1/2, 1/3, and 1/4 of the maximum height, respectively.

©2021. Japan Geoscience Union. All Right Reserved.

Hierarchical cluster analysis of F-net moment-tensor-solution catalogue in Japan

*Hisahiko Kubo[1], Takeshi Kimura[1], Katsuhiko Shiomi[1]

1. National Research Institute for Earth Science and Disaster Resilience

The spatial distribution of earthquakes is heterogeneous in response to background stresses and underground structures. Therefore, finding regional characteristics of seismic activity from seismic catalogs leads to the understanding of background stresses and underground structures that affect the way earthquakes occur. Kubo et al. (2020, SSJ) applied a dimensionality reduction technique of unsupervised machine learning to the moment tensor solution catalog of F-net of NIED and demonstrated that earthquakes with similar properties are embedded in the same region in the dimensionality-reduced space. In this study, we apply hierarchical clustering, which is also a kind of unsupervised machine learning, to the F-net moment tensor solution catalog to obtain the hierarchical structure of earthquake clusters and investigate the regional characteristics of seismic activity in Japan.

We used the moment tensor solution dataset provided by Kubo et al. (2020, SSJ). This dataset is based on the F-net moment tensor solution catalog and includes additional information on double couple and CLVD. The target parameters in the clustering of this study are latitude, longitude, and depth of earthquakes, and x and y of the source-mechanism diagram (Kavernia et al. 1996; Kagan 2005). A large x means that the reverse fault component is dominant, and a small x means that the normal fault component is dominant. A large y means that the strike-slip fault component is dominant. As a preprocessing for the cluster analysis, an axis transformation using principal component analysis was applied to latitude and longitude, and then each parameter was normalized.

There are two types of clustering methods: hierarchical clustering and non-hierarchical clustering such as k-means. Although hierarchical clustering is more computationally expensive, it has the advantage of obtaining a hierarchical structure of data with information about the relationships among clusters. In this study, we used the agglomerative method of hierarchical clustering, and the Ward method was used to calculate the distance between clusters. Agglomerative Clustering of scikit-learn was used as the analysis code.

Here, as a preliminary analysis, we examined the top 10 clusters obtained by hierarchical clustering. We found that the top 10 clusters consisted of earthquake groups with different fault types (normal fault, reverse fault, and strike-slip fault), different regions (eastern and western Japan), and different source depths (less than 20 km, 20-100 km, and greater than 100 km). This result indicates that groups of earthquakes with similar properties can be extracted by the hierarchical clustering of the moment tensor solution catalog. Further investigation of the lower clusters is expected to extract more local earthquake groups.

Keywords: Hierarchical clustering, Moment tensor solution, Unsupervised machine learning, Regional characteristics of seismic activity

©2021. Japan Geoscience Union. All Right Reserved.

[J] Poster | M (Multidisciplinary and Interdisciplinary)：M-IS Intersection

Thu. Jun 3, 2021 5:15 PM - 6:30 PM JST | Thu. Jun 3, 2021 8:15 AM - 9:30 AM UTC | Ch.17_2

[M-IS21] Chemosynthetic community and mud volcano: biology, geochemistry, and geophysics of fluid discharge

convener:Yusuke Miyajima(Geomicrobiology Research Group, Research Institute for Geo-Resources and Environment, Geological Survey of Japan, National Institute of Advanced Industrial Science and Technology), Kayama Hiromi WATANABE(Japan Agency for Marine-Earth Science and Technology), Akira Ijiri(Japan Agency for Marine-Earth Science and Technology), Tomohiro Toki(Faculty of Science, University of the Ryukyus)

Fluid discharge at mud volcanoes, cold seeps, and hydrothermal vents brings subsurface materials to the Earth's surface. Unique chemosynthesis-based ecosystems are fueled by the substances provided by discharged fluids, and have played a role in the evolution and diversification of life. Knowing fluid geochemistry, driving forces, and geological background of fluid discharge provides key to understand the distribution and evolution of chemosynthetic ecosystems. Multidisciplinary studies from viewpoints of geology, biology, geochemistry, and geophysics are essential to reveal the relationship between fluid discharge and material cycling, environmental changes, and natural hazards, in addition to elucidate spatio-temporal variation of chemosynthesis-based ecosystems. This session welcomes talks and posters focusing on organisms and geological phenomena related to mud volcanoes, cold seeps, hydrothermal vents, and other similar environments. We aim to understand interactions between geosphere, biosphere, and human both on land and in ocean through Earth history.

[MIS21-P01] Origin of noble gases in surface sediments from submarine mud volcanoes off Tanegashima

*Yuki Mitsutome[1], Tomohiro Toki[2], Takanori Kagoshima[3], Naoto Takahata[4], Yuji Sano[5], Yama Tomonaga[6] (1.University of the Ryukyus Graduate School of Science and Engineering, 2.Faculty of Science, University of the Ryukyus, 3.University of Toyama, 4.Atmosphere and Ocean Research Institute, the University of Tokyo, 5.Division Ocean and Earth Systems, Atmosphere and Ocean Research Institute, the University of Tokyo, 6.Eawag, Swiss Federal Institute of Aquatic Science and Technology)

[MIS21-P02] Subsurface structures and fluid transportation visualization by acoustic mapping in a shallow methane hydrate area off Sakata, eastern margin of the Sea of Japan

*Miho Asada[1], Mikio Satoh[1], Toshiyuki Yokota[1], Shusaku Goto[1] (1.NATIONAL INSTITUTE OF ADVANCED INDUSTRIAL SCIENCE AND TECHNOLOGY (AIST))

[MIS21-P03] Chemosynthesis, surface ruptures and possible methane eruption on the Kuroshima Knoll: a review from previous studies

*Takeshi Matsumoto[1] (1.Faculty of Science, University of the Ryukyus)

[MIS21-P04] Community composition and connectivity of hot vent endemic animals on the Izu-Bonin-Mariana Arc

*Hiromi Kayama WATANABE[1], Chong Chen[1], Shigeaki Kojima[2], Hiroyuki Yamamoto[1] (1.Japan Agency for Marine-Earth Science and Technology, 2.Atmosphere and Ocean Research Institute, the University of Tokyo)

[MIS21-P05] Population Genetic Structure and Gene Expression Plasticity of the Deep-Sea Vent and Seep Squat Lobster *Shinkaia crosnieri*

*Yao Xiao[1] (1.Hong Kong University of Science and Technology)

[MIS21-P06] A Decade to Study Deep-Sea Science

*Hiromi Kayama WATANABE[1], Kerry Howell[2] (1.Japan Agency for Marine-Earth Science and Technology, 2.University of Plymouth)

Origin of noble gases in surface sediments from submarine mud volcanoes off Tanegashima

*Yuki Mitsutome[1], Tomohiro Toki[2], Takanori Kagoshima[3], Naoto Takahata[4], Yuji Sano[5], Yama Tomonaga[6]

1. University of the Ryukyus Graduate School of Science and Engineering, 2. Faculty of Science, University of the Ryukyus, 3. University of Toyama, 4. Atmosphere and Ocean Research Institute, the University of Tokyo, 5. Division Ocean and Earth Systems, Atmosphere and Ocean Research Institute, the University of Tokyo, 6. Eawag, Swiss Federal Institute of Aquatic Science and Technology

A submarine mud volcano is a small hill where sediments with high pore pressure rise as a mud diapir and vent on the seafloor. In Japan, mud volcanoes have been found in the Kumano area of the Nankai Trough and off Tanegashima. In this study, we analyzed noble gases collected from the sediments of four mud volcanoes out of the 15 mud volcanoes discovered in the forearc region off Tanegashima. The purpose of this study is to analyze the measurement results of noble gases in the sediments of the mud volcanoes off Tanegashima, to discuss the origin of the gases, and to compare them with noble gas data from other marine areas.

The sampling was conducted during voyages using the *R/V Hakuho-Maru* from August 19 to September 1, 2015 and August 9 to 18, 2019. MV1 and MV14 sediment samples were collected during the 2015 voyage, and MV2 and MV3 samples were collected during the 2019 voyage. In MV1 and MV14, after collecting the piston corer, a hole was drilled in a PVC pipe and a copper tube was set in it, filled with surface sediment, and sealed with a metal clamp. For MV2 and MV3, copper tubes were set in pre-drilled holes in the pipes of the multiple corer and sediments were collected in the same way as for piston coring. The noble gases in the surface sediments in the copper tube were measured using a noble gas mass spectrometer at ETH Zurich and the Atmosphere and Ocean Research Institute of the University of Tokyo. As a result, the helium isotope ratio ($(^3He/^4He)_{raw}$) ranged from 0.23 to 0.96 R_A, all of which were lower than the value of 1 R_A in atmospheric equilibrium seawater (ASW). 0.23 R_A was the smallest value in MV1, and 0.96 R_A was the largest value in MV14. In MV3, we sampled at three depths, with the deeper depths showing higher values than the shallower ones. The $(^3He/^4He)_{raw}$ values of MV2 is 0.63 R_A. The results of $^4He/^{20}Ne$ values are as follows: MV3-1 shows the highest value of 18.4, followed by MV1, MV2, MV3-2, MV14, and MV3-3 shows the lowest value of 0.81. All the mud volcanoes are significantly higher than ASW, beyond the error range. The concentrations of heavy noble gases (Ar, Kr, and Xe) were obtained for MV1 and MV14, and it can be said that MV14 is slightly higher than MV1 for all noble gas concentrations. In both mud volcanoes, the concentrations are higher than those of ASW.

The $(^3He/^4He)_{corr}$ results corrected for the influence of ASW are about 0.2 R_A for MV1, 0.6 R_A for MV2, 0.3-0.6 R for MV3, and 0.9 R_A for MV14. The contribution of the mantle-derived helium was about 2% for MV1, 7% for MV2, 4-7% for MV3, and 12% for MV14. In the four mud volcanoes, the influence of crustal helium was about 88-98%, suggesting that most of the collected helium was of crustal origin. Plotting the helium isotope ratio data obtained in other forearc regions shows two major ranges. The first is in the range of 0.1-0.8 R_A, which is the data from the Oomine Ridge off Kumano and the mud volcanoes in the Gulf of Cadiz. The other is the data at depths of several kilometers below the seafloor with values of ~2.4 R_A, suggesting the presence of mantle-derived helium. The data off Tanegashima corresponds to the lower range of the helium isotope ratio. The NGTs inferred from the heavy noble gas concentrations of MV1 and MV14 were about 150℃ and 100℃, respectively. The NGT estimated from the heavy noble gas concentration is reasonable because the temperature at which the reaction occurs is estimated to be 60-160℃. If the geothermal gradient around Tanegashima is 25-50℃/km, the temperature of 100-150℃

©2021. Japan Geoscience Union. All Right Reserved.

is estimated to be around 2-6 km below the seafloor. According to the velocity structure study, these depths are considered to be in the upper to middle crust around the Off Tanegashima, and the plate boundary is estimated to be located about 10 km below the seafloor, which is not a clear evidence for the origin of these noble gases near the plate boundary.
In the mud volcanoes off Tanegashima, the results of $^{3}He/^{4}He$ in the sediments suggest that about 90% of the helium is of crustal origin, although there are differences in MV1, MV3 and MV14. From the heavy noble gas concentration, the origin temperature of noble gas in MV1 and MV14 is estimated, and the helium corrected from sediments is considered to have come from about 2-6 km below the seafloor. Therefore, the helium isotope ratios and heavy noble gas concentrations in the sediments do not provide clear evidence that the noble gases originated near the plate boundary in either case.

Keywords: off Tanegashima, submarine mud volcano, noble gas

©2021. Japan Geoscience Union. All Right Reserved.

Subsurface structures and fluid transportation visualization by acoustic mapping in a shallow methane hydrate area off Sakata, eastern margin of the Sea of Japan

*Miho Asada[1], Mikio Satoh[1], Toshiyuki Yokota[1], Shusaku Goto[1]

1. NATIONAL INSTITUTE OF ADVANCED INDUSTRIAL SCIENCE AND TECHNOLOGY (AIST)

Shallow methane hydrates (MH) have been reported atop a knoll off Sakata (Sakata knoll, a tentative name), along a reverse fault located at the southwest foot of the knoll, along the eastern margin of the Sea of Japan (Temma and Goto, 2018). Fluid seepage not only helps in generating shallow MH, but also assists in the cultivation of chemosynthetic animal communities, and generates carbonate rocks from a mixture of gas-containing fluid and seawater. The distribution of chemosynthetic animal communities and rocks on and below the seafloor in this area is a slight indicator of fluid emission, including gas, in turn suggesting the distribution of buried shallow MH. However, the relationship between the distribution of the communities and rocks, and the route of gas emission is unclear.

Prior observation cruises in this area acquired data from: acoustic mapping using research vessels and autonomous underwater vehicles (AUVs), optical observations using remotely operated vehicles (ROVs), logging-while-drilling (LWD) measurements, and sediment sampling (Morita, 2015; Temma and Goto, 2018; Yokota, 2020). These results reveal a depression bordered by steep slopes atop the knoll (~1 km× ~300–400 m in diameter, ~12 m deep), two terraces on its northern and southern sides, a single hill near its center, and swells on the top around the depression (~15 km×~5–10 km in diameter, ~120 m of relative height from the southwestern foot of the knoll). The distribution of backscatter strength was the largest on the steep slopes, relatively large on the terraces within the depression and the surrounding swells, and continued southwestwards along the knoll. The shallow subseafloor structure showed an anticline along the topography of the knoll. Faults developed were more in number on the southwestern slope of the knoll, compared to a few found in the shallowest layer. A large acoustic blanking which developed directly beneath the depression prevented the visibility of shallow subsurface structures. Relatively common smaller acoustic blankings on the northeast side of the knoll, seemed to cut the layers.

To determine the detailed distribution of chemosynthetic communities and carbonate rocks on the seafloor, optical seafloor mapping was performed with a 1K20 cruise using Kaiyomaru no.1 (Kaiyo Engineering Co. Ltd.), and ROV-*Kaiyo3000* with *SeaXerocks 1* (high-resolution 3D mapping system, Kaiyo Engineering Co. Ltd.) in June 2020, in and around the depression. The seawater was turbid with increased biomass in the depression. Methane hydrates remained unconfirmed on the seafloor. The two terraces and swells were extensively covered with sediments, but rare rock outcrops and small biological mats were observed.

Since shallow subseafloor structures beneath the depression were unrecognizable because of acoustic blanking, it was difficult to extract information corresponding to the distribution of communities, rocks, and subseafloor structures. Nevertheless, we recognized larger visible faults just outside the depression, most of which stopped below the top layer of the sediment without reaching the seafloor. No communities or rocks were observed directly above these faults, suggesting the likelihood of less fluid and gas discharge through surface sediment. More communities and rocks on the steep slope surrounding depression than in the surrounding areas should be assisted by larger amount of fluid seepage through

©2021. Japan Geoscience Union. All Right Reserved.

the exposure of the layers.

This study was conducted as part of the methane hydrate research project funded by the Ministry of Economy, Trade and Industry (METI).

References:
Temma and Goto (2018) 33rd investigative commission for methane hydrate development, METI (in Japanese)
Morita (2015) FY2014 AUV survey in shallow methane hydrate fields in Japan Sea, Japan Geoscience Union meeting 2015, MIS24-02, abstract (May 27, Chiba)
Yokota (2020) Results of high-resolution 3D seismic reflection survey, Research and development of shallow methane hydrate, FY2020 Achievements Report Meeting, Research and development project for shallow methane hydrate, AIST (in Japanese)

Keywords: shallow methane hydrate, acoustic mapping, 3D pictorial mapping system, different scale observation matchup

©2021. Japan Geoscience Union. All Right Reserved.

Chemosynthesis, surface ruptures and possible methane eruption on the Kuroshima Knoll: a review from previous studies

*Takeshi Matsumoto[1]

1. Faculty of Science, University of the Ryukyus

Kuroshima Knoll is located about 40km south of Ishigaki Island in the southwest Ryukyu arc. A Calyptogena colony was first discovered during the survey on seafloor fractures on the knoll by use of a deep-tow camera system in 1996. After this expedition, a reconnaissance survey on the eastern edge of the summit of the knoll was carried out at 24° 07-08' N, 124° 11-13' E by use of ROV Dolphin-3K and DSV Shinkai2000 in 1997 (Cruise ID: NT97-14). The purpose of the expedition was to detect the distribution pattern of the chemosynthetic communities and relationship between their situation and the basement rocks of the knoll. The survey revealed a living white Calyptogena colony (chemosynthetic communities) in the survey area (depth: 812-682m). Dense colonies of Calyptogena (both living and dead) were observed. A living tube worm is also found in this place. Doming structures and sedimentary mounds which were apparently formed recently together with brecciated rocks were also observed. These suggest that compressional stresses are predominant in the eastern part of the summit. Pipe-like calcareous sandstone "chimneys" (both standing and lying) were also observed near the mounds. It is estimated that the top of the Kuroshima Knoll is composed of the Miocene to Early Pleistocene Shimajiri Group overlain by the Pleistocene Ryukyu Group and that they are covered with recent calcareous sediments. The whole survey area seems to be suffered from fracture and brecciation. It is estimated that cold water seep and gas eruption have occurred since late Pleistocene era, accompanied with rock fracturing. Since then, calcareous sandstone chimneys might have been formed. (Matsumoto et al., 1998, JAMSTEC J. Deep Sea Res.).

Thus, a series of research cruises up to 2001 suggested the existence of methane hydrate under the seafloor of the knoll. After those expeditions, total 33 dives by ROV Dolphin-3K, ROV Hyper-Dolphin, DSV Shinkai2000 and DSV Shinkai6500 were operated from 2002 to 2004 for reconnaissance survey in the vicinity of 24° 07' 48" N 124° 11' 30" E (depth: 686-622m). Based on the video images from these dives, a seafloor mapping on the knoll was carried out in order to detect the area of the communities of chemosynthetic fauna and methane eruption. Calcareous sandstones, dead Calyptogena and living Bathymodiolus colonies spread over the wide area on the knoll. 35 methane bubble gushing were also observed. The area where methane may be existing beneath the seafloor of the knoll was estimated to be about 40,000 square meters in the survey area (Matsumoto and Aoki, JpGU2014, MIS22-P05).

It is necessary to examine if the sub-seafloor beneath the knoll is within the temperature and pressure conditions for methane hydrate stability. The temperature and depth records at 17 ARGO float stations around the knoll (there are no ARGO float stations just above the knoll) were examined to draw a temperature-depth profile. The result shows that the temperature at the summit (water depth : 640m) is too high (6 degrees Celsius in autumn, 9 degrees Celsius in spring) for methane hydrate to exist stably throughout the year (less than 7 degrees Celsius at pressure of 6MPa, according to the methane hydrate stability curve for bottom water with a salinity of 3.46%, Tishchenko et al., 2005). The water depth of the seafloor should be 750m or more if a possible sub-seafloor methane hydrate is stable. The observed bubbles are gushing directly from the methane that was formed sub-seafloor beneath the knoll.

©2021. Japan Geoscience Union. All Right Reserved.

Keywords: Kuroshima Knoll, Calcareous chimney, Methane, Cheomosynthesis

©2021. Japan Geoscience Union. All Right Reserved.

Community composition and connectivity of hot vent endemic animals on the Izu-Bonin-Mariana Arc

*Hiromi Kayama WATANABE[1], Chong Chen[1], Shigeaki Kojima[2], Hiroyuki Yamamoto[1]

1. Japan Agency for Marine-Earth Science and Technology, 2. Atmosphere and Ocean Research Institute, the University of Tokyo

Lush biological communities associated with deep-sea hydrothermal vents are sustained by high primary production through chemosynthesis. These communities are island-like, being discretely distributed on the normal deep-sea floor lacking in primary production. Nevertheless, planktonic larval dispersal among vents means the compositions of benthos inhabiting vent fields —even those hundreds of kilometres away —are often similar. The 2800 km long Izu-Bonin-Mariana (IBM) Arc is a submarine volcanic arc located off Japan to Guam, and host a number of vent communities. Here, we present the similarity of community composition of these vent communities, and the genetic connectivity among local populations of the vent crab *Gandulfus yunohana* on the IBM Arc as a case study to identify dispersal barriers and source-sink relationships of the deep-sea vent sites and animal populations.
Our similarity analyses using presence/absence data of 41 taxa in 10 deep-sea vent communities on the IBM Arc showed that the communities are subdivided into three major groups; Izu, Shallow (< 1000m) Bonin-Mariana, and Deep (> 1000m) Bonin-Mariana. This pattern of subdivision indicates that both water depth and tectonic discontinuity contribute to the realized distribution of deep-sea vent animals on the IBM Arc. Genetic analyses of *G. yunohana* in the vent communities on Myojin Knoll, Bayonaise Knoll (Izu Arc) and Nikko Seamount (Mariana Arc) suggest the populations on the Izu Arc are the source for those on the Mariana Arc. Although this vent crab is distributed continuously on the IBM Arc, its uneven dispersal is indicative of geographic restrictions to larval dispersal. Vents located on the northern part of the IBM Arc, within the Japanese EEZ, are known to produce ore-quality sulfide deposits and are being eyed as targets or deep-sea mining. Knowledge on the dispersal and settlement dynamics of vent endemic animals, like those presented herein, are required for an accurate evaluation of the ecosystems' resilience for the disturbance that is key to sustainable exploitation.

Keywords: Faunal composition, Gene flow, Mining impact

©2021. Japan Geoscience Union. All Right Reserved.

Population Genetic Structure and Gene Expression Plasticity of the Deep-Sea Vent and Seep Squat Lobster *Shinkaia crosnieri*

*Yao Xiao[1]

1. Hong Kong University of Science and Technology

Shinkaia crosnieri (Decapoda: Munidopsidae) is a squat lobster that dominates both deep-sea hydrothermal vent and methane seep communities in the Western Pacific. Previous studies comparing *S. crosnieri* living in these two types of habitats have suffered from methodological and/or sample size limits. Here, using transcriptome-wide single nucleotide polymorphisms (SNPs) markers from 44 individuals of *S. crosnieri*, we reveal the extent of genetic connectivity between a methane seep population in the South China Sea and a hydrothermal vent population in the Okinawa Trough, as well as their signatures of local adaptation. Analysis of differentially expressed genes (DEGs) between these two populations and population-specific genes (PSGs) revealed that a large number of unigenes, such as cytochrome P450 (CYP), glutathione *S*-transferase (GST) and peroxiredoxin 6 (Prdx6) related to oxidoreductase, and sulfur dioxygenase (ETHE1) and chondroitin 4-sulfotransferase 11 (CHST11) related to sulfur metabolism, showed opposite expression patterns in these two populations. Data subsampling in this study revealed that at least five individuals of *S. crosnieri* per site are required to generate reliable results from the differential gene expression analysis. Population genetic analyses based on 32,452 SNPs revealed clear genetic differentiation between these two populations with an F_{ST} value of 0.07 ($p < 0.0005$), and physical oceanographic modeling of the ocean currents in middle and deep layers also suggests a weak connection between these two sites. Analysis of outlier SNPs revealed 345 unigenes potentially under positive selection, such as sarcosine oxidase/L-pipecolate oxidase (PIPOX), alanine-glyoxylate transaminase/serine-glyoxylate transaminase/serine-pyruvate transaminase (AGXT), and Cu-Zn superoxide dismutase (SOD1). Among the differentially expressed genes and genes with amino acid substitutions between the two sites are those related to oxidation resistance and xenobiotic detoxification, indicating local adaptation to the specific environmental conditions of each site. Overall, exploring the population structure of *S. crosnieri* using transcriptome-wide SNP markers resulted in an improved understanding of its molecular adaptation and expression plasticity in vent and seep ecosystems.

Keywords: Deep sea, Population genetics

©2021. Japan Geoscience Union. All Right Reserved.

A Decade to Study Deep-Sea Science

*Hiromi Kayama WATANABE[1], Kerry Howell[2]

1. Japan Agency for Marine-Earth Science and Technology, 2. University of Plymouth

Deep-sea occupied most parts of Earth’ s ecosystem, however, only a limited knowledge has been accumulated due to the physical and technical restriction of observation and sampling methods. Deep-sea is not a homogeneous environment, where various environments such as hydrothermal vent fields which are supported by chemosynthetic primary production, and hadal trench area which is occupied by specific microbes and faunas. Therefore, multi-disciplinary approaches, not only biological survey, but also physical and chemical observation that enable us to estimate how animals behave in invisible deep-sea, are required. Here I will introduce some projects including Challenger 150 program associating with the Decade of Ocean Science, and discuss how we can contribute to these projects.

Challenger 150 program is constituted with Decade working group in Deep-Ocean Stewardship Initiative (DOSI), SCOR WG-159, and Deep-Sea Special Interest Working Group in Challenger Society in UK. The program attempts to archive social outcomes related to SDGs, with scientific output about diversity, connectivity, functionality and resilience of deep-sea ecosystem. Local and topical committees will be organized and contribution of deep-sea researchers are anticipated.

References

Howell et al. 2020 A Blueprint for an Inclusive, Global Deep-Sea Ocean Decade Field Program. Front. Mar. Sci., 25 November 2020 | https://doi.org/10.3389/fmars.2020.584861; Howell et al. 2020. A Decade to Study Deep-Sea Life. Nature Ecology & Evolution. https://doi.org/10.1038/s41559-020-01352-5

Keywords: The Decade of Ocean Science, Challenger 150 Program

©2021. Japan Geoscience Union. All Right Reserved.

[J] Poster | M (Multidisciplinary and Interdisciplinary)：M-GI General Geosciences, Information Geosciences & Simulations

Thu. Jun 3, 2021 5:15 PM - 6:30 PM JST | Thu. Jun 3, 2021 8:15 AM - 9:30 AM UTC | Ch.20_2

[M-GI33] Data-driven geosciences

convener:Tatsu Kuwatani(Japan Agency for Marine-Earth Science and Technology), Hiromichi Nagao(Earthquake Research Institute, The University of Tokyo), Kenta Ueki(Japan Agency for Marine-Earth Science and Technology), Shin-ichi Ito(The University of Tokyo)

It is important to extract essential processes and structures from observed data sets in order to understand and predict the dynamic behavior of the earth and planetary systems. Recently, many powerful methodologies have been proposed to extract useful information from high-dimensional data sets in mathematical and information sciences. This session aims to provide an opportunity to gather various geoscientists to have a productive discussion for interdisciplinary collaborations.

[MGI33-P01] Numerical modeling of mantle melting degree based on major element composition of melt

*Kenta Ueki[1], Satoru Haraguchi[2,1], Hikaru Iwamori[1] (1.Japan Agency for Marine-Earth Science and Technology, 2.Earthquake Research Institute, The University of Tokyo)

[MGI33-P02] Bayesian modeling of the equation-of-state by integration of various data sets for liquid iron in Earth's outer core

*Taroujirou Matumura[1], Yasuhiro Kuwayama[2], Kenta Ueki[3], Tatsu Kuwatani[3], Ando Yasunobu[1], Kenji Nagata[4], Shin-ichi Ito[5], Hiromichi Nagao[5] (1.Research center for computational design of advanced functional materials, AIST, 2.Department of Earth and Planetary Science, The University of Tokyo, 3.Research Institute for Marine Geodynamics, Japan Agency for Marine-Earth Science and Technology, 4.Research Center for Advanced Measurement and Characterization, National Institute for Materials Science (NIMS), 5.Earthquake Research Institute, The University of Tokyo)

[MGI33-P03] Superresolution of X-ray CT images of rock core samples and applications to serpentinite in the Oman ophiolite

*Shoui Suzuki[1], Atsushi Okamoto[2], Katsuyoshi Michibayashi[3], Toshiaki Omori[1] (1.Kobe University, 2.Tohoku University, 3.Nagoya University)

Numerical modeling of mantle melting degree based on major element composition of melt

*Kenta Ueki[1], Satoru Haraguchi[2,1], Hikaru Iwamori[1]

1. Japan Agency for Marine-Earth Science and Technology, 2. Earthquake Research Institute, The University of Tokyo

Determining the mantle melting degree is essential to understand the physical and chemical conditions of the mantle, the process of melt generation, and for estimating the chemical composition of the source mantle based on the chemical composition of volcanic rocks. Due to the low thermodynamic degrees of freedom during partial melting of mantle peridotite, the composition of the partial melt is controlled by the phase relation, including phase assemblage of residual minerals and the melt fraction. Therefore, it is expected that the melt fraction can be expressed only as a function of melt composition, although it is generally expressed as a function of temperature with a fixed bulk composition of the source rock and a fixed pressure. Based on this background, we conduct numerical modeling of mantle melting degree based on the major element composition of the melt.
We compiled the previously reported experimental results of mantle peridotites at pressures corresponding to the upper mantle. Both hydrous and anhydrous experiments are included in the compiled database. We use melting experiments in which the melting degree at a given bulk composition was reported. We conduct a regression analysis based on the data-driven method in Ueki et al. (2018 and 2020). Based on the method, a small number of essential variables are automatically selected to obtain a model of robustness and high predictive capacity. A model that calculates the degree of melt based on the melt composition without temperature and pressure information is constructed based on our analysis. This model will allow us to estimate the physical and chemical conditions of the source region of various natural primitive magmas.

Keywords: mantle, melting, data driven

©2021. Japan Geoscience Union. All Right Reserved.

Bayesian modeling of the equation-of-state by integration of various data sets for liquid iron in Earth’s outer core

*Taroujirou Matumura[1], Yasuhiro Kuwayama[2], Kenta Ueki[3], Tatsu Kuwatani[3], Ando Yasunobu[1], Kenji Nagata[4], Shin-ichi Ito[5], Hiromichi Nagao[5]

1. Research center for computational design of advanced functional materials, AIST, 2. Department of Earth and Planetary Science, The University of Tokyo, 3. Research Institute for Marine Geodynamics, Japan Agency for Marine-Earth Science and Technology, 4. Research Center for Advanced Measurement and Characterization, National Institute for Materials Science (NIMS), 5. Earthquake Research Institute, The University of Tokyo

Bayesian modeling of the equation-of-state (EoS) was demonstrated to constrain P-wave velocity (V_P) and density (ρ) of liquid iron under Earth’s outer-core conditions. We collected six data sets obtained by high-pressure (P) and high-temperature (T) experiments and *ab initio* molecular dynamics simulations in previous works. These data sets were integrated into one to estimate the parameters of EoS. However, as the type of observed data depends on the approach, integrated data set includes some unobserved data. To analyze such data set, we performed an analysis based on Bayesian inference. Our analysis successfully estimated the posterior probability distribution of the parameters and unobserved data by using the Hamiltonian Monte Carlo method. These posterior probability distributions enable us to calculate P– V_P and P– ρ profiles of liquid iron along the adiabatic P–T profile together with the associated credible intervals. Bayesian modeling of the EoS enables estimation of EoS’s parameters, integration of data sets that include unobserved data and evaluation of uncertainty ranges of physical properties, such as V_P and ρ, which are important for comparison with seismological properties of the core.

©2021. Japan Geoscience Union. All Right Reserved.

Superresolution of X-ray CT images of rock core samples and applications to serpentinite in the Oman ophiolite

*Shoui Suzuki[1], Atsushi Okamoto[2], Katsuyoshi Michibayashi[3], Toshiaki Omori[1]

1. Kobe University, 2. Tohoku University, 3. Nagoya University

Recently, the X-ray computed tomography (CT) scanner has been commonly used for the onboard analyses of cores of scientific drilling, which provides us the 100 to 1000 m scale continuous data of various structures (lithological or sedimental layering, fractures, pores etc) of rocks. However, the resolution of such X-ray CT for the cores (for example, ~0.17 mm by the X-ray CT of Drilling Chikyu) is slightly low compare to reveal the shape and geometry of mineral grains and thin fractures. In contrast, the resolution of X-ray CT in usual laboratories is high (~0.01 mm or less). Therefore, if we can link the high resolution X-ray CT in the lab of the limited samples to the low resolution drilling core CT data, we can obtain the valuable big data for the analyses of multi-scale structures.

For this purpose, we have tried to apply sparse superresolution techniques to the rock samples with veins. The sample is a serpentinezed dunite in the Moho transition zone taken by the Oman Drilling project (CM1A). We took the X-ray CT images of the samples with the voxel size of 10, 20, 40 and 80 micrometers. The X-ray CT image reveals that distribution of magnetite and spinel grains and fractures filled with serpentine. We consider that each image is expressed by sparse representation; an image consists of a small number of basis images. The algorithm consists of two processes: dictionary learning and superresolution processes. In dictionary learning process, basis images are obtained by feature extraction from multiple X-ray CT images. In super-resolution process, a reconstructed high resolution image is obtained from a low resolution X-ray CT image by using common sparse representations. By using the sparse superresolution algorithm, we obtained results that sparse superresolutions provide fine structure from low resolution X-ray CT image.

Keywords: Oman Drilling Project, Image Superresolution, Sparse Representation

©2021. Japan Geoscience Union. All Right Reserved.

[J] Poster | M (Multidisciplinary and Interdisciplinary)：M-GI General Geosciences, Information Geosciences & Simulations

Thu. Jun 3, 2021 5:15 PM - 6:30 PM JST | Thu. Jun 3, 2021 8:15 AM - 9:30 AM UTC | Ch.18_2

[M-GI34] Earth and planetary informatics with huge data management

convener:Ken T. Murata(National Institute of Information and Communications Technology), Susumu Nonogaki(Geological Survey of Japan, National Institute of Advanced Industrial Science and Technology), Rie Honda(Department of Science and Technology, System of Natual Science, Kochi University), Keiichiro Fukazawa(Academic Center for Computing and Media Studies, Kyoto University)

Increasingly large and complex data are produced by observations and numerical simulations in earth and planetary sciences. The target of this session is to discuss a broad range of practices and new knowledge of informatics, international standard and modelling, including techniques for large-scale data processing and numerical simulation, data preservation and publication, data transfer and collection and other data technologies with a vision to advance an emerging data-intensive science, namely "geoplanetary informatics".

[MGI34-P01] An attempt of local government disaster prevention WebGIS

*Ken T. Murata[1], Asanobu Kitamoto[2], Tomohiro Kawanabe[3], Keiichiro Fukazawa[4], Kazuya Muranaga[1], Kazunori Yamamoto[1], Yuki MURAKAMI[1] (1.National Institute of Information and Communications Technology, 2.National Institute of Informatics, 3.Institute of Physical and Chemical Research, 4.Kyoto University)

[MGI34-P02] Development of interface for PTZ Camera to use image processing technique

*Yuki MURAKAMI[1], Ken T. Murata[1], Michiharu Niimi[2], Yoshihide Kagatani[3], Minehito Ageno[3], Kazunori Yamamoto[1], Tomohiro Kawanabe[4] (1.National Institute of Information and Communications Technology, 2.Kyushu Institute of Technology, 3.GEO Solutions Co.Ltd., 4.Institute of Physical and Chemical Research)

[MGI34-P03] Development of LPWA and visual IoT techniques (2)

Mehdad Shirazi[1], *Takamichi Mizuhara[1], Toshiki Aoki[1], Yuua Kagebayashi[1], Takeshi Murata[2], Kazunori Yamamoto[2], Kazuya Muranaga[3] (1.CLEALINK TECHNOLOGY CO., LTD., 2.National Institute of Information and Communications Technology, 3.Systems Engineering Consultants Co.,LTD.)

[MGI34-P04] HpFP: development of high-speed data transfer applications (2)

Yasunori Kakizawa[1], Ayahiro Takaki[1], *Takamichi Mizuhara[1], Kazuya Muranaga[3], Kazunori Yamamoto[2], Takeshi Murata[2] (1.CLEALINK TECHNOLOGY CO., LTD., 2.National Institute of Information and Communications Technology, 3.Systems Engineering Consultants Co.,LTD.)

[MGI34-P05] Programming Techniques for visual IoT on Raspberry Pi (4)

Toshiki Aoki[1], *Takamichi Mizuhara[1], Takeshi Murata[2], Kazunori Yamamoto[2], Kazuya Muranaga[3] (1.CLEALINK TECHNOLOGY CO., LTD., 2.National Institute of Information and Communications Technology, 3.Systems Engineering Consultants Co.,LTD.)

[MGI34-P06] A large-scale distributed cloud system for research works on Earth and Planetary sciences

Kazunori Yamamoto[1], Kazuya Muranaga[2], *Ken T. Murata[1], Keiichiro Fukazawa[3], Atsushi Higuchi[4], Takeshi Nanri[5], Tomohiro Kawanabe[6], Yoshitaka Ohyoshi[7] (1.National Institute of Information and Communications Technology, 2.SEC, 3.Kyoto University, 4.Chiba University, 5.Kyushu University, 6.Institute of Physical and Chemical Research, 7.Virtual)

[MGI34-P07] Activity of preparing training data for study of space plasma with collaboration of observation, MHD simulation and machine leaning

*Keiichiro Fukazawa[1], Tomoki Kimura[2], Terumasa Tokunaga[3], Shin ya Nakano[4] (1.Academic Center for Computing and Media Studies, Kyoto University, 2.Frontier Research Institute for Interdisciplinary

Sciences, Tohoku University, 3.Department of Systems Design and Informatics, Faculty of Computer Science and Systems Engineering, Kyushu Institute of Technology, 4.Department of Statistical Modeling, Institute of Statistical Mathematics)

[MGI34-P08] Development of a multi-station airglow imaging system using commercial cameras

*Shin Suzuki[1] (1.Faculty of Regional Policy, Aichi University)

[MGI34-P09] Super-resolution and colorization of small body images by Generative Adversarial Network

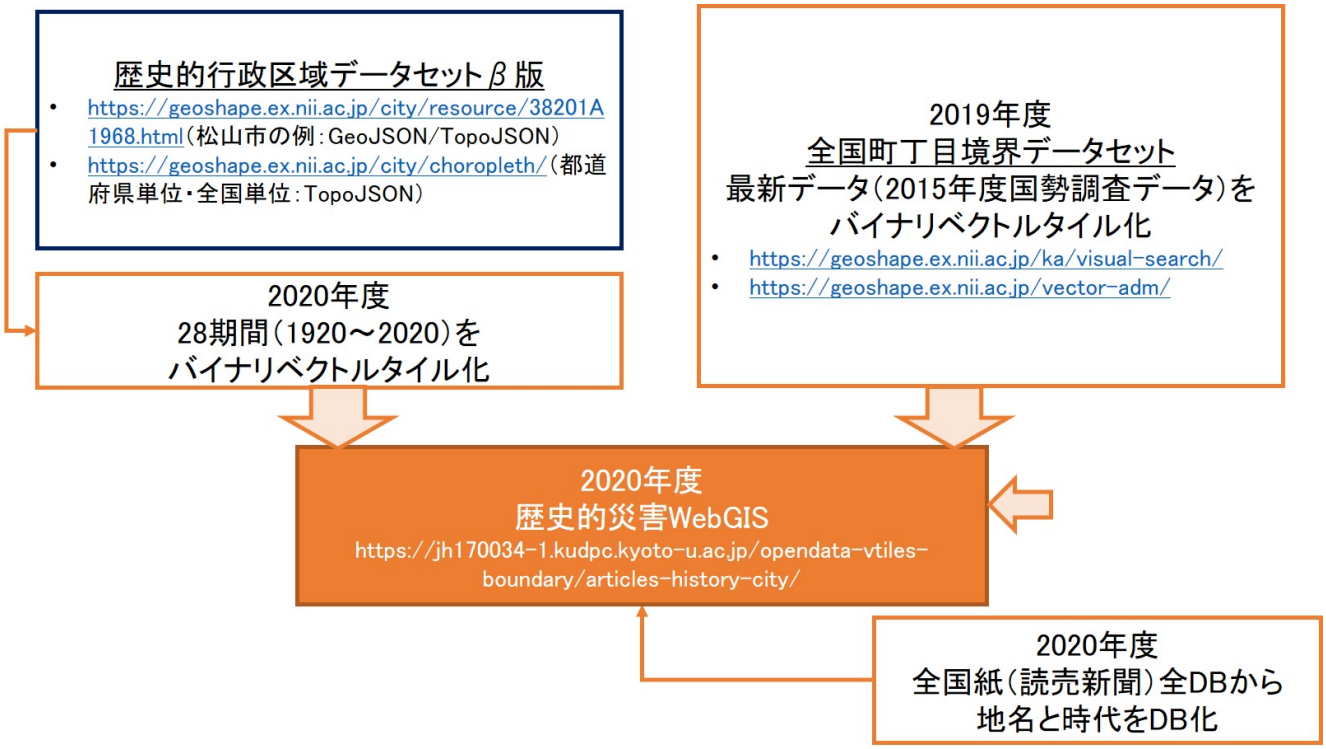
Rintaro Kishi[1], Ren Hashimoto[1], *Rie Honda[1], Kimikazu Tanase[1], Yasuhiro Yokota[2], Seiji Sugita[3], Tomokatsu Morota[3], Shingo Kameda[4], Naoya Sakatani[4], Eri Tatsumi[5], Yuichiro Cho[3], Toru Kouyama[6], Manabu Yamada[7], Masahiko Hayakawa[2], Hidehiko Suzuki[8], Kazuo Yoshioka[3], Chikatoshi Honda[9], Kazunori Ogawa[2], Hirotaka Sawada[2] (1.Kochi University, 2.ISAS/JAXA, 3.Univ. of Tokyo, 4.Rikkyo Univ., 5.Instituto de Astrofisica de Canarias, Univ. of La Laguna, 6.AIST, 7.Chiba Inst. Tech, 8.Meiji Univ., 9.Univ. of Aizu)

An attempt of local government disaster prevention WebGIS

*Ken T. Murata[1], Asanobu Kitamoto[2], Tomohiro Kawanabe[3], Keiichiro Fukazawa[4], Kazuya Muranaga[1], Kazunori Yamamoto[1], Yuki MURAKAMI[1]

1. National Institute of Information and Communications Technology, 2. National Institute of Informatics, 3. Institute of Physical and Chemical Research, 4. Kyoto University

In this study, we build up a local government disaster prevention WebGIS by linking historical administrative area dataset with newspaper article dataset. Specifically, for Chikuma City, Nagano Prefecture, we visualize local information on various natural disasters occurred in the past in this era. Binary vector tiles that can speed up rendering make it possible to visualize past natural disaster occurrence locations extracted from newspaper articles on the current WebGIS map. This database and Web application will be provided to various user organizations for research and development, regardless of whether they are academia or private companies.



©2021. Japan Geoscience Union. All Right Reserved.

Development of interface for PTZ Camera to use image processing technique

*Yuki MURAKAMI[1], Ken T. Murata[1], Michiharu Niimi[2], Yoshihide Kagatani[3], Minehito Ageno[3], Kazunori Yamamoto[1], Tomohiro Kawanabe[4]

1. National Institute of Information and Communications Technology, 2. Kyushu Institute of Technology, 3. GEO Solutions Co.Ltd., 4. Institute of Physical and Chemical Research

In recent years, the government and companies aim at realization of smart society. Smart city is an element of smart society, and it produces safe and reliable life with feedback results of data aggregation and processing from sensors installed in a city. A Pan, Tilt and Zoom controllable camera (PTZ camera) is a kind of visual sensor. PTZ cameras set up in elevated spots of a city can help realization of automatic city monitoring system. The system monitors a situation of city in a normal period automatically. If the system detects anomaly points in a city, it focuses on the point. The system needs two core techniques: PTZ control and image processing. We developed an interface between PTZ control and image processing, and report results of PTZ control. The interface decides PTZ values from a pixel of an image. The PTZ values depend on not only position of the pixel but also target camera and zoom level, so a user must calibrate the target camera. However, it is difficult for the user to calibrate every camera in a city. We also developed self-calibration program, and packaged PTZ control and self-calibration program to use easily.

Keywords: Visual IoT, PTZ Control

©2021. Japan Geoscience Union. All Right Reserved.

Development of LPWA and visual IoT techniques (2)

Mehdad Shirazi[1], *Takamichi Mizuhara[1], Toshiki Aoki[1], Yuua Kagebayashi[1], Takeshi Murata[2], Kazunori Yamamoto[2], Kazuya Muranaga[3]

1. CLEALINK TECHNOLOGY CO., LTD., 2. National Institute of Information and Communications Technology, 3. Systems Engineering Consultants Co.,LTD.

Visual Internet of Things (IoT) is a class of IoT that collects rich visual data. In general, the visual IoT device is equipped with a video transmission equipment such as a camera. The involved technologies are advanced video transmission techniques and information extraction from images by image recognition techniques. However, since the video data size is larger than the sensor data size, one of the issues of visual IoT is high-performance video transmission in networks in which the bandwidths are limited. In this paper, we design and develop a real-time monitoring system using visual IoT device. Our system is based on a novel protocol, named high-performance video transmission (HpVT), for field monitoring via 4G LTE mobile networks. The performance of our system is evaluated in real fields to conclude that we can achieve full high-definition (full-HD) resolution video transmission with as high frame rate as 30 fps. We introduce an original carrier board for LoRa communication system development. Basic examinations in outdoor environments and our application to visual IoT syste are discussed.

Keywords: IoT, LPWA, Image

©2021. Japan Geoscience Union. All Right Reserved.

HpFP: development of high-speed data transfer applications (2)

Yasunori Kakizawa[1], Ayahiro Takaki[1], *Takamichi Mizuhara[1], Kazuya Muranaga[3], Kazunori Yamamoto[2], Takeshi Murata[2]

1. CLEALINK TECHNOLOGY CO., LTD., 2. National Institute of Information and Communications Technology, 3. Systems Engineering Consultants Co.,LTD.

For LFNs (Long-Fat Networks) with 10 Gbps or more and satellite networks with large latency, a variety of TCP-based protocols have been proposed which show high performance on large latency network conditions. However, such TCP protocols are essentially unable to archive large bandwidth on high latency networks accompanied with packet-losses that are inevitable on practical LFNs or satellite networks. To overcome this issue, we designed a new data transfer protocol on TCP/IP transport layer built on top of UDP: High-performance and Flexible Protocol (HpFP). It constantly monitors latency (RTT) and packet losses, and conducts rate control and retransmission control based on them to enable higher bandwidth data transfer than 10 Gbps even on packet-loss conditions over LFNs. The basic concepts are addressed and protocol design of the HpFP are discussed. An applications to transfer many data files in small size (e.g., 1MB x 10000 files) with almost wire-rate bandwidth (10 Gbps) is also addressed. In this study we develop a tool to bind multiple connection of HpFP aiming at higher throughput on a broadband network faster than 100Gbps. In the near future, big data transfer with high speed is expected on LFNs such as SINET5.

Keywords: HCP, LFN, BigData

©2021. Japan Geoscience Union. All Right Reserved.

Programming Techniques for visual IoT on Raspberry Pi (4)

Toshiki Aoki[1], *Takamichi Mizuhara[1], Takeshi Murata[2], Kazunori Yamamoto[2], Kazuya Muranaga[3]

1. CLEALINK TECHNOLOGY CO., LTD., 2. National Institute of Information and Communications Technology, 3. Systems Engineering Consultants Co.,LTD.

The recent emergence of low-cost single board computers such as Raspberry Pi and Arduino, which are used as sensing devices with connectivity to Internet gateways and cloud services, has led to Internet of Things (IoT) architectures in the real world. Visual IoT is one of the classes of IoT that poses crucial end-to end challenges due to the need for sensing and processing of visual data. One of the significant roles of the visual IoT is information extraction from images by using image recognition techniques. In this paper, we present a programming environment of visual IoT on Raspberry Pi, and develop a couple of applications. The first one is an application for real-time information extraction and the second one is an augmented reality (AR)-oriented application. The performance of both applications is examined in outdoor fields using 4G LTE mobile networks to prove that our environment has a potential for many types of visual IoT devices. Our presentation this year focuses on a remote operation function of PTZ-type IP camera (https://www.youtube.com/watch?v=cNCGVany0BQ).

Keywords: IoT, Camera, Image

©2021. Japan Geoscience Union. All Right Reserved.

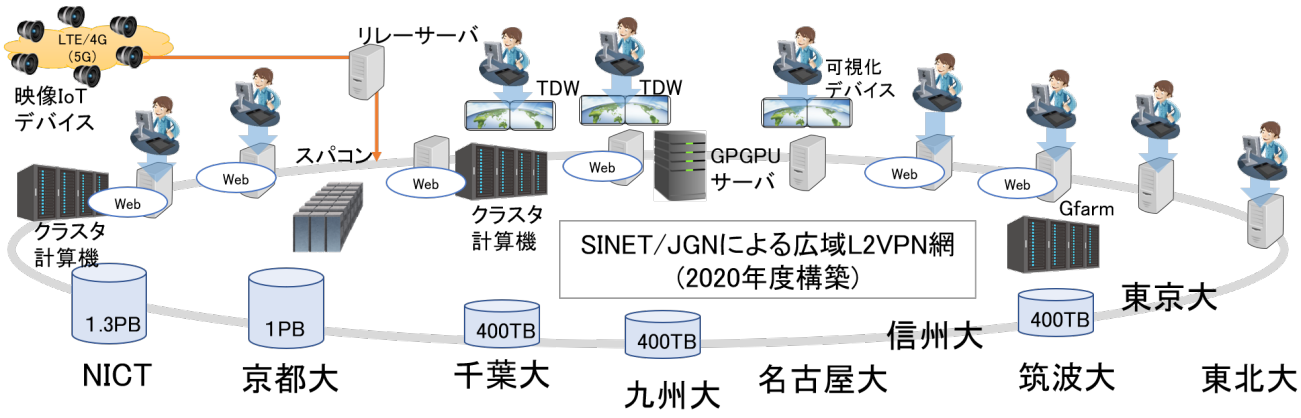
A large-scale distributed cloud system for research works on Earth and Planetary sciences

Kazunori Yamamoto[1], Kazuya Muranaga[2], *Ken T. Murata[1], Keiichiro Fukazawa[3], Atsushi Higuchi[4], Takeshi Nanri[5], Tomohiro Kawanabe[6], Yoshitaka Ohyoshi[7]

1. National Institute of Information and Communications Technology, 2. SEC, 3. Kyoto University, 4. Chiba University, 5. Kyushu University, 6. Institute of Physical and Chemical Research, 7. Virtual

NICT, National Institute of Information and Communications Technology, has been developing large-scale data transfer technology (HpFP) and high-speed communication technology (HpVT) in association with Clearlink Technology Co., Ltd. Since 2018, we have been conducting a wide-area system to verify out techniques using actual data in the Joint Usage/Research Center for Interdisciplinary Large-scale Information Infrastructures. Each base university (Tohoku University, Tokyo University, Nagoya University, Kyoto University, Kyushu University) and research bases (Tohoku University, Tokyo University, Nagoya University, Kyoto University, Kyushu University) is connected via JGN and SINET, high-speed backbone networks, using the highly functional communication protocol HpFP. By 2020, we have built an L2VPN network service (named as “JHPCN wide area distributed cloud”) that transfers and shares data at high speed between the information infrastructure centers of Chiba University, Kyoto0 University, Kyushu University, and NICT. Furthermore, we verified the performance of this environment and confirmed that the data transmission speed between bases can be achieved at or occasionally higher than that of a general LAN environment. As a result, researchers can freely utilize the huge computer resources provided by each research base; it has become possible to realize unprecedented big data science.

Keywords: JHPCN, Cloud system



©2021. Japan Geoscience Union. All Right Reserved.

Activity of preparing training data for study of space plasma with collaboration of observation, MHD simulation and machine leaning

*Keiichiro Fukazawa[1], Tomoki Kimura[2], Terumasa Tokunaga[3], Shin ya Nakano[4]

1. Academic Center for Computing and Media Studies, Kyoto University, 2. Frontier Research Institute for Interdisciplinary Sciences, Tohoku University, 3. Department of Systems Design and Informatics, Faculty of Computer Science and Systems Engineering, Kyushu Institute of Technology, 4. Department of Statistical Modeling, Institute of Statistical Mathematics

The machine learning (ML) has become a powerful tool to find the relation between variables thanks to the deep learning technique. This performs greatly in the classification, regression and recently generative modeling in the engineering and commercial areas. However, due to the satisfaction of physical laws in the scientific research area, the application of ML has some difficulties. In particular, the generative modeling is very sensitive to scientific data since the generated data is not guaranteed by the physical laws.

To overcome these problems, we have tried to apply ML to space plasma physics for several years and then reconfirmed the importance of preparing the training data. For example, when we classify the aurora in the observation results with ML, we have to prepare the huge amount of aurora observational image to learn the feature with high accuracy. It takes a lot of time to prepare the aurora image if considering the augmentation. Thus, we are developing the web site to classify the image including the aurora or not with the expectation of citizen science cooperation. In this study we show the web site for preparing the classification image and the initial results of it. In addition, our database of global simulation data of magnetosphere using real solar wind data and formatted aurora image by All-Sky-Imager will be shown.

Keywords: machine learning, space plasma, database

©2021. Japan Geoscience Union. All Right Reserved.

Development of a multi-station airglow imaging system using commercial cameras

*Shin Suzuki[1]

1. Faculty of Regional Policy, Aichi University

Atmospheric gravity waves significantly contribute to the wind/thermal balances in the mesosphere and lower thermosphere (MLT) through their vertical transport of horizontal momentum originated from meteorological disturbances in the lower atmosphere. Airglow imaging is a useful technique to observe two-dimensional structure of small-scale (<100 km) gravity waves in the MLT region and has been widely used to investigate behaviours of the waves. Recent studies with simultaneous/multiple airglow cameras have derived spatial extent of the MLT waves. Such network imaging observations are advantageous to ever better understanding of coupling between the lower and upper atmosphere via gravity waves and will become increasingly important. In this study, we newly developed low-cost airglow cameras to enlarge the airglow imaging network. Each of the cameras has a fish-eye lens with a 185-deg field-of-view and equipped with a CCD video camera (WATEC WAT-910HX) ; the camera is small (W35.5 x H36.0 x D63.5 mm) and inexpensive, much more than widely-used airglow camera, and has a CCD sensor with 768 x 494 pixels that is highly sensitive enough to detect the mesospheric OH airglow emission perturbations. For multipoint network observations using the system, however it is necessary to improve on data flow to make vast amounts of image data available to the public.

In this presentation, we will share some results of performance evaluation of the new camera and development of data flow. Outreach and educational activities based on this research will be also reported.

Keywords: camera network, airglow, mesosphere

©2021. Japan Geoscience Union. All Right Reserved.

Super-resolution and colorization of small body images by Generative Adversarial Network

Rintaro Kishi[1], Ren Hashimoto[1], *Rie Honda[1], Kimikazu Tanase[1], Yasuhiro Yokota[2], Seiji Sugita[3], Tomokatsu Morota[3], Shingo Kameda[4], Naoya Sakatani[4], Eri Tatsumi[5], Yuichiro Cho[3], Toru Kouyama[6], Manabu Yamada[7], Masahiko Hayakawa[2], Hidehiko Suzuki[8], Kazuo Yoshioka[3], Chikatoshi Honda[9], Kazunori Ogawa[2], Hirotaka Sawada[2]

1. Kochi University, 2. ISAS/JAXA, 3. Univ. of Tokyo, 4. Rikkyo Univ., 5. Instituto de Astrofisica de Canarias, Univ. of La Laguna, 6. AIST, 7. Chiba Inst. Tech, 8. Meiji Univ., 9. Univ. of Aizu

Super-resolution plays a big role in the choice of the landing site in the small body exploration. Conventionally, analytical techniques such as the reconstruction of higher resolution images using slightly shifted multiple images. In this study, we examined the method named SRGAN, based on Generative Adversarial Network, for estimation of a high-resolution image from the low-resolution image via learning and applied it to the images of asteroid Ryugu obtained by the ONC - T camera onboard Hayabusa2. The experimental result shows the improvement of images is confirmed visually and its calculation time is about 1sec for a 1024 x 1024 pixel image, which is fast compared with the conventional method.

In addition, we also examined the colorization of the single-band image by the method named pix2pix, which is also one of the methods of GAN. Multi-band images are utilized to speculate the type of surface material on the small bodies. However, obtaining multi-band images at the lowest altitude is difficult because the FOV of the cameras moves very fast relative to the surface. We also examined to generate pseudo color images from single-band images based on the learning of the pairs of single band images and pseudo color images. We will report the result of these experiments for asteroid Ryugu images obtained by Hayabusa2’s ONC-T.

Both methods are expected to help to make the decision-making process during the active small body exploration smooth by reducing the time required for analysis and improving the limited information at the maximum.

Keywords: GAN, small body expoloration, super resolution, colorization

©2021. Japan Geoscience Union. All Right Reserved.

[J] Poster | M (Multidisciplinary and Interdisciplinary)：M-TT Technology & Techniques

Thu. Jun 3, 2021 5:15 PM - 6:30 PM JST | Thu. Jun 3, 2021 8:15 AM - 9:30 AM UTC | Ch.20_3

[M-TT42] Frontiers in Geochemistry

convener:Tsuyoshi Iizuka(University of Tokyo), Yoshio Takahashi(Department of Earth and Planetary Science, Graduate School of Science, The University of Tokyo), Urumu Tsunogai(Graduate School of Environmental Studies, Nagoya University)

The Earth and planetary sciences have been advanced through utilizing chemical approaches and state-of-the-art analytical techniques. Recent analytical developments allow us to obtain highly precise and accurate data, but at the same time require deepen knowledge on the methodology to use the data correctly and effectively. This session aims at providing an opportunity for various researchers to get together and have a strategic discussion on frontiers in geochemistry and cosmochemistry. In particular, researchers who would like to apply innovative analytical techniques will have chances to discuss with those who work on devising new geochemical methods. We welcome a wide range of cutting-edge geochemical topics, including technical developments, which have a potential for breakthrough of the Earth and planetary sciences. Any presentations related to the direction of future geochemistry and cosmochemistry are also welcome. We expect wide-ranged and future-oriented discussion to further develop geochemistry and cosmochemistry. Note that presentation language in this session can be either English or Japanese.

[MTT42-P01] High-precision La isotope measurements to apply early Solar System chronology and nuclear cosmochronology

*Mitsuru Suzuki[1], Tsuyoshi Iizuka[1], Kota Yamamoto[1], Takafumi Hirata[1] (1.The University of Tokyo)

[MTT42-P02] **Factors limiting the accuracy and precision of peak positions and intensity ratios in Raman spectra: Optimisation of optics and measurement environment for carbon isotope ratio measurements of CO_2**

*Yuuki Hagiwara[1], Junji Yamamoto[1] (1.Hokkaido University)

[MTT42-P03] Development and evaluation of wet-flow type isotope analyses for fluid-inclusions in speleothems

*Ryu Uemura[1] (1.Nagoya University)

[MTT42-P04] Sub-microgram sulfur isotope analysis for the biological, geological, and extraterrestrial samples by sensitivity-improved EA/IRMS

*Nanako O. Ogawa[1], Toshihiro Yoshimura[1], Takeru Kochi[2,1], Junichiro Kuroda[2,1], Yoshinori Takano[1], Naohiko Ohkouchi[1] (1.JAMSTEC, 2.AORI, Univ. Tokyo)

High-precision La isotope measurements to apply early Solar System chronology and nuclear cosmochronology

*Mitsuru Suzuki[1], Tsuyoshi Iizuka[1], Kota Yamamoto[1], Takafumi Hirata[1]

1. The University of Tokyo

In the nature, La consists of two isotopes, ^{138}La and ^{139}La. ^{138}La is expected to be synthesized only by supernovae likewise short-lived radionuclides ^{92}Nb and ^{98}Tc. ^{92}Nb, which decays to ^{92}Zr with a half-life of 37 Myr, is one of the important chronometers for planetary differentiation in the early Solar System. It has been recently shown that ^{92}Nb was heterogeneously distributed in the early Solar System (Hibiya et al., in review). Thus, the use of ^{92}Nb as a chronometer requires the calibration of the heterogeneous distribution. The long-lived nuclide ^{138}La ($T_{1/2}$=105 Gyr) can be used as an index of the ^{92}Nb heterogeneity because of having the same origin as ^{92}Nb. Moreover, combining ^{138}La with ^{98}Tc, which decays to ^{98}Ru with a half-life of 4.2 Myr, potentially allows us to precisely constrain the timing and location of the supernova explosion which introduced these nuclides into the parental molecular cloud of the Solar System. Thus, ^{138}La analysis can be a strong tool for both the early Solar System chronology and nuclear cosmochronology.

So far, La isotope analysis has been conducted for limited samples such as Ca-Al-rich inclusions (CAIs) and several chondritic bulk samples. The results revealed that CAIs have ^{138}La excesses of up to 60±16 ε (2SD) (Shen and Lee, 2003), whereas for bulk meteorite sample ^{138}La anomalies are marginally resolvable only for carbonaceous chondrites (12±8 ε (2SD)) (Shen et al., 1994). To apply ^{138}La anomaly for the early Solar System chronology and nuclear cosmochronology, it is necessary to improve the precision of La isotope analysis.

In this study, we tested the precision of La isotope measurements by multiple collector ICP mass spectrometry (MC-ICP-MS). With this instrument, we can adopt the external calibration technique for instrumental mass bias effect for La having only two isotopes. Meanwhile, MC-ICP-MS analysis requires the correction of isobaric interferences on ^{138}La from ^{138}Ba and ^{138}Ce. The very low abundance of ^{138}La (0.1%) also makes it difficult to carry out a high-precision analysis. While 10^{11} Ωamplifiers are often used in mass spectrometries, we adopted 10^{13} Ωamplifier on 138 amu and 10^{10} Ωamplifier on 139 amu to improve the precision.

We measured a La standard solution NIST 3127a. Adopting the external calibration technique has improved the precision 10–20 times better than La standard bracketing method. Moreover, the isobaric interferences of ^{138}Ba and ^{138}Ce were corrected for by monitoring ^{137}Ba and ^{140}Ce, increasing the precision about 2 times compared to when no interference corrections made. As a result, we achieved an internal precision of ±1.4 ε (2SE) for a 80 ppb La standard solution.

Keywords: La, supernova, early Solar System, MC-ICP-MS

©2021. Japan Geoscience Union. All Right Reserved.

Factors limiting the accuracy and precision of peak positions and intensity ratios in Raman spectra: Optimisation of optics and measurement environment for carbon isotope ratio measurements of CO_2

*Yuuki Hagiwara[1], Junji Yamamoto[1]

1. Hokkaido University

Raman spectroscopy has been established as one of the most versatile quantitative analytical methods in materials science research due to its non-destructive analysis and high spatial resolution. Experimental calibration is performed to relate Raman spectral characteristics to the state of materials to quantify density, pressure, temperature, concentration, strain, etc. In recent years, Raman spectroscopy has been used to improve and develop non-destructive local isotope analysis methods for H_2O, CO_2, CH_4, HCO_3^-, CO_3^{2-}, N_2, humic acid, calcite, etc. However, the accuracy of these methods is still far from being applied to the measurement of isotope ratios in natural samples. For example, Arakawa et al. (2007)[1] and Yokokura et al. (2020)[2] reported 1 σ = 20‰ and 8.7‰, respectively, for the accuracy of carbon isotope ratio measurements of CO_2. In Yokokura et al. (2020)[2], the reason for the improvement in measurement accuracy is that the focal length of the monochromator is longer, the pixel resolution is higher, and the measurement time is longer, but it is not clear which factors contribute most to the improvement. Other parameters such as excitation wavelength, grating engraving number and size, slit width, detector noise characteristics, reciprocal line dispersion, and pixel size can also have a significant effect on measurement accuracy, but the relationship between these parameters and measurement accuracy is not well understood. Once we know which optics can be upgraded most efficiently to improve the accuracy of our measurements, we will be able to overcome the 1 σ = 8.7‰ barrier reported by Yokokura et al. (2020)[2] while reducing cost and time. In this study, we use simulated CO_2 Raman spectra to evaluate how the above parameters affect the accuracy of intensity ratio measurements.

The factors limiting the accuracy of Raman spectroscopy can be divided into three main categories: (1) noise, (2) spectral resolution, and (3) thermal and mechanical stability of the instrument.

To obtain the shot noise, the efficiency of Raman scattering (count/sec) is used as an input parameter, and the average number of photons (e-) arriving at the detector in a certain time interval is estimated from the quantum efficiency of CCD (%) and A/D count (e-/count). The square root of this value was then randomly generated as shot noise according to Poisson statistics. Dark noise and readout noise were randomly generated as Poisson and Gaussian distributed noise, respectively, using the measured values of 1.00×10^{-5} (e-/pix/sec) and 3.36 (e-/times$^{0.5}$). The effect of the instrumental spectral resolution on the peak bandwidth was introduced following the model of Liu et al. The projection of the slit on the CCD and the spectrum of the sample were assumed to be Gaussian distributed, and the resulting bandwidth was calculated to be the square root of (spectral resolution)^2+(natural bandwidth)^2.

Based on the above model, it is possible to generate spectra taking into account the effects of noise and spectral resolution by assuming the analysis time (sec), the number of vertical pixels (pix) (i.e. binning width), the shape of the Raman spectrum, the peak position (cm^{-1}), the natural bandwidth (cm^{-1}) and the amplitude (count/sec). It is possible to generate spectra taking into account the effects of noise and spectral resolution. In this study, the Raman spectra of CO_2 generated by the above method with varying the parameters were fitted with the spectrum analysis software (GRAMS/AI) to investigate which parameters affect the measurement accuracy such as peak position and intensity ratio. Finally, we estimate under what conditions the carbon isotope ratio of CO_2 can be measured with an accuracy of ‰.

©2021. Japan Geoscience Union. All Right Reserved.

Keywords: Raman spectroscopy, Carbon isotope ratio, Quantification, Spectral resolution, Noise

©2021. Japan Geoscience Union. All Right Reserved.

Development and evaluation of wet-flow type isotope analyses for fluid-inclusions in speleothems

*Ryu Uemura[1]

1. Nagoya University

Cavity-ringdown spectrometers (CRDS) are used for hydrogen/oxygen stable isotope ratio analyses of fluid inclusions in speleothems. Several methods for analyzing fluid inclusions in stalagmites have been developed [(e.g., 1-3)]. However, stable isotope ratio analysis of water in fluid inclusions has a problem of memory effect [(3)]. In this study, we develop and evaluate a method for measuring isotope ratios in fluid inclusions to improve the sample throughput by reducing the memory effect.

The measurement line consists of a water extraction unit and a detector (CRDS, Picarro 2140-i) that measures the water isotope ratio. Stalagmite sample was crushed under a vapor stream (i.e., moisturized carrier gas) in which the isotope ratio and concentration are constant. This wet flow type method has been improved due to various developments [(1-2)].

We succeeded in producing a stable water vapor concentration (± 6 ppm, standard deviation for 10 minutes). The repeated measurement precision(1 σ) of working standard water (in the range of 0.1-0.4 μL) was ±0.1-0.2 ‰, ±0.1-0.2 ‰and ±0.2-0.6 ‰for $\delta^{17}O$, $\delta^{18}O$ and δD, respectively. As reported in previously, the precision became worse as the sample volume was 0.1 μL or less. By adjusting the introduction rate of water vapor, the accuracy could be maintained even at 0.05 μL.

References: (1) Affolter et al., Clim. Past, 2014; (2) De Graaf et al., Rapid Commun Mass Spectrom., 2020; (3) Uemura et al., Geochim. Cosmochimi. Acta, 2016

Keywords: speleothem, stable isotope, fluid inclusion, CRDS

©2021. Japan Geoscience Union. All Right Reserved.

Sub-microgram sulfur isotope analysis for the biological, geological, and extraterrestrial samples by sensitivity-improved EA/IRMS

*Nanako O. Ogawa[1], Toshihiro Yoshimura[1], Takeru Kochi[2,1], Junichiro Kuroda[2,1], Yoshinori Takano[1], Naohiko Ohkouchi[1]

1. JAMSTEC, 2. AORI, Univ. Tokyo

The natural isotopic composition of sulfur ($\delta^{34}S$) is a useful, strong tool in geochemistry, ecology, environmental and planetary sciences. However, the scope of application is often limited by analytical capability. In the case of a sulfur isotope as well, it was often limited by analytical requirements for a large sample size (>60 μgS), and complicated preparatory procedures. To achieve precise measurement of $\delta^{34}S$ within small and limited quantities of samples, and to expand the scientific applicational range of the tool, we have developed a robust, sensitivity-improved sulfur isotopic analysis system by optimizing a commercial continuous-flow elemental analyzer/isotope-ratio mass spectrometer (EA/IRMS). Our EA/IRMS system successfully reduced the quantity of the required sample to 0.4 μgS or less to obtain reliable data of the sulfur abundances and isotopic compositions. In this presentation, we introduce the overview of the sensitivity-improved EA/IRMS for $\delta^{34}S$ with some application results from natural samples, such as gypsum, meteorites, and sulfur-containing organic compound such as methionine from biological samples.

Geological Samples: We established the conventional method to obtain $\delta^{34}S$ from gypsums and foraminiferal carbonates, with precisions of ±0.2‰ from samples of 0.5-2 μgS. The method was applied to study the sulfur cycle and evaporite formation during the Messinian Salinity Crisis. We will introduce the method details and the partial results of the project, as the main results will be presented and discussed by Kochi *et al.* at Session M-IS16 in this meeting.

Extraterrestrial Samples: We will also present the preliminary results of δ34S for carbonaceous chondrites (Murray, Murchison, Yamato 793321). The isotopic composition of bulk sulfur was obtained by analyzing the original (pre-treated) powders and the SOM extracted residues for these samples. The analytical techniques are going to be applied to investigate sample material recovered from the C-type asteroid Ryugu, as part of the Hayabusa2 SOM analysis team objectives [1,2].

Compound-Specific Samples: When combined with the compound-isolation/purification benefits of high-performance liquid chromatography (HPLC), the improved sulfur EA/IRMS can be applied to organic molecules, spanning a wide range of polarities and molecular weights, as well as investigate compound-specific isotope analysis. We will present the obtained $\delta^{34}S$ of Methionine separated from natural samples.

References

[1] Ogawa *et al.* Quantification and Isotopic Measurements of Submicrogram Scales Carbon and Nitrogen from Extraterrestrial Materials Through Nano-EA/IRMS. Lunar and Planetary Science Conference. No. 2326. (2020)

[2] Yoshimura *et al.* Major and Trace Element Composition in Acid-Soluble Extracts of Murchison and Yamato Meteorites. Lunar and Planetary Science Conference. No. 2326. (2020)

Keywords: Sulfur isotope, Compound specific isotope analysis, Messinian Salinity Crisis, C-type asteroid Ryugu, Hayabusa2

©2021. Japan Geoscience Union. All Right Reserved.

[J] Poster | M (Multidisciplinary and Interdisciplinary)：M-ZZ Others

Thu. Jun 3, 2021 5:15 PM - 6:30 PM JST | Thu. Jun 3, 2021 8:15 AM - 9:30 AM UTC | Ch.19_2

[M-ZZ46] Marine Manganese Deposits: Origin, Exploration, and Development

convener:Akira Usui(Marine Core Research Center, Kochi University), Katsuhiko Suzuki(Submarine Resources Research Center, Japan Agency for Marine-Earth Science and Technology), Yoshio Takahashi(Department of Earth and Planetary Science, Graduate School of Science, The University of Tokyo), Takashi Ito(Faculty of Education, Ibaraki University)

Marine manganese deposits occur in all world oceans, as nodules, crusts, and massive oxide aggregates. The deposits are known as potential resources of Co, Cu, Ni, REE as well as geological archives of surface environments. However, the controlling parameters on the regional and temporal variations in chemical and mineralogical composition have not been well understood yet. In the session, various factors in growth, enrichment and circulation of metals, paleoenvironment, formation age are discussed with the results of exploration and environmental impact studies from viewpoints of geosciences, engineering, and environments.

[MZZ46-P01] Detrital minerals in hydrogenetic ferromanganese crusts as an alternative tool for archiving marine geological environments

*Akira Usui[1], Takashi Ito[2], Hirokuni Oda[3], Hitoshi Hasegawa[4] (1.Marine Core Research Center, Kochi University, 2.Ibaraki University, 3.AIST, 4.Kochi University)

[MZZ46-P02] Fluxes of sinking particles in the exploration area for cobalt-rich ferromanganese crusts in the Northwest Pacific

*Kyoko Yamaoka[1], Atsushi Suzuki[1], Yuichiro Tanaka[1], Masahiro Suzumura[2], Ayumi Tsukasaki[2], Tatsuo Fukuhara[3], Takeshi Fujii[3], Junpei Minatoya[4], Nobuyuki Okamoto[4], Yoshiaki Igarashi[4] (1.Geological Survey of Japan, National Institute of Advanced Industrial Science and Technology, 2.Environmental Management Research Institute, National Institute of Advanced Industrial Science and Technology, 3.KANSO Co., Ltd., 4.Japan Oil, Gas and Metals National Corporation)

[MZZ46-P03] Submarine erosion of basement sedimentary rocks around ferro-manganese crust fields

*Takashi Ito[1], Masaki Saito[1], Eri Shimizu[2], Takashi Miyazaki[3], Bogdan S. Vaglarov[3], Katsuhiko Suzuki[3], Akira Usui[4] (1.Faculty of Education, Ibaraki University, 2.JOGMEC, 3.JAMSTEC, 4.Center for Advanced Marine Core Research, Kochi University)

[MZZ46-P04] Local structure of rare earth elements in marine ferromanganese oxides by extended X-ray absorption fine structure analysis

*Makoto Nagasawa[1], Yoshio Takahashi[1] (1.Department of Earth and Planetary Science, Graduate School of Science, The University of Tokyo)

[MZZ46-P05] Reconstruction of rotation by paleomagnetic analysis of manganese nodules collected in the South Pacific

*Wataru Katanoda[1,2], Hirokuni Oda[2], Masafumi MURAYAMA[3], Akira Usui[3] (1. Kochi university Graduate school of Integrated Arts and Science, 2.National Institute of Advanced Industrial Science and Technology, 3.Kochi university)

[MZZ46-P06] Lamina-scale analysis of chemical composition of the mid-Cretaceous northern Shimanto belt, Kochi, Japan: implications for formative processes of bedded ferromanganese deposits

*Go-Ichiro Uramoto[1], Takaumi Nagata[1], Yoshiro Nishio[1] (1.Kochi University)

[MZZ46-P07] Biodiversity and connectivity of deep-sea amphipods at seamounts with cobalt-rich ferromanganese crusts in the Northwest Pacific

*Akira Iguchi[1], Eri Ikeuchi[1], Hiroyuki Yokooka[2], Hideki Sugishima[2], Kazumasa Ikeda[3], Ryuichi Miwa[4], Miyuki Nishijima[1], Nozomu Iwasaki[5], Yuichiro Tanaka[1], Taiga Kunishima[6], Shogo Kato[7], Junpei Minatoya[7], Yoshiaki Igarashi[7], Nobuyuki Okamoto[7], Atsushi Suzuki[1] (1.National Institute of Advanced Industrial Science and Technology, 2.IDEA Consultants, Inc., 3.Okamoto Glass Co., Ltd., 4.Kaiyo Engineering Co., Ltd., 5.Faculty of Geo-Environmental Science, Rissho University, 6.Wakayama Prefectural Museum of Natural History, 7. Japan Oil, Gas and Metals National Corporation)

Detrital minerals in hydrogenetic ferromanganese crusts as an alternative tool for archiving marine geological environments

*Akira Usui[1], Takashi Ito[2], Hirokuni Oda[3], Hitoshi Hasegawa[4]

1. Marine Core Research Center, Kochi University, 2. Ibaraki University, 3. AIST, 4. Kochi University

Since iron and manganese oxides have been precipitated in the world oceans since 20Ma or older, most of the deep-sea floors are covered with ferromanganese crusts and nodules. The hydrogenetic ferromanganese crusts are in particular noted as potential paleoceanographic archives as well as future metal resources. They can be used as a tape recorder for deciphering the historical changes in marine geological environments, as indicators of environmental changes. We have reported laminated structure or compositional changes of major chemical composition on various scales and their regional changes. However, most of the data that read the variations are growth structure of major iron-manganese oxide only, which is the principal hydrogenetic components. In this study, we paid special attention to other minor components useful to read the history. The goal is to utilize better techniques for further research and development for more reliable criteria for identification of mineral particles similarly to marine sediment cores. The target materials are the substrate rocks on the seafloor, terrigenous mineral particles (river output, eolian dust), remains and traces of organisms, extraterrestrial materials, volcanic ash, hydrothermal precipitates, and authigenic precipitates. We tried to identify the materials using high-resolution optical/electron microscopes, microscale analysis, X-ray CT, analysis software, acid leach, gravity separation, etc. As a result, together with the earlier reports on magnetic minerals, we found that microfossil assemblage, cosmic spherules, weathering products, chemical precipitates. We have several issues in the processes of separation, age models, and identification of the factors of the spatiotemporal fluctuations, but expect better future in archiving the paleoenvironmental information from the detrital components in marine manganese deposits.

Keywords: paleoceanography, manganese crusts, ocean sediments

©2021. Japan Geoscience Union. All Right Reserved.

Fluxes of sinking particles in the exploration area for cobalt-rich ferromanganese crusts in the Northwest Pacific

*Kyoko Yamaoka[1], Atsushi Suzuki[1], Yuichiro Tanaka[1], Masahiro Suzumura[2], Ayumi Tsukasaki[2], Tatsuo Fukuhara[3], Takeshi Fujii[3], Junpei Minatoya[4], Nobuyuki Okamoto[4], Yoshiaki Igarashi[4]

1. Geological Survey of Japan, National Institute of Advanced Industrial Science and Technology, 2. Environmental Management Research Institute, National Institute of Advanced Industrial Science and Technology, 3. KANSO Co., Ltd., 4. Japan Oil, Gas and Metals National Corporation

To assess the environmental impact of deep-sea mining, it is important to understand natural spatial/temporal variations and their mechanisms. As part of the environmental baseline survey in the exploration area for cobalt-rich ferromanganese crusts in the Northwest Pacific, we have conducted sediment trap observations around five seamounts (JA02, JA03, JA04, JA06, JA17). The sinking particles mainly consisted of biogenic carbonate, and total mass fluxes were low (~5 mg m^{-2} d^{-1}), which are consistent with the characteristics of the oligotrophic open ocean. The JA17 Seamount, which is located in the northernmost portion of the area (~24Nº), showed relatively elevated total mass fluxes and a seasonal peak corresponding to the spring bloom. The sinking particles also contained higher biogenic opal, suggesting contribution of diatoms. On the other hand, the total mass fluxes at other seamounts showed seasonality with a sharp peak in late summer (August–September), although satellite data indicated the lowest primary production in summer. This discrepancy could be explained by short-lived or subsurface blooms induced by passing typhoons (Yamaoka et al., 2020).

We also measured elemental composition of the sinking particles collected around JA06 Seamount located in the south of the area. The results demonstrated that elemental fluxes in the area are controlled by four major processes: lithogenic (Al, Ti, Fe), carbonate (Mg, Ca, Sr), biogenic (+scavenging) (Ni, Zn, Cd, Pb), and scavenging (V, Mn, Co, Cu, REE). The estimation of excess flux based on the composition of upper continental crust demonstrated that >85% of total Mn, Co, Ni, Cu, Zn, Cd, and Pb fluxes were attributable to scavenging (+biogenic uptake). Scavenging-dominant metal fluxes are likely ubiquitous in the oligotrophic open ocean. Interestingly, the excess fluxes of Mn (1.3–7.0 μg m^{-2} d^{-1}) and Co (0.04–0.1 μg m^{-2} d^{-1}) for sinking particles in this study roughly corresponded to the metal fluxes into ferromanganese crusts (1.9–3.0 μg m^{-2} d^{-1} for Mn and 0.03–0.11 μg m^{-2} d^{-1} for Co) estimated by Sato and Usui (2018). Recently, Usui et al. (2020) presented evidence of ongoing precipitation of Fe-Mn oxide particles (a few micrometers in diameter) from normal seawater at 900–4500 m depth based on *in situ* 15-year exposure tests. Such particulate precipitates could be a common source of Mn for both cobalt-rich crusts and sinking particles.

Keywords: seamount, sinking particle, ferromanganese crust

©2021. Japan Geoscience Union. All Right Reserved.

Submarine erosion of basement sedimentary rocks around ferro-manganese crust fields

*Takashi Ito[1], Masaki Saito[1], Eri Shimizu[2], Takashi Miyazaki[3], Bogdan S. Vaglarov[3], Katsuhiko Suzuki[3], Akira Usui[4]

1. Faculty of Education, Ibaraki University, 2. JOGMEC, 3. JAMSTEC, 4. Center for Advanced Marine Core Research, Kochi University

The ferromanganese crust Sample HPD#958R12 collected from the depth of 1424 m at Takuyo-Daigo Seamount in the western Pacific Ocean was used as a research target to investigate the seamount erosion around the crust formation site. The number of fish tooth fossil samples separated from the 7-layers within the surficial 4 cm of this crust is 25 to 54, and the mass is about 0.1 mg to 0.2 mg. The fish tooth fossils for each of these strata were chemically treated and yield the $^{87}Sr/^{86}Sr$ ratio ranging from 0.70809 to 0.70880. The Sr isotopic composition of each fish tooth group in all layers is significantly lower than the coeval seawater Sr isotope ratio estimated from the ^{10}Be age of each layer of the crust. No specific pattern is observed in the growth direction. Based on these results, it was clarified that the teeth of fish contained in the crust include not only the fish that lived during the crust growth but also the older tooth fossils with lower Sr isotope ratio. The field observation by JAMSTEC ROV and the examination of the collected samples reveal that the exposed sedimentary rocks near the summit of Takuyo-Daigo Seamount are hard, phosphatized Cretaceous reef deposits. The results of this study clearly suggest that the following mechanism are very common, i.e. these phosphatized basement rocks are physically eroded and the washed-out fish teeth are contained in the growing layer of the crust. It was shown that the phenomena of physical erosion of hard sedimentary rocks and chemical precipitation of manganese oxide coexist in the seamounts.

Keywords: ferromanganese crust, fish tooth fossil, Strontium isotope

©2021. Japan Geoscience Union. All Right Reserved.

Local structure of rare earth elements in marine ferromanganese oxides by extended X-ray absorption fine structure analysis

*Makoto Nagasawa[1], Yoshio Takahashi[1]

1. Department of Earth and Planetary Science, Graduate School of Science, The University of Tokyo

Introduction
Marine ferromanganese oxides (MFMO), which is a mixture of nanoparticles of iron oxides and manganese oxides, formed as nodules or crusts at seafloor has been also of great interest as promising materials as metal resources. Among various elements enriched to MFMO, total abundance of rare earth elements (REE) enriched to MFMO reachs 2000 mg/kg. However, the extraction of REE other than by acidic solutions has not been reported for MFMO. In particular, high extraction rate of the target ions by aqueous solution at circumneutral pH is preferred, considering its possible influence on environment and ease to handle it for the refining processes.
In this study, speciation of REE, or yttrium (Y), in MFMO was conducted by extended X-ray absorption fine structure (EXAFS) analysis to reveal REE species adsorbed at the surface of MFMO or incorporated into MFMO. The species is highly important to understand their enrichment to the materials and also their extraction rate under various conditions. More specifically, formation of inner- and outer-sphere complexes at the solid-water interface is a most important factor controlling the extraction rate.

Sample and experimental
Typical marine ferromanganese nodules (D535) at the seafloor (water depth: 5222 m) employed in this study was collected in the Central Pacific, which is most likely formed by precipitation directly from seawater. This hydrogenetic process was also supported by iron and manganese ratio and other geochemical and mineralogical characteristics reported previously (Takahashi et al., 2007). Total REE abundances in D535 were 1920 mg/kg (Y: 130 mg/kg). EXAFS for Y at K-edge was employed to clarify the local structure of Y, or REE, in D535 at beamline BL01B1 in SPring-8.

Results and discussion
EXAFS spectra in k space for hydrated Y^{3+}, Y adsorbed on MnO_2 and goethite, and Y in D535 showed that the spectrum of Y in D535 is very similar to that of Y adsorbed on MnO_2. More quantitative analysis was conducted by the fitting of each shell in the spectra in R space for Y on MnO_2 and Y in D535 using backscattering and phase shift parameters given by FEFF. The fitting results quantitatively revealed that Y forms inner-sphere complex on MnO_2. It is suggested thta inner-sphere complexation of Y^{3+} in MnO_2 is essential as the host phase of trace elements under seawater condition with high salinity, because high ionic strength inhibits formation of outer-sphere complex as adsorbed species due to the ion-exchange reaction with other abundant cations in seawater.

Keywords: Rare earth element, Extended X-ray absorption fine structure, Speciation

©2021. Japan Geoscience Union. All Right Reserved.

Reconstruction of rotation by paleomagnetic analysis of manganese nodules collected in the South Pacific

*Wataru Katanoda[1,2], Hirokuni Oda[2], Masafumi MURAYAMA[3], Akira Usui[3]

1. Kochi university Graduate school of Integrated Arts and Science, 2. National Institute of Advanced Industrial Science and Technology, 3. Kochi university

Marine manganese nodules are believed to grow at or within the deep-sea sediments, and assumed uplifting and overturn during the growth without burial. We try to reconstruct the rotation and overturn during the growth process based on a paleomagnetic perspective using the manganese nodules collected with deep sea clay sediments.The Earth's magnetic field averaged over thousands of years can be approximated by a geocentric axial dipole, and the remanent magnetization direction recorded on the surface of a manganese nodule growing in a magnetic field is expected to correspond to the magnetic field direction at that time. If the manganese nodule has not been rotated during the growth process, the paleolatitude can be determined by determining inclination from the remanent magnetization direction. On the other hand, if the manganese nodule has rotated, the paleolatitude calculated from inclination will be different from the actual latitude, and the amount of rotation can be detected from this discrepancy.

The nodules were collected by a box corer (158˚30'64" W, 12˚00'03" S) from a depth of 5248 m in the GH83-3 Hakurei-maru cruise conducted by the Geological Survey in 1983 in the Penrhyn Basin. This is a spherical sample (B92-1-1; 74 mm long, 60 mm wide, and 66 mm high). The nodules were marked at the apex (center) with a white dot on board as a reference for the vertical direction.

The sample was split in half lengthwise on the plane including the white dot and the center of the nodule, and the vertical slice sample A was taken from the section as well as another vertical slice. Both slices were divided into five rows of strips, and then further divided in the growth direction into five subsamples. The samples were further divided into five or ten subsamples in the direction of growth to allow confirmation of changes in paleomagnetic and rock magnetic parameters with growth. The natural remanent magnetization of the subsamples was measured using a pass-through superconducting rock magnetometer (2G Enterprises Model 760R) at the National Institute of Advanced Industrial Science and Technology (AIST), and the primary remanent magnetization component was determined by stepwise alternating current demagnetization experiments and analysis of the demagnetization curve. Furthermore, rock magnetic properties such as magnetic hysteresis, isothermal remanent magnetization acquisition curve, and First Order Reversal Curve (FORC) were measured using a vibrating sample magnetometer (Lakeshore VSM 8604).

The paleomagnetic data confirmed that the paleomagnetic inclination of the samples near the surface near the white marker for both samples A and B are in good agreement with the expected geomagnetic inclination value (-23 degrees) at the sample collection point. This confirms that the surface layer of the sample records the current geomagnetic field. In addition, the paleomagnetic inclination tends to become deeper as we go back in time, indicating the sample was rotating. We discuss the possibility of rotation of manganese nodule during growth on the sediments, and the types and origin of magnetic minerals based on rock magnetic data.

Keywords: manganese nodule, paleomagnetism, geomagnetic inclination, growth process

©2021. Japan Geoscience Union. All Right Reserved.

©2021. Japan Geoscience Union. All Right Reserved.

Lamina-scale analysis of chemical composition of the mid-Cretaceous northern Shimanto belt, Kochi, Japan: implications for formative processes of bedded ferromanganese deposits

*Go-Ichiro Uramoto[1], Takaumi Nagata[1], Yoshiro Nishio[1]

1. Kochi University

The mid-Cretaceous has been identified as a super-greenhouse world with tropical sea surface temperatures in excess of 35˚C. In addition to the mid-Cretaceous climate being characterized by extreme warmth, it was also associated with significant tectonic, geochemical, and biotic perturbations[1]. Subsequently, it has been considered that the formation of the ferromanganese deposits occurred in the limited area in the marine environments[2]. However, available studies have mainly focused on the shallow marine sequences in North America and Africa. Data from the Pacific region are still limited despite the fact that the paleo-Pacific constituted the largest open ocean in the mid-Cretaceous, thus the Pacific region is critical for gaining a better understanding of the formation of metallic minerals in marine environments during the climatic evolution of the greenhouse Earth.

The mid-Cretaceous sequence of pelagic chert and ferromanganese deposits of the northern Shimanto-belt is widely distributed in the Aki area, Kochi, Japan. Bulk sample analysis of the northern Shimanto belt in the previous study[3] suggested that the mineral component including metallic elements was of hydrothermal origin. To examine the more detailed formative processes of the ferromanganese deposits, we conducted observations of microstructures in the pelagic sequence and identified the tens-to-hundreds micrometer-scale lamina in the ferromanganese deposits. The elemental analysis by EPMA and laser ablation ICP-MS analyses indicated that the lamination is consists of (1) a high abundance of metallic elements such as iron and manganese and (2) metallic elements with silicate. Besides, we could identify the variations of the metallic element abundance in the chert sequence. Based on these results, we will discuss the formative processes of the ferromanganese minerals in the pelagic environment of the northwestern Pacific in the mid-Cretaceous.
References: Jenkyns, 2010. Gcubed; Roy, 2006, Earth-Sci Rev.; Fujinaga et al., 2011, Shigen Chishitsu.

Keywords: northern Shimanto belt, mid-Cretaceous, ferromanganese deposit

©2021. Japan Geoscience Union. All Right Reserved.

Biodiversity and connectivity of deep-sea amphipods at seamounts with cobalt-rich ferromanganese crusts in the Northwest Pacific

*Akira Iguchi[1], Eri Ikeuchi[1], Hiroyuki Yokooka[2], Hideki Sugishima[2], Kazumasa Ikeda[3], Ryuichi Miwa[4], Miyuki Nishijima[1], Nozomu Iwasaki[5], Yuichiro Tanaka[1], Taiga Kunishima[6], Shogo Kato[7], Junpei Minatoya[7], Yoshiaki Igarashi[7], Nobuyuki Okamoto[7], Atsushi Suzuki[1]

1. National Institute of Advanced Industrial Science and Technology, 2. IDEA Consultants, Inc., 3. Okamoto Glass Co., Ltd., 4. Kaiyo Engineering Co., Ltd., 5. Faculty of Geo-Environmental Science, Rissho University, 6. Wakayama Prefectural Museum of Natural History, 7. Japan Oil, Gas and Metals National Corporation

To compare biodiversity and connectivity between seamounts with cobalt-rich ferromanganese crusts in the Northwest Pacific, we performed molecular ecological analysis targeting deep-sea amphipods, which are well diversified group in deep-sea area. We established baited traps in several sites and succeeded in collecting many amphipods specimens, likely including several species with different life characters. With these amphipod specimens, DNA barcoding and MOTUs community analysis detected different community structures among depths and seamounts. In addition, we also performed population genetic analysis by targeting several putative species and detected connectivity patterns between seamounts. Our molecular ecological approach using deep-sea amphipods around cobalt-rich ferromanganese crusts demonstrates its usefulness for performing environmental baseline studies and impact assessments in consideration of future deep-sea mining projects.

Keywords: Seamounts, Cobalt-rich ferromanganese crust, Amphipods, DNA barcoding, Connectivity

©2021. Japan Geoscience Union. All Right Reserved.